MODIFICATION OF CONNEXIN 43 EXPRESSION IN VASCULAR SMOOTH MUSCLE

Penelope-Jane Linnett BSc(Hons) *ANU* BVSc *Syd*

A thesis submitted for the degree of
Master of Philosophy

at the
Australian National University

July, 2002

STATEMENT

The contents of this thesis are original and all experiments were planned and carried out by the author under the supervision of Dr. Caryl Hill and Dr. Klaus Matthaei, except where otherwise stated or referenced.

The oligonucleotide primers (Cx43F, Cx43R, Cx43R2, Cx43R3, CMVF, pEGFPR) were designed by Dr. Caryl Hill and Dr. Klaus Matthaei, whilst the HOTT3 and HOTT7 primers were designed by Mr. David Mann. Preparation and testing of the smooth muscle cells was carried out by Ms. Haruyo Hickey. The set up and culture of the embryonic stem cells was done by Dr Klaus Matthaei, and the blastocyst injections were performed by Ms Helen Taylor. The blood pressure measurements in Chapter 4 were done by Mrs Kate MacKenzie.

Penelope-Jane Linnett

ACKNOWLEDGEMENTS

I wish to acknowledge the following: Dr Caryl Hill, Dr Klaus Matthaei, Wayne Damcevski, David Mann and Matthew Newhouse. Special thanks must go to Sue Henderson, Professor Ian Hendry, Haruyo Hickey, Dr Nesrin Ozarak and Dr Shaun Sandow.

Finally, I wish to acknowledge the very special support and guidance provided to me by Dr Paul Cooper.

ABSTRACT

Transgenic mice overexpressing Cx43 in specific regions of the vasculature were generated to examine the hypothesis that vascular function (specifically blood pressure) is influenced by increased connexin (Cx) 43 expression. The creation of a DNA construct containing a restricted portion of the SM22α promoter (SM22α / Cx43) to drive Cx43 gene expression, met the tissue specific requirement of the mice. Unfortunately, the establishment of a temporal and tissue specific transgenic mouse line to ensure that the mouse would not succumb to embryonic or neo-natal mortality, exceeded the time limitations of the current project.

When tested *in vitro* in murine aortic smooth muscle cells (prior to transformation into BALB/c embryonic stem cells), this DNA construct (SM22α / Cx43 / pBs KSII-) produced inconclusive results. This construct was, however, used to generate a transgenic mouse line with a truncated-promoter in the germ-line. It was found that only 204 to 103 bp of the SM22α promoter was present and so the functional capability of the truncated-promoter was unknown. Subsequently, this mouse line was interbred to increase the gene copy number and hence, the Cx43 expression level. A second attempt produced mice with the full-promoter in the germ-line.

Preliminary analyses on both mouse lines revealed the following: the aortic and tail artery tissues of all transgenic mice were more fragile than the control mouse; and the blood pressures of all mice, as determined by tail-cuff plethysmography, were within the normal range. Western blotting was used to determine the Cx43 protein levels in the aortae and tail arteries of the mice. In the single transgenic-promoter mice, there was no significant increase in Cx43 expression in either the aorta or tail artery. The double transgenic truncated-promoter mice had significantly increased Cx43 protein levels in the aorta, with no change in the tail artery, which indicates that the truncated-promoter

was minimally functional. In the single transgenic full-promoter mice, aortic Cx43 protein levels were significantly increased with a trend towards increased Cx43 in the tail arteries, which demonstrated that the SM22α / Cx43 construct was functional *in vivo*.

Together, the Cx43 expression data and the blood pressure measurements. suggest that increased Cx43 expression does not cause hypertension or hypotension in the mouse. The results obtained from this thesis provide the groundwork for further experimentation into the physiological effects of Cx43 overexpression in the vasculature and changes in vascular reactivity.

PUBLICATIONS AND PRESENTATIONS

Some of the work emanating from this thesis was presented at scientific meetings. The following abstract was published in conjunction with one of these presentations.

Linnett, P-J., Matthaei, K.I., Hickey, H. and Hill, C.E. (1999) Tissue and temporal specific expression of connexin 43 in mice. *Proceedings of the Australian Neuroscience Society* **10**: 225.

Other presentations:

Neuroscience Colloquium, Kioloa, NSW. (1999)

Neuroscience Seminar, John Curtin School of Medical Research, ACT. (1999)

TABLE OF CONTENTS

Abbreviations

AIS	Analytical Imaging System
ATP	adenosine triphosphate
4-AP	4-aminopyridine
bp	base pair(s)
bpm	beats per minute
BRF	Biomolecular Resource Facility
BSA	bovine serum albumin
cAMP	cyclic adenosine monophosphate
cGMP	cyclic guanosine 3',5'-monophosphate
cDNA	complimentary DNA
cm	centimetre
Ca^{2+}	calcium
CAT	choramphenicol acetyltransferase
CIAP	calf intestinal alkaline phosphatase
CMV promoter	cytomegalovirus promoter
COOH-	carboxy-
CT	carboxy-tail or carboxy terminal tail
Cx	connexin
Cx43	connexin 43 gene
dNTP	deoxynucleotidetriphosphate
dox	doxycycline
Da	dalton
DFS	doxycycline free serum
DMEM	Dulbecco modified Eagles medium
DNA	deoxyribonucleic acid
DTT	dithiothreitol
EDTA	ethylenediaminetetraacetic acid
ES cell	embryonic stem cell
EtOH	ethanol
FCS	foetal calf serum
g	gram(s)
G418	geneticin

GA	glycyrrhetinic acid (18α- and 18β-)
GFA	glutamine:fructose-6-phosphate-amidotransferase
hr	hour(s)
HCl	hydrochloric acid
I/P	intraperitoneal
IGF	interleuken growth factor
kb	kilobase(s)
kDa	kilodalton(s)
kV	kilovolt(s)
K^+	potassium
KCl	potassium chloride
L	litre(s)
L-amp plate	L-ampicillin agar plate
LB	Luria-Bertani broth
LIF	leukaemia inhibitory factor
mg	milligram(s)
min(s)	minute(s)
ml	millilitre(s)
mM	millimolar
mRNA	messenger RNA
M	molar
MCS	multiple cloning site
$MgCl_2$	magnesium chloride
ng	nanogram(s)
nm	nanometre(s)
NaCl	sodium chloride
Na_2HPO_4	sodium hydrogen phosphate
NaOAc	sodium acetate
NaOH	sodium hydroxide
NEB	New England Biolabs
NH_2-	amino-
oligo	oligonucleotide
OD	optical density
pBs KSII-	pBluescript plasmid

per os	by mouth
pmol	picomole
PBS	phosphate buffered saline
PBS-T	phosphate buffered saline with Tween-20
PCR	polymerase chain reaction
rpm	revolutions per minute
rtTA	reverse transactivator
s / sec(s)	second(s)
SDS	sodium dodecyl sulphate
SM22α	smooth muscle 22α gene
T_A	annealing temperature
T_m	melting temperature
Taq	*Thermus aquaticus*
TEA	tetraethylammonium
TRE	tetracycline response element
Tris	tris(hydroxymethyl)aminomethane
Tris-HCl	tris-hydrochloride
µg	microgram(s)
µl	microlitre(s)
µm	micron(s)
U	unit(s)
UTR	untranslated region
UV light	ultraviolet light
v/v	volume per volume
V	volt(s)
VDCC	voltage-dependent calcium channel
w/v	weight per volume
X-gal	5-bromo-4-chloro-3-indolyl-β-Dgalactose

Chapter 1 – Introduction

This thesis examines the hypothesis that vascular function is influenced by connexin expression by specifically determining the effects of increased connexin (Cx) 43 expression on blood pressure. To date, over fourteen individual mammalian connexins have been described (Beyer *et al.* 1990; Goodenough *et al.* 1996; Kumar and Gilula, 1992, 1996; Lo, 1999), with three having been identified in vascular smooth muscle: Cx43, Cx40 (Beyer *et al.* 1992; Little *et al.* 1995a; Christ *et al.* 1996; Severs *et al.* 1996; Xie *et al.* 1997; Hill *et al.* 2002) and Cx37 (Nakamura *et al.* 1999; Hill *et al.* 2002).

The characteristics of gap junctions, as determined by the properties of their component Cx properties, permit the selective intercellular passage of various ions, metabolites and small molecules (< 1 kD) between adjacent coupled cells (Loewenstein, 1981; Beyer *et al.* 1990; Bennett *et al.* 1991; Beny and Pacicca, 1994; Bruzzone *et al.* 1996; Goodenough *et al.* 1996; Veenstra, 1996). Such coupling can vary both within, and between, vascular beds. Changes in the distribution and expression of the vascular connexins have been correlated with a number of disease states such as hypertension, atherosclerosis, coronary heart disease and renal failure (Brink, 1998; Severs, 1999; Kwak *et al.* 2002).

In order to investigate aspects of some of these disease states, and in particular hypertension, the primary aim of this thesis was to produce a transgenic mouse model that would selectively overexpress Cx43 in the arterial system. This would enable an examination of the physiological effects of such overexpression on a number of aspects of vascular function, in particular the effect on blood pressure.

1.1 The Circulatory System

1.1.1 General overview

The circulatory system consists of the heart and an extensive system of arteries, veins and lymph vessels that are responsible for the supply of essential substances, such as oxygen and nutrients, and the removal of metabolic by-products. In this regard, the circulatory system is essential for the maintenance of homeostasis, including temperature regulation, systemic humoral communication, and adjustments to oxygen and nutrient supply in different physiological states (Berne and Levy, 1988; Tortora and Grabowski, 1993).

The vascular system consists of three general types of vessels that can be subdivided on a functional basis: the aorta and arteries (a distributing system), the microcirculation (a diffusion and filtration system), and the veins (a collecting system).

1.1.2 Types of arteries

Arteries have traditionally been classified into three types: large or elastic arteries (eg. the aorta), medium or muscular arteries (eg. the coronary, mesenteric and middle cerebral arteries), and small arteries and arterioles. In general, large diameter vessels with a media consisting of smooth muscle cells and elastic laminae, are referred to as elastic arteries, whilst vessels with a much reduced or absent medial elastic lamina are referred to as muscular arteries (Duling *et al*. 1991; Luff, 1991). The latter generally decrease in diameter as they approach the periphery at which point, the media consists of only 1 to 2 smooth muscle cell layers, and where the vessel is commonly referred to as an arteriole (Mulvany and Aalkjaer, 1990). Elastic arteries may give rise to elastic or muscular branches, although the reverse does not occur (Bunce, 1970). Functionally, elastic arteries serve as conduction tubes that facilitate the passage of blood (Berne and Levy, 1989).

1.1.3 Arterial morphology

In all arteries, the vessel wall is divided into three distinct layers: the intima, media and adventitia (Gutterman, 1999). Although variations in the characteristics of each layer have been observed in different vascular beds, the general arrangement of the endothelial and smooth muscle cells is similar in all arteries. A description of the morphology based upon several publications is presented in Figure 1.1 and Section 1.1.3.1 (Rhodin, 1967, 1980; Gabella, 1981; Ross and Reith, 1985; Deitweiler, 1989; Mulvany and Aalkjaer, 1990; Duling *et al.* 1991; Luff, 1991), with the latter concentrating on the vascular smooth muscle cells, which are of particular relevance to the current study.

1.1.3.1 Vascular smooth muscle cells

Vascular smooth muscle cells, the predominant cell type in the media, are mononucleate and are arranged in helical or circular layers around the larger blood vessels with a generally decreased pitch (defined as the degree of angle in relation to the parallel arrangement of the vessel) in more peripheral vessels (Rhodin, 1967; Luff, 1991). The structural arrangement of vascular smooth muscle cells reflects both functional and regulatory variations between different blood vessels, both in different parts of the vasculature and within the same vascular region (Jacobsen *et al.* 1966; Bevan and Torok, 1970; Shiraishi *et al.* 1986; Frid *et al.* 1997).

The size of vascular smooth muscle cells varies considerably in different vascular beds ranging from 30 to approximately 2000 μm in length (Burnstock, 1970; Gabella, 1981) and from 3 to 20 μm in width (Komuro *et al.* 1982; Todd *et al.* 1983; Shiraishi *et al.* 1986). The overall shape of vascular smooth muscle cells has been shown to vary along the one vascular bed, between different vascular beds and between different animals (Gabella, 1981; Todd *et al.* 1983; Shiraishi *et al.* 1986; Gabella, 1991;

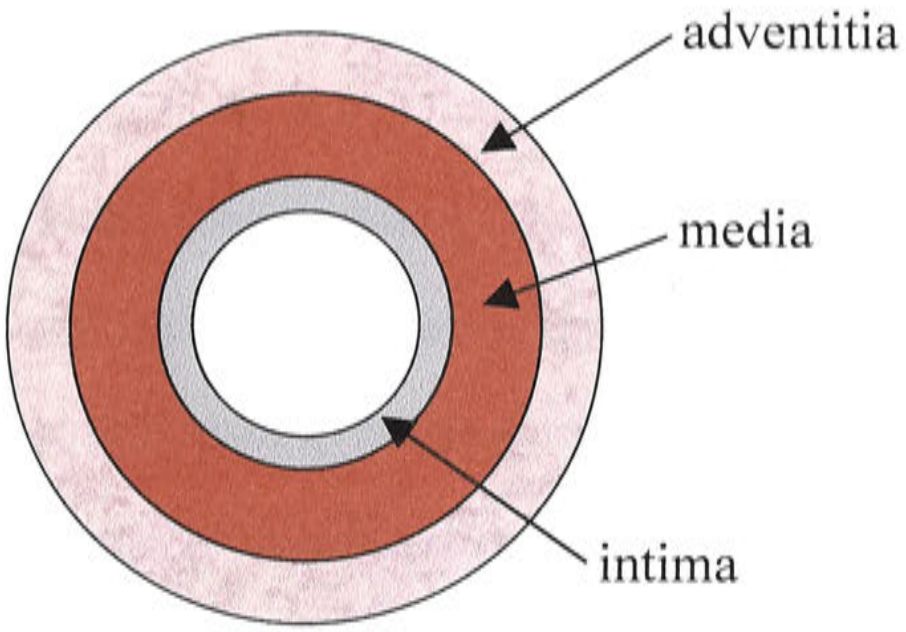

Figure 1.1 Schematic representation of the X-sectional appearance of an artery

The intima consists of a tubular lining of endothelial cells which are joined by tight (occluding) junctions and gap (communicating) junctions, with the specific arrangement of junctions varying in different blood vessels, tissues and animal species. In elastic arteries, the intima is usually relatively thick, consisting of the lining endothelium with its basal lamina, a subendothelial layer of connective tissue with both collagenous and elastic fibres, and the concentrically arranged internal elastic lamina. In muscular arteries, the subendothelial connective tissue is sparse and in some arteries, the basal lamina of the endothelium contacts the internal elastic membrane.

The medial layer consists of either single or multiple layers of smooth muscle cells that vary in size, shape and arrangement in different blood vessels. These cells are connected by tight and gap junctions, with collagen fibres often being present in the region between smooth muscle cells. In both elastic and muscular arteries, the smooth muscle cells produce extracellular collagen and elastic fibres. Arterioles have one layer of smooth muscle cells and a small artery may have up to about eight layers of smooth muscle cells. Muscular arteries often have a distinct external elastic lamina.

The adventitia confers structural support to the vessel, as well as connecting it to the surrounding tissues. It is composed of connective tissue and extracellular collagen fibres which contain cellular components such as fibroblasts, macrophages, and sympathetic, parasympathetic and sensory nerve fibres, and Schwann cells. The thickness of the adventitia varies considerably depending on the type and location of the blood vessel.

Kohler *et al.* 1999), as well as during development (Hill and Sandow, unpublished results) and maturation (Cliff, 1967; Miller *et al.* 1987).

A variety of forms of vascular smooth muscle cells have been found to coexist within the vascular wall (Giuriato *et al.* 1995; Frid *et al.* 1997). Phenotypically distinct vascular smooth muscle cells, characterized by different patterns of ultrastructural morphology, cytoskeletal protein and ion channel expression, electrical responses, capacity for extracellular matrix synthesis, migration and growth, have been identified in the adult arterial media and in culture (Ko *et al.* 1999; Kohler *et al.* 1999; Halayko and Solway, 2001). Thus, specific types of vascular smooth muscle cells may be differentially involved in the processes associated with vascular disease (Frid *et al.* 1997; Seidel, 1997). A characteristic property of vascular smooth muscle cells is their ability to modulate between the contractile phenotype and the synthetic phenotype, which is characterized by a reduction in myofilament content and an increase in synthetic organelles (Campbell *et al.* 1981), for the synthesis of extracellular matrix molecules (Blackburn *et al.* 1997). In the adult mammalian vascular system, vascular smooth muscle cells are found predominantly in the contractile state, but during vascular disease (in hypertension, for example) or following injury or during atherosclerotic plaque formation, the secretory synthetic type is expressed (Rennick *et al.* 1993; Lindop *et al.* 1995; Ross, 1996; Dzau *et al.* 1993; Severs, 1999).

Abnormal growth of vascular smooth muscle cells plays an important role in the pathogenesis of many vascular diseases including atherosclerosis and hypertension (Jackson and Schwartz, 1992; Christ *et al.* 1996; Haefliger *et al.* 1997b; Shimokawa, 1999). In hypertension, the vascular pathology is characterized by hypertrophy of the media, which in turn results in elevated blood pressure (Weissberg *et al.* 1995), whilst development of the intimal cells occurs in atherosclerosis (Blackburn *et al.* 1995; Schwartz *et al.* 1995; Schwartz, 1999). It has been suggested that these changes are

related to the position of the particular vessel in the vascular tree (Nakamura *et al.* 1998).

In hypertension, hypertrophy of the media is greater in the smaller arteries or arterioles than in the larger arteries, such as the coronary artery (Isoyama *et al.* 1992). Thus, in this state, the main pathological change in the vascular smooth muscle cells varies according to the size and position in the vasculature of the specific blood vessel. In the small arteries or arterioles, the smooth muscle cells undergo hyperplasia rather than hypertrophy (Mulvany *et al.* 1985; Berk *et al.* 1989) whilst in the larger arteries, they undergo hypertrophy rather than hyperplasia (Owens *et al.* 1981; Berk *et al.* 1989). Morphologically and biochemically there is little to distinguish these cells from normal vascular smooth muscle cells other than the hypertrophy / hyperplasia and a tendency to form multiple branches (Lindop *et al.* 1995; Weissberg *et al.* 1995).

1.1.4 Arterial function

As a functional whole, vascular smooth muscle cells contribute to the control of total peripheral resistance, and arterial and venous tone (Christ *et al.* 1996). These cells are in close contact with the endothelial cells which maintain the homeostatic state of the blood vessel by producing factors that regulate vessel tone, coagulation state, cellular responses (eg. proliferation), and leukocyte movements (Kunsch and Medford, 1999).

Contraction of the smooth muscle cells assists in the maintenance of blood pressure (Sherwood, 1993; Tortora and Grabowski, 1993). Contraction is initiated by an increase in the cytoplasmic concentration of calcium resulting from the release of calcium from the sarcoplasmic reticulum and/or from the influx of calcium from the extracellular space though voltage-dependent calcium channels (VDCC: L-type and T-type, of which the L-type VDCC is a major contributor to vascular tone) or receptor operated nonselective channels (Tortora and Grabowski, 1993; Martens and Gelband,

1998). The specific mechanisms involved in the entry and activity of calcium vary amongst vascular beds (van Breemen *et al.* 1995; Hirst and Edwards, 1989; Jagger and Ashmore, 1999). Calcium increase in the cytosol activates myosin light chain kinase, an enzyme that uses ATP to phosphorylate the myosin so that it can bind to actin for contraction to occur. Smooth muscle tone, which is integral for the maintenance of vascular tone and tension, is maintained by the continual entry and removal of calcium from the cytosol of smooth muscle cells, resulting in the preservation of a state of continual partial contraction (Sherwood, 1993; Tortora and Grabowski, 1993).

1.1.5 Gap junctions

The coupling of vascular smooth muscle cells via gap junctions is essential for the co-ordination, modulation and propagation of the contractile activity of vascular smooth muscle cells (Segal and Duling, 1986; Hirst and Edwards, 1989; Duling *et al.* 1991; Christ *et al.* 1993a,b; Segal, 1994; Brink *et al.* 2000). The absence or reduction in gap junctions in tumours or transformed cells (Loewenstein, 1979; Ruch *et al.* 1998) and their corrective effects on cell proliferation when connexins, their constituent proteins, are transfected into these cells (Mehta *et al.* 1991; Rose *et al.* 1993), suggests that gap junctions also play an important role in the control of cell growth and development (Loewenstein, 1987; Bennett *et al.* 1991; Loewenstein and Rose, 1992; Warner, 1992; Goodenough *et al.* 1996; Lo, 1996).

Analysis of connexin gene knockout animals and naturally occurring connexin mutations, has indicated that gap junctional communication has diverse functions in the development and physiological activity of not only the vascular system, but also of several organ systems (Lo, 1996; Martyn *et al.* 1997; Chanson *et al.* 1999; Waldo *et al.* 1999).

Gap junctions are dynamic structures, continually undergoing the process of formation and degradation (Christ *et al.* 1996; Spray, 1998). Compared with many

other membrane proteins, this appears to be rapid in normal adult vascular tissues with, for example, Cx43 half-life between 1.5 and 3 hours in primary cultures of neonatal myocytes (Beardslee *et al.* 1998) as well as in other cultured cells (Fallon and Goodenough, 1981; Yancey *et al.* 1981; Laird *et al.* 1991; Darrow *et al.* 1995; Laing and Beyer, 1995; Darrow *et al.* 1996; Laing *et al.* 1997). Regulation of gap junction function and structure by various means, including via the activity of growth and differentiation factors, has been extensively reported (Meda *et al.* 1993; Brissette *et al.* 1994) and will be discussed further in Section 1.1.5.4.

1.1.5.1 Gap junction structure

Dye-tracer studies, high resolution electron microscopy and nuclear resonance imaging (NMR) electron microscopy have enabled the morphological structure of gap junctions to be well characterized (Brightman and Reese, 1969; Makowski *et al.* 1977, 1984; Lampe *et al.* 1991; Yeager and Gilula, 1992; Yeager, 1995). Cell-to-cell contact through gap junctions occurs at sites of close apposition (2 to 3 nm apart) of plasma membranes of adjacent cells (Goodenough and Revel, 1970; Gabella, 1973; Caspar *et al.* 1977; Little, 1995a,b; Unger *et al.* 1999). These sites appear as electron dense pentalaminar structures (Luff, 1991) approximately 10 nm in width (Brink, 1998).

At the molecular level, gap junctions have been described as consisting of a highly conserved group of membrane protein subunits termed connexins; different types and combinations of which allow the selective intercellular passage of various ions, metabolites and small molecules (< 1 kD) in different vascular beds and tissues (Loewenstein, 1981; Beyer *et al.* 1990; Bennett *et al.* 1991; Beny and Pacicca, 1994; Bruzzone *et al.* 1996; Goodenough *et al.* 1996; Kumar and Gilula, 1996; Veenstra, 1996; Simon, 1999; Falk, 2000). Each gap junction channel is composed of 12 connexin protein subunits formed by the association of two hemichannels (connexons), one in each opposing cell, comprising a hexagonal array of six connexin polypeptides

which together surround a central pore 1.5 to 2.0 nm in diameter (Loewenstein, 1980, 1987; Figure 1.2).

The characteristic pentalaminar appearance of the gap junctions at the ultrastructural level, together with the arrangement of transmembrane connexins, is illustrated in Figure 1.3. Electron micrographs have shown that gap junctions have variable numbers of closely packed membrane channels, ranging from a few to many thousands (also called gap junction plaques) (Goodenough and Revel, 1970), with the packing morphology varying between different tissues (Shivers and McVicar, 1995).

Since the first connexin cloning studies of Kumar and Gilula (1986) and Paul (1986) that demonstrated the full length amino acid sequences for specific connexins, over fourteen distinct mammalian connexins have been cloned and designated according to their molecular mass (in the range 26 to 60 kD) (Beyer *et al.* 1990; Willecke *et al.* 1991; Kumar and Gilula, 1992; Goodenough *et al.* 1996) or into three major subclasses, α or type II, β or type I and γ or type III (Gimlich *et al.* 1990; Kumar and Gilula, 1996; O'Brien *et al.* 1998). Their presence has been demonstrated in a large variety of organisms (Bennett *et al.* 1995; Waltzman and Spray, 1995; Morley *et al.* 1997), as well as in various mammalian cell types and tissues (Paul, 1986; Waltzman and Spray, 1995; Coppen *et al.* 1999; Lo, 1999). Although connexin expression is conserved among species, it has been shown to be both tissue- and cell-specific, with some cell types expressing multiple connexins (Donaldson *et al.* 1997). Multiple connexins may also be present in the same gap junctional plaque (Nicholson *et al.* 1987).

In vascular smooth muscle, two connexins have been identified - connexin (Cx) 43 and Cx40 (Christ *et al.* 1996), whilst Cx43, Cx40 and Cx37 have been demonstrated in vascular endothelial cells (Beyer *et al.* 1992; Christ *et al.* 1996; Delorme *et al.* 1997). Localization of Cx37 has recently been demonstrated in the medial layer of both the pulmonary artery and aorta (Nakamura, 1999) and in the rat tail artery (Hill and Hickey,

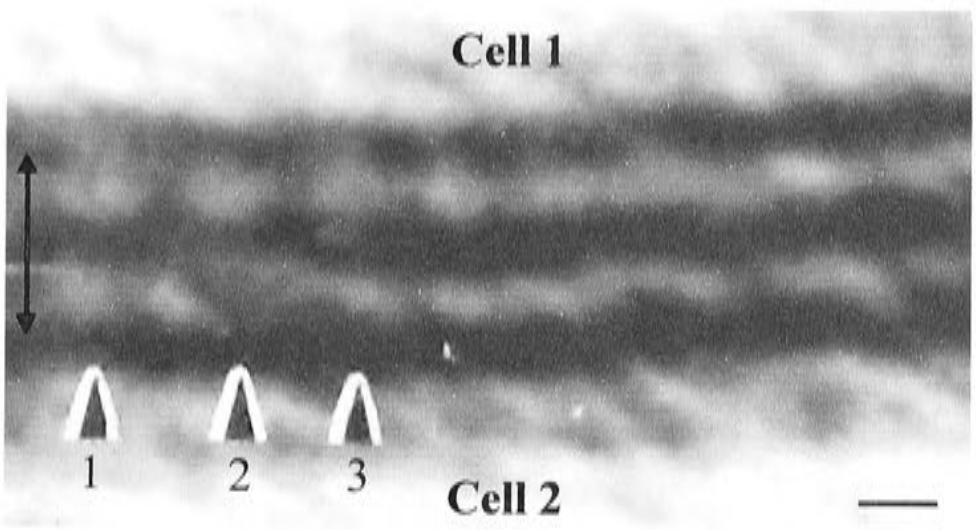

Figure 1.2 Gap junction structure between smooth muscle cells

High power electron micrograph from a 14 day rat iris arteriole showing a typical gap junction between smooth muscle cells and the appearance of connexins at the electron microscope level. The characteristic pentalaminar structure can be seen clearly. The lighter regions (arrows; 1-3) denote individual connexin channel pores. The distance between the connexins is 9 nm. The scale bar represents 5 nm.

(Electron micrograph courtesy of Dr. Shaun Sandow, Division of Neuroscience, John Curtin School of Medical Research, Australian National University).

Figure 1.3 Structure of gap junction channels

Schematic diagram of the structure of gap junction channels between two cells A and B, demonstrating the position of the connexons in the cell membranes and their constituent connexins. Also shown are the lipid bilayers, the intercellular space and some of the molecules which are known to pass through the central pore of each gap junction.

(Modified from Christ *et al*. 1996).

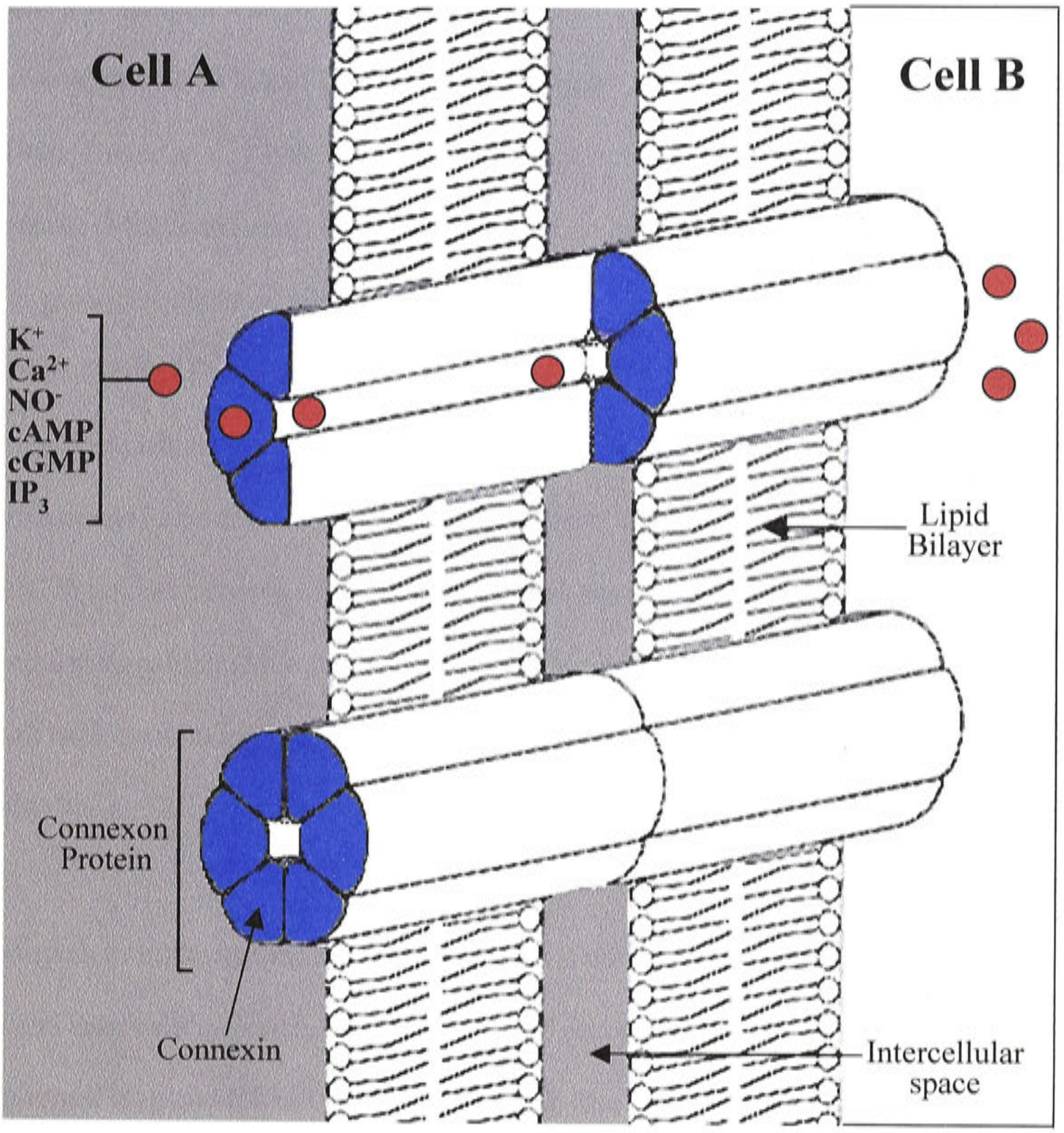
Cell A
Cell B
K^+
Ca^{2+}
NO^-
cAMP
cGMP
IP_3
Lipid Bilayer
Connexon Protein
Connexin
Intercellular space

pers com). Connexins may also have overlapping or complementary expression patterns (Delorme *et al*. 1997).

High resolution ultrastructural studies and sequencing data have shown that the connexins comprise a family of homologous proteins, all of which have four α-helical transmembrane domains that form the channel, two extracellular loops, a cytoplasmic loop, and cytoplasmic NH_2- and COOH- termini (Figure 1.4) (Bennett *et al*. 1991; Locke, 1998; Unger *et al*. 1999) which can influence or regulate the physical properties of the channel (Makowski *et al*. 1977; Kumar and Gilula, 1992; Paul, 1995; Sosinsky, 1996; Yeager and Nicholson, 1996; Nicholson and Bruzzone, 1997; Yeager, 1998; Purnick *et al*. 2000). The extracellular loops of all connexins contain highly conserved cysteine residues, which are important in intercellular recognition and the docking of two hemichannels (connexons) (Yeager and Nicholson, 1996). Studies of the carboxy terminal (CT) tail have shown that it is an important site for channel gating in response to intracellular signalling (Moreno *et al*. 1994; Ek-Vitorin *et al*. 1996; Castro *et al*. 1999) with each domain interacting with the other domains (Verselis *et al*. 1994). The CT tail also has a role in regulating connexin-mediated growth (Omori and Yamasaki, 1999).

Sequence similarity amongst the connexins is concentrated in the transmembrane domains and extracellular loops, whilst most of the sequence and length variation is in the cytoplasmic loop and CT tail (Beyer *et al*. 1990; Haefliger *et al*. 1992; Donaldson *et al*. 1997). Domain swapping experiments have determined that compatibility between the connexins (defined as the ability of adjacent cells expressing different connexins to communicate) is attributable to the second extracellular domain (White *et al*. 1994, 1995).

Figure 1.4 Structure of gap junction channels

Two typical connexins, Cx43 and Cx32, are illustrated, showing the four membrane spanning domains – two extracellular loops, a cytoplasmic loop, and cytoplasmic amino (N) and carboxy (C) termini.

(Modified from Yeager and Nicholson, 1996).

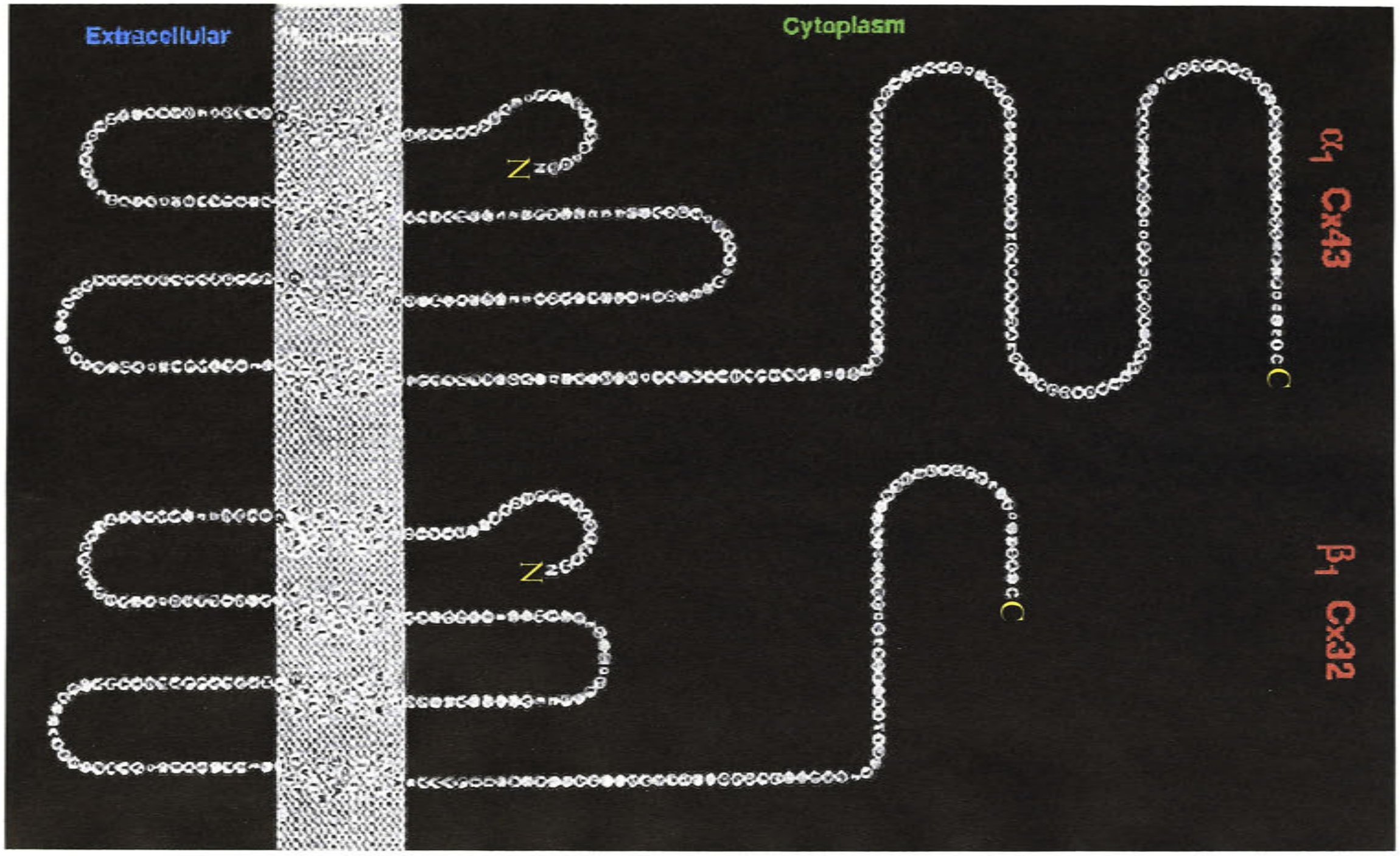
Extracellular
Cytoplasm
Z
Z
C
C
α1 Cx43
β1 Cx32

1.1.5.2 Gap junctions: homomeric, heteromeric, homotypic and heterotypic forms

As alluded to above, each connexon (hemichannel) may be composed of either one type of connexin (homomeric) or multiple connexins (heteromeric). Theoretically, the heteromeric connexon can result in a variety of connexin combinations (Brink, 1998; White and Paul, 1999) which would be physiologically advantageous, in terms of diversity, for intercellular communication. Adjacent cells can contribute different types of connexon to the intercellular channel giving rise to homotypic (when the same connexin is present in both connexons), heterotypic (when each connexon is composed of a different connexin) or heteromeric (when different connexins mix in the connexons) intercellular channels (Figure 1.5) (Bukauskas *et al.* 1995; White and Bruzzone, 1996; Brink *et al.* 1997; Yeh *et al.* 1998; White and Paul, 1999).

Some combinations of connexins, however, will not interact and consequently, are unable to form functional channels. Cx43 and Cx40, for example, are coexpressed in vascular smooth muscle and together, they form homomeric / homotypic channels with distinct permeability and gating properties but not functional homomeric / heterotypic channels (Kanter *et al.* 1993; He *et al.* 1999; Li and Simard, 1999). Conversely, He *et al.* (1999) demonstrated that in vascular smooth muscle cells *in vitro*, Cx43 and Cx40 can form functional channels with unique gating and conductance properties in the form of heteromeric channels, whilst Valiunas *et al.* (2000) have demonstrated that these connexins can form functional heterotypic channels in human HeLa cells.

Electrophysiological studies of heterotypic channels have shown that some exhibit unique properties compared to homotypic channels (Barrio *et al.* 1991; Bruzzone *et al.* 1994; White *et al.* 1994; Darrow *et al.* 1996; Brink *et al.* 1997). Studies of homotypic Cx43, Cx40 and Cx37 gap junction channels (Brink *et al.* 1996; Veenstra, 1996) have shown that they all display symmetric voltage dependence but different kinetics and voltage sensitivities (Brink, 1998). Furthermore, they are all permeable,

Figure 1.5 Connexins in gap junctions

The arrangement of connexins into connexons, intercellular channels and gap junctions is shown. Adjacent cells contribute different types of connexon to the intercellular channel giving rise to heteromeric, homomeric, heterotypic and homotypic channels.

(Modified from White and Paul, 1999).

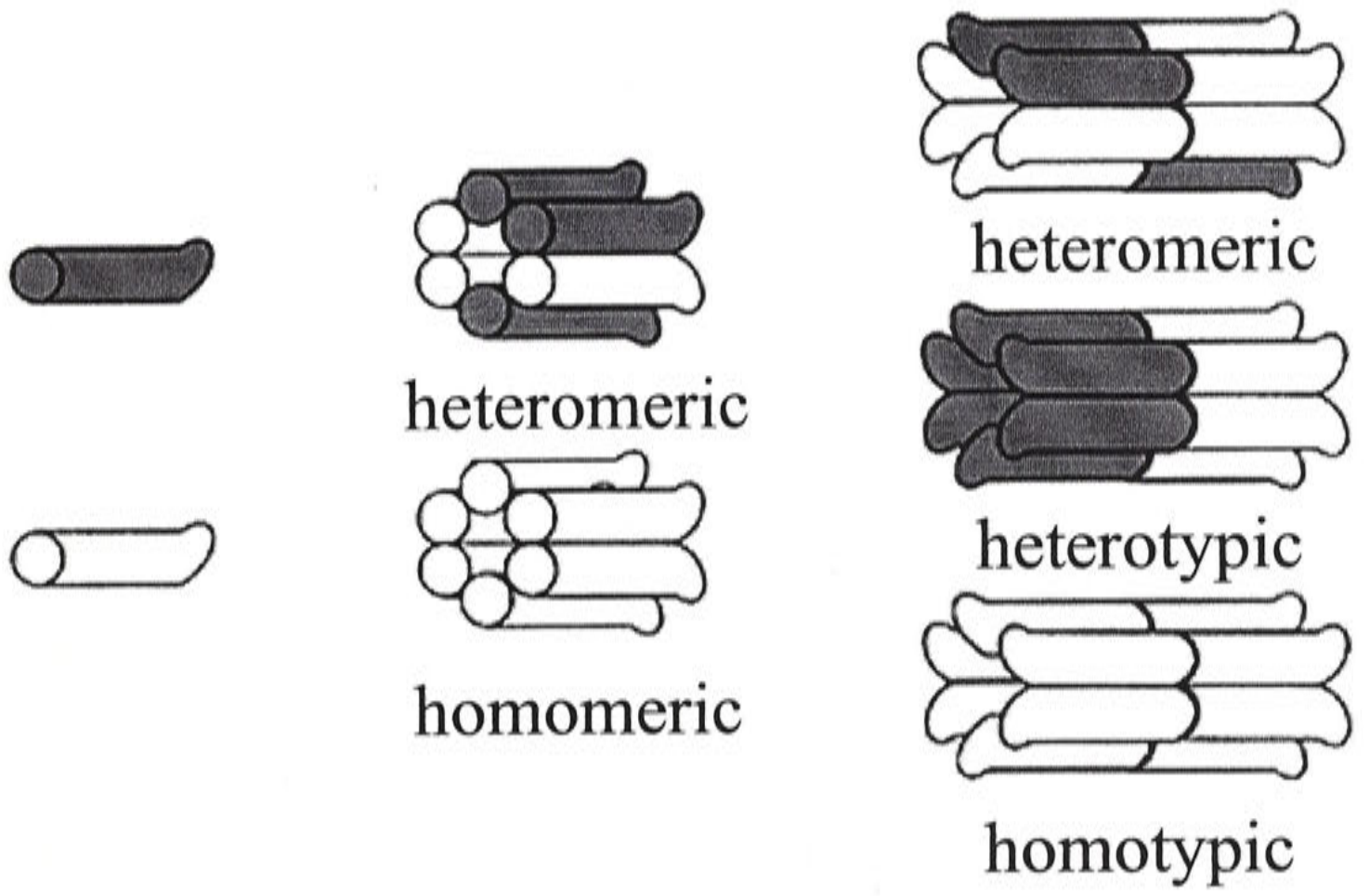
heteromeric
heteromeric
heterotypic
homomeric
homotypic
connexins
connexons
intercellular channels

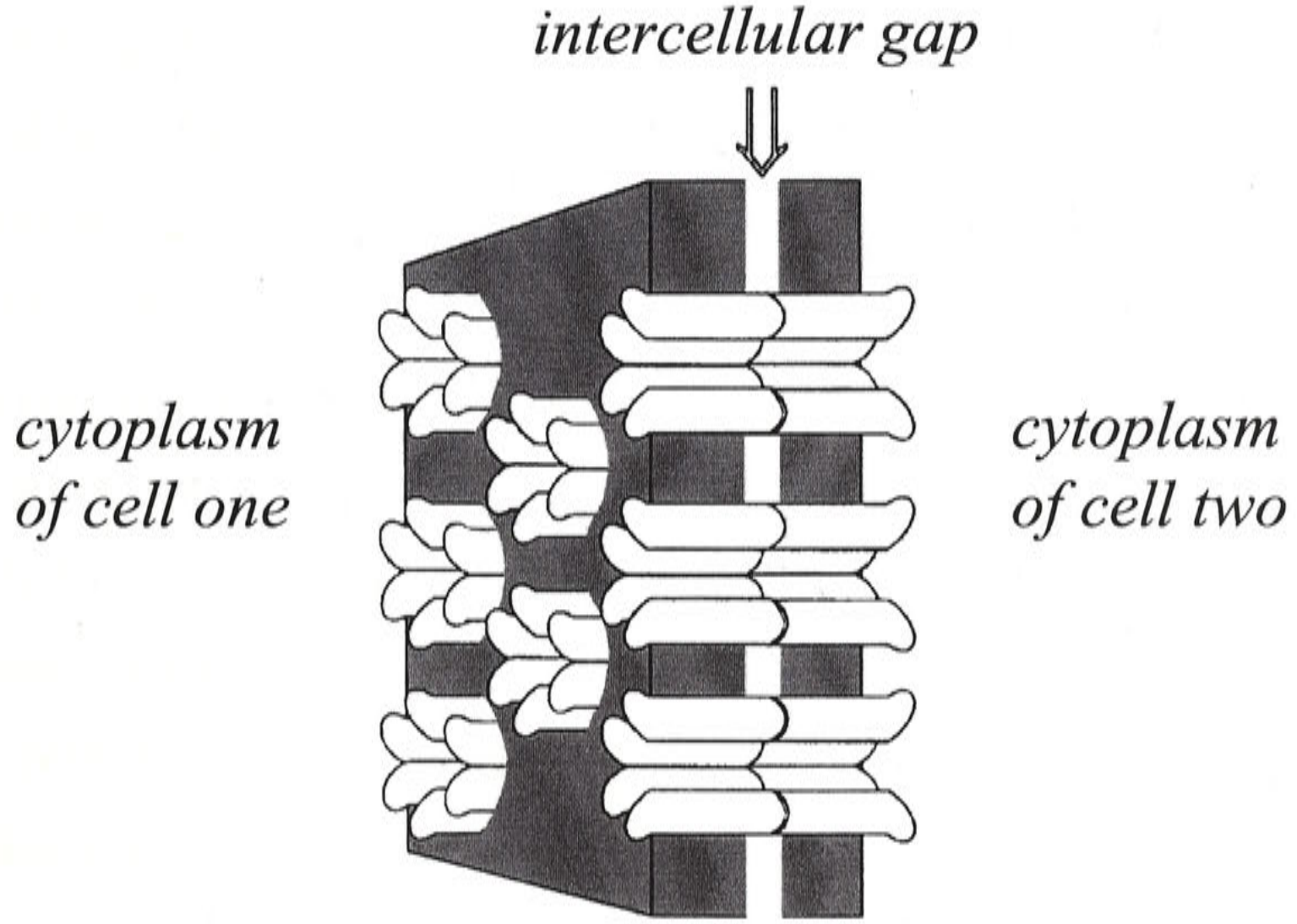
intercellular gap
cytoplasm of cell one
cytoplasm of cell two
gap junction

though at different levels, to fluorescent dye molecules in the range 350 to 450 Da such as Lucifer Yellow or carboxyfluorescein (Robinson *et al.* 1993; Moreno *et al.* 1994; Little *et al.* 1995b; Brink, 1996, 1997; Darrow *et al.* 1996), with Cx37-Cx40 having reduced permeability to 6-carboxyfluroscein compared to Cx43 (Veenstra *et al.* 1994).

1.1.5.3 Gap junction expression

The previous sections have alluded to the fact that different connexins and differences in the characteristics of connexins can confer specific physiological properties on gap junctions (Bruzzone *et al.* 1996; Beyer *et al.* 1990; Willecke *et al.* 1991; Goodenough *et al.* 1996). Since most, if not all cells and tissues express at least two connexins (Nicholson *et al.* 1987; Kanter *et al.* 1992,1993; Darrow *et al*, 1995; Stauffer, 1995; Van Rijen *et al.* 1997; Coppen *et al.* 1999; Lo, 1999; Mehta *et al.* 1999), it follows that the properties of the gap junctions of any cell or tissue are complex.

Physiological analysis of channel formation and gating has revealed unique patterns of connexin-connexin interaction, as well as unique functional characteristics of channels containing more than one type of connexin protein (White *et al.* 1995; White and Bruzzone, 1996). Each connexin has tissue-specific distributions, differential temporal expression and specific channel permeability properties, and is subject to unique types of biochemical regulation (Veenstra, 1992; Bruzzone *et al.* 1996; Kumar and Gilula, 1996; Bevans *et al.* 1998; Goodenough *et al.* 1996). Data from animal model studies and human disease states have shown that genetic defects in each connexin produce distinct developmental and/or physiological defects (Britz-Cunningham *et al.* 1995; Paul, 1995; Anzini *et al.* 1997; Donaldson *et al.* 1997; Ewart *et al.* 1997; Huang *et al.* 1998; Chanson *et al.* 1999; Sullivan *et al.* 1999; White and Paul, 1999; Willecke *et al.* 1999). Specific mutations in Cx32 result in X-linked Charcot-Marie-Tooth disease, a demyelinating peripheral neuropathy (Bergoffen *et al.* 1993; Anzini *et al.* 1997; Balice-Gordon *et al.* 1998; Abel *et al.* 1999; Fischbeck *et al.*

1999) whilst congenital hereditary bilateral cataracts have been associated with a missense mutation in Cx50 (White and Paul, 1999; Xu and Ebihara, 1999).

Mutations in Cx43 (also referred to α1 connexin, and is the predominant gap junction gene in developing and adult heart tissue) have been shown to be associated with atrial defects (eg. visceroatrial heterotaxia; Britz-Cunningham *et al.* 1995) and other congenital cardiac abnormalities (Reaume *et al.* 1995). In the transgenic (overexpressing Cx43) and knockout Cx43 mice, there are major right ventricular cardiac defects (Reaume *et al.* 1995; Ewart *et al.* 1997; Martyn *et al.* 1997; Ya *et al.* 1998) leading to failure of pulmonary gas exchange and neonatal lethality at birth. Consequently, Cx43 appears to play an important role in cardiac morphogenesis with the precise level of Cx43-mediated gap junctional communication also being potentially critically important (Reaume *et al.* 1995; Ewart *et al.* 1997).

Coexpression of multiple connexins enables cells to achieve levels of intercellular communication that could not be achieved by expression of a single connexin (Koval *et al.* 1995). Coexpression also enables functional compensation to occur (Minkoff *et al.* 1999) as has been demonstrated in Cx43 knockout mice. In this mouse, the absence of gross abnormalities, other than the (critical) heart defect, has been taken as evidence that the loss of Cx43 can be compensated for by other connexins whose distributions overlap (De Sousa *et al.* 1997; Houghton *et al.* 1999). Furthermore, in preimplantation embryos lacking Cx43, a low level of intercellular coupling is maintained by gap junction channels having characteristics of Cx45 (α6 connexin; De Sousa *et al.* 1997). Cx32 has also been suggested to compensate for the absence of Cx43 in some instances (Houghton *et al.* 1999). The ability of one type of connexin to either induce or suppress the expression of other connexins during development (van Kempen *et al.* 1995) has been demonstrated with respect to Cx45 in the Cx43 knockout mice (De Sousa *et al.* 1997) as well as with other connexin combinations.

Depending on the surrounding microenvironment to which cells are exposed, the extent of intercellular communication may also vary during development and aging (Mombouli and Vanhoutte, 1999). Modification of the Cx43 gene in mice has highlighted the importance of this connexin in heart morphogenesis (Reaume *et al.* 1995; Ewart *et al.* 1997; Huang *et al.* 1998; Sullivan *et al.* 1999). In the Cx43 knockout mouse, abnormal cardiac tissue growth has been observed during development (Sullivan *et al.* 1999). Responses to other stimuli (pharmacological, hormonal or oncogenic) may also be distinct to a particular connexin or group of connexins (Mehta *et al.* 1999).

1.1.5.4 Regulation of gap junction function

Many aspects of the regulatory processes of gap junctions have been elucidated as a result of physical, biochemical and cloning studies. Regulation of gap junction function, and hence gap junction-mediated communication, can occur both acutely (gating) and over a longer time period. In the latter, overall connexin expression levels are altered, with or without switching to functionally different connexin isoforms (Bennett *et al.* 1991; Beyer, 1991).

Dye coupling experiments and dual whole-cell voltage-clamp experiments (Flagg-Newton *et al.* 1979; Schwarzmann *et al.* 1981; Little *et al.* 1995b; White *et al.* 1995; Darrow *et al.* 1996; Kwak and Jongsma, 1996; Bevans *et al.* 1998; Ebihara *et al.* 1999; Manthey *et al.* 1999; Srinivas *et al.* 1999) have been used extensively to determine the functional state of gap junctions. Dye coupling studies have provided information about the extent of diffusional coupling and permeability of the channels, whilst dual whole-cell voltage-clamp experiments have allowed the gap junctional conductance (g_j), which depends on the number of channels present, the conductance of each channel (γ_j) and their probability of being 'open', to be determined (Kwak and Jongsma, 1996). As the majority of these studies have been done in the adult animal, there is a lack of comparable data for the immature and developing animal.

Gap junctions can 'open' and 'close' (or be in an 'intermediate' state) rapidly in response to various stimuli (Moreno *et al.* 1994; Morley *et al.* 1997); an ability which may enable cells to adapt quickly to different physiological conditions. In human corporal cells, for example, the mean open time for Cx43 channels ranged from 0.43 to 5.25 seconds while the mean closed time was in the range of 0.21 to 1.49 seconds (Brink *et al.* 1997). At any one time, the proportion of channels open depends on the characteristics of the constituent connexin/s in conjunction with such variables as the calcium concentration, transjunctional voltage, phosphorylation state, cytoplasmic pH and levels of cAMP (Laing and Beyer, 1995). These are briefly discussed below.

In prolonged transjunctional voltage, where the voltage differs between two cellular interiors (Revilla *et al.* 1999), vascular smooth muscle cell Cx43 gap junction channels are prone to prolonged closures (Brink *et al.* 1996). Phosphorylation (Kwak *et al.* 1995a,b; Kwak and Jongsma, 1996) and changes in intracellular pH (Bennett *et al.* 1991; Morley *et al.* 1997; Francis *et al.* 1999) are known to be important regulators of gap junctional communication. Phosphorylation has been implicated in connexin trafficking, assembly, insertion into membranes, degradation and retrieval from the plasma membrane (Laird, 1996; White and Bruzzone, 1996; Stahl and Sies, 1998). It also influences the gating of gap junction channels, as do changes in intracellular pH and the concentration of calcium (Obaid *et al.* 1983). The effect phosphorylation exerts on junctional coupling is dependent on two factors: the type of connexin and the type of kinase involved (Kwak *et al.* 1995a,b; Kwak and Jongsma, 1996). Phosphorylation is associated with both increases and decreases in junctional coupling (Musil and Goodenough, 1991; Kwak and Jongsma, 1996; Hertlein *et al.* 1998), probably in consequence to conformational changes in the connexin/s that make up the channel. Changes in the phosphorylation state of Cx43, for example, appear to correlate with changes in the functional state of the gap junctions formed by this protein (Saez *et al.* 1993, 1997; Moreno *et al.* 1994; Lau *et al.* 1996; Warn-Cramer *et al.* 1998). Saez *et al.*

(1997) showed reduced functional coupling of neonatal rat cardiac myocytes after treatment with staurosporine, a protein kinase inhibitor. In contrast, Crow *et al.* (1990) demonstrated that in transformed mammalian fibroblasts, phosphorylation of Cx43 on tyrosine in the presence of *v-src* is correlated with inhibited communication.

With respect to the regulation of gap junctions and changes in pH, Morley *et al.* (1997) showed that the closure of Cx43 channels is significantly impaired by the truncation of the CT domain at amino acid 257, with a loss of pH sensitivity. This implies that the pH gating of Cx43 results from an interaction between the CT domain and the rest of the channel. Trexler *et al.* (1999) demonstrated that the CT domain of Cx43 enhanced the pH sensitivity of truncated Cx40, and that the CT domain of Cx40 restored the pH sensitivity of truncated Cx43. Similar results have also been obtained by Gu *et al.* (2000). Thus, the regulatory domain of one connexin can specifically interact with a channel formed by another connexin, which may be an important factor in the regulation of heteromeric channels (Section 1.1.5.2).

Functional differences between the various connexins are likely to be physiologically relevant (Peters, 1997) with respect to the selective permeabilities to small signalling and regulatory molecules, such as cAMP and cGMP (Spray and Bennett, 1985; Spray and Burt, 1990; Moreno *et al.* 1994; Veenstra *et al.* 1995; Nicholson *et al.* 2000). cAMP and cGMP play important roles in the mediation of the contractile process and can alter the functional status of gap junctions (Burt and Spray, 1988; Burt, 1990; Bevans and Harris, 1999). Peters (1997) and Brink (1998) have suggested that cAMP and cGMP are of a size, charge and conformation that may cause them to diffuse selectively and thus exert their effects differentially between cells with different connexin expression. Other studies however, have shown that as a whole, gap junction channels appear to be poorly selective (Tsien and Weingart, 1976; Beblo and Veenstra, 1997; Wang and Veenstra, 1997) allowing the diffusion of small solutes, including second messenger molecules, to occur relatively easily.

Other regulatory factors influencing gap junction function include the number, size and spatial distribution of gap junctions; these being important determinants of passive electrophysiological properties (Beblo *et al.* 1995). In cultured smooth muscle cells, gap junctions are numerous between cells with a synthetic phenotype but few are observed between contractile cells (Rennick *et al.* 1993). This may be important for vessel development, following injury, or in various vascular disease states (Christ *et al.* 1996). Increased expression of Cx43 has been observed in some forms of hypertension (Bastide *et al.* 1993; Gabriels *et al.* 1998) and atherosclerosis (Blackburn *et al.* 1995).

Recent advances in the cloning of connexins have made it possible to manipulate the regulation of cellular growth and neoplastic transformation associated with intercellular communication (Ruch *et al.* 1998). It has been proposed that the loss of gap junctional communication leads to uncontrolled cell growth (Pitts *et al.* 1988; Loewenstein and Rose, 1992). Support for this contention comes from a number of studies (Mehta *et al.* 1991; Zhu *et al.* 1991; Rose *et al.* 1993; Hirschi *et al.* 1996; Temme *et al.* 1997; Naus, 1998; Rae *et al.* 1998; Mehta *et al.* 1999). In general, an inverse relationship exists between cell growth and connexin expression and intercellular coupling (Bennett *et al.* 1991; Beyer, 1991; Loewenstein and Rose, 1992). In Cx32 (β_1) knockout mice, susceptibility to spontaneous and chemically induced hepatocarcinogenesis is increased (Temme *et al.* 1997). In mouse and human lung carcinoma cell lines, Ruch *et al.* (1998) have shown that expression of Cx43 is reduced compared to control. However, conflicting evidence is provided by Sia *et al.* (1999) in their study of gap junctional communication in quiescent mammary epithelial cells, where Cx43 expression was reduced but a high level of intercellular communication was maintained.

A number of other factors have been shown to influence gap junctional activity. These include: hormonal regulation (parathyroid hormone, isoproterenol, oestrogens),

anaesthetics (halothane, isoflurane), calmodulin binding, cadherins (the calcium-dependent cell-cell adhesion molecules), neurotransmitters (dopamine, acetylcholine and γ-aminobutyric acid), and selective pharmacological agents (heptanol, Gap 27 mimetic peptide, 18α- and 18β-glycyrrhetinic acid (GA) and tetraethylammonium) (Davidson *et al.* 1986; Peracchia, 1991; Schiller *et al.* 1992; Hertig *et al.* 1996; Proulx *et al.* 1997; Wang and Rose, 1997; Chaytor *et al.* 1998; Yamamoto *et al.* 1999; He and Burt, 2000).

1.1.6 Gap junctions and arterial function

Gap junctions enable coupling between smooth muscle cells, between endothelial cells and in some cases, between adjacent smooth muscle and endothelial cells (Rhodin, 1967; Somlyo and Somlyo, 1968; Gabella, 1981; Duling *et al.* 1991; Luff, 1991; Beny, 1999). Dye tracer studies performed in isolated arterioles indicate that in some vessels, gap junctional coupling between endothelial cells is more extensive than that between the underlying medial smooth muscle cells (Little *et al.* 1995b). Connections between endothelial cells and the innermost smooth muscle cells have been suggested to occur through discontinuities in the internal elastic lamina of smaller coronary arteries and arterioles, with heteromeric gap junctions (Section 1.1.5.2) sometimes being present at these sites (Severs, 1999). In such cases, communication occurs mainly in a unidirectional fashion from the endothelium to the smooth muscle layer (Little *et al.* 1995b; Beny, 1999), although bi-directional coupling is possible (Hill *et al.* 2001).

Whilst the full functional gamut of gap junctional coupling remains to be elucidated, it has been established that this coupling is important for the regulation and co-ordination of blood flow both within and into tissue beds. The localized application of various vasoconstrictor and vasodilator substances (acetylcholine and norepinephrine, for example) onto the arteriolar surface has been shown to induce both a local and a

generalized response (vasoconstriction or vasodilation) which is propagated proximally and distally along the vessel (Duling and Berne, 1970; Segal and Duling, 1986; Segal *et al.* 1989; Delashaw and Duling, 1991; Gustafsson and Holstein-Rathlou, 1999). This response is referred to as the conducted vasomotor response. However, not all substances that are capable of inducing local vasoconstriction or vasodilation initiate a propagated vascular response – sodium nitroprusside, for example (Segal *et al.* 1989).

The ability of local vasomotor responses (constriction or dilation) to be conducted relates to the stimulus (Delashaw and Duling, 1991), whilst the actual conduction of the response has been shown to be due to electrotonic transmission of the signal along the vascular wall through gap junctions between adjacent cells in some vessels (Segal and Duling, 1989; Xia and Duling, 1995; de Wit *et al.* 2000; Emerson and Segal, 2000). Basically, vasomotor responses may originate in either the endothelial or smooth muscle cell layer, with the expression of the final mechanical response depending on the specific signal transduction pathway involved (Hill *et al.* 2001).

The connexin knockout mice models have demonstrated the important role played by gap junctions in the vasomotor response, particularly in cardiac conduction and morphogenesis. Cx40-deficient mice have impaired conduction of endothelium-dependent vasodilator responses along intact skeletal muscle arterioles (de Wit *et al.* 2000), and cardiac conduction abnormalities (Kirchhoff *et al.* 1998; Simon *et al.* 1998). Cx40 has been proposed to be important in the heteromeric coupling of the endothelium and vascular smooth muscle (de Wit *et al.* 2000). Cardiac conduction abnormalities have also been observed in the Cx40 and Cx43 double-deficient knockout mice (Kirchhoff *et al.* 2000). In Cx45-deficient mice, vascular development is defective (Kruger *et al.* 2000; Kumai *et al.* 2000), whilst in the Cx37 knockout mice, females are infertile due to failure of intercellular signalling (Simon *et al.* 1997). Overall, these

results support the contention that connexins play a vital role in intercellular communication in the vasculature, and hence the conducted vasomotor response.

Antagonism of gap junction activity by pharmacological agents provides a useful tool for examining gap junction function although, to date, no agent has been shown to be universally effective. The specificity of action of these agents has been questioned and is indeed variable at best. The long chain alcohols, heptanol and octanol, for example, have been shown to block gap junction activity in a variety of tissues and cell cultures (Burt and Spray, 1989; Takens-Kwak *et al.* 1992; Bastiaanse *et al.* 1993; Christ *et al.* 1993b; Deutsch *et al.* 1995; Zhang *et al.* 1996; Largo *et al.* 1997; Proulx *et al.* 1997). Christ *et al.* (1993b, 1999), for example, have shown that alpha-adrenoceptor agonist stimulated contraction is inhibited by heptanol in rat aortic smooth muscle cells, whilst in the rabbit superior mesenteric artery, heptanol abolishes rhythmic contractile activity and inhibits contractions evoked by phenylephrine (Chaytor *et al.* 1997). In myoblasts, l-octanol and β-glycyrrhetinic acid inhibit gap junctional intercellular communication (Proulx *et al.* 1997). Inhibition of gap junction activities by β-glycyrrhetinic acid has also been observed in rat hepatocytes (Eugenin *et al.* 1998) and guinea-pig mesenteric arterioles (Yamamoto *et al.* 1999). In rabbit jugular veins, 18α-glycyrrhetinic acid blocks heterocellular endothelium-vascular smooth muscle coupling (Griffith and Taylor, 1999) and in immature rat irideal arterioles, it blocks spontaneous depolarisations and contractions (Hill *et al.* 1999).

Another putative gap junction antagonist, Gap 27, a synthetic peptide possessing sequence homology with the extracellular loop 2 of Cx43, has been shown to block the acetylcholine induced endothelium-dependent relaxation in rabbit mesenteric arteries (Chaytor *et al.* 1998; Dora *et al.* 1999; Hutcheson *et al.* 1999) and jugular veins (Griffith and Taylor, 1999). Other synthetic peptides consisting of regions of the connexin extracellular loop sequences have been shown to inhibit gap junctional activity between

smooth muscle cells in mesenteric arteries (Chaytor *et al.* 1997). Calero *et al.* (1998), for example, showed that a synthetic 17mer peptide formed by amino acids 271 to 287 of Cx43 interfered, in a sequence specific manner, with the acidification-induced uncoupling of Cx43. Similarly, dye coupling and dual whole-cell voltage clamp have been used to demonstrate, via the synthetic oligopeptide P180-195 which corresponds to a segment of the second extracellular loop of Cx43, selective inhibition of Cx43 gap junction channels (Kwak and Jongsma, 1999). The selective block of gap junction channel expression with connexin-specific antisense oligodeoxynucleotides has also been documented (Moore and Burt, 1994; Minkoff *et al.* 1999).

A variety of pharmacological agents (agonists) have been used to study the activation or promotion of gap junction activity. Two examples are the potassium channel inhibitors tetraethylammonium (TEA) and 4-aminopyridine (4-AP) (Jones *et al.* 1978; Kannan and Daniel, 1978; Peracchia, 1991). These agents are nonselective inhibitors of K^+ channels. In vascular smooth muscle, it has been suggested that tetraethylammonium induces rhythmic contractions by promoting gap junction activity (Takens-Kwak *et al.* 1992; Christ *et al.* 1996).

Thus, both *in vivo* and *in vitro*, diverse mechanisms of gap junction regulation exist that can vary between vascular beds and within vascular beds and for different connexins, that are susceptible to manipulation via a number of mechanisms.

1.2 Vascular Control Mechanisms

The control of blood flow in the vasculature is mediated by a variety of mechanisms, which can result in either arterial constriction or dilation. Such mechanisms include neural, humoral, myogenic, metabolic, endothelial-derived and physical factors (Wilson, 1979; Tortora and Grabowski, 1993; Bylund, 1995).

Differences in the activity of one or more of these mechanisms can result in specific control of different regions of the vasculature (Bylund, 1995), which can result in both systemic and localized control of blood flow and vascular resistance (tone) (Bevan and Purdy, 1973; Johnson, 1978; Burnstock and Ralevic, 1994). Control of vascular tone is important in the small arteries and arterioles, as they are the major resistance vessels, containing more than 50% of the total systemic vascular resistance (Berne and Levy, 1989; Sherwood, 1993). The integration of the vascular response occurs through electrical and mechanical coupling of vascular smooth muscle cells (Hirst and Edwards, 1989); factors that are moderated by the autonomic nervous system (Janssen and Smits, 2002).

Neurotransmitters released from the autonomic nervous system act on specific receptors located on the smooth muscle cells and/or endothelial cells to modify vascular tone (Todd, 1980; Bevan, 1988). Contraction or relaxation of many blood vessels occurs in response to either an increase or decrease in intracellular calcium (Walsh *et al.* 1995), initiated via various pathways and signalling mechanisms. However, nerve-mediated vascular responses vary between vascular beds and between different regions along the one blood vessel (Bylund, 1995), as well as within the same vascular bed during development (Sandow and Hill, 1999). Not only can signalling pathways vary, but the type of neurotransmitter released, their associated pre- and post-synaptic receptors and pathways associated with such receptors, and mechanisms of intracellular calcium, may also vary.

Thus, in order to understand the implications of variable gap junctional activity in the vasculature, an understanding and recognition of other factors associated with vascular control is required. One such entity that is relevant to this thesis, in terms of its influence on the vascular smooth muscle cells, is the neurovascular control provided by the endothelium.

1.2.1 Endothelium derived factors

The endothelium plays an important role in maintaining vascular resistance and blood flow in many vascular beds (Griffith and Henderson, 1989; Mombouli and Vanhoutte, 1999), by releasing a variety of vasodilator mediators, including nitric oxide, endothelium-derived hyperpolarizing factor (EDHF) and prostaglandins (Moncada *et al.* 1991; Fleming and Busse, 1999; Shimokawa, 1999). In some cases, this function may be hampered by the release of vasoconstrictors. Nitric oxide and EDHF activity (release) have also been linked to the activity of various neurotransmitters (Griffith *et al.* 1988; Toda and Okamura, 1998).

Nitric oxide is synthesized from L-arginine via the enzyme nitric oxide synthase (Palmer and Moncada, 1989; Vanhoutte and Feletou, 1998). In smooth muscle cells, nitric oxide mediates vasodilation via the activation of guanylate cyclase and cyclic 3', 5'-guanosine monophosphate (cGMP) signaling pathways (McDonald and Murad, 1995). In endothelial cells, activation of nitric oxide synthase, which is calcium / calmodulin dependent (Bredt and Snyder, 1992), may occur via receptor activation, by shear stress and/or aggregating platelets (Fleming and Busse, 1995; Arnal *et al.* 1999; Takamura *et al.* 1999). Nitric oxide synthase has been shown to co-localize with acetylcholine and vasoactive intestinal peptide (VIP) in parasympathetic nerves (Lumme *et al.* 1996; Yoshida and Toda, 1997), and to be present in sensory nerves (Lumme *et al.* 1996).

The labile substance EDHF (Feletou and Vanhoutte, 1999) induces hyperpolarization of smooth muscle cells due to an increase in potassium conductance (Komori and Suzuki, 1987), which in turn leads to reduced intracellular calcium and relaxation (Walsh *et al.* 1995). The exact nature and mechanisms of action of EDHF are unknown to date (Mombouli and Vanhoutte, 1997, 1999; Feletou and Vanhoutte, 1999). Although both EDHF and nitric oxide cause endothelium-dependent dilation, the

dilatory response is often tissue specific. In most vascular diseases, the vasodilator function of the endothelium is attenuated (Mombouli and Vanhoutte, 1999).

1.2.2 Endothelial influences in vascular disease

Furchgott and Zawadzki (1980) first demonstrated the role of the endothelium in the acetylcholine induced relaxation of isolated rabbit aorta where a factor, subsequently shown to be nitric oxide, caused relaxation of vascular smooth muscle (Ignarro *et al.* 1987; Palmer *et al.* 1987; Moncada and Palmer, 1991; Feletou and Vanhoutte, 1999).

Subsequently, it has been shown that the endothelium can control vascular smooth muscle tone primarily by the release of mediators of vasodilation (prostacyclin and EDHF, for example) in response to factors such as increases in the level of shear stress, neurotransmitters (such as acetylcholine and noradrenaline), endothelial produced autacoids, platelet products and coagulation derivatives (including serotonin and thrombin) and hormones (angiotensin II) (Vanhoutte and Miller, 1989; Vanhoutte and Boulanger, 1995; Shimokawa, 1998; Boulanger, 1999; Burnstock, 1999; Feletou and Vanhoutte, 1999; Fleming and Busse, 1999; Mombouli and Vanhoutte, 1999; Takamura *et al.* 1999).

In a number of blood vessels, selective α_2-adrenergic agonists can cause endothelium-dependent relaxations and stimulate post-junctional α_2-adrenoceptors on vascular smooth muscle cells to result in a contraction (Vanhoutte and Miller, 1989; Aburto *et al.* 1993). Although these receptors are more abundant in hypertensive blood vessels, the responses they evoke are very sensitive to functional agonists such as nitric oxide (Vanhoutte and Miller, 1989).

A summary of the effects of the main endothelium-derived vasodilators (nitric oxide, endothelium-derived hyperpolarizing factor and prostacyclin) and endothelium-derived contracting factors (vasoconstrictor prostaglandins, endothelin and reactive oxygen species) on vascular smooth muscle cells, is shown in Figure 1.6.

Figure 1.6 Activity of endothelial vasodilators and vasoconstrictors

Summary of the effects of endothelial-derived vasoconstrictors and vasodilators on the contraction and proliferation of the underlying vascular smooth muscle cells. The figure also demonstrates coupling between adjacent endothelial cells (1), between adjacent smooth muscle cells (2) and between endothelial and smooth muscle cells (3).

Modified from Shimokawa, 1999.

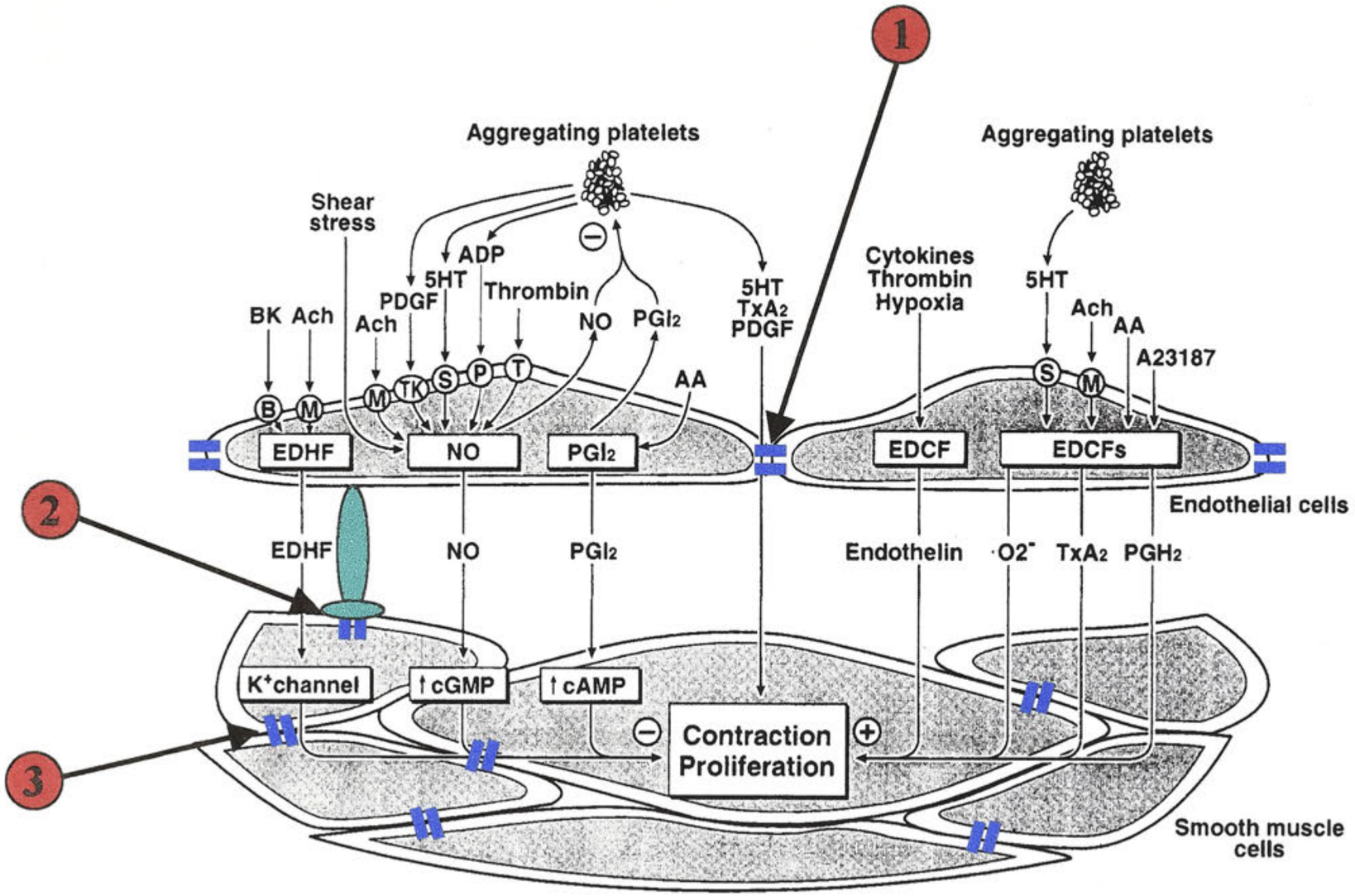
1
Aggregating platelets
Shear stress
ADP
5HT
PDGF
Thrombin
NO
PGI2
5HT
TxA2
PDGF
BK
Ach
Ach
AA
B
M
M
TK
S
P
T
EDHF
NO
PGI2
Aggregating platelets
Cytokines
Thrombin
Hypoxia
5HT
Ach
AA
A23187
S
M
EDCF
EDCFs
Endothelial cells
2
EDHF
NO
PGI2
Endothelin
·O2-
TxA2
PGH2
K+channel
↑cGMP
↑cAMP
Contraction
Proliferation
3
Smooth muscle cells

Under normal conditions, an accurate and balanced release of relaxing and contracting factors contribute to vascular perfusion (Tortora and Grabowski, 1993). In disease states however, such as hypertension, atherosclerosis, coronary artery disease, diabetes and heart failure, this balance is shifted (Sherwood, 1993). Arteries obtained from hypertensive animal models have demonstrated, for example, that endothelium-dependent vasodilation is reduced (Vanhoutte and Miller, 1989; Vanhoutte and Boulanger, 1995; Shimokawa, 1998), with the mechanisms underlying this dysfunction being variable between different types of hypertension.

Endothelial dysfunction in most arterial diseases is characterized by either decreased secretion of vasodilator mediators, increased production of endothelium-derived vasoconstrictors, and/or resistance of vascular smooth muscle to endothelium-derived vasodilators (Vanhoutte and Boulanger, 1995; Shimokawa, 1998; Mombouli and Vanhoutte, 1999). Endothelial dysfunction differentially affects shear stress- or hormone-induced endothelium-dependent vasodilation in vascular beds for two reasons: firstly, the distribution of endothelial receptors for acetylcholine, ADP, UTP, bradykinin, serotonin, vasopressin and catecholamines (stimulators of endothelial vasodilators) may vary, as well as the signal transduction pathway/s to which they are coupled, within an artery or be modified by the physiological conditions present in the artery (Furchgott, 1983; Vanhoutte and Miller, 1989; London and Safar, 1996; Mombouli and Vanhoutte, 1999).

1.3 Vascular Disease and Gap Junctions

1.3.1 Gap junctions in injury and vascular disease

Remodelling of vascular structures in response to haemodynamic signals associated with changes in blood flow readily occurs as a result of changes in a variety of physiological, developmental and pathological stimuli. Such changes are often

reflected by changes in the properties of the vascular connexins. Under selected disease processes that result in vascular cell injury and proliferation, such as many forms of hypertension, atherosclerosis and ischaemia, altered expression levels of various connexins, in particular Cx40 and Cx43, have been observed (Bastide *et al.* 1993; Peters *et al.* 1994; Kwak *et al.* 2002). As this thesis is primarily concerned with the role of connexins in vascular disease, a summary of the role of vascular connexins in disease processes will now be presented.

Vascular tissues are known to respond to changes in the mechanical loads imposed on them by changes in blood pressure (stretch) and thus, changes in blood flow (shear stress), with adjustments in vasomotor tone in the short term and then structural remodelling when these loads persist (De Paola *et al.* 1992; Langille, 1993; Davies, 1995; Hayoz and Brunner, 1997; Cowan *et al.* 1998; Mulvany, 1999). This transition involves the expression of various genes that affect cell proliferation, cell death, and connective tissue proliferation and reorganization (Sutcliffe and Davidson, 1990; Malek *et al.* 1993; Birukov *et al.* 1995; Davies, 1995; Hayoz and Brunner, 1997; Cowan *et al.* 1998; Mulvany, 1999). In vascular smooth muscle cells, stretch force has been shown to enhance cell proliferation, modulate cell phenotype (Birukov *et al.* 1995) and change the expression of contractile proteins (Reusch *et al.* 1996). Furthermore, Inoue *et al.* (1998) showed that stretch force on rat aortic smooth muscle cells enhanced cell-mediated low density lipoprotein oxidation via superoxide anion production; a potential mechanism in the theoretical link between hypertension and atherosclerosis (Kunsch and Medford, 1999).

Tissue remodelling due to changes in mechanical load has been shown to involve extensive changes in intercellular communication. Cowan *et al.* (1998) found that both mechanical and fluid shear stress caused increased expression of the gap junction protein Cx43 in vascular smooth muscle cells exposed to stretch, and in endothelial cells exposed to fluid shear stress. As discussed below, the smooth muscle cells are largely

responsible for effecting the remodelling responses by activation of the stretch-sensitive expression of connexins. Stretch-sensitive expression of connexins has been shown to be related to the activity of selected ion channels (Ou *et al.* 1997; Ziambaras *et al.* 1998); low dose progesterone, for example, induces the gravid rat myometrium to contract and hence, increases myometrial Cx43 expression (Ou *et al.* 1997).

Stretch-activated nonselective ion channels are present on arterial smooth muscle cells (Ohya *et al.* 1997; Setoguchi *et al.* 1997). The opening of these channels causes Ca^{2+} and Na^{+} influx and membrane depolarization, which contribute to the myogenic contractile response. Ohya *et al.* (1998) showed that activation of stretch-activated channels was enhanced in vascular smooth muscle in small mesenteric arteries from spontaneously hypertensive rats compared with control. It was suggested that this phenomenon may contribute to increased myogenic responses to mechanical stress in spontaneously hypertensive rats, as well as to the generation of hypertrophy and remodelling of arterial tissues in hypertension. Other mechanisms, however, may also contribute to this vascular remodelling.

Further changes in the activity of ion channels are illustrated by the activity of L-type Ca^{2+} currents which are present in normal vascular smooth muscle cells (Welsh *et al.* 1998) and have been shown to be larger in vascular smooth muscle cells from spontaneously hypertensive rats compared with responses in control rats (Rusch and Hermsmeyer, 1988; Ohya *et al.* 1993; Wilde *et al.* 1994). Other stretch-dependent mechanisms could include phospholipases A and C (Sadoshima and Izumo, 1993), voltage-dependent Ca^{2+} channels (including L-type Ca^{2+} channels) (Langton, 1993; Arii *et al.* 1999) and Ca^{2+}-dependent K^{+} channels (D'Angelo and Meininger, 1994; Dopico *et al.* 1994; Takamura *et al.* 1999).

The neural, hormonal and other control mechanism/s responsible for the altered activity of stretch-activated channels have yet to be elucidated. However, Ohya *et al.* (1997), in their study of spontaneously hypertensive rats (SHR), proposed three

possibilities: 1) that increased expression of the channel proteins would explain the increased opening (greater availability) of the stretch-activated channels; 2) that changes in the expressed phenotype of channel protein or its regulatory protein for stretch-activated channels may differ between the SHR and control rat; and 3) that differences in lipid characteristics of vascular smooth muscle cells between SHR and control rats may contribute to enhanced activation of stretch-activated channels in the hypertensive animal model (Tsuda *et al.* 1988a,b; Dominiczak *et al.* 1991; Andreeva *et al.* 1995). Indeed, an increased viscosity of the lipid bilayer in hypertension has been suggested to be responsible for the multiple abnormalities of membrane transport systems that exist in genetic (inherited) hypertension (Bohr *et al.* 1991b; Dominiczak *et al.* 1991).

Generally, in vascular smooth muscle cells, up-regulation of Cx43 gap junctions occurs after injury to arteries (Yeh *et al.* 1997; Severs, 1999) and in the early stages of atherosclerosis (Blackburn *et al.* 1995), where phenotypic transformation of the smooth muscle cells occurs concurrently. With further growth and accumulation of extracellular matrix material, the number of gap junctions decreases (Blackburn *et al.* 1995) in line with the reduced intercellular communication reported in cultured smooth muscle cells isolated from atherosclerotic lesions (Andreeva *et al.* 1995). The initial increase in gap junctional communication between vascular smooth muscle cells appears to be linked both to the phenotypic transition process itself and subsequent maintenance of the synthetic state (Blackburn *et al.* 1995; Severs, 1999).

Whilst the conditions of vascular cell coupling in culture often differ from that *in vivo* (Christ *et al.* 1996; Hill *et al.* 2001), such studies are useful for demonstrating some of the fundamental activities of vascular smooth muscle cell coupling in normal and diseased states. In cultured smooth muscle cells, immunodetectable Cx43 expression is high between synthetic phenotype cells but low between contractile cells (Rennick *et al.* 1993; Ko *et al.* 1999). Upregulation of Cx43 gap junctions *in vivo* has also been associated with the transition of contractile vascular smooth muscle cells to the synthetic

state (Rennick *et al.* 1993), which may be an important factor during atherosclerotic plaque formation, blood vessel development or following injury.

Endothelial responses to mechanical stress related to repair of injury, may also result in upregulation of Cx43 channels (Gabriels and Paul, 1998). In addition, this upregulation may facilitate communication with other Cx43-expressing cell types, such as monocytes and macrophages (Beyer and Steinberg, 1991; Polacek *et al.* 1993), polymorphonuclear leukocytes (Jara *et al.* 1995) and lymphocytes (Krenacs and Rosendaal, 1995).

The influence of growth factors and cytokines on the expression of connexins in cultured smooth muscle cells has emerged (Mensink *et al.* 1996; Yeh *et al.* 1996). Mensink *et al.* (1996) demonstrated that the magnitude and nature of the observed effects on the primary human smooth muscle cell gap junctions, were growth factor- and cytokine-specific; some causing a transient increase (basic fibroblast growth factor), a transient decrease (interleukin-6) or a persistent decrease (interferon gamma), in intercellular communication. This raises the possibility of co-operative interactions between extracellular signalling and direct intercellular communication in the modulation of vascular smooth muscle cell function in arterial disease and injury.

1.3.2 Hypertension

Hypertension has been identified as the most important risk factor in both coronary heart disease and cerebrovascular disease in human populations (World Health Organization, 2000). Chronically elevated blood pressure induces degenerative arterial disease predominantly affecting the heart, brain and kidneys (Sherwood, 1993; Tortora and Grabowski, 1993; Baldwin *et al.* 1999; Neutel *et al.* 1999). In humans, blood pressure over 120 / 80 (normal) is considered indicative of hypertension (Berne and Levy, 1989). A summary of the control mechanisms of blood pressure and the types and causes of hypertension is presented below.

1.3.2.1 Blood pressure control mechanisms

Regulation of blood pressure is complex, involving both multiple environmental and intrinsic (eg. genetic) factors. In both normal and hypertensive individuals, several interconnected negative feedback systems control blood pressure by adjusting cardiac output and peripheral vascular resistance. These systems include the cardiovascular centre in the medulla, which influences the parasympathetic and sympathetic divisions of the autonomic nervous system and other neural systems (baroreceptors and chemoreceptors), hormonal (epinephrine, norepinephrine, antidiuretic hormone, angiotensin II, atrial natriuretic peptide, histamine and kinins) and local (physical changes and chemical mediators) negative feedback systems (Tortora and Grabowski, 1993; Janssen and Smits, 2002).

1.3.2.2 Types and causes of hypertension

There are two types of hypertension: primary and secondary. In humans, about 90% of hypertensive cases are primary (essential) and idiopathic, with the remaining 10% being secondary to renal disease or less commonly, to narrowing of the renal artery by an atheromatous plaque (renovascular hypertension). Both essential and secondary hypertension may be either benign or malignant depending on the clinical course (Robbins and Kumar, 1987). A number of disease states also display hypertension, such as primary aldosteronism, Cushing's disease (hyperadrenocorticism) and pheochromocytoma.

Elevated blood pressure is usually caused by a combination of several abnormalities. Epidemiological evidence suggests that genetic inheritance, psychological stress, and environmental and dietary factors (excess body weight, increased salt and perhaps decreased calcium and potassium intakes) contribute to an increased prevalence of hypertension (Robbins and Kumar, 1987; Detweiler, 1989; Kreutz *et al*. 1992; Sherwood, 1993; Shimkets and Lifton, 1996; Redon, 2001).

Over fifty different genes have now been identified as having an important role in the regulation of blood pressure (Garbers and Dubois, 1999). Interestingly, males are at greater risk than females of developing hypertension as demonstrated by ambulatory blood pressure measurements in human patients (Wiinberg *et al.* 1995) and hypertensive rat models (Chen and Meng, 1991; Reckelhoff *et al.* 1998, 1999). Also, elderly people have a higher cardiovascular risk, which may be the result of age-associated functional and structural changes to the arterial tree (Lakatta and Mitchell, 1987; Bortolotto *et al.* 1999). Aging decreases the distensibility of large elastic arteries independently of blood pressure changes (Bortolotto *et al.* 1999).

Manipulating components of the mechanisms controlling blood pressure has generated a number of animal models of experimental hypertension. Based on their phenotypic traits, models exhibiting the following have been generated: elevated cardiac output (essential hypertension), renal hypertension, neurogenic hypertension, increased salt loading and reduced renal mass, increased adrenal steroids (aldosterone and corticosterone), angiotensin II stimulation, and genetic (hereditary) hypertension (Bohr and Dominiczak, 1991; De Paola *et al.* 1992, 1999; Johns *et al.* 1996). Computer models, together with animal experimentation, have also been used to elucidate the conceptual bases of hypertensive mechanisms (Guyton *et al.* 1988). Data obtained from studies on these models indicate that the most likely contributors to the primary defects in the pathogenesis of hypertension are alterations in neurohumoral regulatory mechanisms (sympathetic nervous system, renin-angiotensin system and endothelium-derived vasoactive factors), cellular growth control, steroid action, lipid metabolism, and cell membrane function (ion transport, signal transduction and cell calcium handling) (Zicha and Kunes, 1999; Cvetkovic and Sigmund, 2000).

The initial haemodynamic response to increased blood pressure is an increase in cardiac output (Benowitz and Bourne, 1989). Functional and morphological changes in the resistance vessels have been suggested to result from a chronic elevation in blood

pressure. Changes in vascular morphology such as hypertrophy of the muscular arterial walls, occur through vascular autoregulation, increasing the peripheral resistance to a level sufficient to maintain hypertension despite the cardiac output and extracellular fluid volume returning to normal (Detweiler, 1989; Haefliger *et al.* 1997b, 1992; Bohr *et al.* 1991a,b; Schiffrin and Deng, 1999).

Sympathetic innervation also contributes to the maintenance of elevated blood pressure (Folkow, 1978); adrenergic factors representing one of the mechanisms that determine variability in blood pressure (Koepke *et al.* 1988; Umemura *et al.* 1992; Lembo *et al.* 1998; Altman *et al.* 1999; Baldwin *et al.* 1999; Makaritsis *et al.* 1999a,b). The adrenergic receptors are G-protein coupled receptors located in the cell membranes of such tissues as the brain, kidney, sympathetic neurones and blood vessels (Tavares *et al.* 1996). Animal and human studies have demonstrated that sympathetic activation directly promotes cardiac and vascular alterations that are associated with hypertension, independently of the rise in blood pressure (Mancia, 1997). This has been shown to occur, for example, in the hypertrophication or remodelling process of the vascular smooth muscle cells (Heagerty *et al.* 1993; Giannattasio *et al.* 1995) during the development of hypertension.

Since hypertension is a complex multifactorial disease, specific causes of hypertension are difficult to determine. However, morphological changes occur in the small arteries of hypertensive animals and humans that have been positively correlated with elevated blood pressure (Cowan *et al.* 1998; Mulvany, 2002a).

1.3.2.3 Vascular morphology in hypertension

As mentioned above, vascular tissues respond to changes in blood pressure and flow by adjusting vasomotor tone. When these loads or variations there-of persist, structural remodelling often occurs. Fluid dynamic studies *in vitro* have shown a close relationship between flow characteristics and altered morphology and function (Davies

et al. 1986; De Paola *et al.* 1992, 1999; Malek *et al.* 1993; Burnstock, 1999; Mulvany, 2002b).

Although the determinants of remodelling in hypertensive vascular disease have yet to be completely characterized, examples found to date include growth factors and vasoactive peptides, such as angiotensin II (Chung and Unger, 1999; Romero and Reckelhoff, 1999; Kim and Iwao, 2000), endothelin (Schiffrin, 1995; Rosendorff, 1997), and pulse pressure (the difference between peak systolic and minimum diastolic pressure; Baumbach *et al.* 1991; Christensen, 1991; Baumbach, 1996; Schiffrin and Deng, 1999). Schiffrin and Deng (1999), for example, have shown changes in systolic, diastolic and mean blood pressure to be closely correlated with the remodelling present in the small gluteal subcutaneous arteries of hypertensive humans. Furthermore, a complex interaction between endothelin, angiotensin II, α_1-adrenergic agonists, calcium and other growth factors has been described (Rosendorff, 1996).

The morphological remodelling that occurs in small arteries of hypertensive animals and humans is well documented, and is largely attributable to changes in the vascular smooth muscle cells (Huttner *et al.* 1982; Lee *et al.* 1983; Mulvany and Aalkjaer, 1990; Heagerty *et al.* 1993). Hypertrophy of the vascular smooth muscle of the arterial wall leads to thickening of the vessel wall and a decrease in lumen diameter, resulting in an increase in the media to lumen ratio (Aalkjaer and Mulvany, 1995; Cooper and Heagerty, 1997; Sharifi *et al.* 1998; Schiffrin and Deng, 1999) and an augmented cross-sectional media area (Mulvany *et al.* 1996; Sharifi *et al.* 1998). Resistance to blood flow is subsequently increased, which contributes to the elevated peripheral resistance seen in essential hypertension (Folkow, 1982; Korner and Angus, 1992). Medial growth may also occur as a result of deposition of increased intercellular matrix due to a greater than normal collagen to elastin ratio (Sharifi *et al.* 1998).

The remodelling process involves the expression of many genes which influence cell growth, cell death, and connective tissue elaboration and reorganization (Sutcliffe

and Davidson, 1990; Malek *et al.* 1993; Davies, 1995) and consequently, extensive intercellular communication. Sutcliffe and Davidson (1990) have shown that *in vitro* stretching alone does not cause hypertrophy or hyperplasia of the vascular smooth muscle cells of the porcine aorta. In this study, transduction of mechanical force into elastin gene expression by vascular smooth muscle cells contributed to the development of a thickened arterial media, characteristic of hypertensive blood vessels.

In terms of intercellular communication, it has been suggested that in endothelial cells, hypertension may either increase the ratio of gap junctions to the lateral endothelial membrane surface area, or alternatively, may result in abnormal gap junction morphology (Huttner *et al.* 1982). Studies on vascular smooth muscle cells from hypertensive animals and humans have concluded that since the cells have abnormal contractile oscillations, hypertension alters gap junctional communication (Webb *et al.* 1992; Sunano *et al.* 1994; Watts *et al.* 1994; Watts and Webb, 1996). This altered gap junctional communication has reportedly been associated with increased abundance and size of gap junctions (Grunwald *et al.* 1982). It has been suggested that in hypertension gap junctional communication may be enhanced by one or more of the following: an increase in the transcription of genes encoding for connexins, an increase in the translation of connexin mRNA, an increase in plaque size or by increasing processes such as protein phosphorylation (Bennett *et al.* 1991).

Early in the hypertensive process, expression of the gap junction protein Cx43 in the vascular smooth muscle has been shown to increase (Grunwald *et al.* 1982; Peters *et al.* 1994), as does expression of Cx40 in the endothelium (Bastide *et al.* 1993). Recently, however, Rummery *et al.* (2002) demonstrated that in the SHR rat, the development of hypertension is accompanied by a decrease in Cx 40 expression.

A mediator of vascular smooth muscle hypertrophy, cAMP, has been shown to increase both conduction velocity and Cx43 expression via a signalling cascade (Peters *et al.* 1997). The expression of Cx43 is increased specifically in regions of blood

vessels where the blood flow becomes non-laminar and the endothelial cells are subjected to shear stress (Bastide *et al.* 1993; Gabriels and Paul, 1998; De Paola *et al.* 1999). Increased Cx43 plaque size has also been reported. It has been suggested that the localized release of basic fibroblast growth factor after endothelial cell injury may result in these increases in Cx43 expression (Lau *et al.* 1996; Gabriels and Paul, 1998). Haefliger *et al.* (1997a,b), De Paola *et al.* (1999) and Haefliger and Meda (2000) concluded that Cx43 expression, organization and function are regionally mapped to haemodynamic forces, and that localized mechanical forces (stretch and shear forces) induced by hypertension are major tissue-specific regulators of Cx43 expression.

Alterations in the structure and function of the vascular smooth muscle cells and associated gap junctions, in particular Cx43, are correlated with the increased peripheral vascular resistance characteristic of hypertension in animals and humans. The functional vascular changes that occur with elevated blood pressure are complex and variable.

1.4 Thesis Aims and Outline

1.4.1 General overview

The properties of gap junctions, together with those of the autonomic nervous system, pacemaker cells, myogenic mechanisms, and electrotonic current spread (hyperpolarizing and depolarizing mechanisms and their associated currents passing though gap junctions), confer physiological advantages throughout the vascular tree, in terms of adaptability and flexibility to both local and systemic influences (Christ *et al.* 1996). It is these attributes that most likely explain the observed diversity in the regulation and function of all vascular tissues throughout the cardiovascular system, in both homeostatic and disease states. The integration and co-ordination of responses amongst vascular smooth muscle cells are vital to the local modulation of vasomotor

tone, and to the maintenance of circulatory homeostasis (Simon, 1999; Brink *et al.* 2000).

A thorough knowledge of intercellular communication between vascular smooth muscle cells and, to a degree, between endothelial cells, is essential to understanding not only the pathogenesis of hypertension, but also a wide variety of other vascular pathologies. The nature and regulation of the gap junction channel proteins, the connexins, and the signals that pass between the cells, are of great interest as they represent potential targets for the modification of blood flow and for repair and growth of blood vessels.

The preceding literature survey reveals the need for experimental work to provide more information on the relationship between vascular structure and function. Although reliably identified, functional characterization of gap junction channels formed by connexins in vascular tissue is limited (Li and Simard, 1999).

Increased expression of the gap junctional protein Cx43 has been observed in hypertensive subjects (Blackburn *et al.* 1997; Haefliger *et al.* 1997a), although the cause and significance of this increase and its function in relation to hypertension, remains to be elucidated. Connexins have been shown to be important in the co-ordination of mechanical contraction of vascular smooth muscle cells (Segal and Duling, 1986; Segal 1994). It is possible that Cx43 has a role in the mediation and modulation of vascular tone in the resistance arteries. In fact, the increased expression of Cx43 in vascular smooth muscle cells during hypertension suggests that they are involved in the adaptive response to elevated blood pressure (Blackburn *et al.* 1997; Donaldson *et al.* 1997; Haefliger *et al.* 1997b). How the change in Cx43 expression participates in the adaptive process remains to be elucidated, as does the question of whether the increase in Cx43 expression is due to or causes, high blood pressure.

Further studies are currently required to determine the role of Cx43 in hypertensive states. The general aim of this study is to initiate studies in this area.

1.4.2 Thesis aims

The primary aim of this thesis was to determine the effect on blood pressure of selectively overexpressing Cx43 in blood vessels, specifically in the media. In order to achieve this, a DNA construct was made, containing a restricted portion of the SM22α promoter from the murine SM22α gene, to direct specific arterial expression in order to avoid overexpression of Cx43 in the heart, which has been shown to be lethal. Following the development of the DNA construct, a transgenic mouse line was produced by firstly, expressing the construct *in vitro* and then injecting into blastocysts, the construct with embryonic stem cells.

The SM22α / Cx43 transgenic mice would be expected to exhibit tissue specificity but not temporal specificity. This circumvents any congenital cardiac abnormalities caused by Cx43 overexpression, but will not prevent or ameliorate any developmental complications from occurring, both in the vascular smooth muscle and systemically. The physiological effect of overexpressing Cx43 or any connexin in the vasculature, apart from the heart, has not as yet been reported. Thus, the results obtained from this study using control and transgenic SM22α / Cx43 mice will enable some conclusions concerning the overexpression of Cx43 in the smooth muscle cells of the vasculature to be drawn. The rest of this thesis reports this work and is divided into:

The general methods (Ch. 2)

The design, development and evaluation of the DNA construct (Ch. 3)

The generation and assessment of the SM22α / Cx43 transgenic mouse (Ch. 4) and the final discussion is presented in Ch. 5.

Chapter 2 – Materials and Methods

A variety of molecular biology techniques were used in the design, construction and verification of the DNA construct for the generation of the transgenic mice. Evaluation of the construct prior to injection into murine blastocysts was performed using cell cultures of murine vascular smooth muscle cells and murine embryonic fibroblasts, which were transfected and analyzed by immunohistochemistry and fluorescence microscopy. Chimaeric mice were generated from embryonic stem cells and bred to produce germ-line transgenic mice. These mice were analyzed by PCR, immunohistochemistry, blood pressure measurements and Western blotting.

2.1 Recombinant DNA Techniques

The following experimental protocols were used in the design, construction and evaluation of the DNA constructs.

2.1.1 Oligonucleotide design and preparation

The design of the various oligonucleotides will be discussed in the relevant chapters. A summary of the general approach is presented here.

The sequences for the genes and cDNAs used in this thesis were downloaded from GenBank and converted into a text file suitable for reading on a Power MacIntosh (7200/90) computer with the Microsoft programme Word 6. The programmes Amplify (Bill Engels, University of Wisconsin, USA) and MacVector (Stratagene) were also used. After the region of interest of each gene was selected, it was imported into MacVector and a restriction enzyme analysis performed to obtain the restriction enzyme cutters and non-cutters list, and also an annotated sequence. Using Amplify, two

primers (one forward and one reverse) were designed, one on either side of the selected region, and subsequently checked for stability, primer dimer, loops, primability of match and fragment size. The primers were compared against the Genebank database to test their specificity (ie: their ability to anneal to other non-required sequences) before ordering their synthesis from Life Technologies (GIBCO-BRL), SigmaGenosys or the Biomolecular Resource Facility at the John Curtin School of Medical Research, Australian National University (ANU). A summary of the oligonucleotides used is presented in Table 2.1.

Primers were supplied in either ammonium hydroxide or as purified lyophilised powder. Purification of the former group of primers was carried out by n-Butanol precipitation. A small volume of the oligonucleotide (100 µl) was diluted in 1 ml butan-1-ol and mixed well by vortexing, before centrifugation for one minute at 13 000 rpm. The supernatant was removed and the tube inverted on a clean tissue to fully drain the remaining butan-1-ol. The pelleted oligonucleotide was then rinsed carefully with ether, centrifuged for 1 minute, the ether removed and the pellet dissolved in 100 µl of $T_{10}E_{0.1}$ (10 mM Tris-HCl, 0.1 mM EDTA pH 8). After spectrophotometric analysis, aliquots of the oligonucleotide (5 pmol / µl in 200 µl MilliQ water (UF final filter, Millipore) were made and stored at -20°C for future use.

Lyophilised primers were made up according to the manufacturer's directions by adding 0.5 ml $T_{10}E_{0.1}$ buffer to each and mixing well. After spectrophotometric analysis to check the supplied concentration, aliquots of the oligonucleotide were made (5 pmol / µl) and stored at -20°C for future use.

Primer Name	Gene or Plasmid	No. bases	Sequence	T_m
SM22ex1f	SM22α	24	AAG ACT AGT TCC CAC CAA CTC GAT	70
SM22ex1r	SM22α	24	CGT TTG TGG ACT GGA AGG AGA GTA	72
mSM22F2	SM22α	24	AGC CTT GCA AGA AGG TGG CTT GTT	72
mSM22F6	SM22α	24	CAA AAT ATG GAG CCT GTG TGG AGT	72
mSM22F7	SM22α	23	ACA TCA CTG CCT AGG CGG CCT TT	72
mSM22ex1fb	SM22α	23	GAC TAG TTC CCA CCA ACT CGA TT	68
CnxF	Cx43	24	TGG CTT GGG TTG AAA CTG CCT TAT	70
CnxR	Cx43	24	TCC TCC ACA ATC GAT TGG CAG CTT	72
mCnx43R	Cx43	24	GAT ATT CAG AGC GAG AGA CAC CAA	70
CxF	Cx43	24	AAA CGT CTG CTA TGA CAA GTC CTT	68
Cx43F	Cx43	24	GAG ATG CAC CTG AAG CAG ATT GAA	70
Cx43R	Cx43	24	GAT GTT CAA AGC GAG AGA CAC CAA	70
Cx43R2	Cx43	24	GAG CAG CCA TTG AAG TAG GCG TAT	72
Cx43R3	Cx43	24	CGA TGG CTA ATG GCT GGA GTT CAT	72
mCx435′R	Cx43	23	CAT GTC TGG GCA CCT CCT AAG AA	70
pBi5F	pBi5	22	TTC GAG CTC GGT ACC CGG GGA T	72
pBi5R	pBi5	23	CAA GGG ACA TCT TCC CAT TCT AA	66
HOTT3	pBSKSII-	23	CGC GCA ATT AAC CCT CAC TAA AG	68
HOTT7	pBSKSII-	23	ACG ACT CAC TAT AGG GCG AAT TG	68

Table 2.1 Summary of oligonucleotides used in the present study

2.1.2 The polymerase chain reaction (PCR)

In order to amplify each DNA fragment, PCR was performed in a capillary tube cycler (Corbett Research) in a total reaction volume of 20 µl containing 5 µl of the DNA sample (diluted as necessary), 2 µl of 10 x PCR buffer (Promega), 0.8 µl of each deoxynucleotide triphosphate (dNTP; 5 mM of each dATP, dTTP, dCTP and dGTP), 1.0 µl of each primer (5 pmol / µl) and 1 U of *Taq* DNA polymerase (Promega). The PCR reaction mixtures were pipetted into positive displacement pipette tips using a Cycle Prep automatic pipetter, and the ends either plugged or heat-sealed. In summary, the PCR cycling conditions used to amplify each fragment of DNA were: 94°C for 3 minutes for DNA denaturation (1 cycle), then 10 seconds for annealing followed by the appropriate extension time for each DNA fragment at 72°C (35 to 38 cycles). The final cycle was 72°C for 5 minutes followed by 25°C for 5 minutes. Annealing temperatures and extension times were determined by the melting temperatures of the individual primer pairs and predicted fragment lengths. The PCR conditions for specific primer pairs are listed (Table 2.2).

2.1.3 Restriction endonuclease digests

Restriction endonuclease digests (in a 20 µl total volume) were performed to verify the plasmids and the DNA constructs at each stage of their construction, and prior to larger restriction digests (> 200 µl total volume) as part of the cloning process for each construct. Each restriction digest was carried out in the appropriate buffer (NewEnglandBiolabs (NEB)) (see Table AI.1) for each enzyme (NEB, Pharmacia or Promega).

For each digest, the mix consisted of 2 µl of 10 x NEBuffer, 2 µl of 1 mg / ml acetylated-bovine serum albumin (BSA), 100 ng of DNA or plasmid and MilliQ water to a total volume of 20 µl. To this mix, 0.5 µl (> 10 000 units / ml) to 1.0 µl (< 10 000

Primer Pair	Gene / Plasmid	Annealing temperature T_A (°C)	Extension Time (s) / (mins)	Predicted Fragment size (kb)
SM22ex1f SM22ex1r	SM22α gene	65	30 s	0.493
SM22ex1f HOTT3	SM22α/pBs KSII-	63	30 s	0.586
SM22ex1r HOTT3	SM22α/pBs KSII-	64	30 s	none
HOTT3 HOTT7	SM22α/pBs KSII-	64	30 s	0.635
CnxF CnxR	Cx43 gene	65	30 s	1.390
CnxF CxR2	Cx43/pBs KSII-	65	2	1.018
CnxF HOTT3	Cx43/pBs KSII-	65	2	1.390
HOTT3 HOTT7	Cx43/pBs KSII-	65	2	1.480
HOTT7 CxR2	Cx43/pBs KSII-	65	2	1.268
CnxF Cx43R3	Cx43/pBi5	65	2	1.0 kb
mSM22F2 mCx435'R	EGFP/Cx43/pBi5	65	1.30	0.662
SM22ex1f pBi5R	SM22α/Cx43/ pBs KSII-	61	2	1.987
SM22ex1f pBi5F	SM22α/Cx43/ pBs KSII-	61	2	none
SM22ex1f Cx43R2	SM22α/Cx43/ pBs KSII-	65	2	1.47
SM22ex1f CnxR2	SM22α/Cx43/ pBs KSII-	65	2	1.3
SM22ex1f mCnx43R	SM22α/Cx43/ pBs KSII-	65	2	1.334
SM22ex1f HOTT7	SM22α/Cx43/ pBs KSII-	63	2	3.0

Primer Pair	Gene / Plasmid	Annealing temperature T_A (°C)	Extension Time (s) / (mins)	Predicted Fragment size (kb)
mSM22F2 mCx435'R	SM22α/ Cx43/ pBs KSII-	65	2	0.633
mSM22F6 mCx435'R	SM22α/ Cx43/ pBs KSII-	65	2	0.374
mSM22F7 mCx435'R	SM22α/ Cx43/ pBs KSII-	65	2	0.273
mSM22F6 pBi5R	SM22α/ Cx43/ pBs KSII-	61	2.20	1.699
mSM22F7 pBi5R	SM22α/ Cx43/ pBs KSII-	61	2.20	1.598
CnxF pBi5R	SM22α/ Cx43/ pBs KSII-	61	2.20	1.469
Cx43F pBi5R	SM22α/ Cx43/ pBs KSII-	61	2.20	0.9

Table 2.2 PCR conditions for specific primer pairs

units / ml) of the appropriate enzyme was added. The restriction digest was mixed and incubated for 1 hour at the appropriate temperature for each enzyme according to the NEBiolab catalogue. For larger restrictions used in cloning, the amounts of all reagents were increased proportionally and the incubation time/s increased as determined by regular monitoring on a 1.5 % agarose gel (see Section 2.1.4).

2.1.4 Analytical and preparative separation of DNA fragments

In order to visualize the result either of a restriction digest, PCR, or the purity and concentration of DNA present, gel electrophoresis was carried out at room temperature on 1.5% agarose gels. Each gel was prepared by dissolving 1.5 g of agarose (Difco Laboratories) in 100 ml TAE (40 mM Tris-acetate and 2 mM EDTA pH 8.0) and allowing it to cool to 65°C in a water bath before pouring into a prepared gel tray. Once set, the gel was submerged in TAE in a Biorad Mini-Submarine electrophoresis tank and electrophoresis conducted at 80 V for 1 hour. For cloning purposes, the smaller Pharmacia electrophoresis tank was used and 1.0% agarose gels (0.6 g agarose in 60 ml TAE) made before electrophoresis at 60 V for 2 to 3 hours.

To each 20 µl sample, 5 µl of 5 x loading dye (5 ml 1 M Tris-HCl pH 8.0, 20 ml 0.5 mM EDTA, 7.5 g Ficoll 400, 1 g N-lauryl sarcosine and 50 mg dye (bromophenol blue, xylene cyanol, for example)) was added. The sample was then mixed by shaking and incubated for 5 minutes in a 65°C water bath before loading onto a prepared agarose gel. Appropriate volume adjustments were made for the larger samples loaded for gel purification. Lambda phage DNA digested with *Acc*I or *Hind*III or pTz (Biorad) restricted with *Alu*I (pTz / *Alu*I) were run in parallel with the samples to serve as molecular size markers (see Table AI.2) and to enable quantitative analyses. The λDNA *Eco*RI / *Hind*III (GIBCO-BRL, LifeTechnologies) marker was also used later in the study (see Table AI.2). After electrophoresis, the gel was stained with the fluorescent dye ethidium bromide (500 ml TAE and 50 µl ethidium bromide) for 15 minutes, and

the bands visualized under UV light and photographed with either a NovaLine Gel Documentation System or the SpeedLight Platinum Gel Documentation System (Lightools Research).

2.1.5 Gel purification of restricted DNA fragments

Gel purification of restricted DNA was undertaken to isolate the required fragment of DNA, and to remove unwanted DNA fragments and restriction enzymes. After the restriction step was complete, loading dye was added (at 5 µl / 20 µl mix as described previously), and the whole mix heated in a 65°C water bath for 5 minutes before loading onto a gel (1% agarose / 0.001 M guanosine) prepared for a Pharmacia tank. Transillumination of gels can damage the DNA present and compromise subsequent manipulations (Hartman, 1991; Maueler *et al.* 1994), however the incorporation of 1 mM guanosine in agarose gels has been shown to have a strong, albeit not absolute, protective effect on DNA against UV irradiation (Grundemann and Schomig, 1996).

A small amount (5 µl) of an appropriate marker was also added to one lane of the gel before electrophoresis at 60 V for 2 to 3 hours. Gels were stained in fresh ethidium bromide solution for 15 minutes before being viewed under UV light, quickly photographed and the appropriate band removed using a new scalpel blade. The removed gel band was weighed before using the QIAquick Gel Extraction Kit (Qiagen), as the maximum amount of gel slice per QIAquick column is 400 mg. A small amount of the final eluted sample (1 µl with 9 µl MilliQ water and 2.5 µl loading dye) was subsequently run on a 1.5 % agarose gel to ascertain its purity and for quantitation purposes.

2.1.6 DNA concentration by ethanol precipitation

DNA products were concentrated, as necessary, using ethanol precipitation. Briefly, the volume of each sample was estimated before adding 0.1 volume of 3 M sodium acetate (NaOAc, pH 7.5), followed by 2 volumes of ice-cold 100% ethanol. The mixture was vortexed and placed in a -20°C freezer for 3 hours (or immersed in liquid nitrogen for 5 seconds). After centrifuging at 14 000 rpm for 30 minutes at 4°C, all traces of the supernatant were removed and the pellet rinsed with 1 ml 70% ethanol before further centrifugation at 4°C for 2 minutes. The supernatant was removed and the tube inverted on a tissue to dry. The pellet was resuspended in $T_{10}E_{0.1}$ and stored at 4°C. The new DNA concentration was determined by spectrophotometric analysis at OD_{260} (Sambrook *et al.* 1989).

2.1.7 Dephosphorylation of vector DNA

Dephosphorylation was undertaken on complementary ends (also called compatible cohesive ends) of vector DNA using calf intestinal alkaline phosphatase (CIAP; Boehringer-Mannheim) to catalyze the removal of 5′-phosphate residues from the ends of the vector to prevent self-ligation.

After the quantity of number ends (pmol) per mass (µg) of linear DNA was calculated, the dephosphorylation reaction was set up as follows: to the DNA (restriction digest to 200 µl total volume with MilliQ water), CIAP was added at 1 U per 1 - 2 pmol ends and the mix vortexed before being placed in a 37°C water bath for 15 minutes. The same quantity of CIAP was added again and the mix subsequently incubated at 55°C for 15 minutes. Afterwards, 0.5% sodium dodecyl sulphate (SDS), 5 mM ethylenediaminetetraacetic acid (EDTA, pH 8) and proteinase K (100 µg / ml; to digest the CIAP) were added and the mix vortexed before incubation in a 55°C water bath for 30 minutes. The mix was allowed to cool to room temperature and diluted to 300 µl with $T_{10}E_{0.1}$ (pH 8) prior to phenol extraction to purify the dephosphorylated DNA.

To a 300 µl dephosphorylation mix volume, 150 µl phenol was added and the mix vortexed for 30 seconds before centrifugation at 13 000 rpm for 5 minutes. The upper aqueous supernatant was transferred to a new 1.5 ml eppendorf tube and 150 µl of isoamyl alcohol (IAC) added to remove any remaining phenol. After vortexing the mix for 30 seconds, followed by centrifugation at 13 000 rpm for 5 minutes, the supernatant was transferred to a new 1.5 ml eppendorf tube. Subsequent ethanol precipitation (see Section 2.1.6) removed salt contaminants, and agarose gel electrophoresis (using 1 µl of the sample with 9.0 µl MilliQ water and 2.5 µl loading dye) was undertaken as described previously.

2.1.8 Blunt ending of DNA fragments with Klenow

The Klenow fragment is a proteolytic fragment of *Escherichia Coli* DNA Polymerase I which retains polymerization and 3′ to 5′ exonuclease activity, but has lost 5′ to 3′ exonuclease activity (Sambrook *et al*. 1989). Thus, the Klenow enzyme can be used to fill-in 3′ recessed ends remaining after enzyme restriction to make restriction sites with incompatible ends blunt and hence complementary. Each reaction was performed in the restriction eppendorf tube (volume 60 µl) using the restriction buffer already present. The buffer was supplemented with 5 mM $MgCl_2$, 33 µM of each dNTP and 1 unit Klenow per µg DNA. The mix was incubated at 25°C for 15 minutes and the reaction stopped by the addition of EDTA to 10 mM final concentration, and heating at 75°C for 10 minutes.

2.1.9 Purification of products

Occasionally, purification of products from the various molecular cloning procedures (eg. PCR, ligation reactions, and restriction digests) was performed using the High Pure PCR Product Purification Kit (Boehringer-Mannheim), according to the manufacturer's instructions. The products were always checked by agarose gel electrophoresis afterwards.

2.1.10 Ligation of restriction fragments into vector DNA

In a typical ligation mix, DNA insert, plasmid vector and 1 x T4 DNA Ligase buffer (50 mM Tris-HCl pH 7.8, 10 mM $MgCl_2$, 10 mM DTT, 1 mM dATP, 25 μg / ml of BSA) were added to a volume of MilliQ water to make the final calculated total volume, then mixed before adding 1 μl T4 DNA Ligase (NEB). The ligation was again mixed thoroughly before incubation at room temperature for 30 minutes, followed by overnight incubation at 16°C.

The ligated DNA was transformed into competent *E. coli* cells as described in Section 2.1.11.

2.1.11 Transformation and selection of bacterial clones

Electroporation was used to transform electrocompetent *E. coli* TOP10F′ cells, with ampicillin as the marker to indicate which populations were transformed.

(a) Preparation of electrocompetent cells

Electrocompetent cells were prepared according to standard techniques. Briefly, a 1 in 100 of a fresh overnight culture of TOP10F′ bacterial cells was diluted in 1 L of liquid medium (Luria Broth or LB; bacto-tryptone 5 g, bacto-yeast extract 2.5 g (Difco Laboratories) and NaCl 5 g in 500 ml MilliQ water; adjusted to pH 7 with 5 mM NaOH

before autoclaving at 120°C for 20 minutes). Ampicillin (Sigma; 50 μg / ml) was added to cooled LB agar (50°C) or LB to select and maintain recombinant bacterial strains.

The cells were grown at 37°C with vigorous shaking and the growth of the culture determined by monitoring the OD_{600} regularly until an OD_{600} of 0.5 to 1.0 was attained (the desired concentration; about 4 hours). After harvesting the cells by chilling the flask on ice for 15 - 30 minutes, the cells were centrifuged at 1 000 g at 4°C. The supernatant was removed and the pellet resuspended in a total volume of 1 L cold MilliQ water before further centrifugation.

After removal of the supernatant, the pellet was resuspended in 0.5 L cold MilliQ water, re-centrifuged, and resuspended in 20 ml cold water before centrifuging again. Again the supernatant was removed, and the pellet resuspended in a final volume of 2 to 3 ml of cold 10% glycerol in MilliQ water. The solution was aliquotted into pre-cooled sterile 1.5 ml eppendorf tubes in 40 μl lots and stored at –70°C.

(b) Preparation of L-ampicillin agar plates

The L-ampicillin (L-amp) agar plates were prepared as follows: liquid medium (400 ml of Lauria Broth (LB)) was prepared and 6.0 g of bacto-agar (Difco Laboratories) added before autoclaving at 120°C for 20 minutes. The media was swirled gently to distribute the melted agar evenly throughout the solution before cooling to 50°C in a water bath. Ampicillin (800 μl of 50 mg / ml) was then added and about 20 ml of the media poured into each petri dish. Bubbles forming on the newly poured L-amp plates were removed by flaming the surface with a Bunsen burner before solidification of the agar. When the plates were set, they were air-dried for 60 minutes in a sterile laminar flow hood and stored inverted at 4°C.

(c) Electroporation and plating

Prior to electroporation, an eppendorf tube containing 40 µl of TOP10F′ cells was removed from the -70°C freezer and placed on ice to thaw. Then 1 µl of the ligation mix was added to the tube and the contents mixed thoroughly. The mixture was transferred into an ice-cold 0.2 cm micro-cuvette (Biorad) and electroporated (2.5 kV, 25 µF and 200 ohms, with a resultant field strength of 12.5 kV / cm) with a Biorad Gene Pulser. After pulsing, the cuvette was flushed with 1 ml of cool LB and the transformed cells transferred to a 15 ml Falcon tube to recover for one hour at 37°C with shaking at 250 rpm. Several dilutions of this culture were plated onto L-amp agar plates using a sterile glass spreader to ensure an even distribution, and then dried before incubation at 37°C overnight. In order to enhance potential growth, the cells were sometimes pelleted by centrifugation at 2 500 g for 3 minutes (after shaking), the supernatant removed and the cells resuspended in 300 µl of LB before plating out onto 2 or 3 L-amp plates.

2.1.12 Screening cloned inserts

The cloned inserts were screened by one or more of the following: α-complementation (blue / white colony screening), cracking or PCR.

(a) α-complementation (blue / white colony screening)

α-complementation is commonly used to identify bacterial colonies that contain recombinant plasmids. Deletion mutants of the operator-proximal segment of the lacZ gene of *E. coli* are complemented by β-galactosidase-negative mutants that have an intact operator-proximal region (Ullmann *et al.* 1967). The Lac^+ bacteria that result from α-complementation form blue colonies in the presence of the chromogenic substrate 5-bromo-4-chloro-3-indolyl-β-D-galactoside (X-gal). However, insertion of a fragment of foreign DNA into the multiple cloning site of the plasmid results in the production of an amino-terminal fragment that is not generally capable of α-

complementation (Sambrook *et al.* 1989). Thus, bacteria carrying recombinant plasmids usually form white colonies. However, some blue colonies can have an insert if it is in frame with the lacZ gene and is usually < 1 kb (Matthaei, *pers com*).

For blue / white screening of vectors capable of α-complementation (eg. pBluescript (Stratagene)), 40 µl of a stock solution of isopropylthio-β-D-galactoside (IPTG; 1 M = 238 mg / ml in water) and 10 µl of a solution of X-gal (10% in dimethylformamide) per 20 ml L-amp plate were mixed, spread evenly over the entire surface of the plate using a sterile glass spreader, and allowed to dry prior to plating the transformed cells. L-amp plates were used to maintain antibiotic selection.

(b) Colony cracking

All transformants were analyzed by colony cracking. This method enables the size of the plasmid in individual colonies of transformed cells to be estimated quickly and simply by gel electrophoresis of total colony lysates.

A gel of 1% agarose in TAE buffer (without ethidium bromide) was prepared and when set, placed in a Biorad Mini-Submarine electrophoresis tank to equilibrate with the TAE in the chamber before the samples were loaded. A well-isolated colony (white if screening) was sampled with a sterile toothpick, replicated onto a fresh L-amp agar plate, and resuspended in 25 µl of cracking solution (MilliQ water, 50 mM NaOH (fresh), 0.5% SDS, 5 mM EDTA, 10% glycerol and 0.01% bromocresol green). This procedure was repeated for each colony sampled after which, the replica plate was placed in an incubator at 37°C until the colonies were about 1 to 2 mm in diameter.

All of the cracking samples were subsequently placed in a water bath at 65°C for 30 minutes, allowed to cool to room temperature and loaded onto the prepared electrophoresis gel. Positive clones were identified by their increased band size when compared with uncut vector and with a Supercoiled DNA ladder (GIBCO-BRL, Life Technologies; 0.25 µg / µl).

(c) PCR

All possible positives were identified (pen marked by hand) on the replica plate and sampled with a sterile toothpick as previously. The toothpicks were then twirled in the appropriately labelled eppendorf tube containing 100 µl MilliQ water. All samples were thoroughly mixed and heated for 5 minutes at 65°C; 5 µl of each sample was used in a PCR with the selected plasmid primers to determine the presence and size of the required insert. PCR positives were re-analyzed with gene specific primers, again under standard conditions, to identify whether or not the inserts present were the correct ones for the DNA construct.

A combination of gene specific and plasmid primers was used to deduce the orientation of the insert in the vector. PCR positives thus identified were selected and grown overnight in liquid culture as described below (Section 2.1.13) before purification using the QIAprep Spin Miniprep Kit (Qiagen) according to the manufacturer's directions. This enabled subsequent verification of positive clones by restriction enzyme digestion and sequencing.

2.1.13 Plasmid preparation

Overnight cultures of 3 to 5 positives (Section 2.1.12) were prepared using, for each positive, 2 ml of L-broth and 4 µl (50 mg / ml) of ampicillin in a labelled Falcon tube (replicates of each plasmid were usually made). The tubes were mixed well by hand before the positive colonies from the replica plate were sampled with sterile toothpicks; each of which was swirled in the appropriately labelled liquid media prior to all tubes being placed in an incubator at 37°C with vigorous shaking (280 rpm) overnight.

Each plasmid was purified according to the manufacturer's instructions for the QIAprep Spin Miniprep Kit. To estimate the plasmid yield, 1 µl of the eluted DNA (with 9 µl MilliQ water and 2.5 µl loading dye) was electrophoresed on a 1.5% agarose

gel, with standard markers, and visualized under UV light. The remainder of each overnight culture (850 µl) was pipetted into an appropriately labelled sterile tube and 150 µl of sterile glycerol added to each to form glycerol cultures. The tubes were thoroughly mixed by vortexing and stored at –70°C.

For larger plasmid preparations, the EndoFree Plasmid Maxi and Mega Kits (Qiagen), and the QIAfilter Maxi Kit (Qiagen) were used, according to the manufacturer's instructions.

2.1.14 DNA sequencing

Dye Terminator Sequencing (ABI PRISM BigDye Terminator Cycle Sequencing Ready Reaction Kit, PE Applied Biosystems) was used for DNA sequencing in a capillary cycler. The 20 µl reaction mixture consisted of Terminator Ready Reaction Mix (8 µl), DNA (200 to 500 µg), primer (3.2 pmol / µl) and MilliQ water to 20 µl total volume. The mix was pipetted into a capillary tip and capped. The cycling conditions were as follows: 25 cycles of DNA denaturation for 30 seconds at 96°C, annealing for 15 seconds at 50°C and extension for 4 minutes at 60°C, and then 1 cycle of 25°C for 5 minutes.

Excess dye terminator was removed before sequencing by ethanol / sodium acetate extraction and the DNA concentrated as follows. To a 1.5 ml eppendorf tube, 2.0 µl 3 M sodium acetate (pH 4.6) was added followed by 50 µl of 95% ethanol. The contents of each extension reaction were then pipetted into the appropriately labelled tube, mixed thoroughly and vortexed before leaving at room temperature (to remove unincorporated nucleotides and dye terminator) for 10 minutes to precipitate the extension products. After centrifugation for 15 to 20 minutes at 13 000 rpm, the supernatants were aspirated and the pellets rinsed with 250 µl of 70% ethanol before briefly vortexing and centrifugation for 5 minutes at maximum speed. The supernatants

were aspirated and the pellets dried in a vacuum centrifuge for 10 to 15 minutes or until dry.

DNA products from the dye terminator cycle reaction were sequenced by the Biomolecular Resource Facility, Australian National University. Results were imported into a file suitable for reading on a MacIntosh computer with the program MacVector. The sequence of bases was checked against known sequences of the gene insert and the plasmid.

2.2 Generation of the DNA Construct

During the course of this study, four DNA constructs were generated: SM22α / Cx43 / pBs KSII- (Chapters 3-5), and a smooth muscle specific construct (SM22α / pTetOn) and two temporal specific constructs (Cx43 / pBi5; EGFP / Cx43 / pBi5) (see Appendix II). The design, analysis and use of each construct is presented in the appropriate chapter. This Chapter deals solely with the SM22α / Cx43 / pBs KSII- construct.

2.3 Evaluation of the DNA Construct in Cell Culture

Evaluation of the construct was performed using cell cultures of murine aortic smooth muscle cells and fibroblasts (murine embryonic feeder cells), and immunohistochemistry.

2.3.1 Dissection and culture of aortic smooth muscle cells

Six adult mice, of either sex, were anaesthetized by ether inhalation and killed by cervical dislocation. Each thoracic aorta was excised and placed in a dish containing Dulbecco modified Eagles medium (DMEM; Sigma), with 5% foetal calf serum (FCS), 3.7 g / L $NaHCO_3$, 6 mg penicillin, 10 mg streptomycin and MilliQ water; pH 7.4 and

filter sterilized (complete medium). Adipose and connective tissues were removed and the aorta placed in a fresh dish of FCS / DMEM. The aorta was then cut open to produce a flat sheet and the endothelial cells rubbed off with a sterile cotton bud. The smooth muscle cell layers were subsequently dissected from the adventitia and washed in incomplete medium (DMEM; no FCS) before digestion with collagenase II (3 mg / ml) / DMEM (mixed by gentle trituration to avoid air bubbles forming) in a 37°C water bath, with shaking, for 10 minutes. The supernatant was discarded and a second digestion undertaken with collagenase II (3 mg / ml) and elastase II (3 mg / ml), in a 37°C shaking water bath for 20 minutes. The supernatant was collected into a tube containing 500 µl FCS.

The double enzyme digestion was repeated, again with careful trituration, with a 15 minute incubation time and the supernatant collected into a second tube of FCS. Both tubes were then centrifuged at 1 000 rpm for 3 minutes and the supernatants subsequently discarded. The cells were resuspended in 1 ml of complete medium (FCS / DMEM) by gentle trituration.

Cell viability and number were checked by mixing a small aliquot (10 µl) of the cells with trypan blue (0.01% in distilled water) and loading 10 µl onto a Neubauer haemocytometer. The cells were subsequently diluted and seeded onto glass coverslips previously placed in the bottom of the 24 well plates (500 µl / well; at an estimated 10^6 cells per well) and incubated in complete medium at 37°C in an incubator with an atmosphere of 5% CO_2 in air. After leaving the plates for 72 hours to allow the cells to settle on the coverslips, the culture medium was changed daily. Cells were grown for 6 to 7 days to a confluence level of approximately 60%, before transfection with Lipofectamine Plus (1 mg / ml; GIBCO-BRL, Life Technologies).

This method was later modified as follows as it was found to enhance cell growth: briefly, the peeled smooth muscle cells were washed with Hanks' Solution (800

mg NaCl, 35 mg $NaHCO_3$, 40 mg KCl, 6 mg KH_2PO_4, 6.5 mg Na_2HPO_4, 100 mg D-Glucose and 1 mg Phenol Red; in 100 ml MilliQ water) without calcium and magnesium, to wash off the 5% FCS in DMEM. Digestion with collagenase II (3 mg / ml diluted in Hanks' Solution) in fresh Hanks' Solution at 37°C in a shaking water bath for 10 minutes followed. The solution and tissue were gently triturated, and the supernatant aspirated and discarded before triple enzyme digestion with collagenase II (3 mg / ml), elastase II (3 mg / ml in Hanks' Solution) and trypsin (2 mg / ml) in Hanks' Solution. The mix was incubated for 10 to 15 minutes with shaking in a 37°C water bath. The tissue was gently triturated, then incubated and the supernatant collected as previously described, and the triple enzyme digestion repeated for 5 minutes in a 37°C water bath. After collecting the second supernatant, centrifugation and seeding proceeded as per normal.

The specificity of these cultures was confirmed using positive staining with antibodies against smooth muscle cell myosin (Figure 2.1; see Table AI.3). Briefly, the adhered cells were rinsed in PBS, fixed in paraformaldehyde and then rinsed again in PBS before the addition of the primary antibody (rabbit anti-myosin; 1:1000) and incubation overnight in a humidified chamber at room temperature. After rinsing in PBS, the cells were incubated with fluorescein (FITC)-conjugated affinity-purified donkey anti-rabbit (1:40; Dako) or goat anti-rabbit oregon green (1:100; Molecular Probes) for one hour as previously described, then rinsed in PBS, mounted in buffered glycerol and stored at –20°C.

2.3.2 Culture of fibroblasts

Fibroblasts were used to test the specificity of the construct. They were grown from embryonic mouse cells (derived from 13 day old mouse embryos without the livers and heads) in tissue culture flasks. When 70 to 80% confluent, the cells were trypsinized (Trypsin / Hanks; 1 x Sterile Hanks to Trypsin-EDTA (0.25% trypsin and

Figure 2.1 Confocal micrograph of smooth muscle cells

Confocal images of murine aortic smooth muscle cell. Immunohistochemistry with antibodies against smooth muscle myosin confirmed the specificity of the smooth muscle cell cultures. Scale bar represents 500 μm.

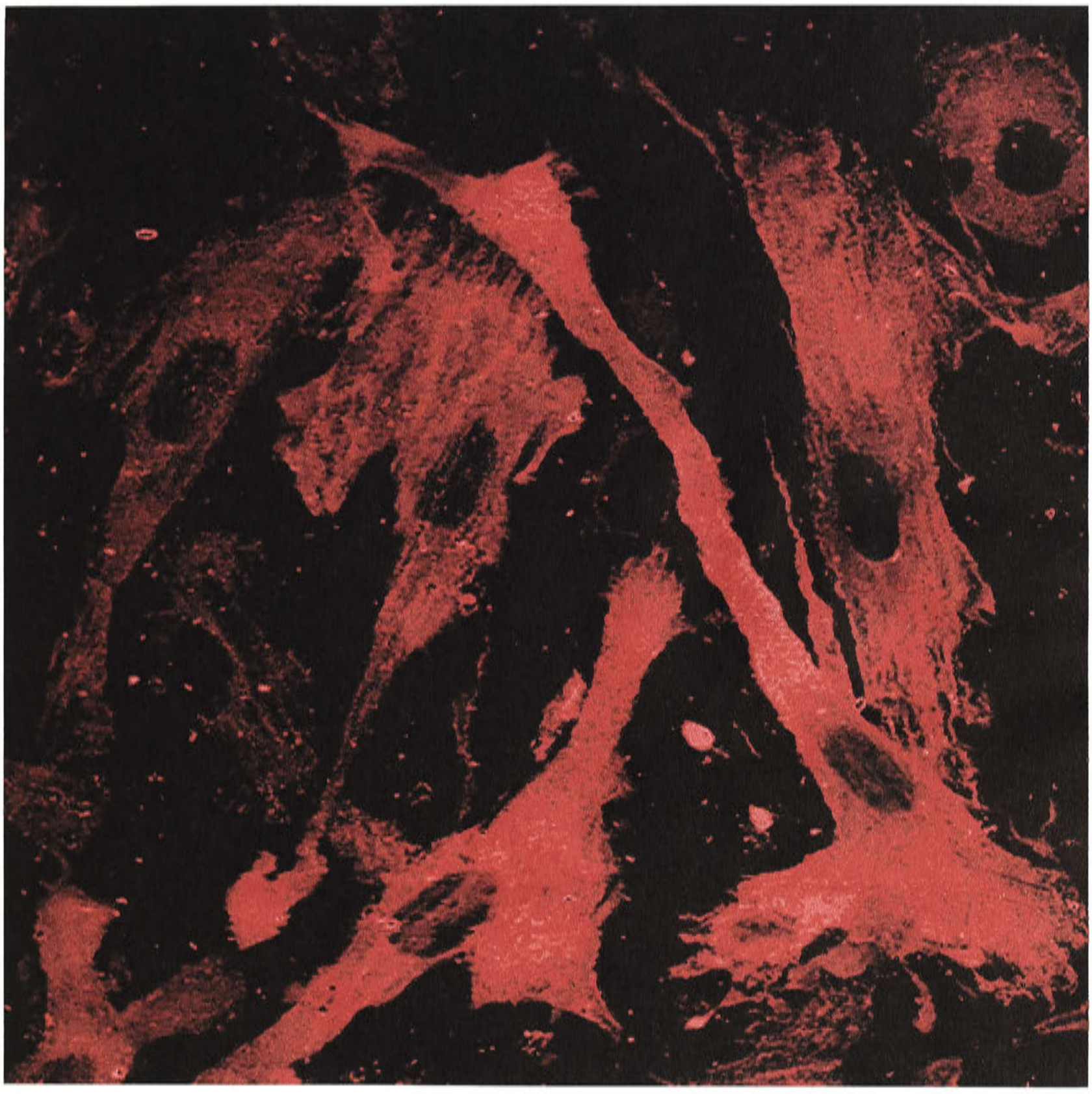

0.02% EDTA; GIBCO-BRL, Life Technologies) to break the seal between the bottom of the culture flask and the cells, and seeded onto glass coverslips in 24 well plates. Incubation was in DMEM (Sigma) containing 1 U / ml penicillin / streptomycin (GIBCO-BRL, LifeTechnologies), 0.1 mM β-mercaptoethanol and 3.4 g $NaHCO_3$; pH 7, and 15% FCS (TRACE) in 1 L sterile water and filter sterilized. Glutamine was replenished weekly (L-Glutamine-200mM; Sigma). Cells were incubated at 37°C in a humidified atmosphere of 10% CO_2 in air and allowed to grow on the coverslips for 2 days (to 60% confluence) before transfection with Lipofectamine Plus.

2.3.3 Transfection of cultured cells

As electroporation was not unsuccessful, transfection of the construct into the cultured cells was undertaken using the transfection reagent Lipofectamine Plus, following the manufacturer's instructions. Preliminary testing was undertaken with this reagent and others: CellFectin (1 mg / ml; GIBCO-BRL, LifeTechnologies), SuperFect Transfection Reagent (3 mg / ml; Qiagen), Lipofectamine (2 mg / ml; GIBCO-BRL, LifeTechnologies), FuGENE 6 (Boehringer Mannheim) and Lipofectamine 2000 (1 mg / ml; GIBCO-BRL, LifeTechnologies)) both in smooth muscle cell cultures and fibroblasts using the control plasmid pJWLacZ (Dr Klaus Matthaei, JCSMR), to determine the best reagent. Two days after transfection, immunohistochemical analysis was performed on the cells.

2.3.4 Immunohistochemistry

Immunohistochemical studies were undertaken using antibodies against Cx43. Briefly, the cells were rinsed in PBS and fixed in 4% (w/v) paraformaldehyde in 0.1 M sodium phosphate buffer pH 7.3, for 5 minutes at room temperature. After washing three times in PBS (5 minutes each), the cells were pre-incubated for 30 minutes with PBS containing 1% (w/v) BSA, 0.3% (v/v) Triton X-100 and 0.04% (w/v) sodium azide

(pre-incubation solution). The primary antibody (mouse anti-Cx43 (1:250; Chemicon or rabbit anti-Cx43, 1:250, Zymed) diluted in the pre-incubation solution was added, and the cells incubated overnight at room temperature in a humidified chamber. After washing three times in PBS (5 minutes each), the cells were washed three times in washing solution containing 1% (v/v) Triton X-100 and 0.04% (w/v) sodium azide in PBS (10 minutes each) before incubation with biotinylated horse anti-mouse (1:500, Jackson Immuno-Research Laboratories Inc.) or biotinylated donkey anti-rabbit mouse (1:500, Jackson Immuno-Research Laboratories Inc.) at room temperature for one hour in a humidified chamber.

Following repeat washing in PBS and in washing solution, the cells were incubated in Texas Red conjugated to streptavidin (1:200, Amersham) for 60 minutes at room temperature in a humidified chamber. After more PBS and washing solution rinses, the cells were mounted in buffered glycerol and stored at -20^{0}C if necessary.

Preparations were examined using either a fluorescence microscope (BH2-RFL, Olympus) fitted with the appropriate filters for fluorescein (excitation filter IF-190 + EY455, dichroic mirror DM500, barrier filter 0-515) and Texas Red (excitation filter IF-545 + BG-36, dichroic mirror DM580, barrier filter R-610), or a confocal laser scanning microscope (Leica TCS 4D), and the number of Cx43 and EGFP labelled cells counted.

Total cell counts were performed directly using either a phase-contrast microscope (for the fibroblasts) or by fluorescence microscopy after staining the cells (smooth muscle cells) in propidium iodide (40 μg / ml diluted in PBS) for 40 minutes, followed by several PBS washes.

Statistical analyses of the total cell counts were undertaken using the computer program GraphPad Prism 2.01 for Windows. A one-way analysis of variance (ANOVA) was performed on the data followed by individual pairwise *t* tests with Bonferroni correction for multiple group comparisons. Significance was assessed at the 5% level.

2.4 *Generation of the Transgenic Mice*

2.4.1 General outline

Transgenic mice were generated as shown in Figure 2.2. The linear DNA construct (either *Pvu*I / *Kpn*I / SM22α / Cx43 or *Pvu*I / *Pvu*II / SM22α / Cx43) was electroporated into BALB/c (white) embryonic stem (ES) cells (where it would recombine with the genome) with a circular selection plasmid (pMClNeoPolyA (pMC1 Neo; Stratagene)) that is not integrated into the chromosome. After selection with G418 (Geneticin; 200 μg / ml; GIBCO-BRL, Life Technologies), resistant (surviving) colonies were isolated and passaged for DNA extraction and storage in liquid nitrogen. Suitable methods for freezing and recovering clones of embryonic stem cells have been published (Chan and Evans, 1991; Ure *et al.* 1992; Ramirez-Solis *et al.* 1993; Hogan *et al.* 1994; Udy and Evans, 1994).

Positive colonies were identified by PCR and subsequently microinjected into blastocysts from a black mouse strain (C57BL/6), which were then reimplanted into the uteri of pseudo-pregnant foster mothers. The chimaeras thus contain cells which have originated from both the introduced transgenic white BALB/c ES cells and the black C57BL/6 cells indigenous to the recipient blastocyst. Chimaeric offspring are therefore black and white.

Confirmation of germ-line chimaeras was achieved by crossing the mice to BALB/c mice and then screening the white progeny (indicating germ-line transmission) by PCR using gene specific primers. Single transgenic mice were interbred to obtain single transgenic, double transgenic and wild type progeny. Breeding germ-line chimaeras gives heterozygous mice that if desired, can be interbred to homozygousity, as is the case for knockout mice.

Briefly, to a 800 μl aliquot of the cell suspension, 10 μg of the linearized DNA and 10 μg of the circular selection plasmid (pMC1 Neo) were added, followed by room

Figure 2.2 Generation of transgenic mice

Schematic diagram showing how transgenic mice were generated. In this thesis, the linear DNA construct was electroporated into cultured BALB/c embryonic stem cells with a circular selection plasmid (pMCl Neo), which was not integrated into the chromosome. Selection with G418 followed, and the resistant (surviving) colonies were passaged; ultimately for freezing and for DNA extraction. Positive colonies were identified by PCR and one to two microinjected into C57BL/6 blastocysts. The latter were then reimplanted into the uteri of pseudo-pregnant foster mothers. The chimaeras were therefore, black and white. Transgenic "founder" mice were identified by PCR screening.

(Modified from a slide provided by Dr Klaus Matthaei, Division of Biochemistry and Molecular Biology, John Curtin School of Medical Research, Australian National University)

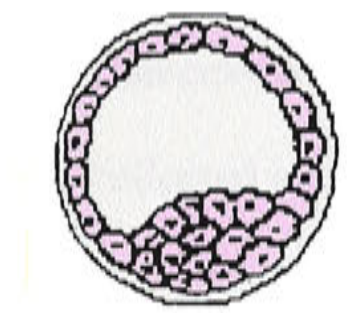

BALBc
Blastocyst

Culture stem cells
in vitro

Electroporate
with transgene
& pMCl Neo

Select for integration
and expand cells

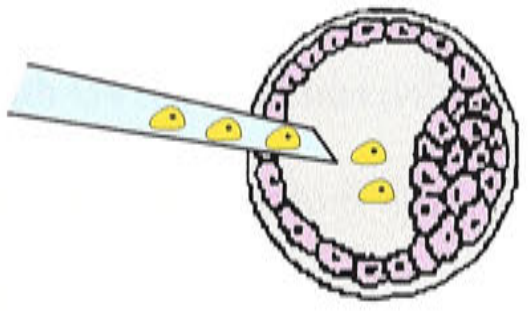

C57Bl/6
Blastocyst

Implant
into foster
mother

Chimaeric
offspring

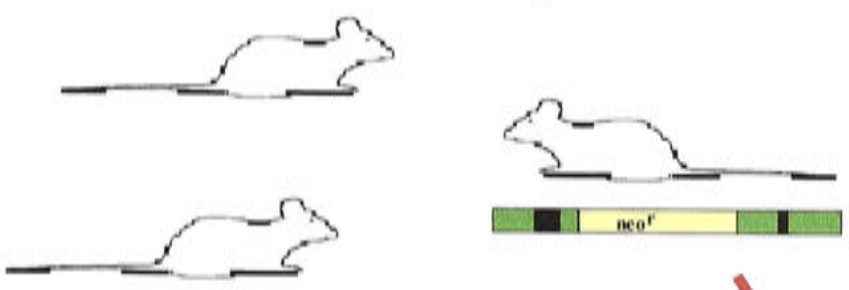

Transgenic
"Founder" mouse

Transgenic mouse
strain

temperature incubation for 5 minutes before transfer to a 0.4 mm electrode gap electroporation cuvette. The cells were pulsed at 0.25 kV, 500 μF in a BioRad gene pulser and collected into a clean tube. After rinsing the cuvette with 800 μl knockout medium (KO DMEM; 500 ml KO DMEM, 0.5 U / ml penicillin / streptomycin; 5 ml non-essential amino acids, 0.1 mM β-MeEtoh, 500 μl leukaemia inhibitory factor (LIF; 1000 U / ml final concentration) and 2 mM L-glutamine) and collecting the medium, an additional 4 ml of KO DMEM was added and mixed into the cell suspension. The cells were seeded onto 5 plates previously seeded with mouse embryonic (feeder) fibroblasts at 1 ml / 100 mm diameter plate, and incubated at 37°C in a humidified incubator with an atmosphere of 10% CO_2 in air.

Twenty-four hours later, cell selection was undertaken every day for about 10 days with G418. The surviving resistant colonies were then individually isolated and passaged in duplicate to 6 well plates: one for DNA isolation and one for passaging for long term storage in liquid nitrogen. By Day 3 non-G418 resistant clones were dying-off, with extensive cell death around days 3 to 5 after starting the selection process.

For each clone, the medium from the well (~ 1 ml) was removed and placed into a labelled tube, centrifuged to pellet the floating cells and the supernatant removed. The well was rinsed twice with PBS, which was added to the tube containing the pelleted cells, before trypsinizing (200 μl / well) for 5 minutes at room temperature. Then 1 ml of warmed KO DMEM with G418 (in a 37°C water bath) was added to the well, mixed by pipetting, and transferred to the same tube. This was repeated with another 1 ml KO DMEM / G418. Finally, the tubes were centrifuged for 10 minutes, the liquid removed and the cells resuspended in 200 μl PBS. The cells were then transferred to a clean eppendorf and stored at 4°C for a maximum of 2-3 hours before DNA extraction.

DNA extraction was performed using the QIAamp Blood Kit (Qiagen) following the protocol for Blood and Body Fluid. Afterwards, the concentration of DNA present

in each clonal sample was measured using a spectrophotometer and calculated. PCRs were performed on 100 ng of DNA from each of the clones using gene specific primers, to identify which clones were positive for the insert. The PCR positives that gave the strongest bands (ie: contain multiple number of copies per cell) when electrophoresed on a 1.5 % agarose gel (see Section 2.1.4), were then frozen in preparation for injection into the blastocysts.

2.4.2 The chimaeras and progeny

Each male chimaera (coat colour black and white) was mated to two female BALB/c mice and each female chimaera was mated to one male BALB/c mouse. Resultant progeny were white (indicating germ-line transmission) or brown (no transmission). Preparation of the tail DNA for PCR is described below, whilst the testing which was undertaken for the SM22α / Cx43 mice is detailed in Chapter 4.

All mice were kept in microisolator cages (Laboratory Products Inc.) in a controlled room with a 12 hour light / dark cycle. Food and water were available *ad libitum*.

2.4.3 Preparation of tail DNA

Three week old mice were ear marked for identification purposes, and the number recorded in the Gene Targeting mouse register. The tips of the tails were then excised (0.3 to 0.5 cm) and placed into eppendorf tubes containing 500 µl lysis buffer (100 mM Tris-HCl pH 8.0, 5 mM EDTA, 0.2% SDS, 200 mM NaCl and MilliQ water to 990 ml; filter sterilized and aliquotted into 25 ml samples for storage at 4°C). Proteinase K (250 µl proteinase K to 25 ml buffer) was added to the lysis buffer just prior to use. All tubes were incubated at 56°C overnight, with rotation, in a hybridization oven.

The following day, the tubes were vortexed and then centrifuged at 6 000 rpm for 10 minutes. The supernatant was poured into clean eppendorf tubes containing 500 µl isopropanol, mixed well and using a sterile Pasteur pipette or ArtTip, the spooled DNA removed into a clean eppendorf tube. After rinsing with 70% ethanol and drying in a vacuum for a minimum of 10 minutes, the DNA was redissolved in 600 µl $T_{10}E_{0.1}$ by heating to 65°C in a water bath for 30 minutes. The OD was then measured at 280 and 260 nm and the DNA concentration calculated. Dilutions of each sample were made (5 µl of sample with 45 µl $T_{10}E_{0.1}$) and 5 µl (~100 ng DNA) used in a PCR reaction. All samples were stored at 4°C.

2.5 Analysis of the Transgenic Mice

Transgenic and control mice were studied using immunohistochemistry, blood pressure measurements and Western blots.

2.5.1 Immunohistochemistry

Two female mice (one transgenic and one control in order to eliminate sex bias) were chosen from two age groups (three and six weeks) and their weights recorded. They were anaesthetized by diluting 0.8 ml xylazine (20 mg / ml; Ilium Veterinary Products) and 1.2 ml ketamine (100 mg / ml; Ilium Veterinary Products) to 10 ml with PBS, and injected intraperitoneally using 100 to 150 µl per mouse. The mice were killed by cervical dislocation. The following tissues were dissected and processed for immunohistochemistry (see Table AI.5): aorta (thoracic and abdominal), mesenteric artery, tail artery, vena cava and ventricle.

Briefly, the dissected tissues were cryo-frozen, sectioned and then placed on microscope slides before fixing in cold acetone. After air drying, the sections were pre-incubated in 2% BSA / 0.2% Triton-X / 0.04% sodium azide for 30 minutes and then

incubated with the primary antibody (anti-rabbit Cx43 polyclonal antibody (1:250; Zymed) diluted in primary antibody solution (0.04% sodium azide, 2% BSA and 0.2% Triton-X) for one hour at room temperature in a humidified chamber. After rinsing and washing with PBS, the secondary antibody (1:100; Cy-3-conjugated anti-rabbit immunoglobulins, Jackson Immunoresearch Laboratories Inc.) diluted in PBS / 0.01% Triton-X was applied for one hour and incubated as before. After rinsing and washing with PBS, the sections were mounted in buffered glycerol and examined using a fluorescence microscope with the appropriate filters.

2.5.2 Western blots

In the current study, Western blots were used to investigate the protein level of connexin 43 and actin in the tail artery and aorta of both control and transgenic mice of either sex.

After recording its bodyweight, each mouse was anaesthetized by inhalation of ether and killed by severing the jugular veins in order to avoid injury to the tail artery. The aorta and tail artery were dissected out and placed into separate dishes containing cold PBS. Adipose and connective tissues were then carefully removed and the tissues placed in fresh dishes of cold PBS. The aorta was cut open so that the blood cells could be carefully removed. Due to its small size, blood in the tail artery was gently squeezed out using a pair of fine forceps. After determining the tissue weights on an analytical balance, the tissues were homogenized in separate pre-chilled homogenizers, containing 1 ml of cold Tris swelling buffer (10 mM Tris-HCl pH 7.9, 10 mM KCl, 1 mM $MgCl_2$ and distilled water to 100 ml) with 0.5 µl phenylmethylsulfonic acid (PMSF; 40 µg / ml in DMSO). This technique was latter modified for each mouse Group 2 to 4 as follows: the tissues were homogenized in 1000 µl of 0.25 mM cold sodium bicarbonate buffer (pH 7.2) with 0.5 µl PMSF.

After homogenization, the samples were pipetted into clean and chilled eppendorf tubes and centrifuged at 800 g for 3 minutes at 4°C. The supernatants were then aspirated into individually labelled clean eppendorf tubes and centrifuged at 17 400 g for 20 minutes at 4°C. The supernatants were discarded and the pellets resuspended in appropriate volumes of either chilled RIPA buffer (Group 1; 150 mM NaCl, 50 mM Na_2HPO_4 pH 7.2, 1% sodium deoxycholate, 1% Triton-X, 0.5% sodium dodecyl sulphate (SDS), 1 mM sodium orthovanadate in distilled water) with added PMSF (1:1000), or 1 x sample buffer without dye (other groups: 100 ml / L glycerol, 120 ml / L UpperTris (Table AI.6), 30 g / L SDS in distilled water). All samples were then stored at –70°C until the protein assays were performed.

The tissue samples were assayed for membrane protein using the Bio-Rad D_C Protein Assay (Bio-Rad Laboratories) according to the manufacturer's directions, and the appropriate dilutions for each sample were calculated. Preliminary testing with the XCell Surelock Mini-Cell System (Invitrogen) had shown that 12 mg of murine tail artery or 1 mg of aorta was the minimum tissue weight required per well in order to produce an adequate band. Subsequently, the proteins were separated on 12% SDS-polyacrylamide gels using Mini-Cell System and the SeeBlue Pre-Stained Standards (Novel Experimental Technology) as a marker. The solutions used are shown in Table AI.6. The proteins were then transferred to nitrocellulose membranes using a Semi-Phor (Hoeffer Scientific Instrumenta) followed by overnight incubation at 4°C (or one hour at room temperature) with 5% skim milk powder in 0.2% Tween20 in PBS (PBS-T) to block non-specific binding. The blocking solution was removed by rinsing the membranes three times in PBS-T, before incubation in anti-connexin 43 rabbit polyclonal antibody (1:500; Zymed) diluted in primary antibody solution (0.04% sodium azide, 1% BSA and PBS-T to 2 ml) for one hour at room temperature or overnight at 4°C on rollers. Control experiments with 10-fold excess of peptide to Cx43 antibody

(peptide block) were also undertaken. After washing in PBS-T for 60 minutes (3 x 10 minutes, then transfer to a new tube for 3 x 10 minutes), the secondary antibody (1:1000; donkey anti-rabbit horseradish peroxidase; Amersham Life Science) diluted in PBS-T was added, and the membranes incubated with agitation at room temperature for one hour, followed by one hour of washing in PBS-T at room temperature. Afterwards, the ECL Western Blotting detection agents (Amersham Pharmacia Biotech) or the Supersignal West Dura Extended Duration Substrate (Pierce) were used to complete the detection process. The membranes were then developed using Xray film and analyzed using the Analytical Imaging System (AIS; Imaging Research Inc.).

2.5.3 Blood pressure recordings

Systolic blood pressure and heart rate were measured in unanaesthetized male and female transgenic and control mice by tail-cuff plethysmography using a Programmed Electro-Sphygmomanometer PE-300 (Narco Bio-Systems), amplifier (to which the tail sensor was connected) and the HyperRat programme (SDR Clinical Technology) on a MacIntosh LC475 computer. Pressure corresponding to the systolic blood pressure is applied externally to the tail in the conscious but restrained mouse, and is measured by a manometer attached to a tail-cuff with blood flow in the tail being detected by a photoresistor (Hoit, 2001). All mice (except one group) were acclimatized to the tail-cuff plethysmography equipment for the recommended 7 days prior to the first recording (Krege *et al.* 1995).

After attaching a tail-cuff and a tail sensor, the mice were warmed to 37°C ± 1°C (basal temperature for a mouse is 37°C) on a HyperRat Heated Baseplate (FUJI PYZ4 Controller) for 15 to 20 minutes. As restraint of some strains of mice is known to decrease tail (and body) temperature (Johnson *et al.* 2000), heating the base-plate to 37°C is considered important as the tail artery dilates, facilitating blood pressure measurements. Readings were taken within 30 minutes, as heating on the plate may

stress mice, leading to a false elevation in the blood pressure reading. A blood pressure reading for each mouse was gained by averaging the figures for four blood pressure measurements that were within 10 mmHg of each other. All measurements were performed between 1300 and 1600 hours.

Statistical analyses comparing blood pressure measurements in control and transgenic mice were undertaken using the computer program GraphPad Prism 2.01 for Windows. A three-way analysis of variance (ANOVA) was performed on the data.

Chapter 3 – Generation of the SM22α / Cx43 Construct and Mouse

3.1 Introduction

A transgenic mouse may be defined as an animal that contains a segment of exogenous DNA that is stably inherited and chromosomally integrated (Mullins and Ganten, 1990; Faraci and Sigmund, 1999). The DNA may originate from the host species, from an unrelated species, or from a combination of the two. The tissue-specific and developmental expression of the gene construct depends upon the nature of the gene construct itself. Phenotypes resulting from such alterations are diverse and may even be phenotypically normal. The latter is due to redundancy in the genome and/or the expression of compensatory mechanisms.

A number of stages are involved in the construction of a transgenic mouse. Briefly, in conventional experiments, pronuclear stage (one cell) murine embryos are collected after fertilization, but before cleavage is initiated. Exogenous cloned linearized DNA is transferred into the genomes of mice by microinjection into the pronuclei (Gordon *et al.* 1980; Gordon and Ruddle, 1981, 1983). The embryos are then implanted into the oviduct or ovarian bursa of a pseudo-pregnant foster mother (previously mated with a sterile male) where they can develop into pups. Therefore, the chimaeras contain cells which will contribute to the germ-line, ensuring the inheritance of the altered gene in succeeding generations.

Alternative methods for introducing genes into the mouse germ-line include, for example, retroviral infection (Nagano *et al.* 2000), nuclear transplantation / transfer (Wakayama *et al.* 1999) and the insertion of genetically engineered embryonic stem cells (Bradley *et al.* 1992) into blastocysts (Hogan *et al.* 1994). The latter method was used in this thesis – chimaeric mice are shown in Figure 3.1.

Figure 3.1 The chimaeric mice

Shown are two photos of two low grade male chimaeras (black and white colouring), each with two BALB/c (white) females. In the top photo, the pups are only a few days old and the female in the lower right corner is clearly gravid. Pink eyes in the BALB/c at birth mean germ-line (grow a white coat), whereas brown eyes (grow a brown coat) mean non-germ-line. In the bottom photo, three pups can be seen – two white (pink) indicating germ line transmission and one brown (no transmission).

Connexin 43 is the predominant gap junction gene in developing and adult cardiac tissue, and has been implicated in many cardiovascular pathologies. In order to develop a transgenic mouse model that selectively overexpresses Cx43 in the vascular system, it was necessary to express Cx43 specifically in vascular smooth muscle. A restricted portion of the smooth muscle (SM) 22α promoter (a promoter confined to vascular smooth muscle cells) from the SM22α gene was used to direct specific arterial expression and thus, avoid cardiac overexpression of Cx43. SM22 is a 22-kDa protein that is expressed exclusively and uniformly in smooth muscle tissues of adult animals (Lees-Miller *et al.* 1987; Shanahan *et al.* 1993) and is one of the earliest markers of differentiated smooth muscle cells (Duband *et al.* 1993).

Previous research by Solway *et al.* (1995) showed that only a 482 bp fragment in the 5'-flanking region of the SM22α gene (- 441 to + 41 bp) was necessary and sufficient to program high level transcription of the SM22α / luciferase reporter gene in both primary rat aortic smooth muscle cells and the smooth muscle cell line A7r5. Subsequent studies delineated a SM22α promoter region specific for expression in arterial smooth muscles *in vivo* (Li *et al.* 1996; Moessler *et al.* 1996). Moessler *et al.* (1996) showed that various promoter constructs of 445 to 2126 bp directed reporter expression initially (and transitorily) in embryonic somites and heart (presumptive right ventricle and outflow tract), and subsequently in the arterial vascular system where it persisted in the adult mouse.

This Chapter describes the cloning of the SM22α / Cx43 / pBs KSII- (SM22α / Cx43) construct and the subsequent generation of the transgenic mice, whilst data obtained from analyses of the mice are presented in Chapter 4. The cloning strategies for the SM22α promoter and Cx43 cDNA are shown in Figures 3.2 and 3.3 respectively, and for the SM22α / Cx43 construct in Figures 3.4 and 3.5.

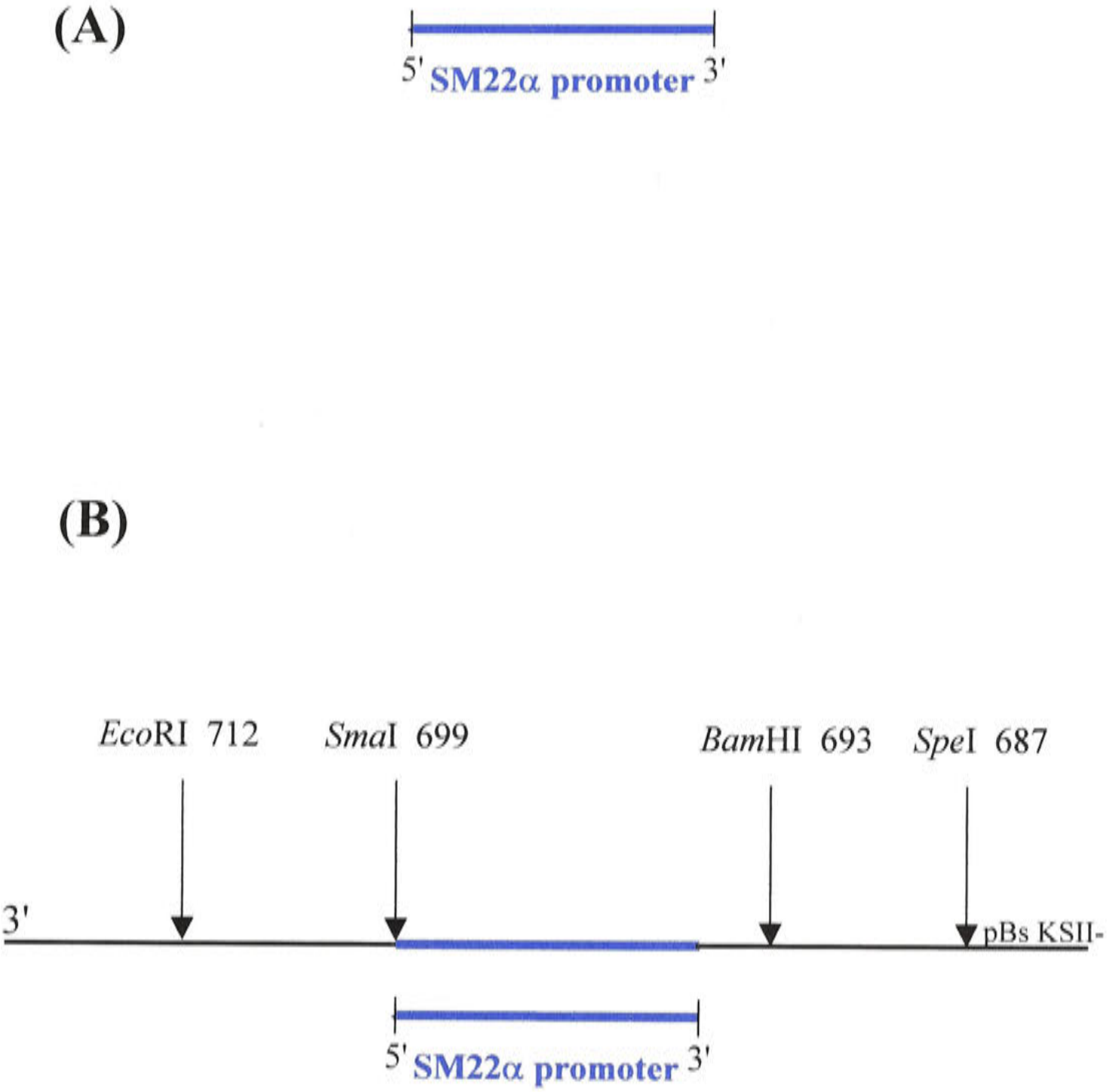

Figure 3.2 Schematic diagram of the cloning of the SM22α promoter

The cloning of the SM22α promoter is shown in **(A)** and **(B)**. The promoter was amplified from a mouse genomic library by PCR **(A)**. For the promoter to function, it had to be in the forward orientation in *Sma*I / pBs KSII- **(B)**.

Figure 3.3 Schematic diagram of the cloning of the Cx43 cDNA

The cloning of the Cx43 cDNA is shown in **(A)**, **(B)** and **(C)**. The cDNA was amplified from mouse genomic DNA by PCR **(A)**. As the ensuing destination site of the Cx43 was in *Pvu*II / *Cla*I restricted pBi5 **(B)**, the Cx43 gene fragment had to be in the reverse orientation in *Cla*I / pBs KSII- **(C)**. Thus, when the Cx43 / pBs KSII- plasmid was cut with *Cla*I and *Eco*RI, the Cx43 gene could be ligated into pBi5 in the correct orientation.

(A)


5'
Cx43 gene cDNA
3'

(B)

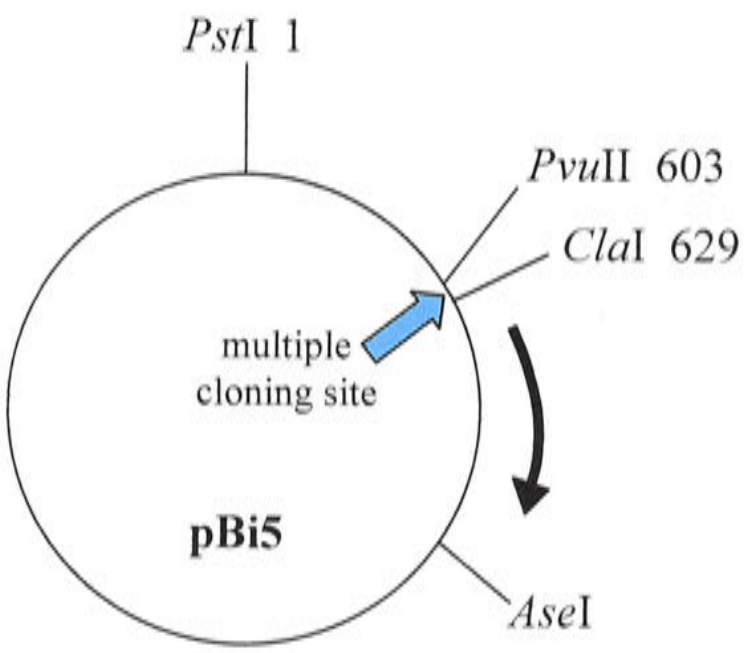
PstI 1
PvuII 603
ClaI 629
multiple
cloning site
pBi5
AseI

(C)

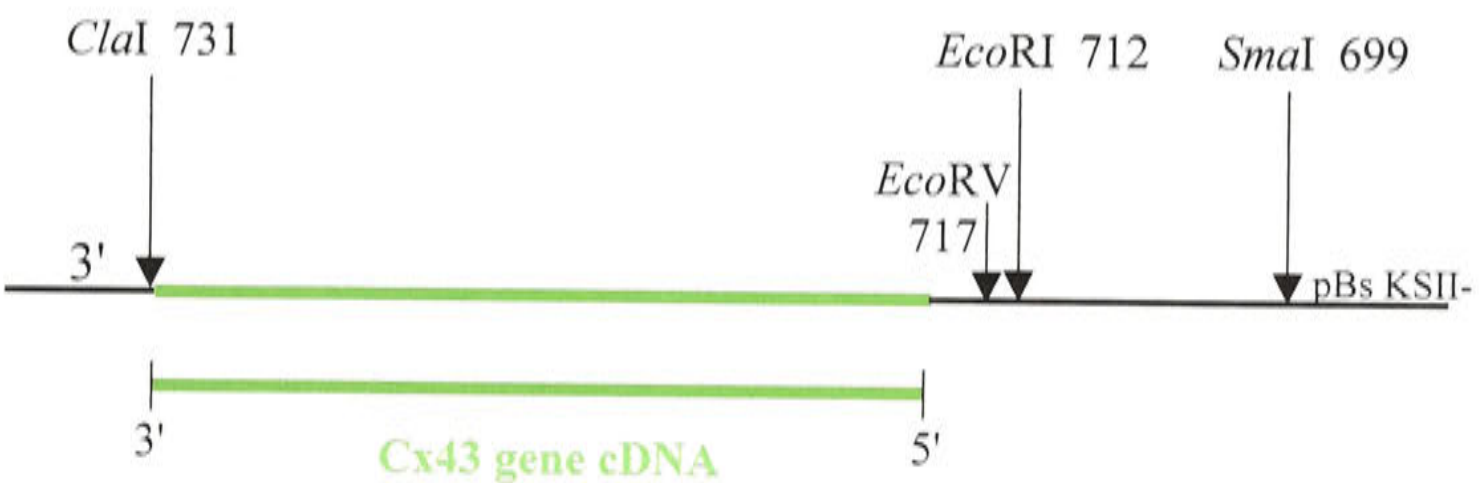
ClaI 731
EcoRI 712
SmaI 699
EcoRV
717
3'
pBs KSII-
3'
5'
Cx43 gene cDNA

Figure 3.4 Schematic diagram of the cloning of SM22α / Cx43 / pBs KSII-

The cloning of the SM22α / Cx43 / pBs KSII- construct is shown in **(A)**, **(B)** and **(C)**. The Cx43 cDNA was excised from Cx43 / pBs KSII- with *Eco*RI and *Cla*I and cloned into the multiple cloning site of *Cla*I / *Pvu*II pBi5. The Cx43 / β-globulin polyA signal fragment was then excised from Cx43 / pBi5 with *Bam*HI and *Ase*I **(A)**. The vector was further restricted with *Sph*I for ease of purification. The SM22α / pBs KSII- plasmid was restricted with *Bam*HI **(B)** before cloning the *Bam*HI / *Ase*I / Cx43 / polyA signal insert into the *Bam*HI / SM22α / pBs KSII- vector **(C)**. The figures are not to scale. The numbers refer to the designated pBs KSII- numbering.

(A)

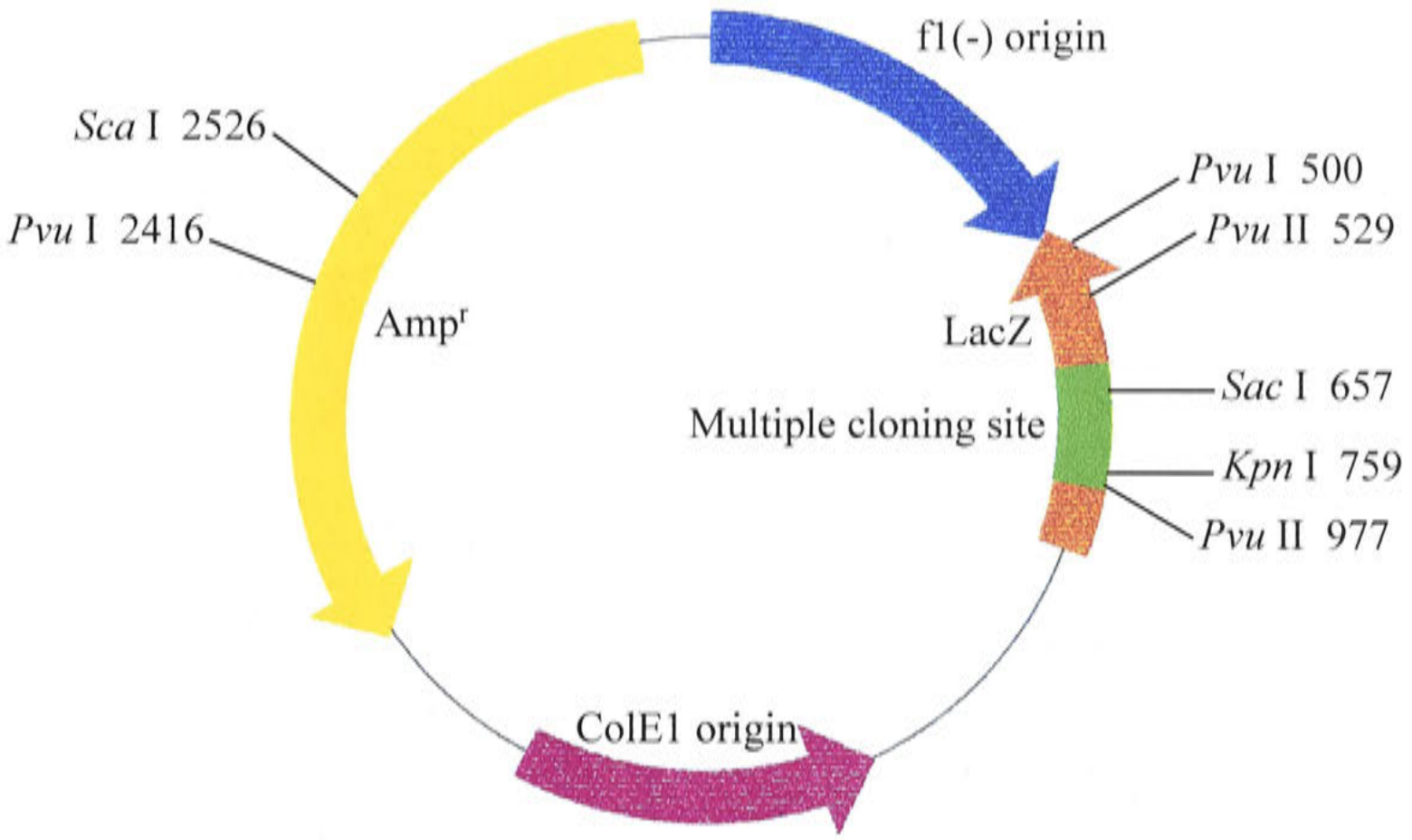
f1(-) origin
Sca I 2526
Pvu I 500
Pvu I 2416
Pvu II 529
Amp^r
LacZ
Sac I 657
Multiple cloning site
Kpn I 759
Pvu II 977
ColE1 origin

(B)

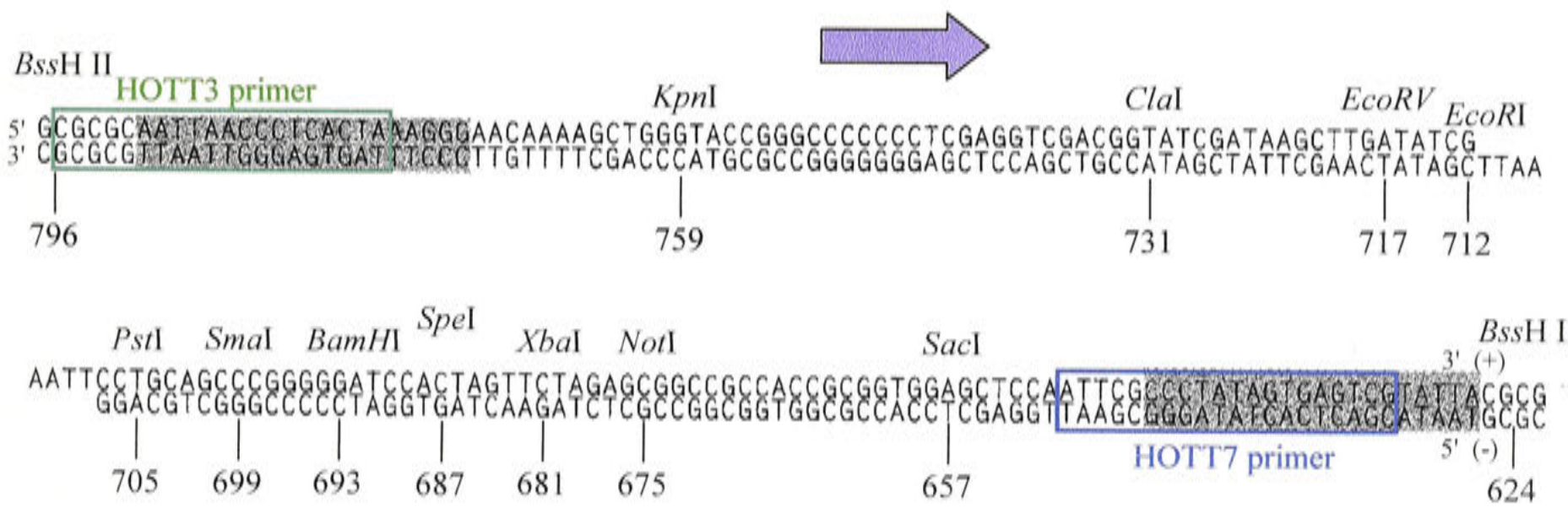
BssH II
HOTT3 primer
KpnI
ClaI
EcoRV
EcoRI
5' GCGCGCAATTAACCCTCACTAAAGGGAACAAAAGCTGGGTACCGGGCCCCCCCTCGAGGTCGACGGTATCGATAAGCTTGATATCG
3' CGCGCGTTAATTGGGAGTGATTTCCCTTGTTTTCGACCCATGCGCCGGGGGGGGAGCTCCAGCTGCCATAGCTATTCGAACTATAGCTTAA
796
759
731
717
712
PstI
SmaI
BamHI
SpeI
XbaI
NotI
SacI
BssH II
3' (+)
AATTCCTGCAGCCCGGGGGATCCACTAGTTCTAGAGCGGCCGCCACCGCGGTGGAGCTCCAATTCGCCCTATAGTGAGTCGTATTACGCG
GGACGTCGGGCCCCCTAGGTGATCAAGATCTCGCCGGCGGTGGCGCCACCTCGAGGTTAAGCGGGATATCACTCAGCATAATGCGC
5' (-)
HOTT7 primer
705
699
693
687
681
675
657
624

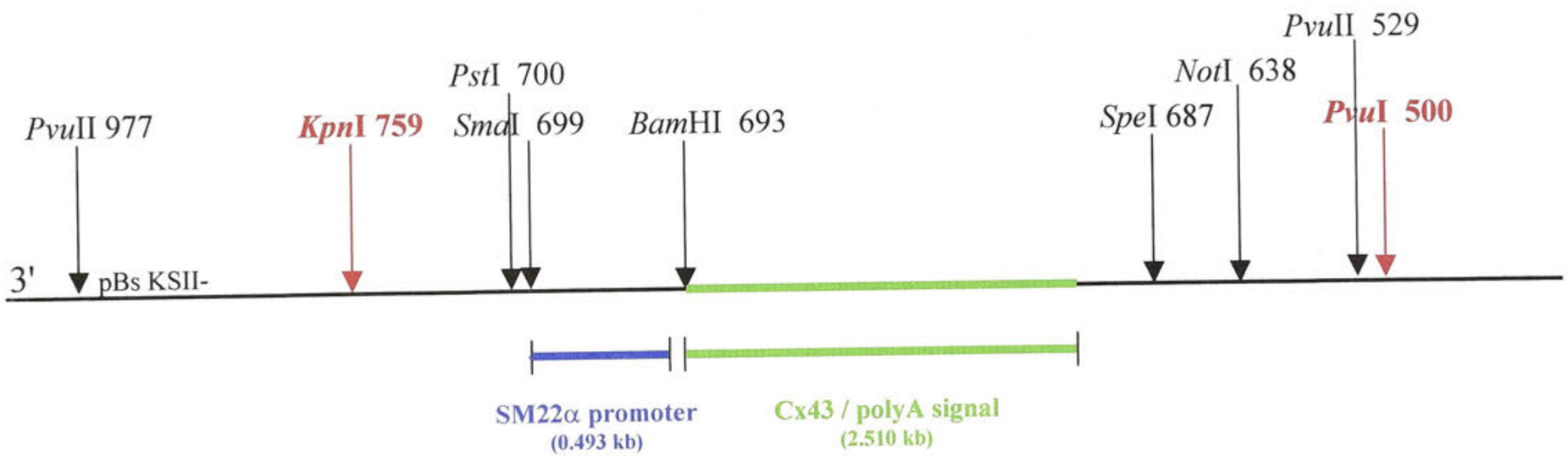

Figure 3.5 Preparation of the SM22α / Cx43 / pBs KSII- plasmid for electroporation

The SM22α / Cx43 / pBs KSII- plasmid was restricted with *Pvu*I and *Kpn*I to excise the SM22α / Cx43 / polyA fragment prior to electroporation into BALB/c murine embryonic stem cells. The numbers refer to the designated pBs KSII- numbering system. Not drawn to scale.

PART I – Cloning of the SM22α promoter and Cx43 cDNA

3.2 Additional Methods

3.2.1 Cloning of the SM22α promoter

3.2.1.1 Isolation of the SM22α promoter

The *Mus musculus* SM22α gene (GenBank sequence accession number Z68618) and SM22α cDNA sequences were downloaded from GenBank and the published restricted SM22α promoter region identified. The general features of the SM22 gene are shown in Figure 3.6A. Two primers, one forward (SM22ex1f) and one reverse (SM22ex1r) were designed on either end of the promoter (see Figure 3.6B; Table 2.2).

The restricted SM22α promoter was amplified from a BALB/c mouse genomic library (LE392, provided by Mr David Mann) by PCR using the SM22ex1f and SM22ex1r primers (see Table 2.2) and *Pfu* DNA polymerase. After agarose gel electrophoresis to check for correct band size (493 bases), the product was generated a further six times using the same primers and PCR conditions to gain sufficient sample for cloning. All six PCR tubes were then combined before assessment by agarose gel electrophoresis. The product was purified and the concentration determined by OD at 260 nm.

3.2.1.2 Construction of the SM22α / pBs KSII- plasmid

The pBluescript plasmid (Figure 3.7) was restricted with *Sma*I and phosphatased by Mr David Mann (Biochemistry and Molecular Biology, JCSMR). The purified SM22α PCR product was blunt-end cloned into *Sma*I / pBs KSII-. The ligation was performed in a 20 µl total reaction volume with 1 µl of T4 DNA ligase (40 000 units / ml). The construct was subsequently electroporated into TOP10F' cells and resulting colonies blue / white screened.

All white colonies were analyzed by cracking and those containing an insert and some not containing an insert, were screened by PCR using the gene specific primers

Figure 3.6 The restricted SM22α promoter

The position of the restricted promoter region in relation to the SM22α gene is shown in **(A)**. The SM22 primers are indicated on the SM22α promoter sequence in **(B)**. The Exon 1 start site and transcription start site is also marked. The mSM22ex1f primer (GAC TAG TTC CCA CCA ACT CGA TT) is not marked as it was largely encompassed by the SM22ex1f primer.

Start site of transcription

Exons are boxed, with open boxes indicating non-coding regions

Restricted promoter region

SM22ex1f

mSM22F2

mSM22F6

mSM22F7

SM22ex1r

Start of Exon 1 and transcriptional start site

End of Exon 1 (+ 65 bp)

(A)

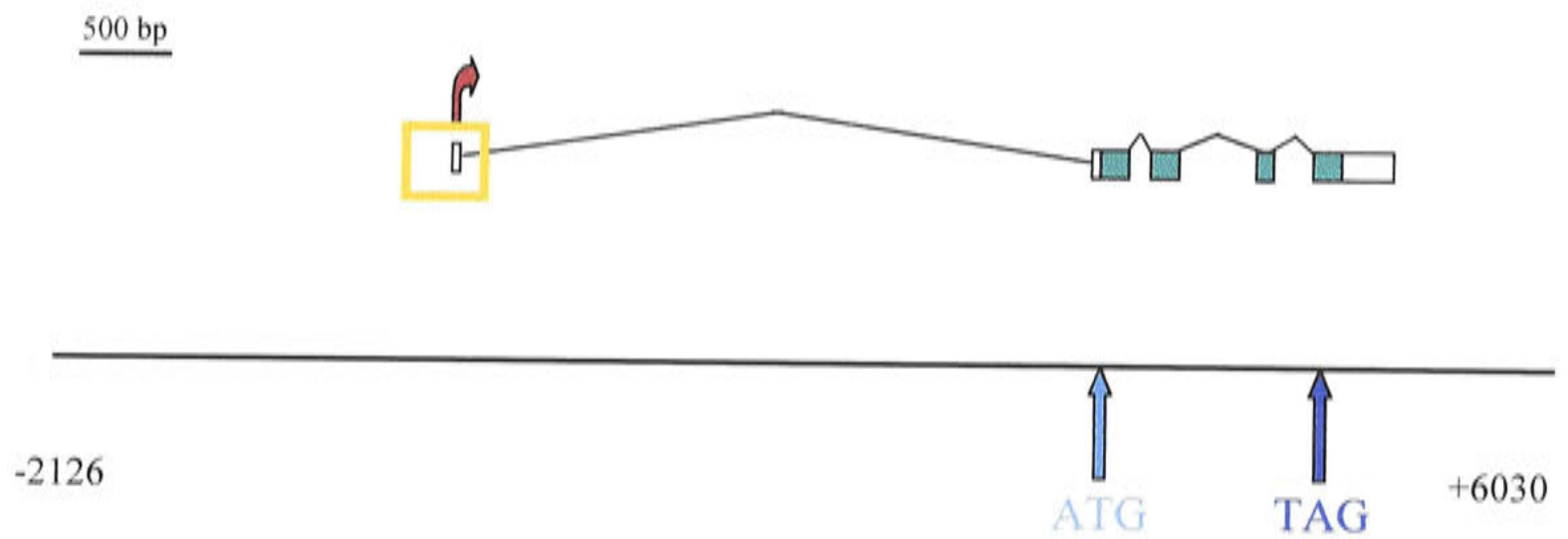

(B)

```
        taccatacct gtgggcagga tgacccatgt tctgccatgc acttggtagc cttggaaagg
        ccactttgaa cctcaatttt ctcaactgtt aaatggagtg gtaactgcta tctcataata
        aaggggaacg tgaggaaggc gtttggatag tgcctggttg cggccaggct gcagtcaaga
-430    ctagttccca ccaactcgat tttaaagcct tgcaagaagg tggcttgttt gtcccttgca
        ggttcctttg ctcgggccaa actctagaat gcctcccccc ttctttctca ttgaagagca
        gacccaagtc cgggtaacaa ggaagggttt cagggtcctg cccataaaag gtttttcccg
        gccgccctca gcaccgcccc gccccgaccc ccgcagcatc tccaaagcat gcagagaatg
        tctccggctg cccccgacag actgctccaa cttggtgtct ttcccaaat atggagcctg
        tgtggagtga gtggggcggc ccgggatggt gagccaagca gacttccatg ggcagggagg
        ggcgccacgg ggcggcagag gggtgacatc actgcctagg cggcctttaa acccctcacc
        cagccgggc cccggcccgt ctgccccagc ccagacaccg aagctactct ccttccagtc
+47     cacaaacgac caagccttgt aagtgcaagt catgggagca gaagggctgt gggctcaatt
        agatccccta gtctcttcta gtttgctggg tggaattggg tccctagaga ccattctctg
        tgttagacaa aaagtctggg ttaaaatgcc taggatgatt tgactggggc aaaagaataa
        atggggtgag agggaggctc aaattcagtc actgtcccac ccataggtgt atgggctatg
        tgttaggccc aaagaggtga caaatgaggc caagggaaca actccatctt tggatctcca
```

Figure 3.7 The pBluescript (pBs KSII + / -) plasmid

The 2.961 kb pBluescript plasmid, derived from pUC19 (GenBank), is shown opposite with selected restriction enzyme sites **(A)**. The KS designation indicates that *lacZ* transcription proceeds from *Kpn*I to *Sac*I. The f1 (-) origin is the filamentous phage origin of replication allowing the recovery of the antisense strand of the *lacZ* gene when a host strain containing the pBluescript II phagemid is co-infected with helper phage. Hence the minus designation (pBs KSII-). The *lacZ* promoter provides α-complimentation for blue / white screening (see Section 2.1.12). The multiple cloning site (657 to 759 bp) is flanked by two promoters (HOTT3 (or T3) and HOTT7 (or T7)) which are shown in **(B)**, with selected restriction enzyme sites pertinent to this study. Amp^r, the ampicillin resistance gene (1975 to 2832 bp), allows antibiotic selection of the vector. The difference between pBs KSII- and pBs KS- is the addition of two *Bss*H II restriction enzyme sites in pBs KSII-.

(A)

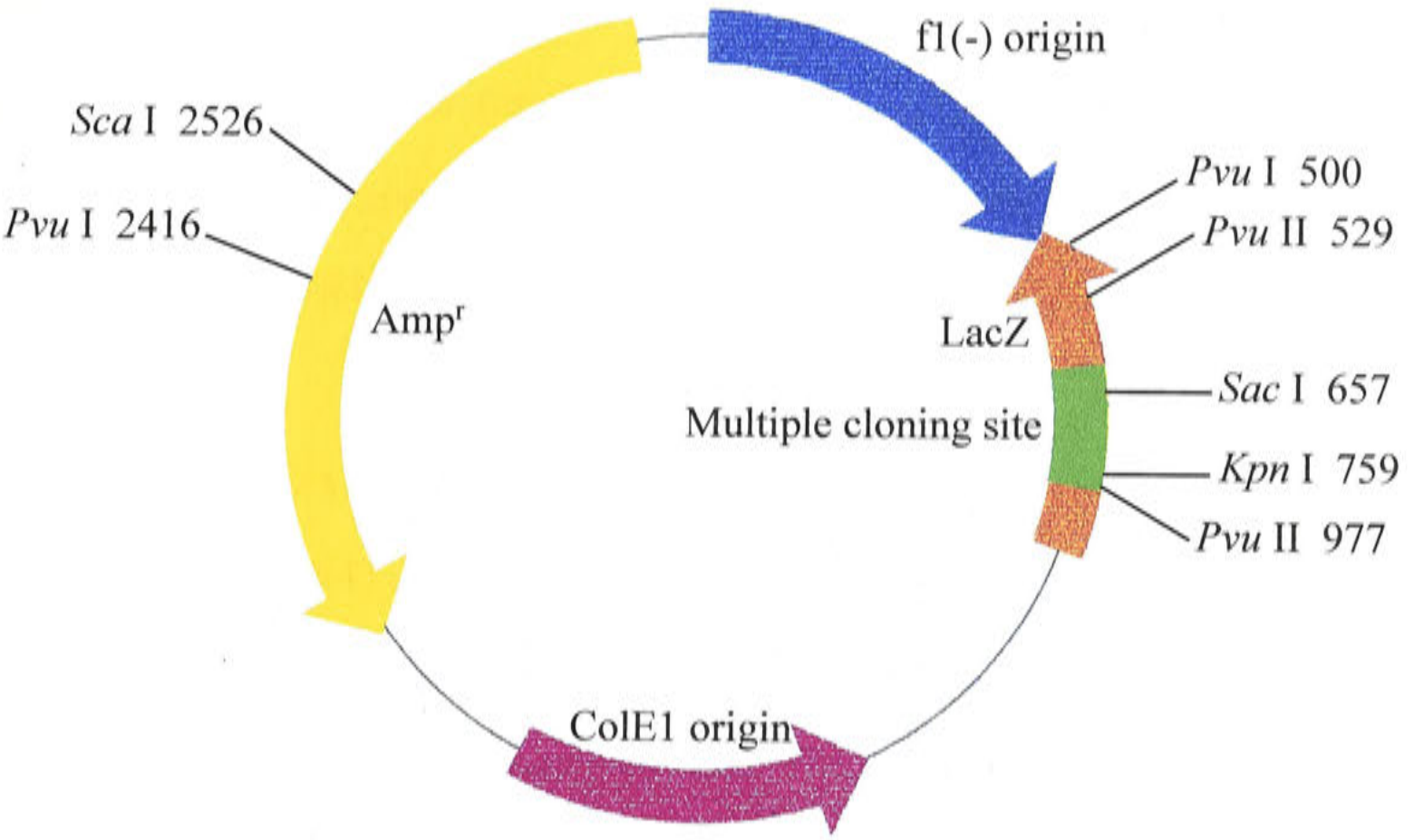
f1(-) origin
Sca I 2526
Pvu I 2416
Pvu I 500
Pvu II 529
Amp^r
LacZ
Sac I 657
Multiple cloning site
Kpn I 759
Pvu II 977
ColE1 origin

(B)

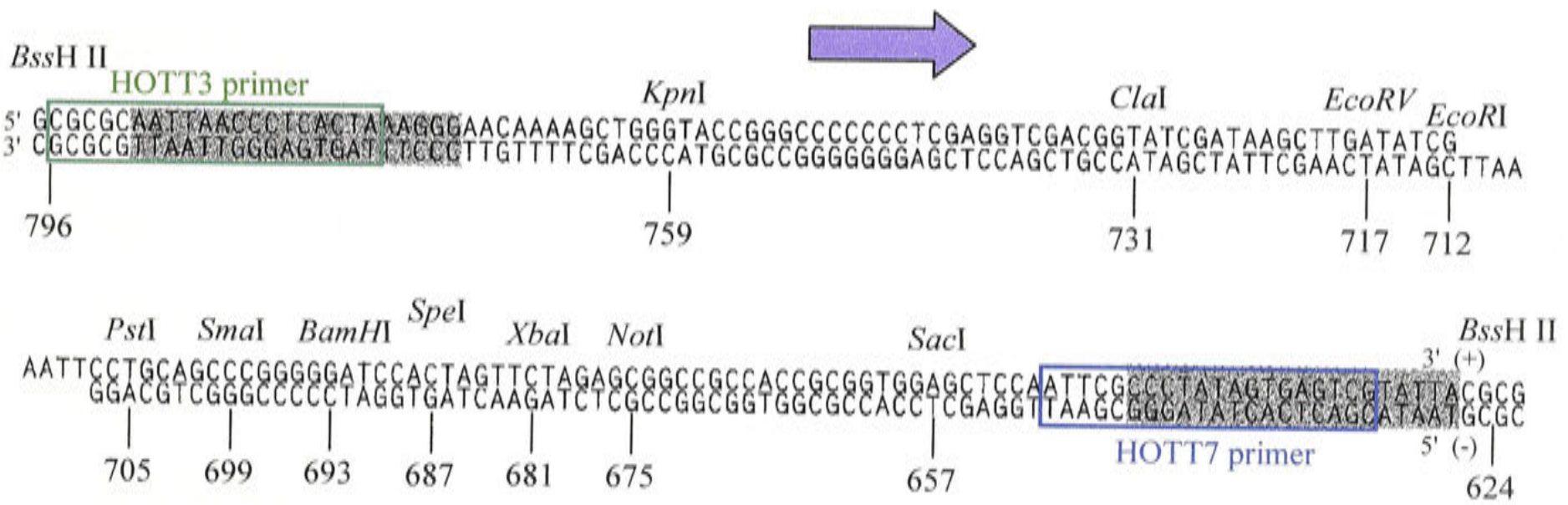
BssH II
HOTT3 primer
KpnI
ClaI
EcoRV
EcoRI
5' GCGCGCAATTAACCCTCACTAAAGGGAACAAAAGCTGGGTACCGGGCCCCCCCTCGAGGTCGACGGTATCGATAAGCTTGATATCG
3' CGCGCGTTAATTGGGAGTGATTTCCCTTGTTTTCGACCCATGCGCCGGGGGGGGAGCTCCAGCTGCCATAGCTATTCGAACTATAGCTTAA
796
759
731
717
712
PstI
SmaI
BamHI
SpeI
XbaI
NotI
SacI
BssH II
3' (+)
AATTCCTGCAGCCCGGGGGATCCACTAGTTCTAGAGCGGCCGCCACCGCGGTGGAGCTCCAATTCGCCCTATAGTGAGTCGTATTACGCG
GGACGTCGGGCCCCCTAGGTGATCAAGATCTCGCCGGCGGTGGCGCCACCTCGAGGTTAAGCGGGATATCACTCAGCATAATGCGC
5' (-)
HOTT7 primer
705
699
693
687
681
675
657
624

SM22ex1f and SM22ex1r, and appropriate controls (pBs KSII- and genomic DNA). The HOTT3 and HOTT7 primers (Table 2.2) were made to the T3 and T7 promoter sites outside the multiple cloning site of pBs KSII-. Positive colonies were further PCR screened using various primer combinations, with two colonies ultimately chosen for restriction enzyme analyses and bi-directional sequencing using the SM22ex1r, SM22ex1f, HOTT3 and HOTT7 primers.

3.2.2 Cloning of the Cx43 cDNA

3.2.2.1 Isolation of the Cx43 cDNA

The *Mus musculus* connexin 43 gene (6.935 kb; Genbank sequence accession number L10388) was downloaded from GenBank. The start and stop codons for the gene were identified using published sequences for the rat and mouse, and sufficient bases added to either side (139 bp forward and 42 bp reverse) for flexibility during the cloning process, to give a fragment of 1.325 kb (3447 to 4772 bp). The selected cloning sequence is shown in Figure 3.8A,B. One forward (CnxF) and one reverse (CnxR) primer were designed on either side of the designated region (Figure 3.8B; Table 2.2) and used to isolate the Cx43 gene fragment from a BALB/c mouse genomic DNA by PCR using *PfuTurbo* DNA polymerase (see Table 2.2). This PCR was repeated four times to generate enough product for cloning. The products were then combined into one sterile eppendorf tube and a small aliquot electrophoresed on an agarose gel to check for correct band size. The PCR product was purified and assessed by agarose gel electrophoresis.

3.2.2.2 Construction of the Cx43 / pBs KSII- plasmid

One hundred nanograms of pBs KSII- (previously quantitated at OD_{260}) was restricted with *Eco*RV and *Cla*I (Figure 3.7). After a four hour incubation (2 hours for the *Eco*RV restriction digest followed by 2 hours for the *Cla*I restriction digest with

Figure 3.8 The Cx43 selected cloning sequence

The position of the selected Cx43 cDNA region (1.325 kb) in relation to the entire Cx43 gene is shown in **(A)**. The Cx43 primers are indicated on the Cx43 cDNA sequence in **(B)**. The Exon 2 start site is also marked, as are the start and stop codons, and the *Cla*I restriction site.

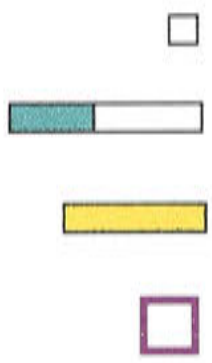

Exon 1

Exon 2 with coding region (green)

Intron (10.5 kb) in the 5'-UTR (untranslated region)

Selected sequence for cloning

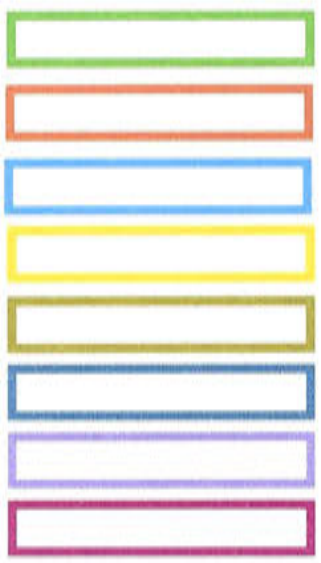

CnxF primer

mCx435'R primer

Rat CxF primer position

Rat Cx43F primer position

mCnx43R primer & rat Cx43R primer position

Rat Cx43R2 primer position

Rat Cx43R3 primer position

CnxR primer

Start and stop codons

Exon 2 start site

*Cla*I restriction site

(A)

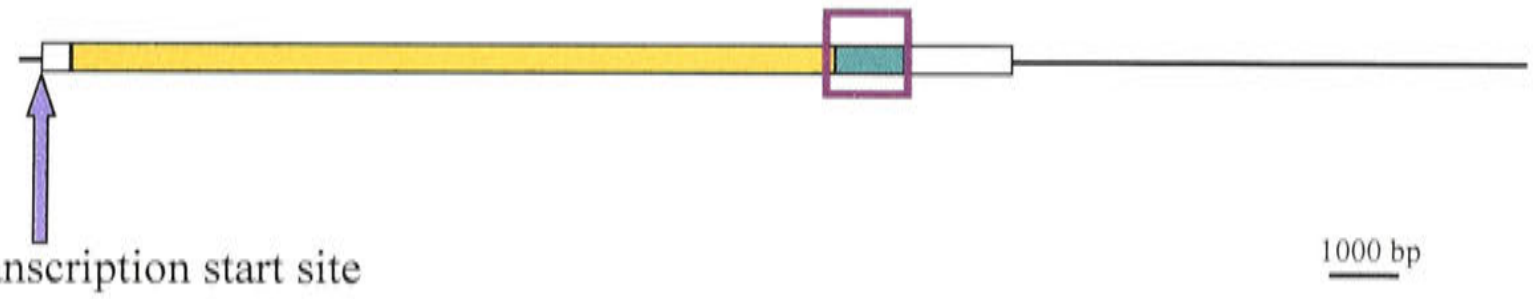

(B)

```
3421 gccagatttg cccttggatt ctgtttggc ttgggttgaa actgccttat tttgactgac
     ccctgaaaaa agaaactata tatgtgaaac catcaattta cagtctacaa tcactgagtt
     gttttcgtgg tttttgtttt tgttttcttt aggaggtgcc cagacatggg tgactggagc
     gccttgggga agctgctgga caaggtccaa gcctactcca cggccggagg gaaggtgtgg
     ctgtcggtgc tcttcatttt cagaatcctg ctcctgggga cagcggttga gtcagcttgg
     ggtgatgaac agtctgcctt tcgctgtaac actcaacaac ccggttgtga aaatgtctgc
     tatgacaagt ccttccccat ctctcacgtg cgcttctggg tccttcagat catattcgtg
     tctgtgccca cactcctgta cttggctcac gtgttctatg tgatgagaaa ggaagagaag
     ctgaacaaga aagaagagga gctcaaagtg gcgcagaccg acggggtcaa cgtggagatg
     cacctgaagc agattgaaat caagaagttc aagtatggga ttgaagaaca cggcaaggtg
     aagatgagag gtggcctgct gagaacctac atcatcagca tcctcttcaa gtctgtcttc
     gaggtggcct tcctgctgat ccagtggtac atctatgggt tcagcctgag tgcggtctac
     acctgcaaga gagatccctg cccccaccag gtggactgct tcctctcacg tcccacggag
     aaaaccatct tcatcatctt catgctggtg gtgtccttgg tgtctctcgc tctgaatatc
     attgagctct tctatgtctt cttcaagggc gttaaggatc gcgtgaaggg aagaagcgat
     ccttaccacg ccaccaccgg cccactgagc ccatccaaag actgcggatc tccaaaatat
     gcttacttca atggctgctc ctcaccaacg gccccactct cacctatgtc tcctcctggg
     tacaagctgg tcactggtga cagaaacaat tcctcctgcc gcaattacaa caagcaagcc
     agcgagcaaa actgggcgaa ttacagcgca gagcaaaatc gaatggggca ggccggaagc
     accatctcca actcccacgc ccagccgttt gatttccctg acgacagcca aaatgccaaa
     aaagttgctg ctggacacga actccagccc ttagctatcg tggatcagcg accttccagc
     agagccagca gccgcgccag cagcagacct cggcctgatg acctggagat ttaaacaggc
     ttgaacatca agctgccaat cgattgtgga ggagaaaaaa aagggtgctt gcagaacgtg
4801 cacctggggt gttcatttcg ttcccgtgga ggtggtactc aacaacctca gtaatgaggc
```

added BSA, MilliQ water and new buffer), the unwanted plasmid fragment and restriction enzymes were removed by guanosine gel electrophoresis. The restricted plasmid was purified and a small aliquot checked by agarose gel electrophoresis.

The blunt-end Cx43 PCR product was then restricted with *Cla*I to make a complementary end for cloning into the *Eco*RV / *Cla*I / pBs KSII- vector (Figure 3.3). After isolation and purification, two hundred and thirty-six ng of the *Cla*I / Cx43 fragment was cloned into 100 ng of *Eco*RV / *Cla*I / pBs KSII- in a 80 µl ligation mix with 1 µl of T4 DNA Ligase (400 000 units / ml; Section 2.1.10). The plasmid was electroporated into TOP10F' cells and blue / white screened.

White colonies were analyzed by cracking (predicted size of 4.326 kb). One possible positive clone, designated C3, was verified by PCR using various connexin and pBs KSII- forward and reverse primers, and by restriction enzyme digests. Bi-directional sequencing with a combination of primers (HOTT3, HOTT7, CnxF, Cx43R, Cx43R2 and Cx43R3) so that each base was unambiguously determined at least twice, was also undertaken. The Cx43 forward primers Cx43F and CxF (provided by Dr Caryl Hill) were also used.

3.3 Results

3.3.1 SM22α / pBs KSII-

Three SM22α / pBs KSII- colonies (designated Clone #121, Clone #137 and Clone #139) amplified the requisite band (around 493 bases) on initial PCR screening with SM22ex1f and SM22ex1r. Subsequent screening on Clone #121 showed that the insert was present and in the correct orientation. As shown in Figure 3.9 (Table 2.2), the HOTT3 / HOTT7 primers amplified a band around the predicted size of 0.635 kb, and insert orientation was determined by the HOTT3 / SM22ex1r PCR (no band was amplified as expected) and the HOTT3 / SM22ex1f PCR (amplified a band around the

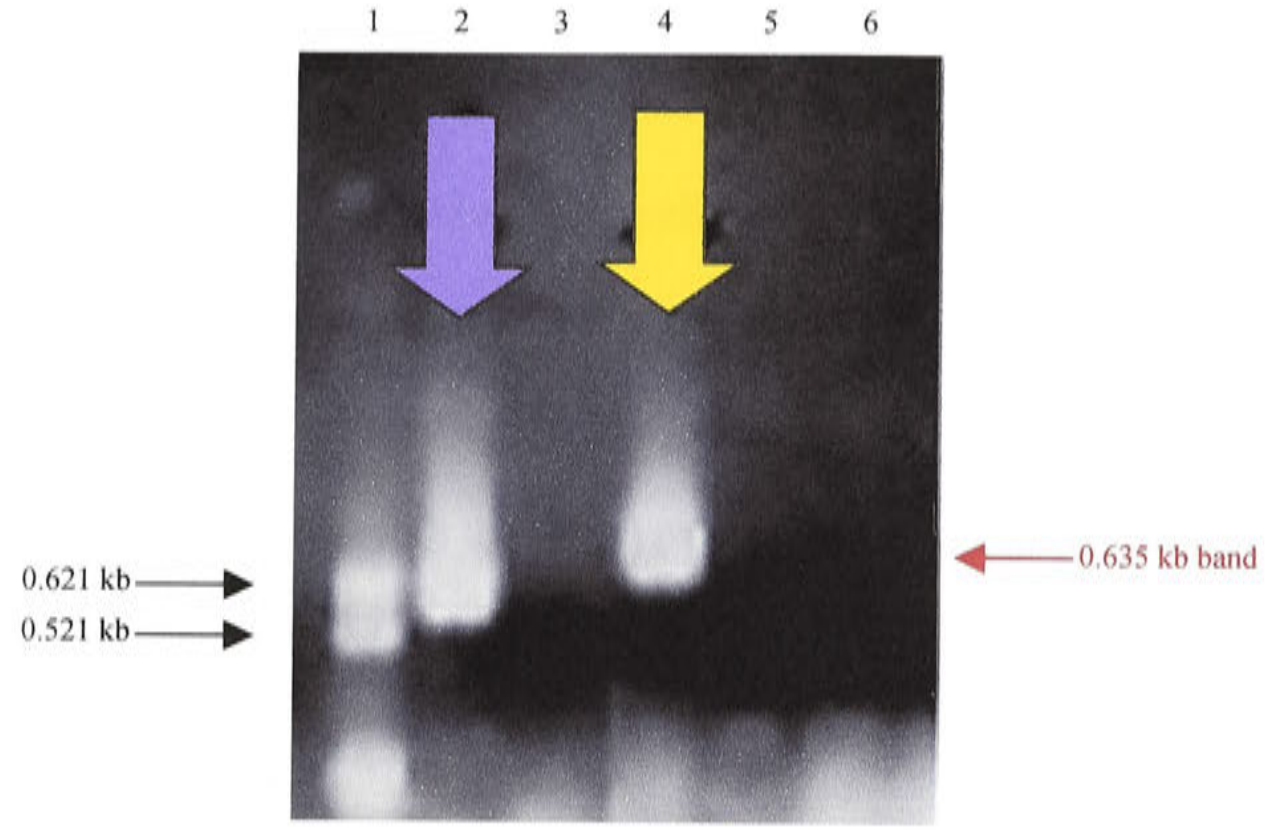

Figure 3.9 PCR screening of SM22α / pBs KSII- Clone #121

Three PCRs are shown, with the pTz / *Alu*I marker in Lane 1. In Lane 2, Clone #121 was screened with HOTT3 and SM22ex1f (positive for reverse orientation; purple arrow) and Lane 3, with HOTT3 and SM22ex1r (negative for reverse orientation). In Lane 4, Clone #121 was screened with HOTT3 and HOTT7 (positive for insert; yellow arrow). The water controls are in Lanes 5 and 6.

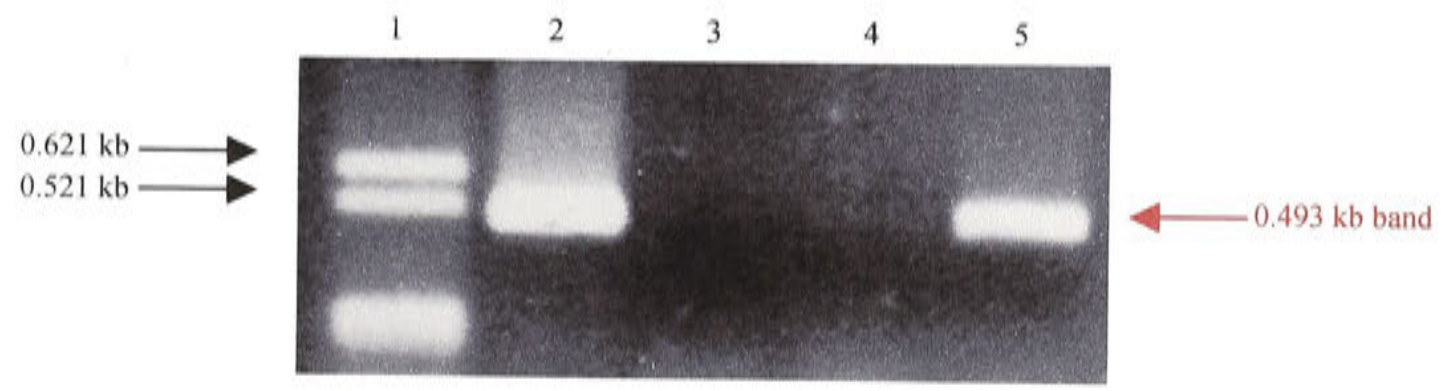

Figure 3.10 PCR screening of SM22α / pBs KSII- clones

PCR screening of Clone #137 and Clone #139 with the SM22ex1f and SM22ex1r primers (expected band size of 0.493 kb) revealed that only Clone #137 was positive (Lane 2). Clone #139 is in Lane 3 (negative), followed by the water control in Lane 4, and SM22α DNA in Lane 5. The pTz / *Alu*I marker is in Lane 1.

predicted size of 0.586 kb). Clones #137 and #139 were screened with the HOTT3 / HOTT7 primers (amplified a band around the predicted 0.635 kb) and the SM22ex1f / SM22ex1r primers (amplified a band around the predicted band size of 0.493 kb). Only Clone #137 was PCR positive for both sets of primers (Figure 3.10).

Subsequently, the two PCR positive SM22α / pBs KSII- clones (#121 and #137) were subjected to restriction analyses: 1) the single pBs KSII- cutters *Eco*RI and *Spe*I (both are non-cutters in the restricted SM22α promoter) each gave a band that corresponded with the predicted fragment size of 3.457 kb; 2) the combination of *Eco*RI and *Spe*I excised the SM22α promoter from SM22α / pBs KSII- giving two fragments that approximated the predicted band sizes of 518 bp and 2.939 kb (Figure 3.11).

Orientation of the SM22α promoter insert in Clones #121 and #137 was confirmed by restriction with the *Xba*I enzyme. *Xba*I cuts once in pBs KSII- (at position 681) and once in the SM22α promoter (at position 87), so an insert in the forward orientation should give bands which correspond with the predicted band sizes of 0.424 kb and 3.033 kb (as in Clone #137). An insert in the reverse orientation when restricted with *Xba*I, would produce two bands around the calculated band sizes of 0.105 kb and 3.352 kb, as was the case with Clone #121. *Bam*HI (a single cutter in pBs KSII- and a non-cutter in the SM22α promoter) restrictions on both clones gave linear bands which approximated the predicted band size of 3.457 kb.

The sequencing data showed that the SM22α / pBs KSII- clones had three (3) bp in the SM22α promoter which differed from the published database sequence (Figure 3.12).

3.3.2 Cx43 / pBs KSII-

The Clone designated C3 was verified by PCR screening (Table 2.2). Briefly, the HOTT3 and HOTT7 primers amplified a band around the predicted fragment size of 1.480 kb, and the HOTT3 and CnxF primers amplified a single band which

Figure 3.11 Verification of the SM22α / pBs KSII- Clones (#121 and #137)

Restriction enzyme digests on Clone #121 are shown in **(A)**, whilst restriction enzyme digests on Clone #137 are shown in **(B)** and **(C)**. The predicted size of the SM22α / pBs KSII- clone was 3.457 kb.

In **(A)**, *Eco*RI and *Spe*I each gave a band which corresponded with the predicted fragment size of 3.457 kb, whilst *Eco*RI and *Spe*I (Lane 5) excised the SM22α promoter, giving two fragments that approximated the predicted band sizes of 0.518 kb and 2.939 kb. An *Xba*I restriction (Lane 6) produced two bands around the calculated band sizes of 0.105 kb and 3.352 kb (the former band could not be visualized on the gel), which confirmed the reverse orientation of the SM22α promoter insert in Clone #121. A *Bam*HI restriction (a single cutter in pBs KSII- and a non-cutter in the SM22α promoter; Lane 8) gave a linear band which approximated the predicted band size of 3.457 kb.

A *Bam*HI restriction on Clone #137 also gave a linear band which corresponded with the predicted fragment size of 3.457 kb **(B)**. Orientation (forward) of the SM22α promoter insert in this clone was confirmed by an *Xba*I restriction, which produced two fragments corresponding with the predicted band sizes of 0.424 kb and 3.033 kb **(C)**.

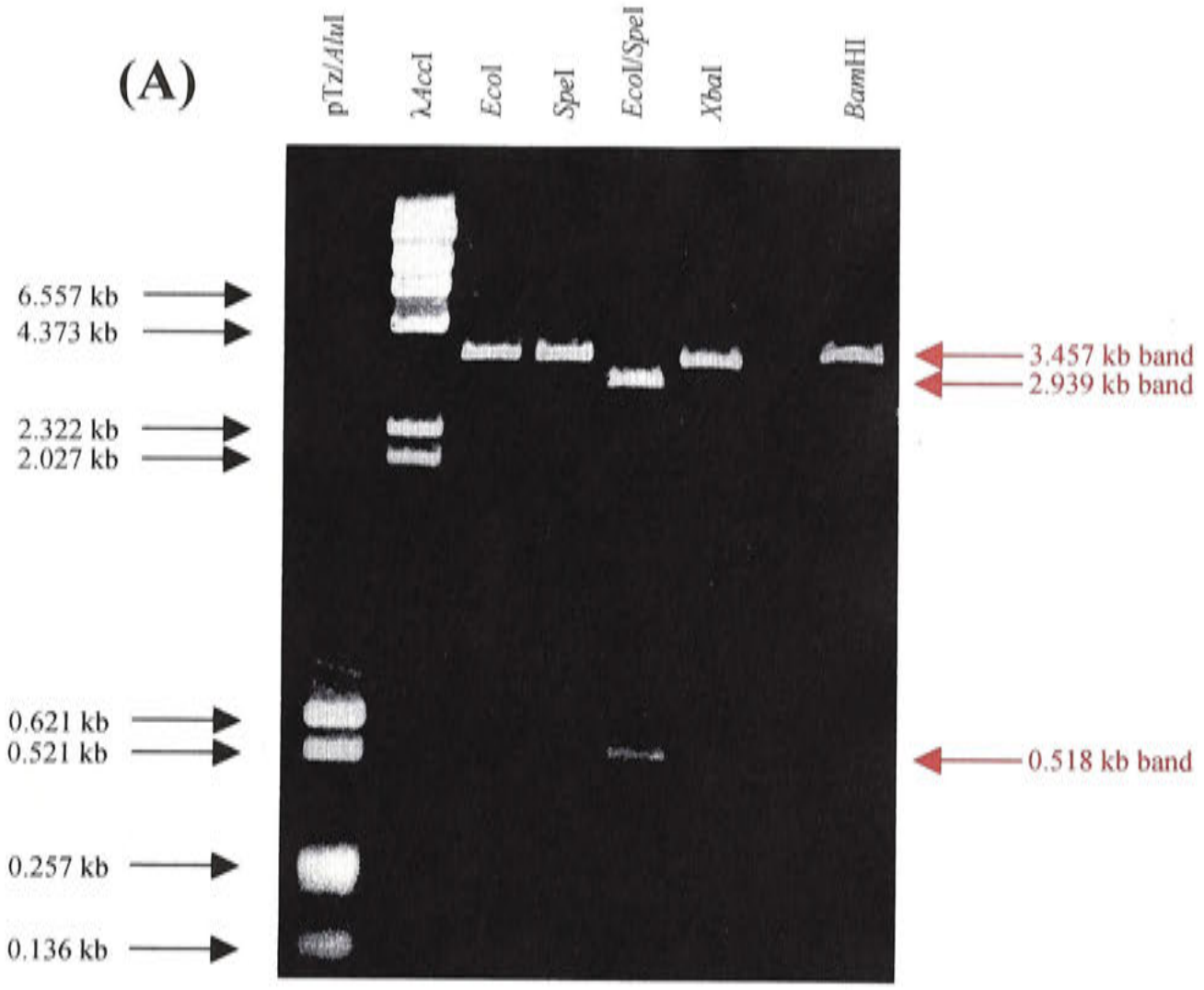
(A)
pTz/AluI
λAccI
EcoI
SpeI
EcoI/SpeI
XbaI
BamHI
6.557 kb
4.373 kb
2.322 kb
2.027 kb
0.621 kb
0.521 kb
0.257 kb
0.136 kb
3.457 kb band
2.939 kb band
0.518 kb band

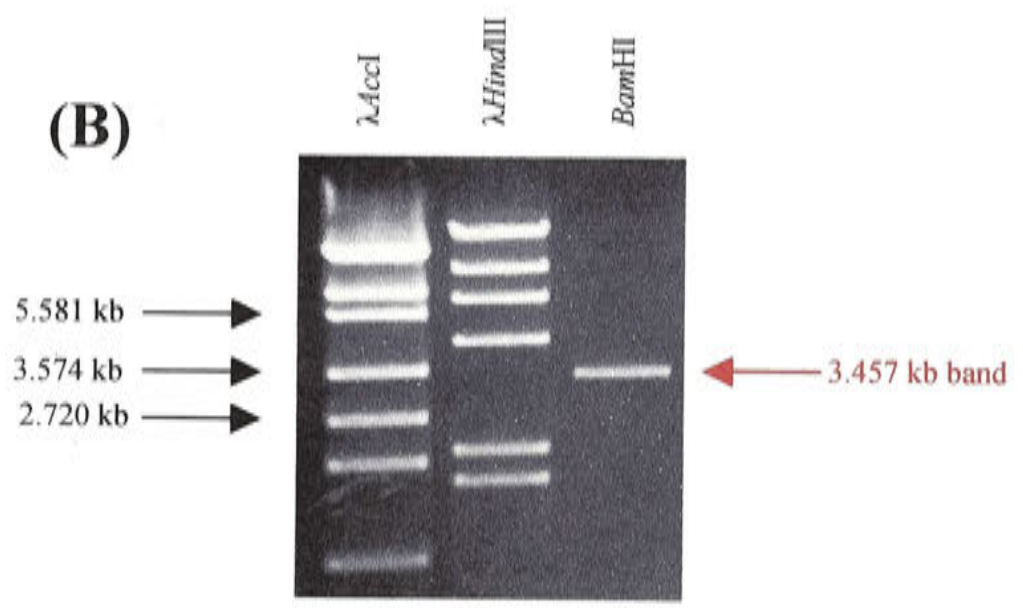
(B)
λAccI
λHindIII
BamHI
5.581 kb
3.574 kb
2.720 kb
3.457 kb band

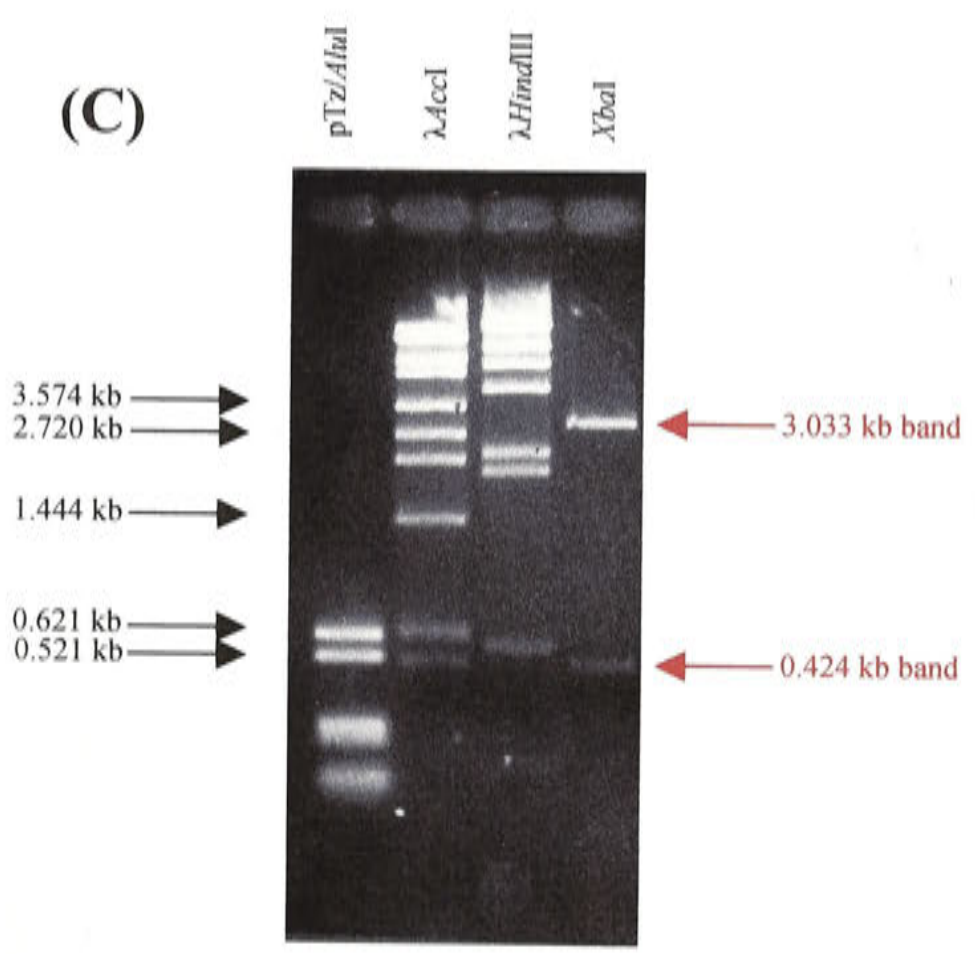
(C)
pTz/AluI
λAccI
λHindIII
XbaI
3.574 kb
2.720 kb
1.444 kb
0.621 kb
0.521 kb
3.033 kb band
0.424 kb band

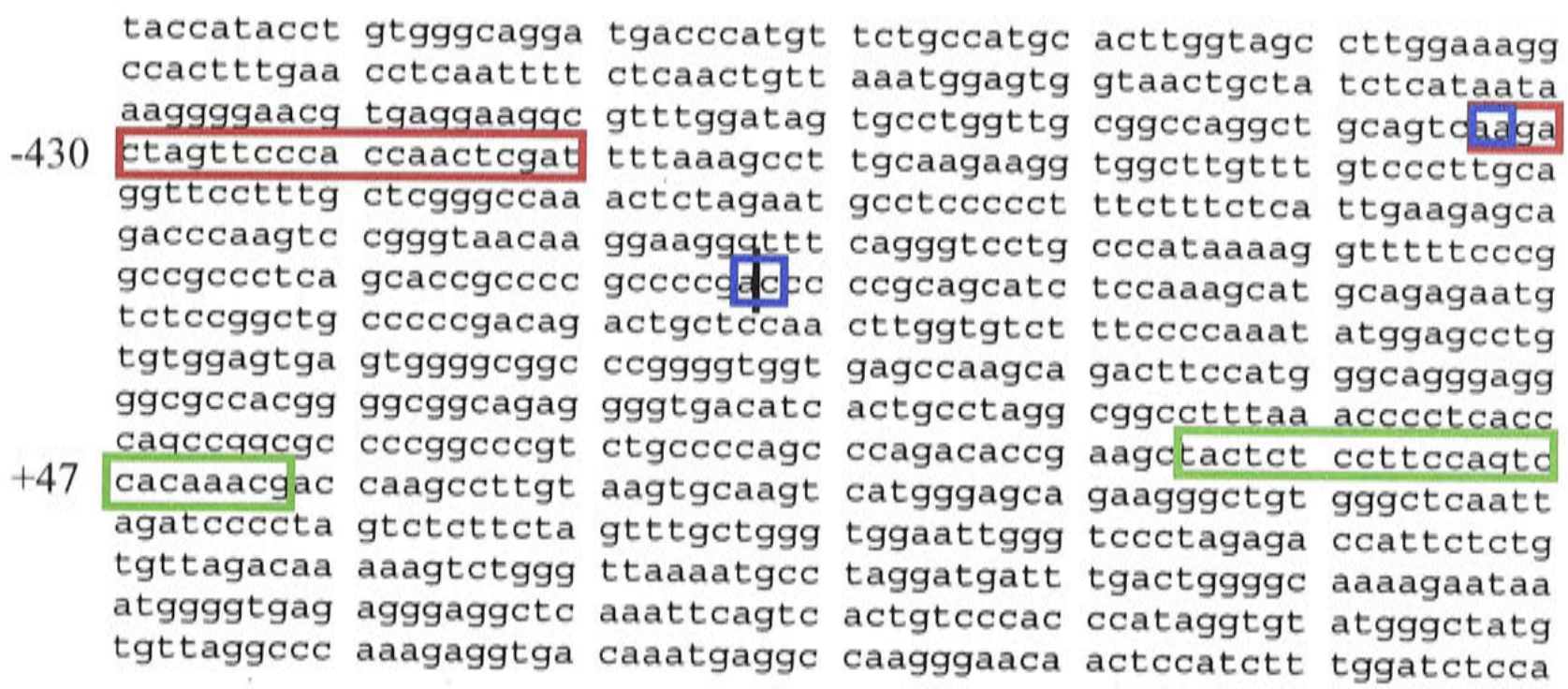

KEY:

SM22ex1f primer

SM22ex1r primer

Figure 3.12 Sequencing of SM22α / pBs KSII- clones

Clones #121 and #137 were sequenced in both directions. The sequences differed from the published sequence by three bases, as indicated by the blue boxes.

An extra C between the A and C

Loss of the two As at the proximal end of the forward primer

approximated the predicted fragment size of 1.390 kb. The HOTT7 and CnxF primers did not amplify any band; the CxR3 and CnxF primers amplified a single band around the predicted fragment size of around 0.680 kb; the CxR2 and CnxF primers amplified a single band around the predicted fragment size of 1.018 kb, and the HOTT7 and CxR2 primers amplified a single band of about 1.268 kb.

Further verification of the C2 clone was by restriction enzyme digests, as shown in Figure 3.13. *Cla*I (a single cutter in pBs KSII- and a Cx43 cDNA non-cutter) gave a linear band which corresponded with the predicted fragment size of 4.326 kb. Single *Bam*HI (single cutter in pBs KSII- and a non-cutter in Cx43) and *Eco*RI (single cutter in pBs KSII- and a non-cutter in Cx43) restriction digests each gave a linear band, which approximated the predicted band size of 4.326 kb. The double restriction enzyme digests *Bam*HI / *Cla*I and *Eco*RI / *Cla*I each excised the Cx43 gene fragment (single band sizes of about 1.417 kb for *Cla*I / *Bam*HI, and 1.384 kb for *Cla*I / *Eco*RI).

Finally, the sequence of the clone did not differ from the published sequence (Figure 3.8).

PART II – Cloning of the Cx43 / pBi5 construct

3.4 Additional Methods

3.4.1 Preparation and verification of the pBi5 plasmid

A small aliquot of the pBi5 plasmid was quantified at OD_{260} and verified by 20 µl restriction analyses using *Aat*II (a single cutter in pBi5 which gave a linear band around the predicted size of 6.083 kb), *Ase*I (cuts twice at 1.827 kb and 3.062 kb, and produced fragments around the predicted band sizes of 4.848 kb and 1.235 kb), *Aat*II / *Ase*I (three fragments were generated around the predicted sizes of 4.086 kb, 1.235 kb and 0.762 kb), *Cla*I (cuts once at 629 bp and produced a linear band approximating the predicted size of 6.083 kb), *Pvu*II (a single cutter at 603 bp, so a linear band of about

Figure 3.13 Restriction enzyme verification of Cx43 / pBs KSII-

The *Cla*I restriction (a single cutter in pBs KSII- and a Cx43 cDNA non-cutter) digest on Cx43 / pBs KSII- gave an expected linear band around the 4.373 kb band of λ*Hind*III **(A)**. This corresponded with the predicted fragment size of 4.326 kb. In **(B)**, the single cutters *Bam*HI (Lane 4) and *Eco*RI (Lane 5) each gave a linear band, which approximated the predicted band size of 4.326 kb. The double restriction enzyme digests of *Bam*HI / *Cla*I and *Eco*RI / *Cla*I are shown in Lanes 5 and 7 of **(C)**. Both combinations excised the Cx43 gene fragment (estimated band sizes of 1.417 kb for *Cla*I / *Bam*HI, and 1.384 kb for *Cla*I / *Eco*RI).

(A)

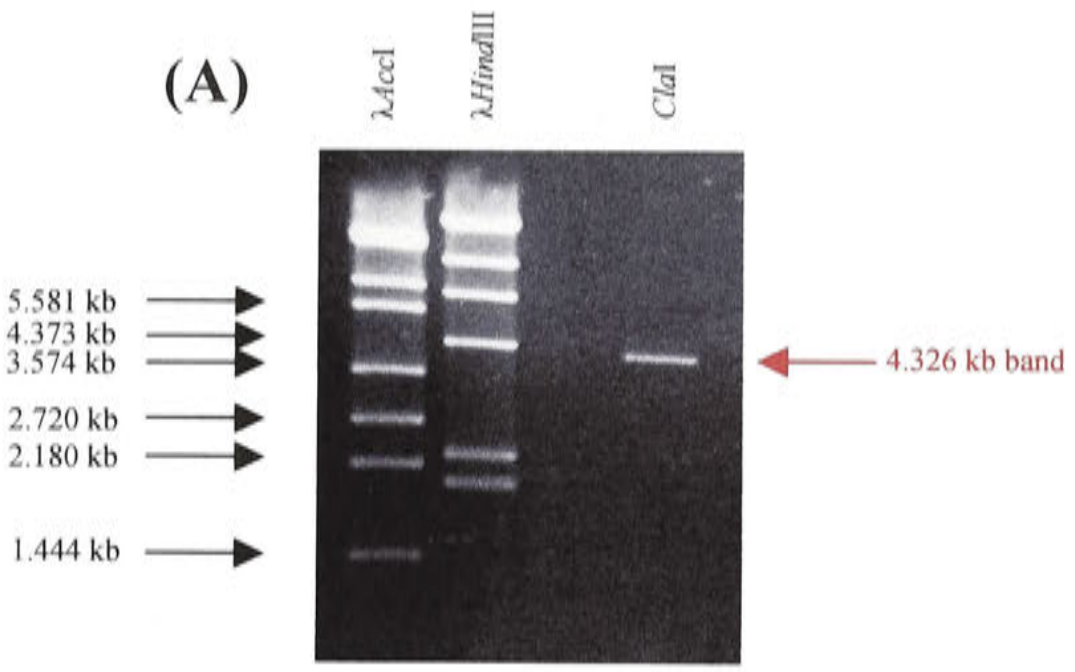
λAccI
λHindIII
ClaI
5.581 kb
4.373 kb
3.574 kb
2.720 kb
2.180 kb
1.444 kb
4.326 kb band

(B)

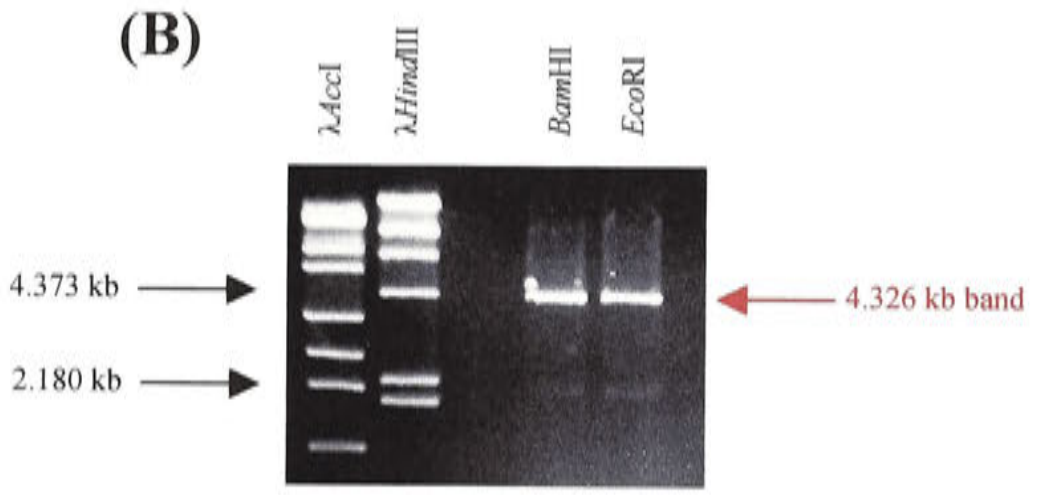
λAccI
λHindIII
BamHI
EcoRI
4.373 kb
2.180 kb
4.326 kb band

(C)

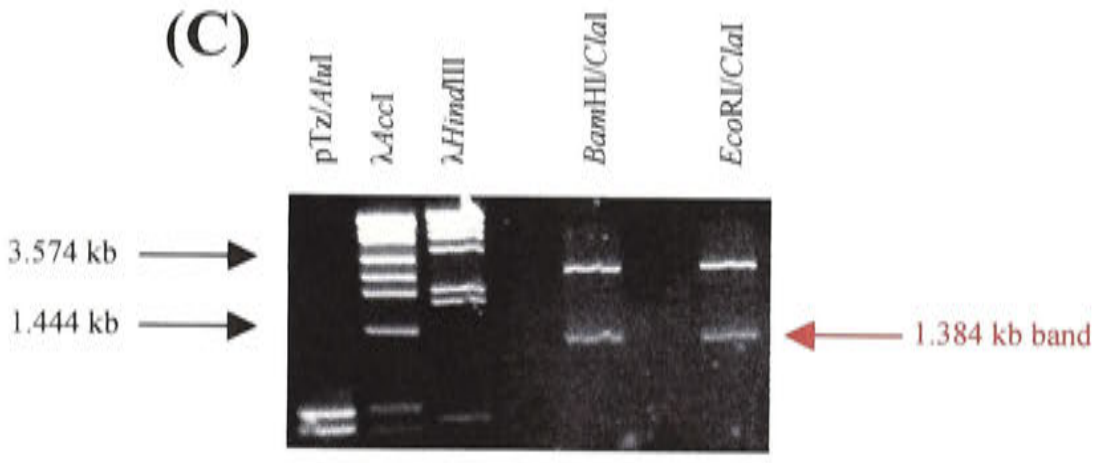
pTz/AluI
λAccI
λHindIII
BamHI/ClaI
EcoRI/ClaI
3.574 kb
1.444 kb
1.384 kb band

6.083 kb was produced), and *Cla*I / *Pvu*II will remove 26 base pairs which will not be visible on a gel, giving a linear band around an estimated band size of 6.057 kb.

One hundred nanograms of the plasmid was then restricted with *Cla*I and *Pvu*II to remove part of the multiple cloning site. The product was assessed by agarose gel electrophoresis before isolation, purification and assessment by agarose gel electrophoresis.

3.4.2 Preparation of the Cx43 / pBs KSII- plasmid

Cx43 / pBs KSII- (2 μg) was restricted with *Eco*RI at 37°C for 1.5 hours and then heat inactivated (65°C for 20 minutes) before blunt-ending with Klenow. The sample was purified and assessed by agarose gel electrophoresis. Two micrograms of *Eco*RI / Cx43 / pBs KSII- were restricted with *Cla*I, isolated by guanosine gel electrophoresis and purified before agarose gel electrophoresis.

3.4.3 Cloning of the insert into the vector

The *Eco*RI / *Cla*I / Cx43 / pBs KSII- insert was ligated into the *Cla*I / *Pvu*II / pBi5 vector with an insert to vector ratio of 5 to 1, and using 100 ng vector with 1 μl of T4 DNA Ligase. Colonies were screened by cracking, with ten positive for the Cx43 insert when compared to the control plasmid. Verification of the Cx43 / pBi5 clones was by PCR using the Cx43R3 and CnxF primers (this reverse primer was chosen as the *Cla*I / Cx43 restriction had removed 13 bases from the original CnxR primer; Table 2.2). The single clone giving the strongest band in the PCRs (designated Clone 20) was chosen for restriction analyses, and together with one other clone (designated Clone 3 (Lane 5); Figure 3.14) was bi-directionally sequenced with the CnxF, CxF, Cx43F and Cx43R2 primers. Two new primers were designed using MacVector to sequence through the multiple cloning site (designated pBi5R and pBi5F). Clone 20 was further verified by restriction analyses.

3.5 Results

Nine Cx43 / pBi5 colonies were PCR positive with the Cx43R3 and CnxF primers, producing a fragment around the predicted band size of 1 kb (Figure 3.14). The clone producing the strongest band (Clone 20) was then subject to restriction analyses (estimated plasmid size of 7.357 kb; Figure 3.15). *Ase*I (cuts twice in pBi5 at 1.827 kb and 3.062 kb, and is a non-cutter in the Cx43 gene fragment) gave fragment sizes which corresponded to the predicted values of 1.235 kb and 6.122 kb; *Aat*II (a single cutter in pBi5 at 3.809 kb) produced a linear band around 7.357 kb; *Ase*I / *Aat*II gave fragment sizes which corresponded to the predicted bands of 1.234 kb, 0.763 kb and 5.359 kb; *Sph*I (a single cutter in pBi5 at 5.411 kb) gave a linear fragment around the predicted size of 7.357 kb), *Bam*HI (a triple enzyme cutter in pBi5 at 0.591 kb, 4.344 kb and 4.362 kb, produced the expected fragment sizes of 2.312 kb, 3.753 kb and 0.018 kb (data not shown); and *Sph*I / *Bam*HI produced three fragments which corresponded with the predicted sizes of 5.027 kb, 1.263 kb, 1.049 and 0.018 kb. In both cases, the 18 bp band was too small to be visualized on the agarose gel.

The sequencing data showed that no base changes had occurred during the cloning process, and the orientation of the construct in pBi5 was confirmed.

PART III – Cloning of the SM22a / Cx43 / pBs KSII- construct

3.6 Additional Methods

3.6.1 Cloning of the SM22α / Cx43 construct

3.6.1.1 Preparation of the SM22α / pBs KSII- plasmid

The SM22α / pBs KSII- plasmid Clone #137 (SM22α in the forward orientation) was verified by repeating the *Spe*I, *Xba*I and *Bam*HI restrictions. Three micrograms of the plasmid were then linearized using *Bam*HI. After assessment by agarose gel

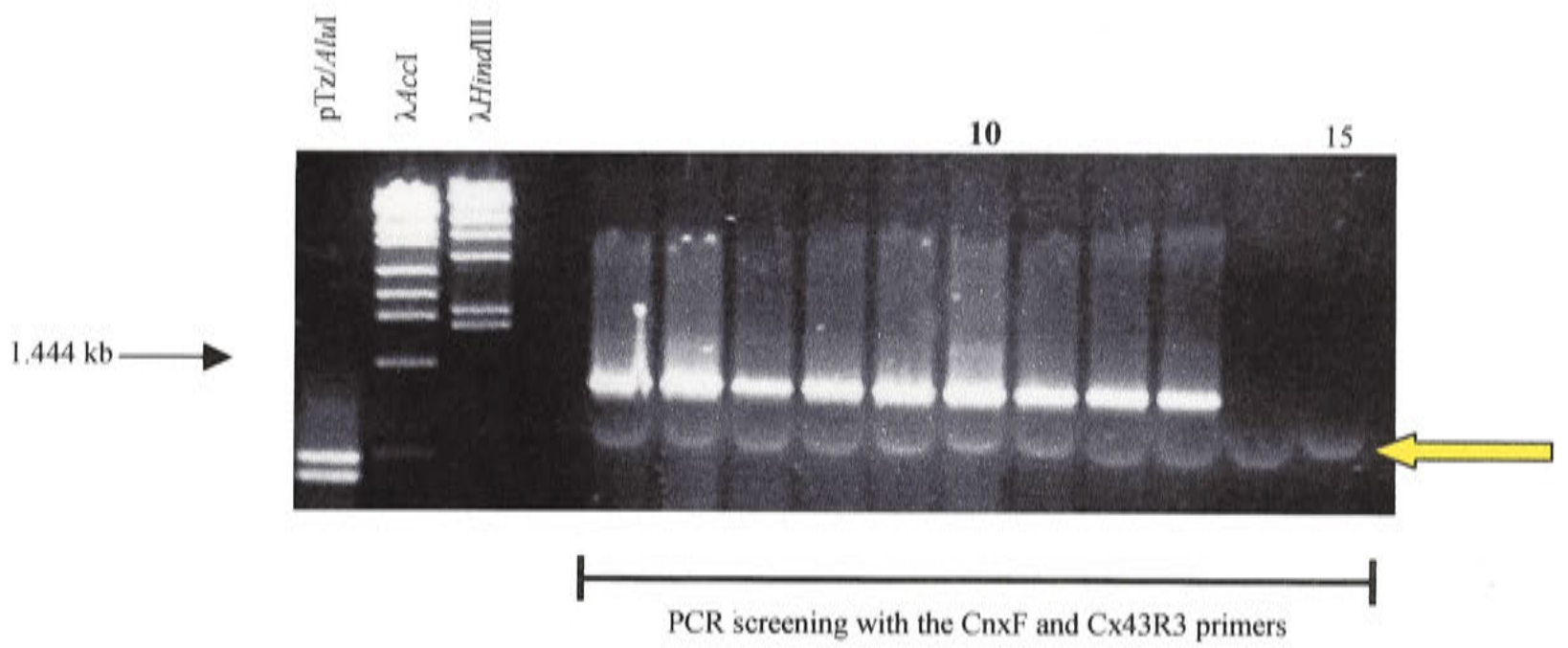

Figure 3.14 PCR testing of Cx43 / pBi5 colonies

The CnxF and Cx43R3 PCR is shown. All colonies except the one in Lane 14 (designated # 47) showed the expected PCR product size of 1 kb. The dye line is indicated by the yellow arrow. The clone in Lane 10 (designated C20) was selected as the potential stock colony. Lane 15 was the water control.

Figure 3.15 Verification of the Cx43 / pBi5 clone

The Cx43 / pBi5 clone (calculated to be 7.357 kb) designated Clone 20 was verified using restriction enzyme analyses. In **(A)**, the single cutter *Aat*II gave a linear band around the predicted band size of 7.357 kb, whilst *Ase*I (cuts twice) produced two fragments of approximately 1.235 kb and 6.122 kb as expected. The *Aat*II / *Ase*I restriction produced three bands which approximated the predicted fragment sizes of 5.359 kb, 1.234 kb and 0.764 kb.

The *Sph*I and *Sph*I / *Bam*HI restrictions are shown in **(B)**. *Sph*I produced a linear band of about 7.357 kb. The *Sph*I / *Bam*HI restriction produced three of the predicted four bands as the 0.018 kb band was too small to be visualized on an agarose gel.

(A)

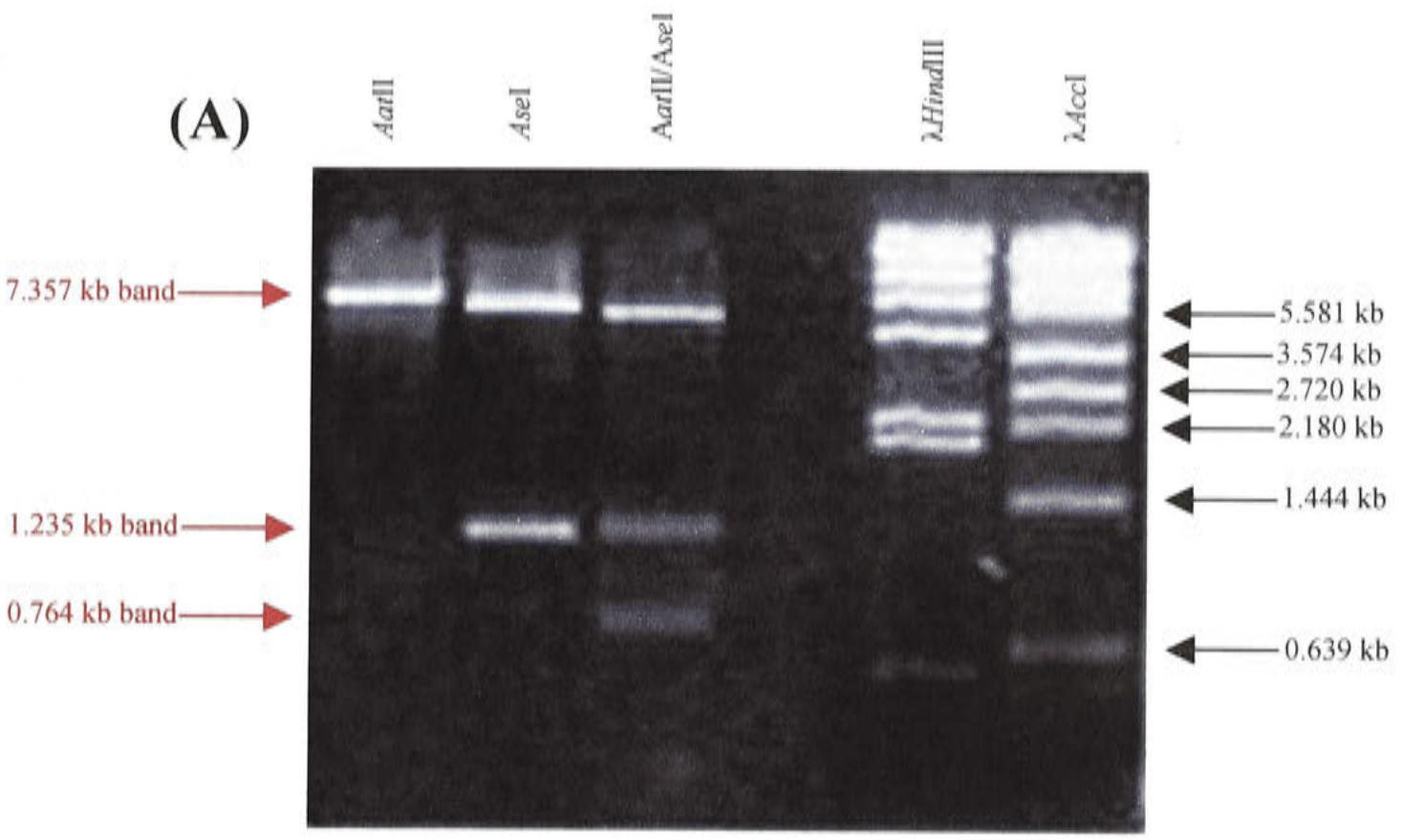
AatII
AseI
AatII/AseI
λHindIII
λAccI
7.357 kb band
1.235 kb band
0.764 kb band
5.581 kb
3.574 kb
2.720 kb
2.180 kb
1.444 kb
0.639 kb

(B)

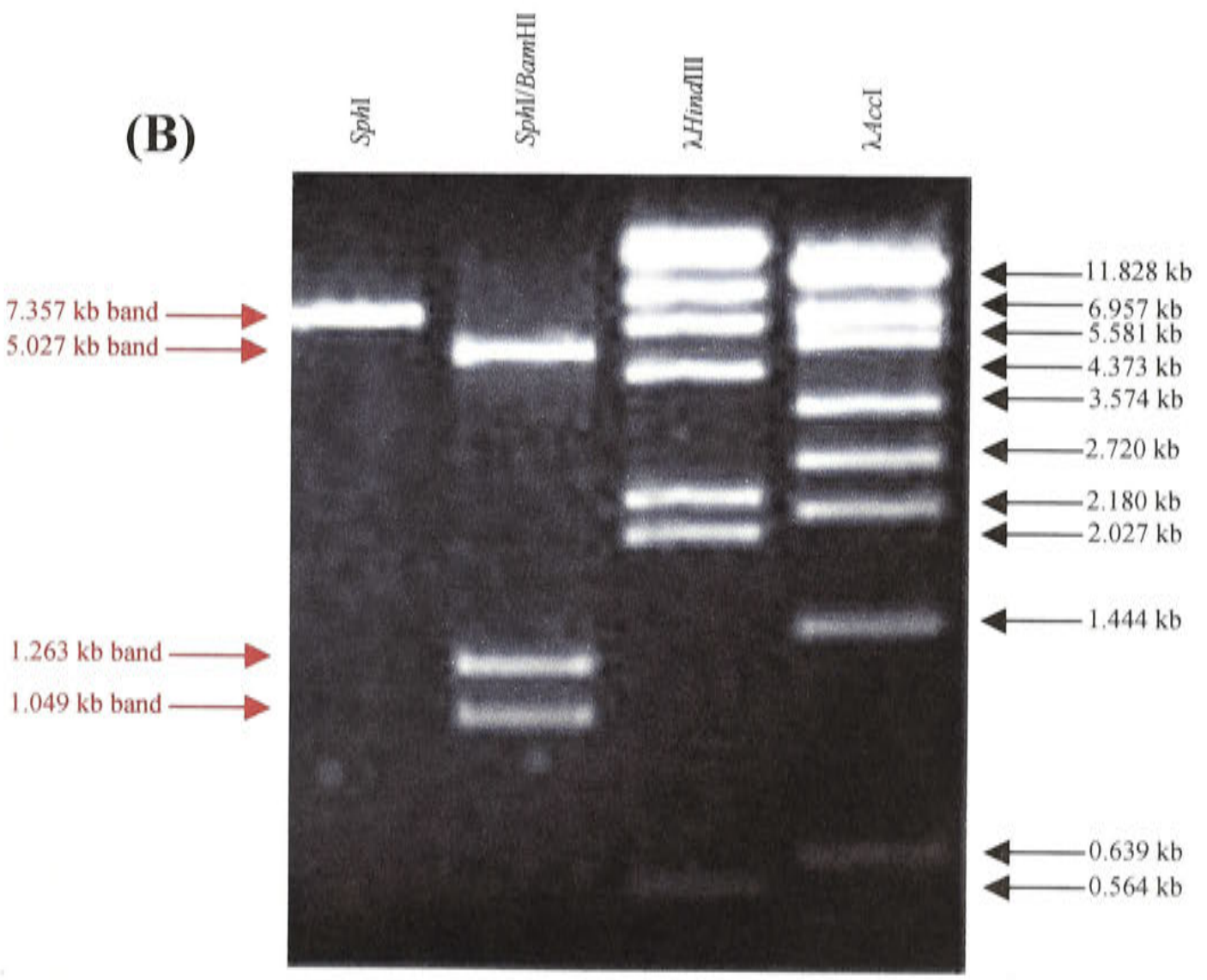
SphI
SphI/BamHI
λHindIII
λAccI
7.357 kb band
5.027 kb band
1.263 kb band
1.049 kb band
11.828 kb
6.957 kb
5.581 kb
4.373 kb
3.574 kb
2.720 kb
2.180 kb
2.027 kb
1.444 kb
0.639 kb
0.564 kb

electrophoresis, the DNA was dephosphorylated and purified before repeat electrophoresis.

3.6.1.2 Preparation of the Cx43 / pBi5 plasmid

The Cx43 / polyA signal fragment was excised from 2.5 μg of the Cx43 / pBi5 plasmid in a large restriction digest with *Bam*HI, *Ase*I and *Sph*I. The DNA was checked, and the fragment isolated and purified.

3.6.1.3 Cloning of the insert into the vector

After the *Bam*HI / *Ase*I / Cx43 / polyA insert was ligated into the *Bam*HI / SM22α / pBs KSII- vector, the 3' ends were filled-in with Klenow. The sample was purified and assessed by agarose gel electrophoresis, before another 1 μl of T4 DNA Ligase was added to the mix, followed by overnight ligation at 16°C. The vector was transformed and resulting colonies screened by cracking. Five positive SM22α / Cx43 / polyA / pBs KSII- (SM22α / Cx43 / pBs KSII-) clones were chosen for verification by PCR screening, restriction enzyme analyses, and bi-directional sequencing using a variety of primers (SM22ex1f, SM22ex1r, CnxF, CxF, Cx43F, Cx43R2, pBi5 3', HOTT3 and HOTT7) so that each base was determined at least twice. The construct was evaluated in cell cultures of murine smooth muscle cells and embryonic fibroblasts using immunohistochemistry.

3.6.1.4 Preparation and electroporation of the SM22α / Cx43 / pBs KSII-

*Kpn*I (a single cutter in pBs KSII- at position 759) and *Pvu*I (a double cutter in pBs KSII- at positions 500 and 2416, and a non-cutter in the SM22α promoter and Cx43 gene fragment) excised the SM22α / Cx43 / polyA signal insert from 4 μg of the SM22α / Cx43 / pBs KSII- plasmid (Figure 3.5). After isolation, purification and assessment by agarose gel electrophoresis, 6 μg of the fragment was co-electroporated into BALB/c

(white) murine embryonic stem (ES) cells with a circular resistance plasmid pMClNeo, and subsequently selected with G418.

The seven antibiotic resistant colonies (diluted in $T_{10}E_{0.1}$ to give a final concentration of 20 ng / µl of which, 5 µl was used in each PCR) were screened by PCR using gene specific primers to confirm which clones possessed a stably incorporated copy of the gene. Two new primers were designed and synthesized to maximize the sensitivity of the PCR for the SM22α promoter: mSM22ex1f (re-synthesized), mSM22ex1fb and mCnx43R (see Table 2.2).

3.6.1.5 Screening of the progeny

Progeny were screened by PCR. To test whether the SM22α promoter was present but truncated in the mice, three new forward primers in the SM22α promoter region were designed and synthesized, mSM22F2, mSM22F6 and mSM22F7 (see Figure 3.6; Table 2.2), and one reverse primer in the Cx43 gene (mCx435'R).

3.7 Results

3.7.1 Cloning of SM22α / Cx43

(a) PCR screening

The PCRs showed that for all five clones, the insert was present and in the correct orientation, which was quite surprising as the cloning was not directional (Figure 3.16). Briefly, the SM22ex1f and pBi5R primers amplified a band around the predicted size of 1.99 kb, the SM22ex1f and Cx43R2 primers amplified a band around the predicted size of 1.47 kb, the SM22ex1f and HOTT7 primers (to screen the whole insert from the promoter through the gene and into pBluescript) amplified a band about 3.5 kb as expected, and the HOTT3 and Cx43R2 primers (to screen from pBluescript to the start of the Cx43 gene) amplified a band size of around the predicted 1.4 kb.

Figure 3.16 PCR screening of SM22α / Cx43 / pBs KSII- colonies

In **(A)**, Lanes 3 to 7 contain the five colonies that were screened by the ensuing PCRs. The SM22ex1f and Cx43R2 PCR produced the expected 1.47 kb band size. The HOTT3 and Cx43R2 PCR **(B)** produced a band which approximated the predicted band size of 1.4 kb, whilst the SM22ex1f and HOTT7 PCR amplified a fragment of about 3 kb. The water control was in Lane 3. The apparent upward slope of the bands in Lanes 4 to 7 inclusive, was due to gel artifact. The relative positions of the primers is shown in **(C)**, which is not drawn to scale.

(A)

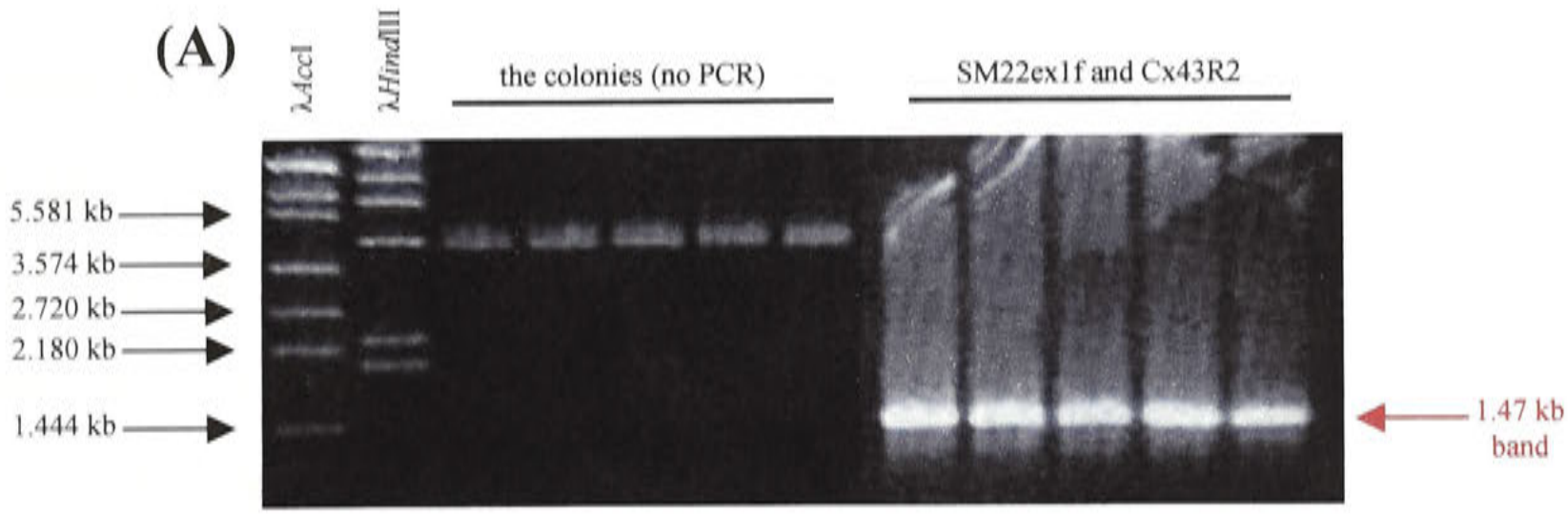
λAccI
λHindIII
the colonies (no PCR)
SM22ex1f and Cx43R2
5.581 kb
3.574 kb
2.720 kb
2.180 kb
1.444 kb
1.47 kb band

(B)

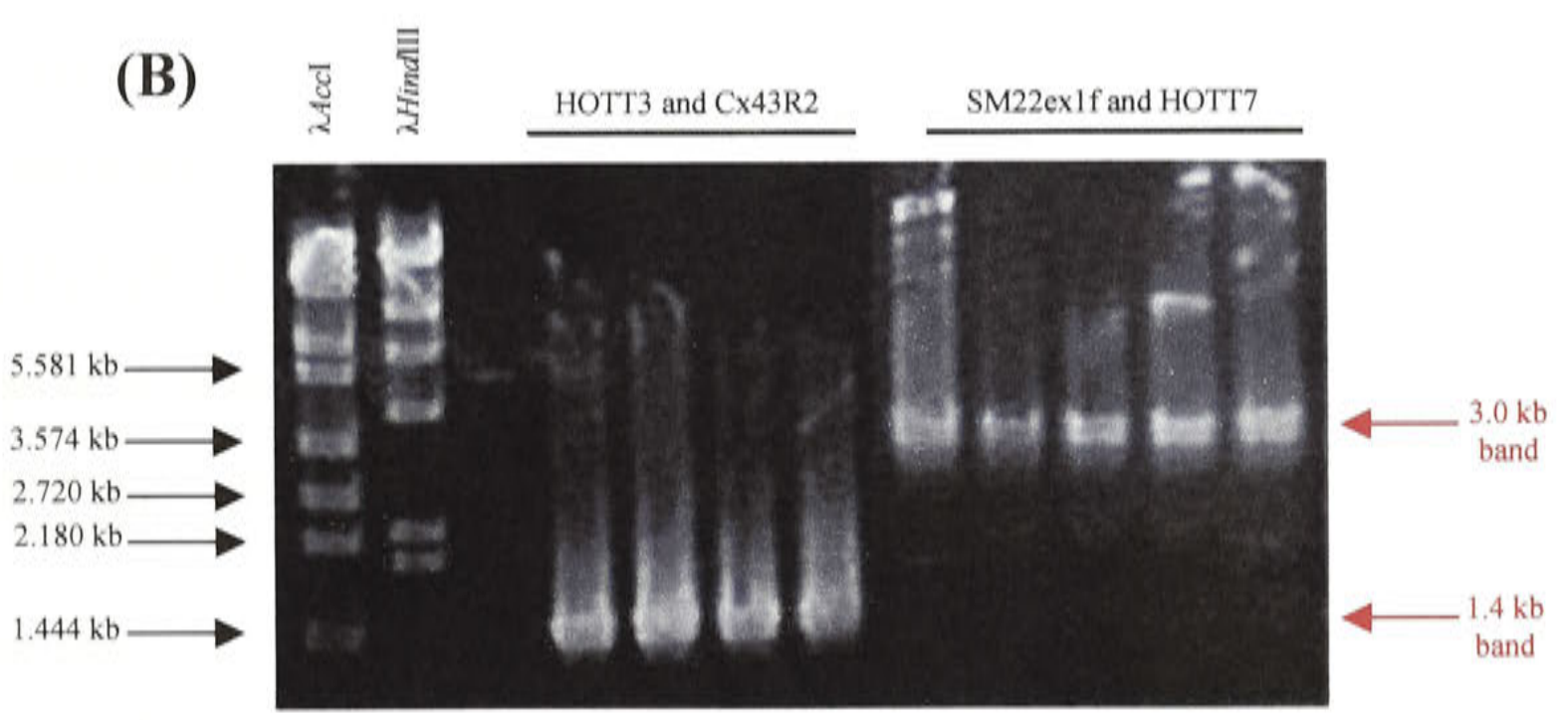
λAccI
λHindIII
HOTT3 and Cx43R2
SM22ex1f and HOTT7
5.581 kb
3.574 kb
2.720 kb
2.180 kb
1.444 kb
3.0 kb band
1.4 kb band

(C)

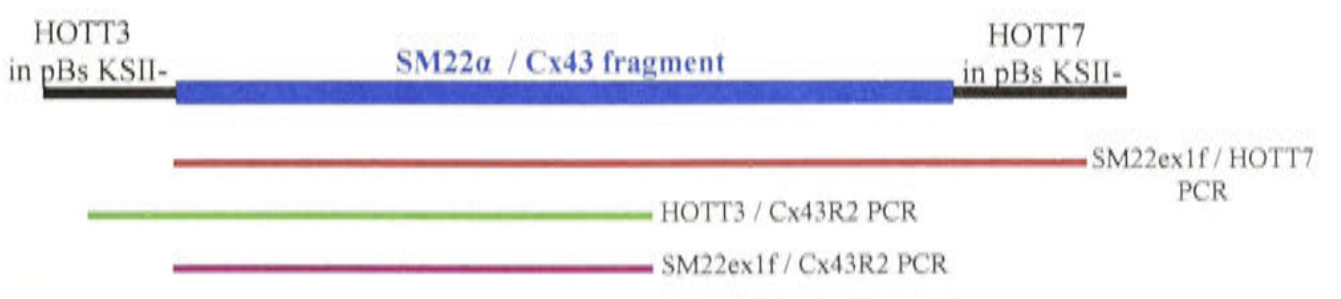
HOTT3 in pBs KSII-
SM22α / Cx43 fragment
HOTT7 in pBs KSII-
SM22ex1f / HOTT7 PCR
HOTT3 / Cx43R2 PCR
SM22ex1f / Cx43R2 PCR

(b) Restriction analyses

Restriction analyses confirmed that for all clones, each segment of the construct was present in the clones. The single cutters *Sph*I (cuts in the SM22α restricted promoter) and *Bam*HI (cuts in pBi5) each gave a single band around the predicted band size of 5.9 kb (Figure 3.17). A single *Not*I restriction produced a linear band of approximately 5.9 kb as expected, and when combined with *Xho*I (a single cutter in pBs KSII-) one band, assumed to be a doublet containing the predicted band sizes of 2.7 kb and 2.9 kb, was produced. A *Bam*HI (a single cutter between the SM22α promoter and the Cx43 / polyA fragment) / *Sac*II restriction produced two bands which approximated the predicted band sizes of 3.09 kb and 2.81 kb.

One colony (designated Clone #57) was chosen, based on band intensity, to be the stock colony. *Kpn*I and *Pvu*I excised the SM22α / Cx43 / polyA insert from SM22α / Cx43 / pBs KSII- (Clone #57) generating three bands around the expected band sizes of 1.045 kb, 1.657 kb and 2.999 kb (the latter was the desired fragment), while the fourth and smallest band (0.199 kb) expected from this restriction digest, was not visible on the gel (Figure 3.18).

(c) Sequencing

The data showed that the restricted SM22α promoter and the Cx43 / polyA signal sequences did not differ from the published genomic sequences and the consensus sequence, apart from the three base pairs in the SM22α promoter as already noted (see Figure 3.12).

3.7.2 Testing in cell culture

Data from the single transfections of SM22α / Cx43 / pBs KSII- in the aortic smooth muscle cells are presented in Figure 3.19A and B. Expression was detected by immunohistochemistry. There was no expression in the fibroblasts (Figure 3.19C) as

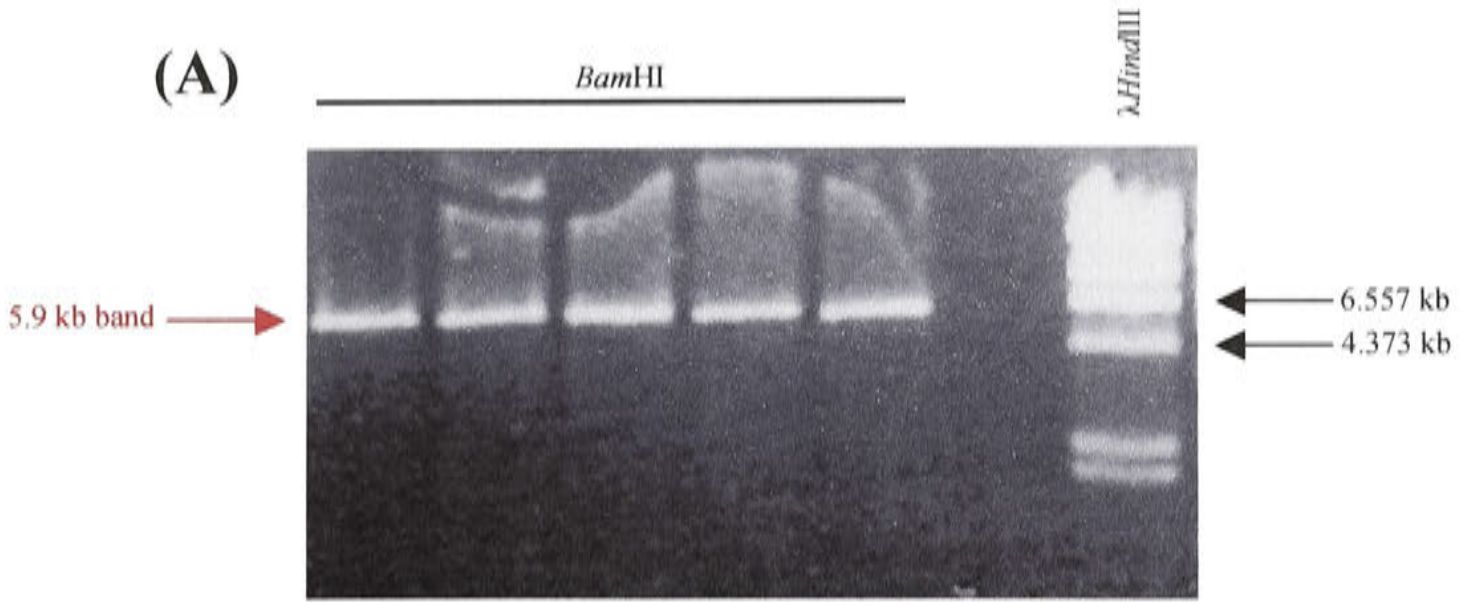

Figure 3.17 Restriction enzyme digests on the colonies

Restriction enzyme analyses performed on five SM22α / Cx43 / pBs KSII- colonies (designated 11, 19, 21, 46 and 57) are shown **(A)**, **(B)** and **(C)**. In **(A)**, *Bam*HI gave a linear band around 5.9 kb for all clones. The *Bam*HI / *Sac*II restriction **(B)** produced three bands, two of which corresponded with the predicted band sizes of 3.09 kb and 2.81 kb, with the third band representing uncut plasmid. The *Not*I / *Xho*I restriction produced two bands as expected around 2.7 kb and 2.9 kb (seen as a doublet), whilst *Not*I gave a linear band around the predicted band size of 5.9 kb **(C)**.

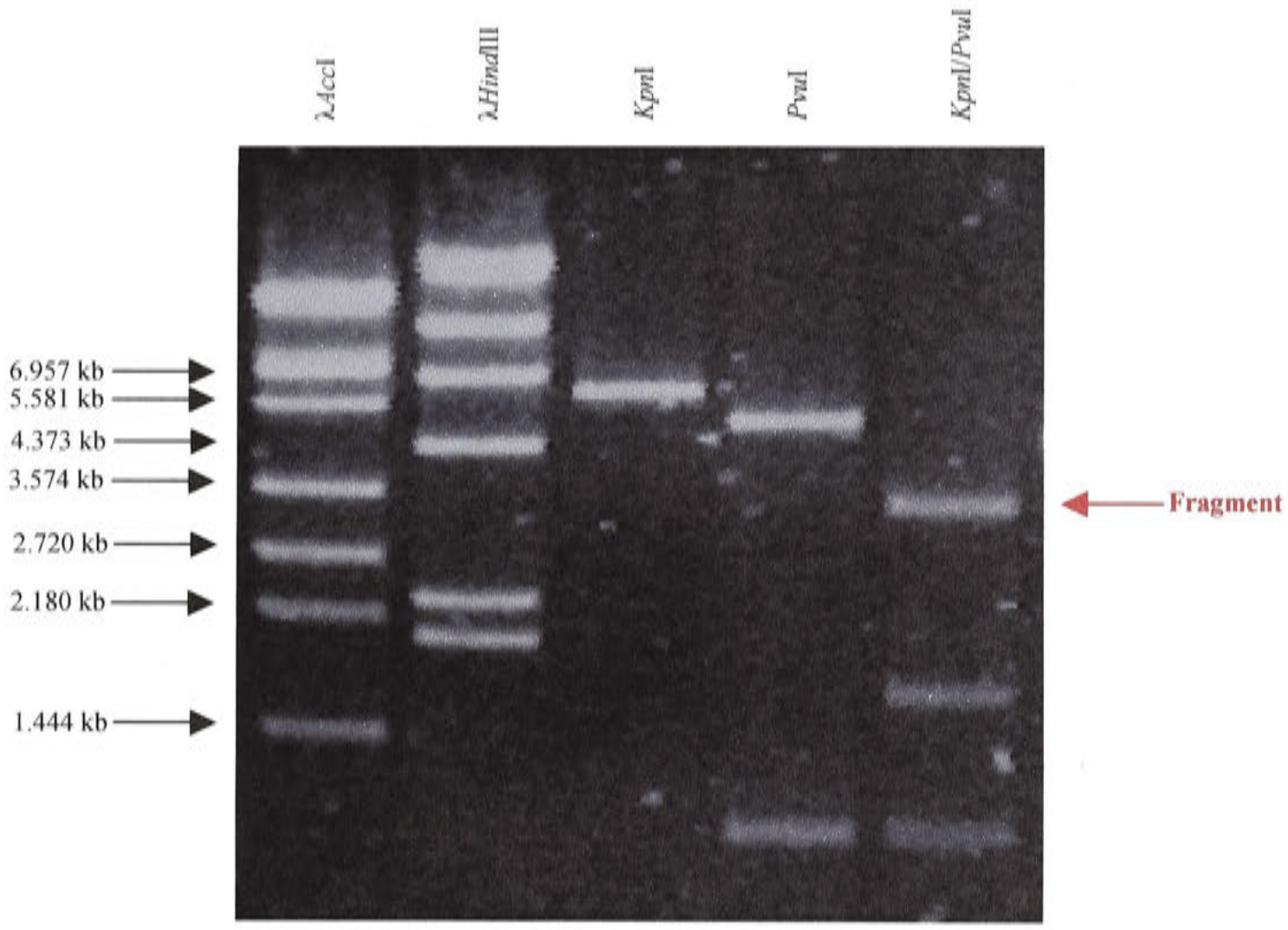

Figure 3.18 Restriction enzyme digests using *Kpn*I and *Pvu*I.

The *Kpn*I restriction gave the predicted fragment size of 5.9 kb whilst the *Pvu*I restriction produced bands which corresponded with the predicted band sizes of 1.045 kb and 4.855 kb. *Kpn*I / *Pvu*I effectively excised the SM22α / Cx43 / polyA signal fragment producing fragments which corresponded with the predicted band sizes of 1.045 kb, 1.657 kb and 2.999 kb (the desired fragment; approximate estimation), with the 0.199 kb not able to be visualized on the gel.

Figure 3.19 Graph of the single transfections of the smooth muscle cells.

Results from single transfections of the smooth muscle cells using the SM22α / Cx43 / pBs KSII- construct are shown **(A)** and **(B)**. **(B)** is an enlarged version of **(A)**. Single transfections of the fibroblasts are shown in **(C)**. The pEGFP-NI (CMV-EGFP) plasmid was used as the control. Expression of the SM22α / Cx43 / pBs KSII- construct was detected by immunohistochemistry using commercial antibodies. The number of labelled cells counted was expressed as a percentage of the total cell count for each slide ($n = 4$ with 2 duplicates per experiment). Each point represents the mean and standard error of the mean.

* Indicates significantly different from control

(A)

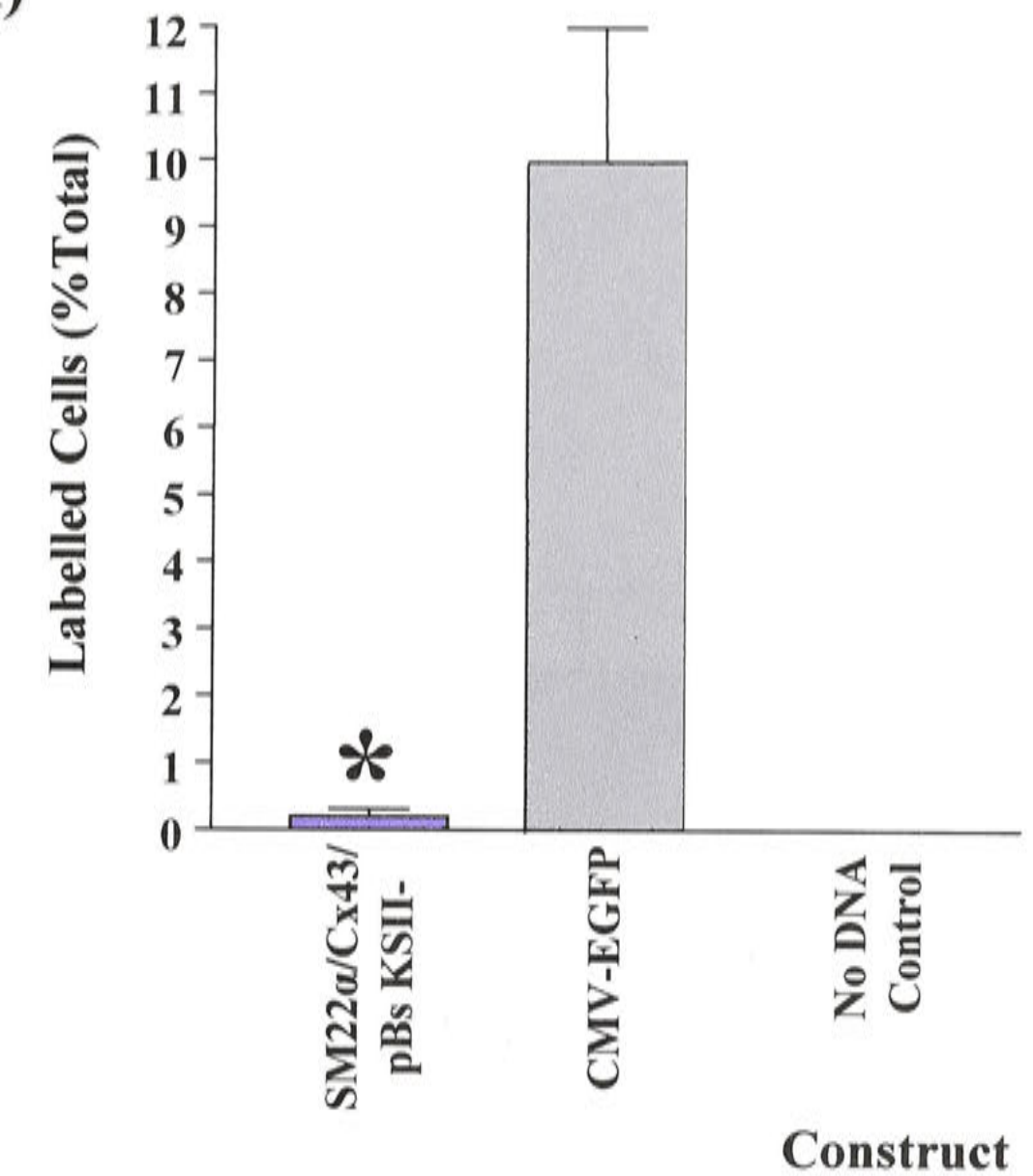
Labelled Cells (%Total)
12
11
10
9
8
7
6
5
4
3
2
1
0
*
SM22α/Cx43/ pBs KSII-
CMV-EGFP
No DNA Control
Construct

(B)

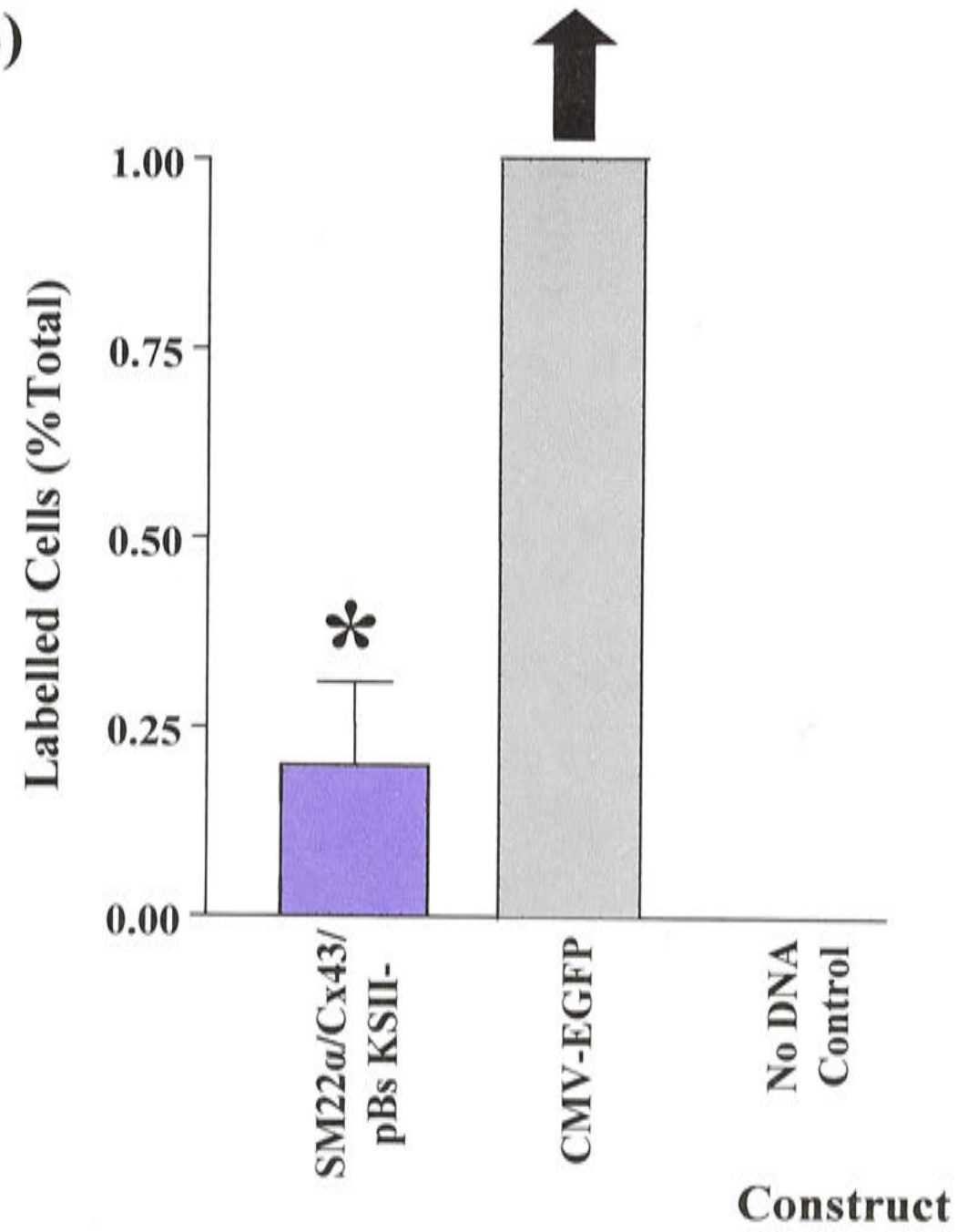
Labelled Cells (%Total)
1.00
0.75
0.50
0.25
0.00
*
SM22α/Cx43/ pBs KSII-
CMV-EGFP
No DNA Control
Construct

(C)

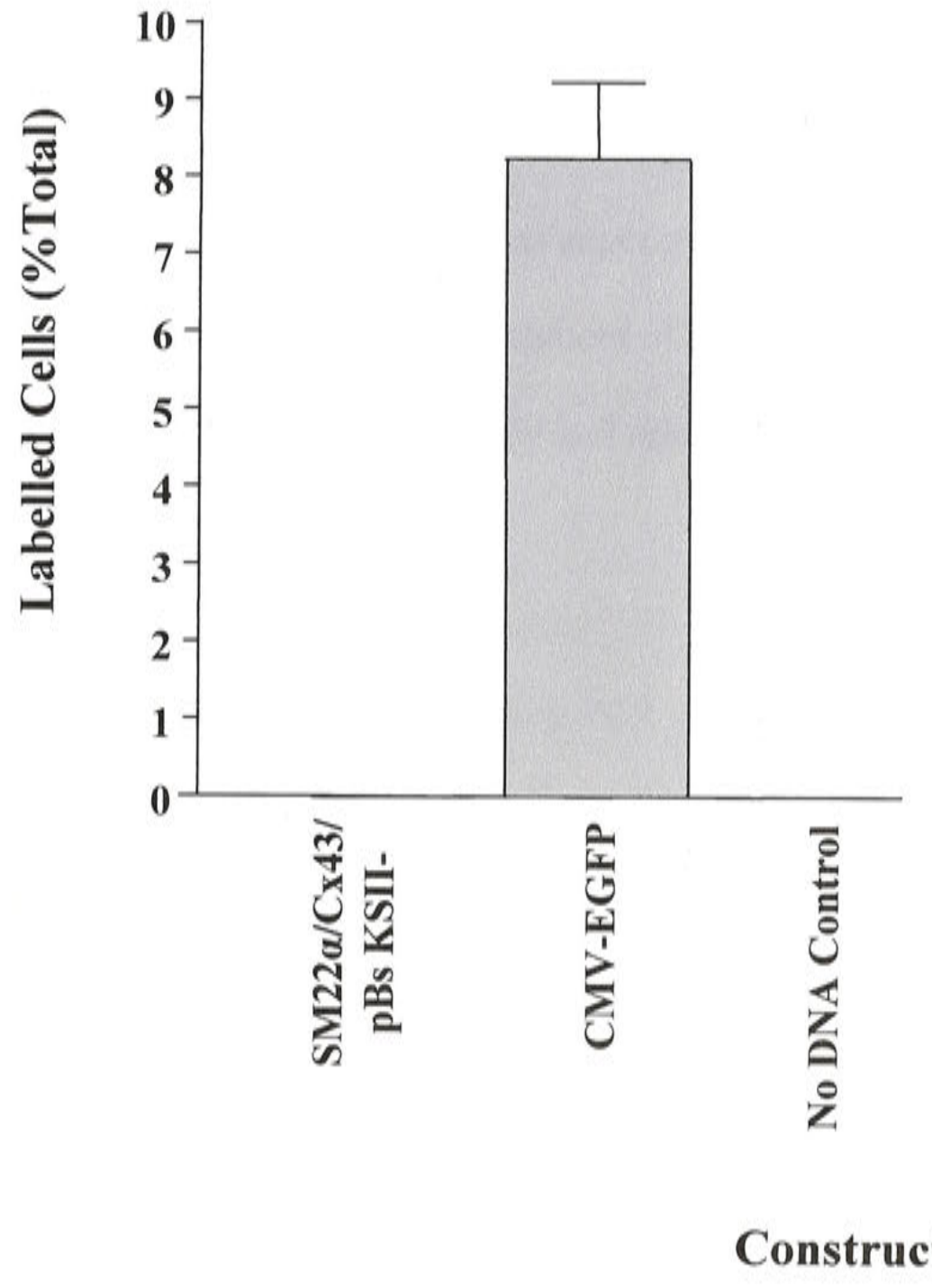
Labelled Cells (%Total)
10
9
8
7
6
5
4
3
2
1
0
SM22α/Cx43/
pBs KSII-
CMV-EGFP
No DNA Control
Construct

expected. There was a low level of expression in the aortic smooth muscle cells (0.20 ± 0.11 %; $n = 4$) which, when compared to the control plasmid (CMV-EGFP; Clontech), was significant ($P < 0.05$) but at a much lower level.

3.7.3 Preparation and electroporation of the SM22α / Cx43 fragment into ES cells

The eluted SM22α / Cx43 / polyA fragment was checked for sample purity and correct band size (Figure 3.20A) before co-electroporation into BALB/c ES cells. Residual DNA was PCR screened using the SM22ex1f and Cx43R2 (amplified a fragment of about 1.2 kb), SM22ex1f and pBi5F (as expected, no band was amplified) and SM22ex1f and pBi5R primers (amplified a fragment of about 2 kb) (Figure 3.20B; see Table 2.2). These PCRs confirmed the integrity and orientation of the fragment.

3.7.4 Identification of positive clones

Antibiotic resistant colonies were screened by PCR using the SM22ex1f and CnxR2 or Cnx43R (amplified bands of about 1.2 kb and 1.3 kb respectively) and CnxF and pBi5R primers (amplified a fragment of about 1.5 kb) (Table 2.2). Only one clone (designated A2) was strongly PCR positive to both sets of primers. Another clone (designated C4) was strongly PCR positive for the CnxF / pBi5R primers but not for the SM22ex1f / CnxR2 primers (Figure 3.21). The new primers synthesized to maximize the sensitivity of the PCR for the SM22α promoter (mSM22ex1f, mSM22ex1fb and mCnx43R) did not improve the PCR results already obtained. Thus, two clones (designated A2 and C4) were microinjected into the BALB/c murine blastocysts.

3.7.5 PCR screening of the progeny

Tail DNA from the white progeny of the mating of the chimaeras (from the A2 and C4 clones) to their BALB/c counterparts were PCR screened using the mSM22ex1f and mCx43R (expected band size of 1.3 kb) and the CnxF and pBi5R primers (expected

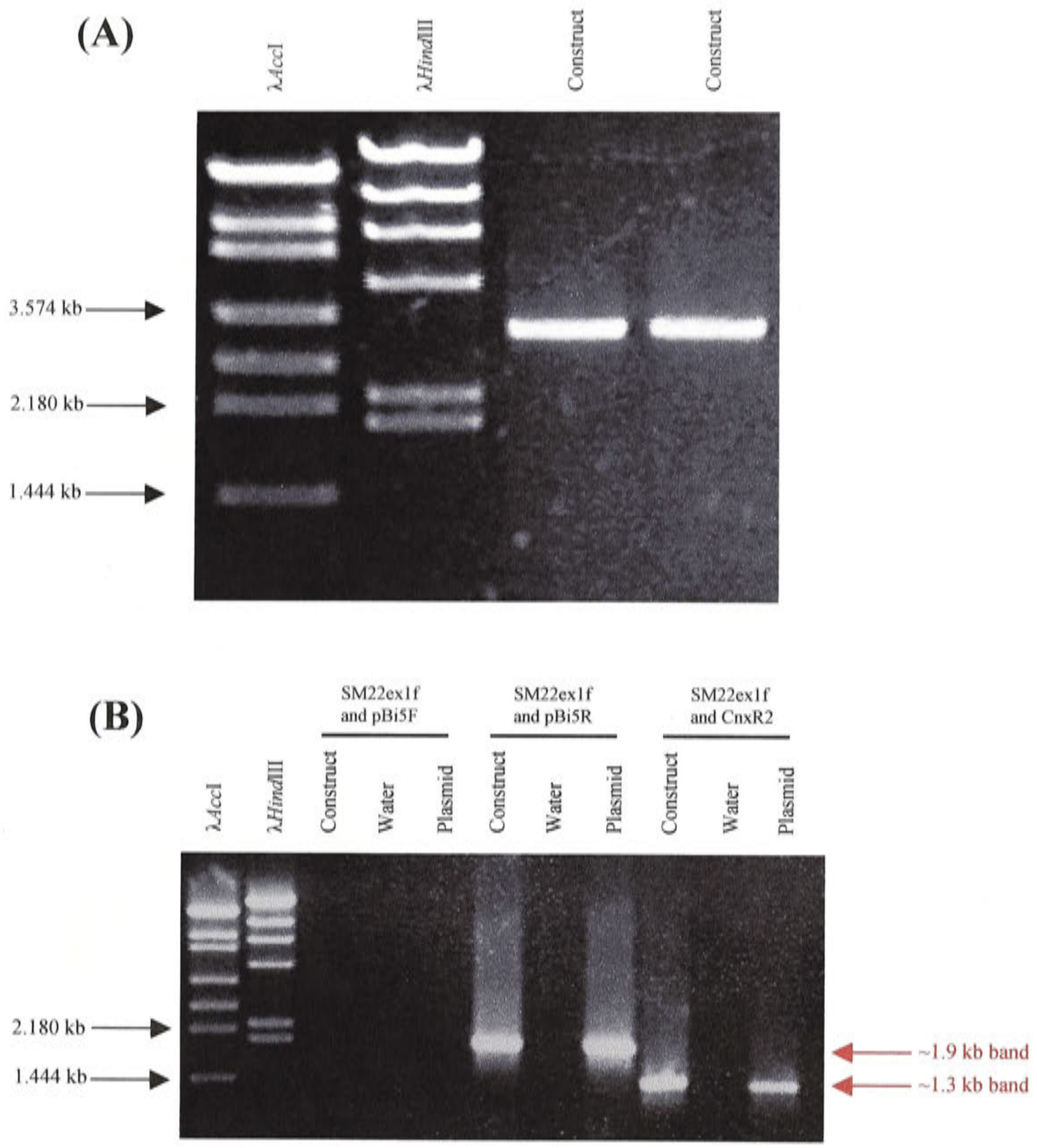

Figure 3.20 The SM22α / Cx43 / polyA signal construct

The isolated and gel purified *Pvu*I / *Kpn*I / SM22α / Cx43 fragment prior to electroporation into murine embryonic stem cells **(A)**. In **(B)**, the residual DNA was PCR screened with the SM22ex1f and pBi5F primers(no band expected) followed by the SM22ex1f and pBi5R primers (a band of 1.9 kb was expected) and the SM22ex1f and CnxR2 primers (expected a band about 1.3 kb). The plasmid (positive control) was Clone #57.

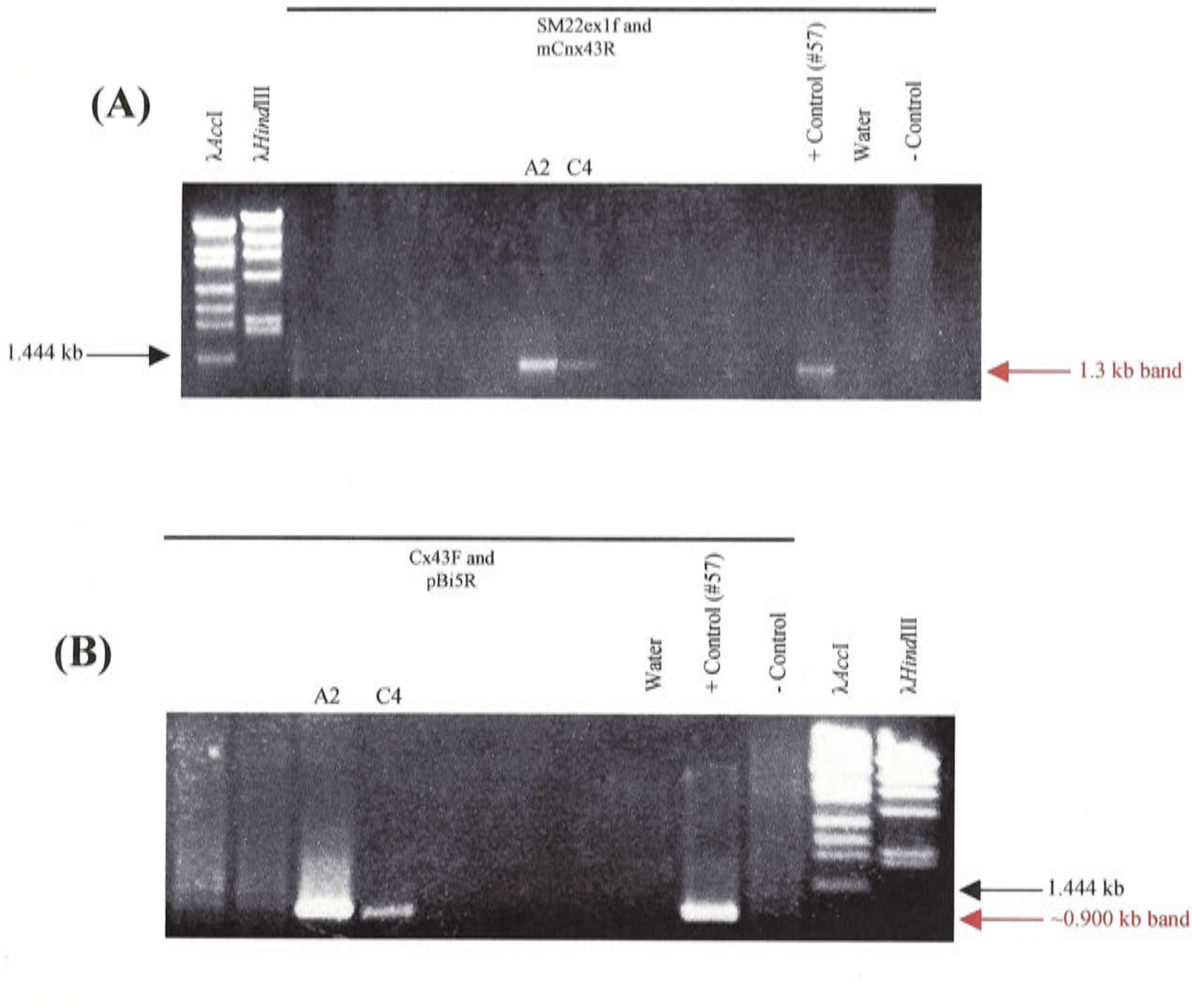

Figure 3.21 PCR testing of the clones

Antibiotic resistant colonies were screened by PCR using a variety of primer combinations. In this figure, the SM22ex1f and mCnx43R (expected 1.3 kb band; **A**) and Cx43F and pBi5R (expected 0.9 kb band; **B**) primers were used.
The positive control was Clone #57 and the negative control mouse genomic DNA. The A2 and C4 clones are marked.

band size of 1.5 kb). For the "C4" tail DNA samples, the mSM22ex1f and mCx43R PCR did not amplify any product from the DNA samples, but the CnxF and pBi5R PCR did amplify a fragment which approximated the predicted band size of 1.5 kb (Figure 3.22). All "A2" tail DNA samples were PCR negative. As these results were unexpected, further PCR testing was undertaken using the mSM22ex1f and HOTT7 primers followed by the mSM22ex1f and pBi5R primers (expected band size of 2 kb). Both PCRs failed to amplify any fragments from the clones; only the positive control (Clone #57) produced a band of the correct size. Repetition of these PCRs using increased primer concentrations produced the same negative results, as did PCR analyses of a new batch of tail DNA samples using the mSM22ex1f and mCnx43R, and CnxF and pBi5R primers.

To test whether the SM22α promoter was present but truncated in the mice, PCRs using three new forward primers in the SM22α promoter region (mSM22F2, mSM22F6 and mSM22F7) were undertaken with the reverse primer mCx435'R. Preliminary testing on Clone #57 produced the appropriately sized bands: mSM22F2 and mCx435'R primers (a band of about 0.633 kb was amplified), mSM22F6 and mCx435'R primers (a band of about 0.374 kb was amplified), and mSM22F7 and mCx435'R primers (a band of about 0.273 kb was amplified) (Table 2.2; Figure 3.23). Subsequent PCR testing of these primers on mouse DNA revealed that the majority of the restricted SM22α promoter was indeed absent (Figure 3.24). According to the PCR results using the mSM22F6 and mSM22F7 forward primers with a reverse primer, it was concluded that perhaps only 100 bp of the promoter was present in the construct. However, as no primers were synthesized between these two primers, the exact length of the truncated promoter is not known.

Subsequently, the single transgenic-promoter transgenic mice were interbred to increase the gene dose rate (and hence Cx43 gene expression) and produce double transgenic mice.

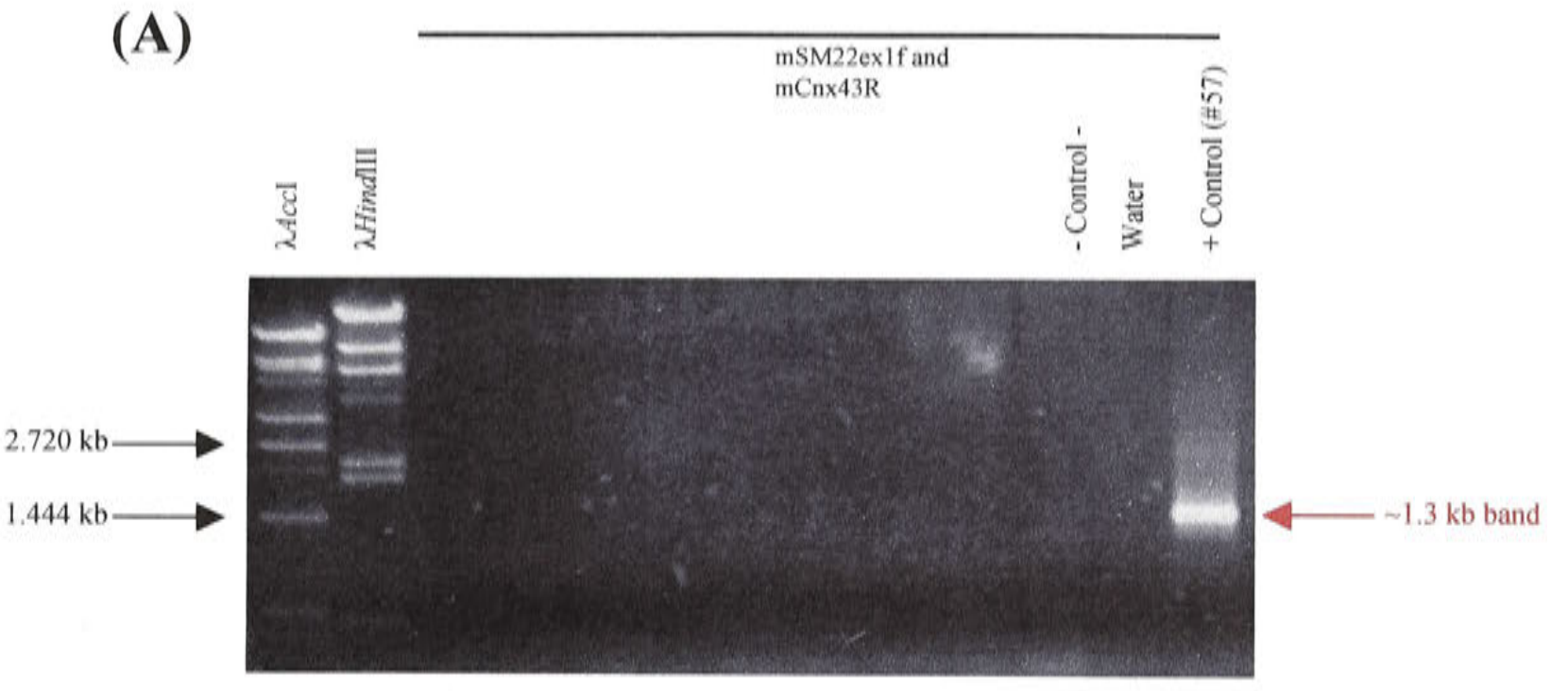

Figure 3.22 PCR screening of the first batch of "C4" tail DNAs

The tail DNAs were PCR screened with the mSM22ex1f and mCnx43R primers **(A)** and the CnxF and pBi5R primers **(B)**. The predicted band size for the mSM22ex1f and mCnx43R PCR was 1.334 kb. The CnxF and pBi5R PCR **(B)** amplified a fragment which approximated the predicted band size of 1.469 kb in Lanes 3, 4, 5 ,7 and 11. The positive control was Clone #57 and the negative control was genomic DNA.

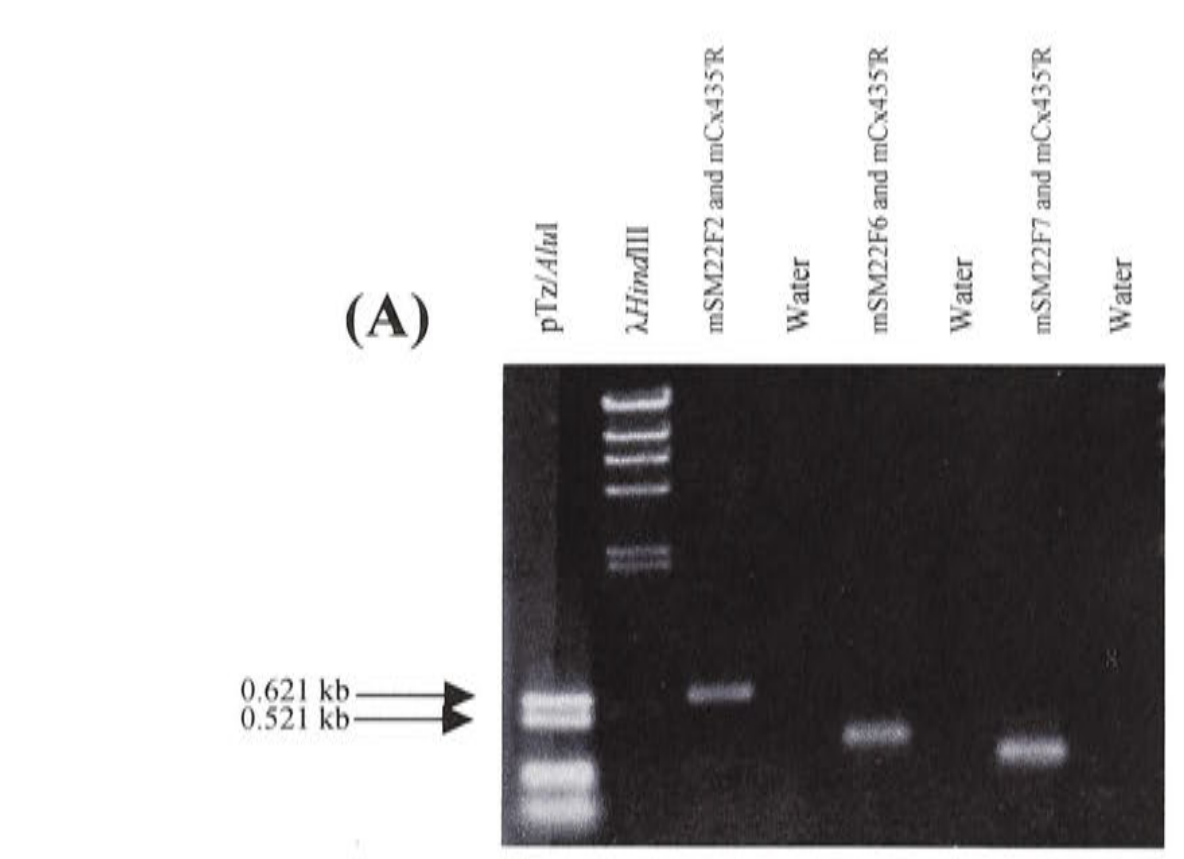

Figure 3.23 Diagnostic PCR testing using the new primers

PCR screening of Clone #57 with the new primers mSM22F2, mSM22F6, mSM22F7 and the reverse mCx435'R primer. In **(A)**, Clone #57 was screened with the mSM22F2 and mCx435'R (expected band size of 0.633 kb), mSM22F6 and mCx435'R (0.374 kb), and SM22F7 and mCx435'R (0.273 kb) primers. The mSM22F7 and pBi5R PCR (expected band size of 1.598 kb) is shown in **(B)**, with 10-fold serial dilutions of Clone #57. The respective water controls are in Lanes 4, 6 and 8. The correct band size (predicted 1.598 kb) was amplified.

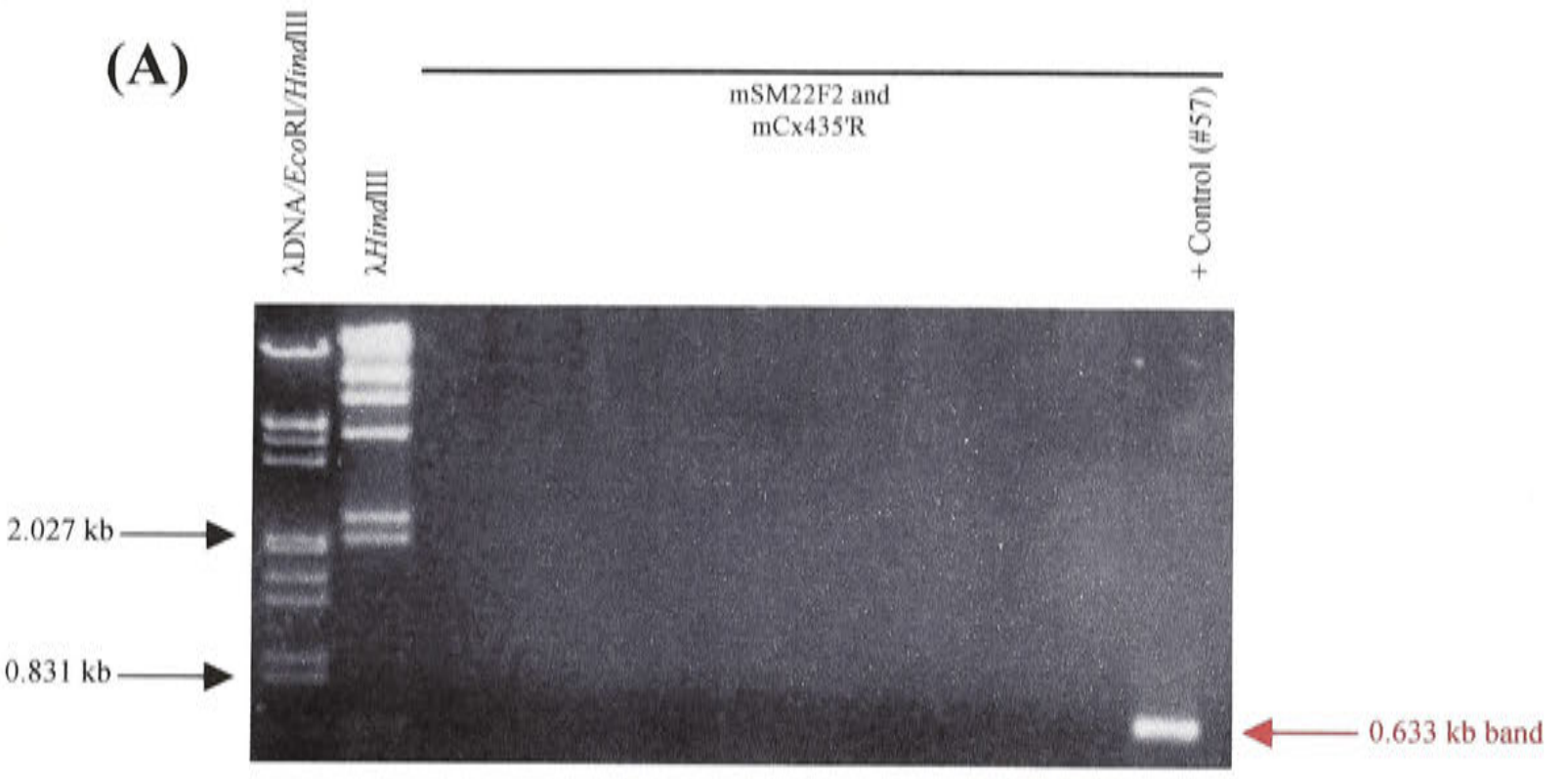

Figure 3.24 Final PCR screening of selected positive tail DNAs

The tail DNAs were screened with the mSM22F2 and mCx435'R primers **(A)**, and with the mSM22F7 and pBi5R primers **(B)**. The Clone #57 positive control had a band that approximated the predicted band size of 0.633 kb. The water and genomic DNA lanes were negative (as expected). In **(B)**, five tail DNAs were PCR positive with a band corresponding with the predicted band size of 1.598 kb; thus showing that only a truncated SM22α promoter was present in the SM22α / Cx43 / polyA signal construct in the genome of these transgenic mice.

3.8 Generation of a Second SM22α / Cx43 Transgenic Mouse

A new enzyme combination (*Pvu*I / *Pvu*II) was chosen to excise the SM22α / Cx43 / polyA signal from SM22α / Cx43 / pBs KSII-. By using *Pvu*I with *Pvu*II this time instead of *Kpn*I, 218 bases were added to the 5' end of the construct to prevent truncation of the promoter from recurring. After running a small restriction digest to check the efficiency of the *Pvu*I and *Pvu*II enzymes, a large restriction digest was set up to excise the SM22α / Cx43 / polyA signal from 30 μg of SM22α / Cx43 / pBs KSII-. The fragment was isolated, purified and subsequently co-electroporated into prepared BALB/c embryonic stem cells with pMCl Neo as previously described. After selection, resistant (surviving) colonies were analyzed by PCR screening. One antibiotic resistant colony (designated B7) was identified by PCR using the mSM22ex1f and mCx435'R, and mSM22F7 and pBi5R primers, and subsequently microinjected into the C57BL/6 blastocysts. Resulting chimaera were mated with BALB/c mice, and the progeny analyzed by PCR which identified the presence of the entire SM22α / Cx43 construct. A double transgenic mouse line was then established.

3.9 Discussion

The SM22α promoter and Cx43 gene fragment were successfully amplified from a mouse genomic library and cloned into pBs KSII-. The sequencing data revealed that *Pfu* DNA polymerase had made three base errors in the reading of the SM22α promoter DNA and no errors in the reading of the Cx43 cDNA. *Pfu* DNA polymerase exhibits the lowest error rate of any of the commercial DNA polymerases (Life Science Catalogue, 2000) (eg. *Taq* DNA polymerase) and thus, would be used again in a similar context. Both SM22α / pBs KSII- and Cx43 / pBs KSII- were then ready to be used in the generation of the SM22α / Cx43 / pBs KSII- construct.

The SM22α / Cx43 / pBs KSII- construct was successfully cloned from the SM22α / pBs KSII- (Clone #137) and Cx43 / pBi5 (Clone C20) plasmids. Testing of the construct *in vitro* in murine aortic smooth muscle cells showed low levels of Cx43 expression, which were similar to background levels. It was concluded that, for the SM22α / Cx43 / pBs KSII- construct, virtually no expression was evident *in vitro*.

There are a variety of methods for introducing DNA into mammalian cells - transfection is reputably the most convenient and reproducible method. Preliminary experiments using electroporation to transform the fibroblasts showed that transfection would be the best method for the current study (data not shown). Transfection is, however, associated with a high DNA mutation frequency of approximately 1% per gene; supercoiled and relaxed DNA are mutated at equal frequencies, whilst linearized DNA leads to a greatly elevated frequency of deletions (Miller *et al*. 1984). This may, in part, explain the low expression rates recorded in the current study.

DNA transfection may be mediated by calcium phosphate, DEAE dextran, electroporation and cationic phospholipids (Kaufman, 1997) – the method of choice being determined by the one most suited to a particular cell type. Lipofectamine Plus Reagent, a cationic lipid reagent with improved transfection efficiency for many adherent cells and with a broader cell type range than the widely used Lipofectamine Reagent (Clontech, 2000), was the transfection reagent of choice for the present study. This reagent was recommended for the murine fibroblasts (Clontech, 1997), although no published data existed for the murine smooth muscle cells. In contrast, in rat smooth muscle cells, Lipofectamine Reagent was recommended (Clontech, 1997, 2000). Although the control experiments in this study showed that for the cultured aortic smooth muscle cells the Lipofectamine Plus Reagent was the best transfection reagent, it may be that the ideal transfection reagent for the combination of these cells and constructs is not as yet established.

Another factor to be considered is the differentiation state of the smooth muscle cells. As these cells are known to readily de-differentiate *in vitro* (Moessler *et al.* 1996), procedural modifications were made to confirm the status of the cells in the current study and to promote differentiation by using insulin for example (data not shown). However, the expression levels for the construct did not improve. In contrast, the CMV-EGFP transfection rates remained relatively constant and at an acceptably high level throughout the experiments. Although it is difficult to determine the differentiation state of the smooth muscle cells, further consideration of this factor would be important in future studies.

The observed low expression levels of the construct are in contrast with the good transfection rates obtained with the CMV-EGFP plasmid. It is now recognized that various promoters are capable of producing different expression levels of genes (Gerolami *et al.* 2000). For example, the CMV promoter can produce high expression levels of many genes in a wide variety of cells after transfection (Almouzni and Wolfe, 1993), but the same situation does not exist for the tissue specific SM22α promoter.

The expression levels obtained using the modified SM22α / Cx43 / pBs KSII- construct are clearly much lower than those for other constructs already published (c.f. Kemp *et al.* 1995; Solway *et al.* 1995; Li *et al.* 1996; Moessler *et al.* 1996). However, direct comparisons cannot be made for several reasons: firstly, the current study used primary cultures of murine aortic smooth muscle cells and murine embryonic fibroblasts in which to test the restricted SM22α promoter (the first such study to do so). Published data concerning the culture and transfection of these cells *in vitro* is lacking. At present there is no recommended transfection reagent for murine aortic smooth muscle cells. However, in the current study, CMV-EGFP was shown to express equally well in both the smooth muscle cells and the fibroblasts. Secondly, all studies so far have used different plasmids, which affect transfection efficiency and thus gene expression.

Linearization of the plasmid, for example, increases the efficiency of integration (Huttner *et al.* 1981; Potter *et al.* 1984). Also, different transfection reagents were used on different cell types. The efficacy, sensitivity and toxicity of a transfection reagent are known to depend on a variety of parameters, some of which have already been discussed. These include, for example, growth rates of cells (Pickering *et al.* 1996), cell type (smooth muscle cell versus endothelial cell, for example) and cell species (rat versus human, for example), absence of serum (Escriou *et al.* 1998), and DNA purity (Clontech, 2000) – which was the same for the constructs in the current study.

The majority of transfection studies thus far have been performed on animal cells but unfortunately, and not surprisingly, not all cell types have been studied. To date, there is a paucity of published data examining the efficient transfection of primary murine smooth muscle cells. The success and effectiveness of the new liposomal and non-liposomal transfection reagents remains to be elucidated. Recently, Hamm *et al.* (2002) demonstrated the effectiveness of the Nucleofectortrade mark technology developed by amaxa biosystems, in the transfection of various primary human cells and stem cells, including human coronary smooth muscle cells. Clearly, more work needs to be undertaken to ascertain the optimal culture conditions and transfection efficiencies of murine embryonic fibroblasts and aortic smooth muscle cells *in vitro*.

Although the SM22α / Cx43 / pBs KSII- construct was shown to be virtually non-functional *in vitro*, it was still possible that the SM22α / Cx43 / pBs KSII- construct would be viable *in vivo*. Therefore, the linear DNA constructs (*Pvu*I / *Kpn*I / SM22α / Cx43 and *Pvu*I / *Pvu*II / SM22α / Cx43) were electroporated into the BALB/c embryonic stem cells (where they would recombine with the genome) with a circular selection plasmid (pMCl Neo). Most of the markers confer resistance to the antibiotic neomycin (Gossler *et al.* 1986; Robertson *et al.* 1986).

DNA introduced into embryonic stem (ES) cells can either randomly integrate, where the entire construct enters the genome stably but non-specifically, or can be subject to homologous (specific) recombination (Roth and Wilson, 1985; Roth *et al.* 1985). Generally, DNA has a two to three-fold higher propensity for random integration (Roth and Wilson, 1985). The ES cell route to transgenesis provides the opportunity to screen for the desired genetic alteration/s before the reintroduction of the ES cells into the mouse (Gossler *et al.* 1986). In the current study, PCR screening of the clones showed that only two colonies were positive for the *Pvu*I / *Kpn*I / SM22α / Cx43 construct (first transformation) and one for the *Pvu*I / *Pvu*II / SM22α / Cx43 construct (second transformation). From previous experience in this laboratory, more positive colonies had been anticipated (Matthaei *pers com*). The reasons for this observation are unknown but it may be due to problems with the construct itself, the ES cells, or a combination of both factors.

Two methods currently exist for the production of ES cell chimaeras: microinjection and aggregation / co-culture of which, the former is reputedly the more successful (Gossler *et al.* 1986). In aggregation, the zona pellucida (outer layer) is removed from morulae-stage embryos, and the morulae allowed to aggregate (co-culture) on a lawn of targeted ES cells. After co-culture, the embryos with the ES cells attached develop into blastocysts before implantation into pseudo-pregnant females (Wood *et al.* 1993a). A comparison of both aggregation and blastocyst injection methods by Wood *et al.* (1993b), however, showed that there was no significant difference in the number of germ-line chimaeras produced by either method. Consequently, in the current study, the two colonies from the first attempt, and the colony from the second attempt, were microinjected into recipient blastocysts.

As most ES cell lines have an XY karyotype, the sex ratio among the chimaeras is biased towards male mice (Robertson *et al.* 1986). Male ES cell lines have the

advantage that the resulting germ-line chimaeras are normally male and so, can father a large number of offspring in a short period of time. In the current study, each male chimaera with a coat colour of any variation of black and white was mated to two female BALB/c mice, and each female chimaera was mated to one male BALB/c mouse. Germ-line transmission has been achieved using male chimaeras with much less than 10% coat colour change (Matthaei *pers com*). PCR analysis using DNA isolated from the tails of three week old mice was used in the current study and if time had permitted, Southerns would also have been done, as they have been suggested to be a better approach (Hogan *et al*. 1994).

PCR analyses of the tail DNAs from the first microinjection, revealed the presence of a truncated form (103 to 204 bp only) of the original restricted SM22α promoter. The exact length of the truncated promoter was not known as no further primers were synthesized. The stage at which the 5'-end of the restricted SM22α promoter was lost is open to speculation. Since the promoter was intact in Clone #57, it is possible that it occurred during electroporation of the construct into the ES cells or, that not all of the promoter was integrated into the genome. Electroporation is known to cause mutations in the DNA. The PCR analyses performed on the A2 clone showed that the entire construct was present, whilst the colony designated C4 was only weakly PCR positive to the SM22α forward and Cx43 reverse primers, compared with the strong band obtained by PCR using the Cx43 forward and pBi5 reverse primers. The A2 clone was equally PCR positive for both sets of primers. Consequently, it is possible that the C4 clone had a truncated-promoter, as the positive PCR result was not entirely convincing. This is supported by the observation that when the C4 clone was incorporated into the germ-line, the resulting progeny contained a truncated-promoter.

Although chimaeric mice from microinjection of the A2 clone were produced, none were germ-line. This may be because the A2 colony was a combination of transgenic and non-transgenic ES cells, with only the non-transgenic cells being

incorporated into the germ-line. In addition, the A2 ES cells were co-transfected with the pMCl Neo transiently and the selective pressure could not be maintained.

In contrast, the colony designated B7 from the second microinjection attempt produced chimaeric pups. Their progeny were identified by PCR screening as possessing the entire DNA construct. Interbreeding of the single transgenic offspring from both the truncated-SM22α / Cx43 and full-SM22α / Cx43 transgenic mouse lines produced double transgenic mice.

In conclusion, the SM22α / Cx43 / polyA fragment was successfully cloned. Although *in vitro* testing of the construct in smooth muscle cells was inconclusive, it was subsequently used to generate two transgenic mouse lines: one with a truncated SM22α promoter in the germ-line and one with the full construct in the germ-line. Interbreeding of each mouse produced double transgenic offspring. Two transgenic mice lines had been successfully generated.

Chapter 4 – Analysis of the SM22α / Cx43 Mouse

4.1 Introduction

Genetically modified mice are increasingly being used to extend the study of the activity of a particular molecule or gene *in vivo*, following cellular studies that were initiated *in vitro*. *In vivo* studies are particularly relevant for the investigation of vascular function and associated disease states (Christ *et al.* 1996). A distinct advantage of a transgenic mouse that survives to and throughout adulthood, is that the potential effect of the removal or modification of a single gene or molecule on mouse physiology and behaviour can be examined using a wide variety of experimental procedures. Various experimental paradigms can, and have been, examined using transgenic and knockout mice.

The phenotypes of transgenic mice can be studied at many levels from behaviour to physiology to cell biology and biochemistry. In this Chapter, studies were undertaken on mice transformed either with a truncated-promoter SM22α / Cx43 mouse (single and double transgenic) or a full-promoter SM22α / Cx43 mouse (single transgenic) to investigate their phenotypes. The expression level of Cx43 in the vasculature, specifically in the aorta and tail artery, was determined using Western blots. The effect of overexpressing Cx43 in the vasculature on blood pressure was also examined.

4.2 Results

4.2.1 General observations

PCR analyses of tail DNA using the mSM22ex1fb / mSM22F7 and mCx435'R primers, and CnxF and pBi5R primers (Table 2.2) identified positive and control mice from the respective litters (single transgenic truncated-promoter, double transgenic

truncated-promoter, single transgenic full-promoter and double transgenic full-promoter). For all groups, there were no obvious phenotypic abnormalities at birth and all were viable, surviving into adulthood. Neo-natal and post-natal deaths were rare.

Either a two- or three-way analysis of variance (ANOVA), or a one-way ANOVA followed by individual pairwise *t* tests with Bonferroni correction for multiple group comparisons, was performed on the data.

4.2.2 Litter sizes and pup gender

The litter sizes and pup genders were recorded for each group (Table 4.1). Interestingly, the full-promoter mice, both single and double transgenic, had slightly smaller litter sizes than did the single and double transgenic truncated-promoter mice ($P > 0.05$). All groups had an approximately equal number of male and female pups.

	Single Truncated-Promoter	Double Truncated-Promoter	Single Full-Promoter	Double Full-Promoter
Litter Size	5.77 ± 0.47 *n* = 31	6.36 ± 0.47 *n* = 14	4.69 ± 0.66 *n* = 16	4.50 ± 0.53 *n* = 14
♂ / ♀	2.91 ± 0.54 ♂ 3.02 ± 0.39 ♀	3.46 ± 0.45 ♂ 3.00 ± 0.38 ♀	2.23 ± 0.33 ♂ 2.67 ± 0.29 ♀	1.86 ± 0.59 ♂ 2.29 ± 0.47 ♀

Table 4.1 Litter sizes and numbers of each sex per group

(*n* = number of litters)

4.2.3 Body weights

A two-way analysis of variance with gender and treatment as explanatory variables was used to examine body mass variation at the end of experiments. Males were significantly heavier (26.35 ± 0.36 g) than females (21.60 ± 0.35 g) ($F_{[1,33]} = 121.2$, $P < 0.0001$). Transgenic mice were lighter than their non-transgenic litter mates ($F_{[5,33]} = 12.6$, $P < 0.0001$), and there was an interaction between transgenic and gender as well ($F_{[5,33]} = 4.07$, $P = 0.0055$) as the difference between male and female weight varied with various transgenic treatments (Figure 4.1). For example, mean weights of males and females of the double truncated-promoter mice were within 1 gram, but all other treatments had at least 2 to 3 grams difference between mean weights of males and females. Comparing only the transgenic groups, the single truncated-promoter mice were heavier (25.0 ± 0.48 g) than both the single full-promoter (22.4 ± 0.58 g) and double truncated-promoter (21.2 ± 0.52 g) mice, although most of the latter change resulted from much smaller male mice.

4.2.4 Organ weights

At the end of the experiments, all mice were weighed and their hearts, lungs, left and right kidneys, livers, spleens, stomach, intestines were removed and the wet weights recorded, to see if there was any difference between the transgenic mice groups and the control mice. As it is known from murine cardiovascular studies that in transgenic and gene targeted mouse lines, the heart and body weights may either increase or decrease (Milano *et al.* 1994; Hein *et al.* 1995; Doevendans *et al.* 1998), changes in other organs would not be unexpected. Wet weights of the various organs are shown in Table 4.2 as absolute weights and relative to body weight.

The single transgenic truncated-promoter male mice had larger hearts, kidneys and livers, but smaller spleens and lungs than the controls. Conversely, the transgenic females had smaller hearts and kidneys, but larger livers, spleens and lungs than

Figure 4.1 Body weight measurements.

The body weight measurements (g) for each mouse group are shown. Each point represents the mean and standard error of the mean.

* Indicates significantly different from control

KEY:

Single Trunc Male/Female = Single transgenic truncated-promoter male / female mice

Double Trunc Male/Female = Double transgenic truncated-promoter male / female mice.

Single Full Male/Female = Single transgenic full-promoter male / female mice.

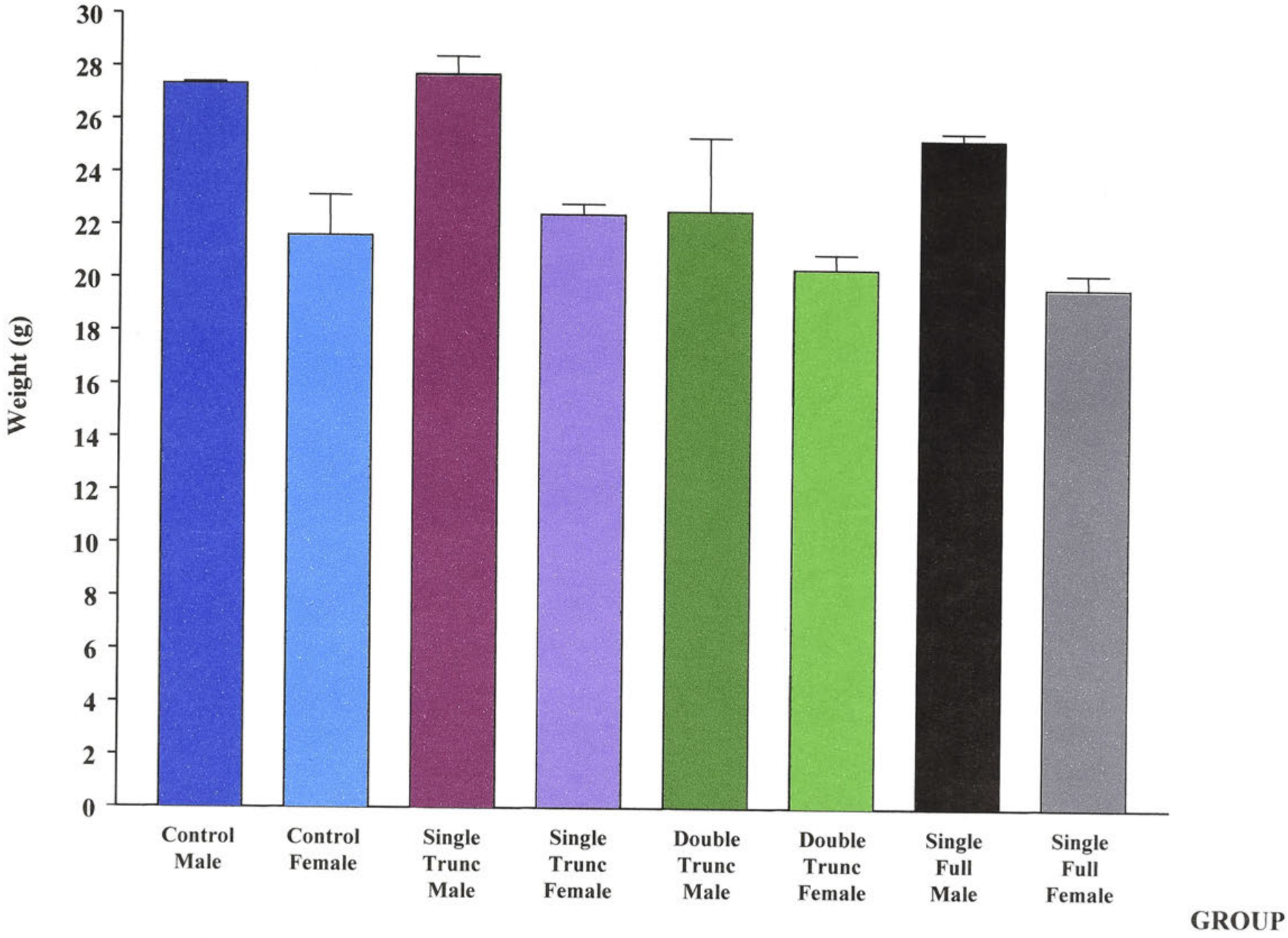
Weight (g)
30
28
26
24
22
20
18
16
14
12
10
8
6
4
2
0
Control Male
Control Female
Single Trunc Male
Single Trunc Female
Double Trunc Male
Double Trunc Female
Single Full Male
Single Full Female
GROUP

Table 4.2 Absolute and relative weights of selected organs

The absolute and relative weights of the hearts, left and right kidneys, livers, spleens and lungs from the control mice, the single and double transgenic truncated-promoter mice, and the single transgenic full-promoter mice are shown. All values represent the mean and standard error of the mean. Significant values are indicated ($*P < 0.05$).

GROUP	TISSUE					
	Heart		Left Kidney		Right Kidney	
	absolute	relative	absolute	relative	absolute	relative
Control male (n = 16)	0.15 ± 0.04g	5.52 ± 1.22	0.26 ± 0.01g	9.77 ± 0.31	0.28 ± 0.03g	10.24 ± 0.82
Control female (n = 11)	0.12 ± 0.03g	5.74 ± 1.30	0.15 ± 0.04g	6.94 ± 1.52	0.15 ± 0.04g	7.02 ± 1.86
Single TruncProm male (n = 11)	0.15 ± 0.02g	5.61 ± 1.52	0.27 ± 0.02g	10.07 ± 0.70	0.30 ± 0.01g	11.06 ± 0.60
Single TruncProm female (n = 11)	0.10 ± 0.02g	5.03 ± 0.57	0.12 ± 0.03g	5.41 ± 0.61	0.17 ± 0.03g	6.87 ± 0.71
Double TruncProm male (n = 5)	0.15 ± 0.03g	*6.17 ± 1.09	0.21 ± 0.02g	8.45 ± 0.42	0.24 ± 0.02g	9.70 ± 0.39
Double TruncProm female (n = 3)	0.095 ± 0.003g	*4.64 ± 0.16	0.11 ± 0.01g	5.39 ± 0.40	0.13 ± 0.02g	6.27 ± 0.70
Single FullProm Male (n = 5)	0.12 ± 0.003g	*4.89 ± 0.16	0.26 ± 0.01g	10.30 ± 0.45	0.25± 0.01g	10.02 ± 0.47
Single FullProm Female (n = 4)	0.10 ± 0.006g	5.08 ± 0.18g	0.11 ± 0.003g	5.45 ± 0.28	0.12 ± 0.007g	5.94± 0.28

KEY:
trunc/fullprom = truncated- or full-promoter; *$P < 0.05$; n = number of individual mice.

GROUP	TISSUE					
	Liver		Spleen		Lung	
	absolute	relative	absolute	relative	absolute	relative
Control male (n = 16)	1.48 ± 0.08g	55.41 ± 2.21	0.10 ± 0.01g	3.55 ± 0.15	0.22 ± 0.03g	8.16 ± 0.89
Control female (n = 11)	1.05 ± 0.05g	50.24 ± 0.93	0.09 ± 0.002g	4.58 ± 0.07	0.21 ± 0.03g	9.98 ± 1.12
Single TruncProm male (n = 11)	1.49 ± 0.02g	59.32 ± 1.81	0.10 ± 0.002g	3.51 ± 0.10	0.22 ± 0.01g	9.02 ± 1.06
Single TruncProm female (n = 11)	1.03 ± 0.05g	52.60 ± 0.98	0.09 ± 0.01g	4.84 ± 0.11	0.21 ± 0.02g	9.99 ± 1.16
Double TruncProm male (n = 5)	1.54 ± 0.06g	*63.59± 0.99	0.08 ± 0.01g	3.38 ± 0.09	0.22 ± 0.03g	9.06 ± 1.03
Double TruncProm female (n = 3)	1.09 ± 0.03g	53.90 ± 1.80	0.09 ± 0.002g	4.58 ± 0.07	0.21 ± 0.03g	9.98 ± 1.12
Single FullProm Male (n = 5)	1.48 ± 0.03g	58.75 ± 0.67	0.09 ± 0.01g	3.70 ± 0.37	0.25 ± 0.03g	10.01 ± 1.15
Single FullProm Female (n = 4)	1.01 ± 0.06g	51.20 ± 1.91	0.08 ± 0.003g	4 .24 ± 0.15	0.20 ± 0.003g	10.36 ± 0.25

KEY:
trunc/fullprom = truncated- or full- promoter; $*P < 0.05$; n = number of individual mice.

controls. The double truncated-promoter mice had smaller hearts (females only), kidneys and spleens and larger livers than did the controls. The relative lung weights for the control and transgenic mice were almost identical. In the single transgenic full-promoter males, all relative organ weights (except the heart) were increased over control, whilst in the females, only the liver and lung weights were increased over control.

Although variation in the carcase weights for each group were observed for the two sexes, the differences were not significant at the 5% level. In general, the female carcase weights for all groups were less than the male carcase weights. In the transgenic double truncated-promoter mice, for example, the female relative carcase weight was 648.7 ± 3.85 g compared to the males' 653.8 ± 4.80 g, whilst in the control single full-promoter mice, the female relative carcase weight was 645 ± 2.44 g and the male relative carcase weight 654.5 ± 4.16 g.

4.2.5 Blood pressure measurements

Data from the blood pressure measurements (as systolic blood pressures) are presented in Figures 4.2 and 4.3. The mice in Figure 4.2 (single transgenic truncated-promoter) were not acclimatized to the equipment prior to the start of the blood pressure recordings, as were the other groups (Figure 4.3). A three-way analysis of variance using the extent of acclimatization to the cuff, transgenic and gender as the major explanatory variable, indicated that none of these variables had a significant effect on blood pressure directly. However, two interactions were significant. The interaction between acclimatization and gender showed that acclimatization affected male mice more than female mice ($F_{[1,58]} = 11.44$, $P < 0.002$) as mean male blood pressure decreased from 111 ± 2.7 mm Hg to 99 ± 2.4 mm Hg with acclimatization. In contrast, female blood pressure actually increased from 101 ± 2.8 mm Hg to 109 ± 2.4 mm Hg with acclimatisation. There was also a weak interaction between the acclimatization

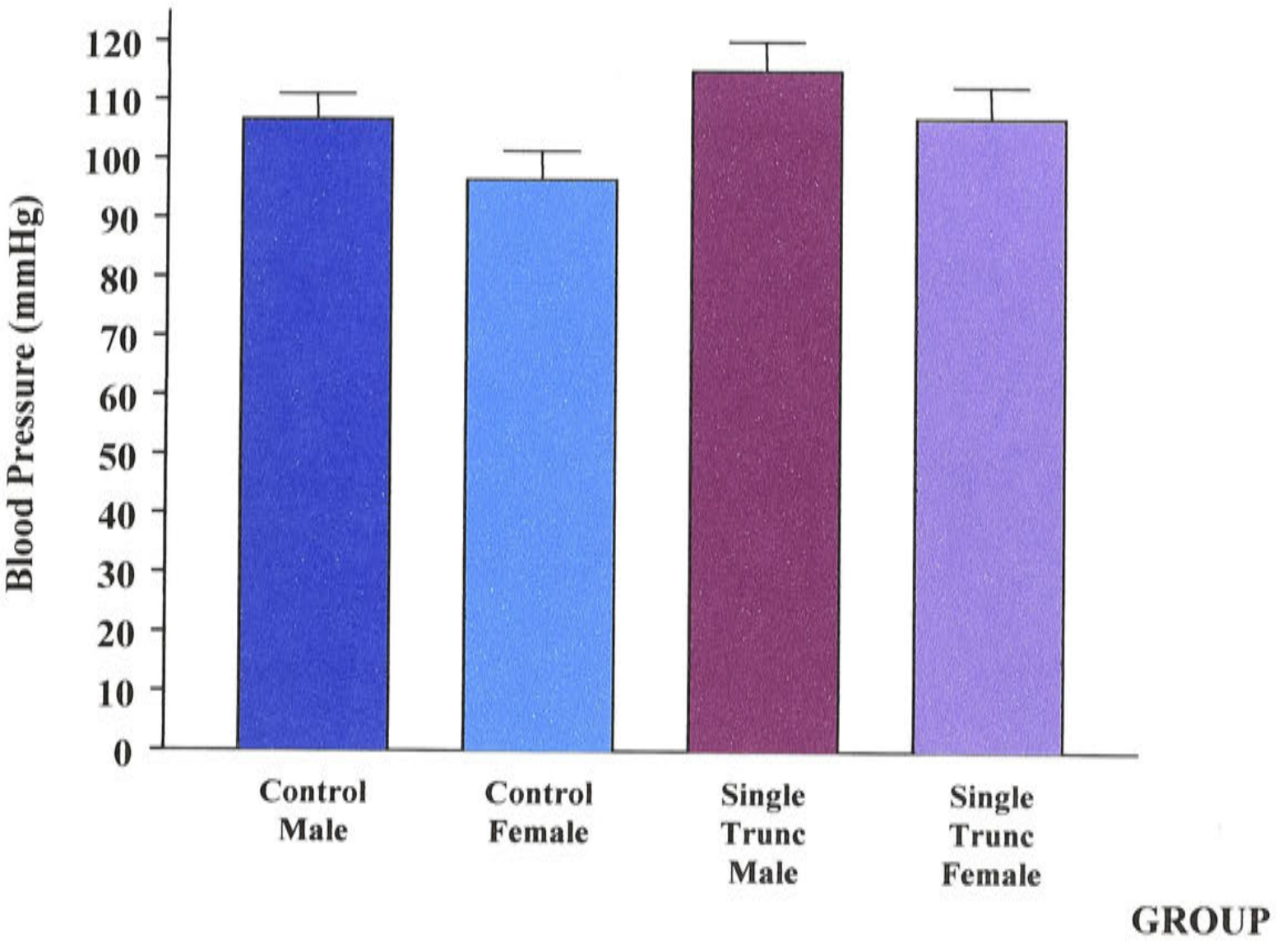

Figure 4.2 Blood pressure measurements

The blood pressure measurements (mmHg) for the first single transgenic truncated-promoter group are shown (n = 6 mice for each group). These mice had no acclimatization period prior to the start of the blood pressure recordings. Each point represents the mean and standard error of the mean.

Figure 4.3 Blood pressure measurements.

The blood pressure measurements (mmHg) for each mouse group are shown. Each point represents the mean and standard error of the mean.

* Indicates significantly different from control

KEY:

Single Trunc Male/Female = Single transgenic truncated-promoter male / female mice

Double Trunc Male/Female = Double transgenic truncated-promoter male / female mice.

Single Full Male/Female = Single transgenic full-promoter male / female mice.

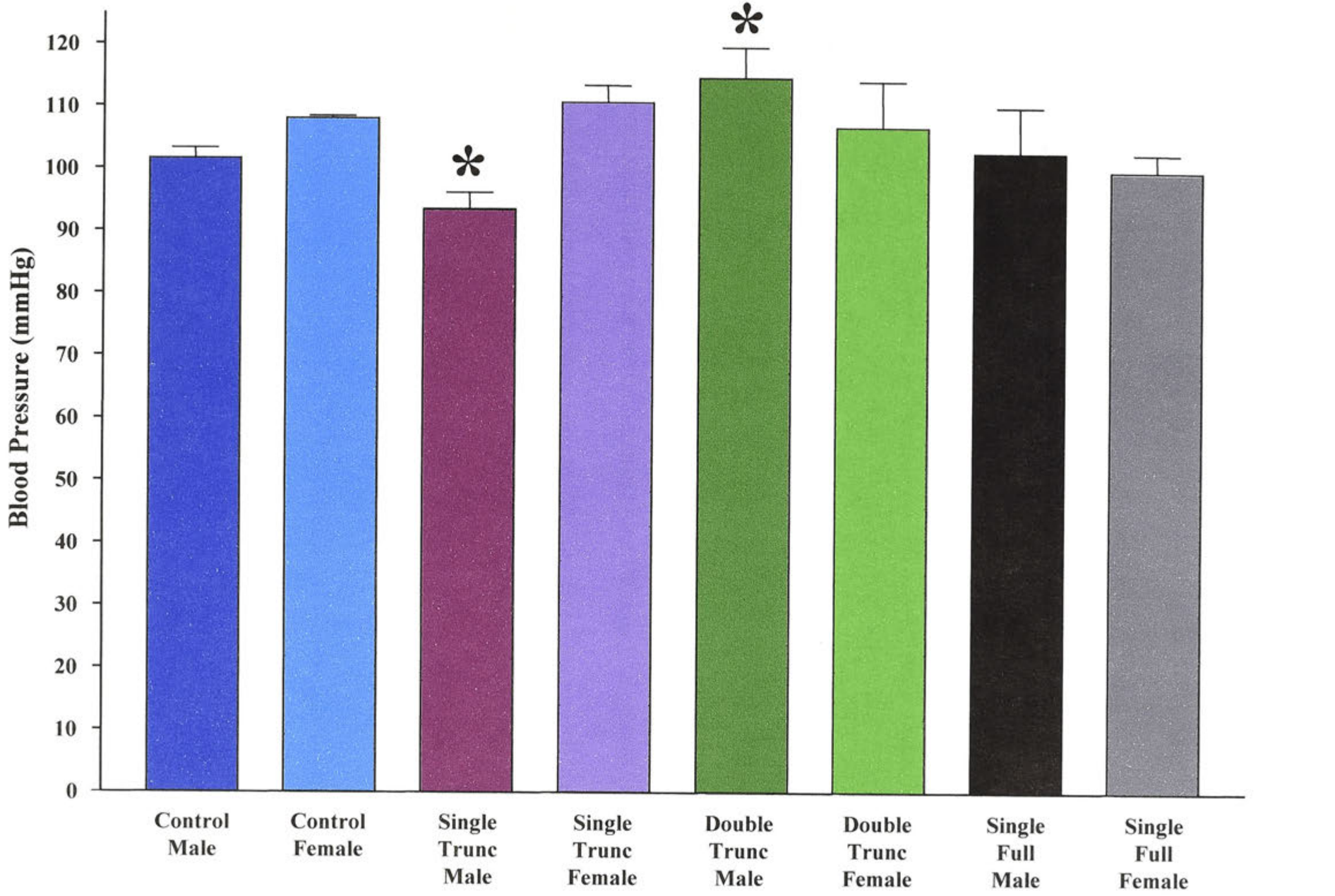
Blood Pressure (mmHg)
120
110
100
90
80
70
60
50
40
30
20
10
0
*
*
Control Male
Control Female
Single Trunc Male
Single Trunc Female
Double Trunc Male
Double Trunc Female
Single Full Male
Single Full Female
GROUP

and whether mice were transgenic or not ($F_{[1,58]} = 4.55$, $P = 0.038$). Non-acclimatized transgenic mice had the highest blood pressure measurements (111 ± 3.4 mm Hg), while control (106 ± 2.6 mmHg) and transgenic acclimatized (102 ± 2.8 mmHg) and control non-acclimatized (101.6 ± 3.2 mmHg) mice all had lower blood pressure measurements.

The variability in the individual blood pressure recordings necessitated several readings on each animal. Examples of the variability are given in Table 4.3, using a selection of individuals from all groups sampled in the current study. There was no correlation between blood pressure and body weight for any group.

The body weights of randomly selected individuals from the single and double transgenic truncated-promoter mice, and single transgenic full-promoter mice were recorded at defined time periods to assess the level of stress and adaptive response to the recording procedure, and hence influence on the blood pressure measurements. Body weight in animals is known to decrease as a stress response (Ettinger, 1989). Body weights were recorded six days prior to the handling / acclimatization period, on the first three days of the recordings and then every second day for six measurements, and on the day of euthanasia (one week after cessation of the blood pressure recordings).

Between the first and second body weight measurements (at the start of the handling / acclimatization period and the blood pressure measurements respectively), both the control and transgenic mice had a slight decrease in body weight (average 0.2 ± 0.01g; $n = 25$).

Mouse	ID	Initial reading	2nd reading	3rd reading	4th reading	5th reading	6th reading	7th reading
1	Single transgenic truncpromoter* male	115.0	88.0	93.0	80.0	110.0	94.0	Not recorded
2	Single transgenic truncpromoter* female	153.0	95.0	105.0	113.0	89.0	87.0	Not recorded
3	Double transgenic truncpromoter* male	76.3	123.3	104.8	106.8	108.3	98	111.8
4	Double transgenic truncpromoter* female	104.5	95.0	113.3	101.8	103.8	106.5	113.8
5	Single transgenic fullpromoter* male	79.3	129.75	113.75	80.0	113.0	153.3	46.0
6	Single transgenic fullpromoter* female	77.25	93.0	91.75	121.5	104.5	90.25	121.50
7	Control controlfemale	105.0	123.5	107.5	114.0	101.0	106.5	113.8
8	Control controlmale	126.25	117.25	109.75	82.75	103.0	108.5	140.5

Table 4.3 Individual Blood Pressure Measurements in mmHg

*trunc/fullpromoter = truncated- or full-promoter mouse

The mice not handled nor acclimatized (control), did not lose any weight during this period. After the first blood pressure measurement, most mice lost an average of 0.8 ± 0.05 g which equated to 3-4% of their total body weight. This was not fluid loss as the weight had not been regained by the following day. By the third to fifth blood pressure reading all mice groups except the double transgenic truncated-promoter males and females were regaining their pre-experimental weight, indicating a reduction in the level of stress experienced by the mice. The double transgenic truncated-promoter males and females started regaining weight by the sixth blood pressure reading. Thereafter, all groups gained weight until euthanasia. All mice not handled gained weight during the experimental period.

4.2.6 Determination of Cx43 expression

The aortae and tail arteries of the transgenic mice (single and double transgenic truncated-promoter and single transgenic full-promoter) were observed during the dissections, to be very fragile when compared to the control vessels. Although the dissections proceeded with great care, homogenisation of the tissues was considerably easier than for the control vessels. Whilst this may have artificially increased the protein values to some degree, the data (presented below) indicate that the magnitude of such an increase was negligible. A more extensive network of connective tissue consistently surrounded the tail arteries in the control mice.

Western blots were used to investigate the protein level of Cx43 in the tail artery and aorta of both control and transgenic mice of either sex. Protein assays were conducted so that equal amounts of protein were loaded per lane, that is 1 mg for the aortae and 12 mg for the tail arteries. Results from the Western blots for Groups 2 to 4 (single transgenic truncated-promoter, double transgenic truncated-promoter, and single transgenic full-promoter mice) are shown in Figure 4.4A to D and presented in Tables 4.4 and 4.5. Data from Group 1 (single transgenic truncated-promoter mice) were

Figure 4.4 Western blot analyses of Cx43 in the aortae and tail arteries

Representative portions of Western blot gels from the aortae and tail arteries of the single and double transgenic truncated-promoter mice, and the single transgenic full-promoter mice. The blots were detected with the Cx43 antibody, followed by the β-actin antibody (as indicated). The actin antibody was supplied by Dr MF Crouch, Division of Neuroscience, John Curtin School of Medical Research, ANU.

A

Aorta
Cx43

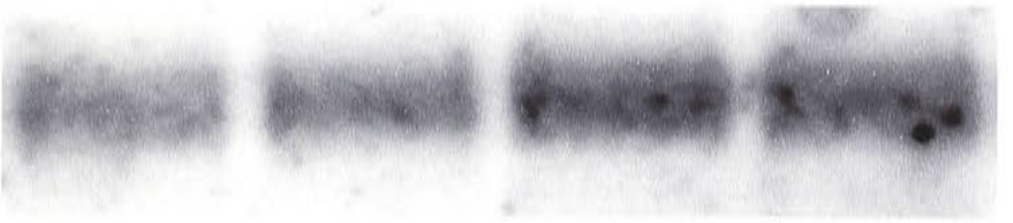

control | single truncated-promoter | double truncated-promoter | single full-promoter

B

Aorta
Actin

control | single truncated-promoter | double truncated-promoter | single full-promoter

C

Tail artery
Cx43

control | single truncated-promoter | double truncated-promoter | single full-promoter

D

Tail artery
Actin

control | single truncated-promoter | double truncated-promoter | single full-promoter

analyzed separately due to different experimental conditions. The data presented are estimates of signal intensity (relative optical density x mm^2), as determined using AIS (Analytical Imaging System)

For Group 1 (single transgenic truncated-promoter mice) Tris-buffer was used to homogenize the aortae (individually processed) and the tail arteries (combined into control and transgenic). There was no significant difference in the aortic Cx43 levels between the control (37.80 ± 16.71; $n = 8$) and transgenic (27.66 ± 10.27; $n = 9$; $P > 0.05$) mice. Similar results were obtained for Cx43 levels in the tail arteries for the control ($2.5 \times 10^{-4} \pm 5.0 \times 10^{-5}$; $n = 2$) and transgenic ($3.5 \times 10^{-4} \pm 5.0 \times 10^{-5}$; $n = 2$; $P > 0.05$) mice. In the latter, the n values refer to data from two groups of mice. There was no significant sex difference at the 5% level for the aortae.

For the second group of single transgenic truncated-promoter mice, and also the double transgenic truncated-promoter and single transgenic full-promoter mice, all tissues were homogenized in sodium bicarbonate buffer and the aortae paired, whilst the tails were combined to give a minimum final concentration of 12 mg wet weight / 10 µl 1x sample buffer. The Western blots were again analysed using AIS to determine the respective Cx43 and actin quantitative gel values. Significant values when compared to control are indicated.

TREATMENT	Aorta Cx43 level	Aorta Actin level	Tail Artery Cx43 level	Tail Artery Actin level
Control	56.56 ± 8.72 $n = 7$	0.09 ± 0.02 $n = 7$	0.25 ± 0.05 $n = 2$	$5.95 \times 10^{-4} \pm 8.5 \times 10^{-5}$ $n = 2$
Sgl Transgenic Trunc. Prom.	63.38 ± 10.30 $n = 5$	0.11 ± 0.04 $n = 5$	0.38 ± 0.08 n = 2	$1.20 \times 10^{-3} \pm 0.0002$ $n = 2$
Dbl Transgenic Trunc. Prom.	173.3 ± 16.97 $n = 4$ $P < 0.05$	0.13 ± 0.03 $n = 4$	0.38 ± 0.005 $n = 2$	$9.80 \times 10^{-4} \pm 6.0 \times 10^{-5}$ $n = 2$
Sgl Transgenic Full Promoter	135.0 ± 8.02 $n = 5$ $P < 0.05$	0.15 ± 0.02 $n = 5$	0.44 $n = 1$	4.98×10^{-4} $n = 1$

Table 4.4 Combined Cx43 and actin quantitative gel values for the aortae and tail arteries.

(n = number of samples analyzed; data presented are estimates of signal intensity (relative optical density x mm^2)).

Briefly, the aortic Cx43 protein values for the single transgenic truncated-promoter mice were not significantly different from the control mice ($P > 0.05$) and similarly for the actin protein values. There was, however, a significant 3 fold difference in the quantity of Cx43 expressed in the double transgenic truncated-promoter mice versus control ($P < 0.05$). The corresponding actin value was not significantly increased ($P > 0.05$). In the aortae of the single transgenic full-promoter mice, the Cx43 protein level increased by 2.4x over control values ($P < 0.05$). The slight increase in the transgenic mice actin levels was not significant ($P > 0.05$). The Cx43 protein levels in the single and double transgenic truncated-promoter tail arteries showed a trend towards an increase ($P > 0.05$), with a similar trend in the single transgenic full-promoter mice.

No definitive conclusions could be drawn from the tail artery data due to the small sample sizes. However, it would seem that the pattern was consistent with that observed with the aortae.

There was a significant sex difference in Cx43 protein ($P < 0.05$) with males consistently having 20 – 30% more Cx43 in the aortae than their female counterparts. There was no corresponding increase in the actin values, as expected. Representative mice from the aortic control, double transgenic truncated-promoter and single transgenic full-promoter mice are shown in Table 4.5. In the tail arteries of the single transgenic truncated-promoter mice, there was a much smaller increase in the Cx43 protein values, 3% between males and females.

TREATMENT (aorta)	Connexin value	Actin value
Control (n = 4; ♂)	65	0.185
Control (n = 4; ♀)	53	0.167
Dble TruncProm (n = 1; ♂)	206	0.09
Dble TruncProm (n = 2; ♀)	157	0.15
Single FullProm (n = 2; ♂)	143	0.16
Single FullProm (n = 2; ♀)	119	0.14

Table 4.5 Representative semi-quantitative aortic Cx43 protein and actin data

(TruncProm/FullProm = Truncated- or Full-promoter)
(*n* = number of samples analyzed; data presented are estimates of signal intensity (relative optical density x mm^2)).

4.2.7 Immunohistochemistry

Immunohistochemical staining indicated no qualitative change in Cx43 levels between the single transgenic truncated-promoter mice and controls in any tissues examined - the thoracic aorta, mesenteric artery, abdominal aorta, tail artery, ventricle and vena cava. No immunohistochemistry was undertaken on the double transgenic truncated-promoter and single transgenic full-promoter mice because of time constraints.

4.3 Discussion

Interbreeding of the single transgenic offspring of both the truncated SM22α / Cx43 (truncated-promoter) and entire SM22α / Cx43 (full-promoter) transgenic mouse lines, produced double transgenic truncated-promoter and double transgenic full-promoter mice. Phenotypic and molecular genetic analysis of transgenic mouse lines has revealed a high level of stability of the transgene integration sites in mice (Aigner *et al.* 1999) and so, upon the establishment of double transgenic lines, breeding programs can be continued to a large number of generations without the need for further stringent molecular genetic analyses.

Interpretation of data obtained from transgenic mice should take into consideration that, in the case of microinjection of DNA into pronuclei (usually the male pronuclei) of mouse zygotes as established by Gordon *et al.* (1980), multiple copies of the transgene are usually integrated in large arrays (Palmiter and Brinster, 1986). However, transgene expression may not necessarily correlate with copy number (Fishman, 1998). The exceptions are the few transgenes which contain all of the elements necessary for position-independent expression, such as the locus control region (LCR) in human β-globin genes (Grosveld *et al.* 1987; Ryan *et al.* 1989), the chicken lysosome locus (Bonifer *et al.* 1994, 1996) and ovine B-lactoglobulin locus (Whitelaw

et al. 1992). LCRs, however, have not been determined for most genes. A method of identifying sites permissive for transgene expression and their use for efficient introduction of single copy genes by homologous recombination has recently been described (Wallace *et al*. 2000).

General physical observations revealed that the single transgenic full-promoter mice had significantly smaller litter sizes than either the single transgenic truncated-promoter or double transgenic truncated-promoter mice. This may represent lowered fertility and/or fecundity rates in this group. The sex ratios were equal in each group, which is consistent with Mendelian ratios, and the neo-natal mortality rate was within normal population limits.

Interestingly, all the transgenic mice were lighter (in bodyweight) than their non-transgenic litter mates, with the double transgenic truncated-promoter males being the lightest. The difference between the male and the female bodyweights in the latter group was almost negligible compared to that recorded for the single truncated- and full-promoter mice. Although the body weights were recorded at the same time each day, the influence of unknown recent feeding on the body weight needs to be considered. Individual weights obtained for the entire digestive tracts, however, indicated that this was not likely to be a problem (data not shown). The bodyweight differences may reflect the presence of the construct, including increased gene copy number, or may be the direct result of the transgene integration site (Milano *et al*. 1994; Hein *et al*. 1995; Doevendans *et al*. 1998).

There were differences in the relative organ weights (heart and kidneys) for the single truncated-promoter mice. The relative lung weight for the control and transgenic mice was almost identical, whilst the transgenic male mice had larger livers than did the control mice. The reason for this is unknown. In the single transgenic full-promoter males, all relative organ weights were increased over control, whilst in the females, only the liver and lung were increased over control. This may simply be a sex-difference.

The value of using the relative weight of a particular tissue rather than absolute weight is evident, allowing more accurate interpretation of the data to be made. The variation in the organ weights, although not statistically significant, is most likely a strain difference and represents no pathological or physiological change. It is known from murine cardiovascular studies, for example, that in transgenic and gene targeted mouse lines, the heart weight and body weight may either increase or decrease (Milano *et al.* 1994; Hein *et al.* 1995; Doevendans *et al.* 1998), and thus changes in other organs would not be unexpected.

There are two methods of obtaining blood pressure measurements in the mouse: indirect (tail-cuff plethysmography) and direct (intra-arterial; telemetry). A close correlation between the two methods in conscious mice and rats exists, with systolic blood pressure as measured by the tail-cuff method, being only 1-9 mmHg higher than intra-aortic measurements (Pfeffer *et al.* 1971; Ikeda *et al.* 1991; Krege *et al.* 1995). Tail-cuff plethysmography allows accurate and reproducible measurements of systolic blood pressure to be obtained (Hoit, 2001), without the surgical invasiveness required for telemetry and the associated anaesthetic complications. Anaesthesia should be avoided where possible as its deleterious effects on blood pressure can last from 24 hours to 4 days post-administration (Janssen *et al.* 1997). Direct intra-arterial assessment in unrestrained and unanaesthetized animals is, nevertheless, regarded as the most physiologically appropriate method of determining the blood pressure (Bunag, 1983; Ferrari *et al.* 1986; Kurtz and St Lezin, 1992; Sponer *et al.* 1993; Mills *et al.* 2000; Butz and Davisson, 2001; Schyvens *et al.* 2001).

Although the blood pressure measurements were quite variable, they were still within the normal limits for mice. Individual tail-cuff measurements are always subject to variability due to animal movement (mice are very active animals compared to rats), stress and associated excessive vasoconstriction. Stress is a major factor in the variability of tail-cuff plethysmography measurements. The heart rate, for example, in

the unanaesthetized resting mouse, varies between 480 and 540 beats per minute (bpm) but during light exercise, the heart rate increases to 600-650 bpm in the BALB/c mouse and during stressful events such as hand restraint, to 750-800 bpm (Kramer *et al*. 1993). As the heart rate varies, concomitant changes occur in blood pressure. It had been hoped in the current study, albeit unsuccessfully, to reduce or even eliminate the variability by extending the number of blood pressure measurements to a total of 16 over 4 weeks. Previous studies have used 60 to 100 tail-cuff measurements for each mouse (Krege *et al*. 1995), which is in direct contrast to those who claim a stable blood pressure measurement with four or five readings (Johns *et al*. 1996). Recently, Janssen and Smits (2002) concluded that the tail-cuff method is more practical when blood pressures between groups have to be compared over long periods.

Although the majority of mice in the current study were handled for three to four days prior to acclimatization on the base-plate, there was still a stress response as determined by the 4% loss in body weight after the first recording. The initial blood pressure recordings were often higher than those subsequently obtained and there was also a noticeable post-recording change in temperament in the mice. They became unco-operative with increased vocalization, until they adjusted to the tail-cuff plethysmography equipment. According to the body weight measurements, this occurred after the third to fifth reading with attainment of the pre-recording weights occurring relatively slowly, indicating a slow adaptive response.

The difference in the blood pressure measurements between the single transgenic truncated-promoter mice in Groups 1 and 2 may be attributed to the lack of handling of by Group 1 prior to commencement of the measurements. An ANOVA on all groups, showed that acclimatization affected male mice more than the female mice, with male blood pressures decreasing whilst the females increased. Non-acclimatized transgenic mice had the highest blood pressures. The reasons for these differences have yet to be elucidated.

In order for definitive results to be obtained, many more mice need to be tested with an increased number of blood pressure recordings for each individual. However, it may be better to utilize the direct intra-arterial (telemetry) method for recording blood pressure in future. This would also eliminate the stresses inherent in handling and restraint.

The increased tissue fragility of the aortae, tail arteries and associated connective tissue of all the transgenic mice was not expected. Similar findings with other transgenic mice have not, as yet, been reported. This may be partly due to lack of study on the vasculature of normal and transgenic mice. The systemic influence of selectively overexpressing the Cx43 gene in the murine vasculature should not be overlooked, nor should the possibility that the insertion of foreign DNA into the genome may have disrupted the function of one or more endogenous genes (Babinet *et al.* 1989). Clearly, the nature and extent of this tissue phenomenon, and its likely systemic effects, need to be ascertained.

Although a larger number of samples for each group must be studied for more conclusive results, some generalizations can be drawn from the Western blot protein data. The slight increase in Cx43 expression in the single transgenic truncated-promoter mice was not statistically significant but the trend suggested an increase, which will require further testing of the mice to establish its significance. It appears unlikely that the truncated promoter is capable of full function, but it may retain minimal function.

In the double transgenic truncated-promoter mice, an increased gene copy number significantly increased aortic Cx43 protein levels with little increase in the tail artery Cx43 protein levels. This indicates that the truncated-promoter appears to be tissue specific. It may also indicate that the construct has been incorporated into the genome in a way that allows overexpression of Cx43 in the elastic vessels in the vasculature. Estimates of the gene copy number would have been obtained by either

Southern blot analysis or dot-blot hybridisation assay (Hogan *et al.* 1994) had time permitted.

The single transgenic full-promoter mice had a 3-fold increase in Cx43 protein levels in the aortae compared to the control mice, with a trend towards increased Cx43 protein levels (2-fold) in the tail arteries. This trend may become significant with further testing as only one sample containing five tails was analyzed. This indicates that the full SM22α promoter is providing tissue specificity for Cx43 overexpression in the aorta (elastic artery) and perhaps in the tail artery (muscular artery). Conclusive evidence will be provided by continuing studies on a range of blood vessels from these transgenic mice.

The control actin values for the aortae and tail arteries remained relatively constant both within and between groups, making this a suitable standard for use in the vasculature of mice. A relationship has been proposed to exist between actin microfilaments and gap junctions (Larsen *et al.* 1979; Hitt and Luna, 1994; Murray *et al.* 1997) due to their close anatomical positioning. However, the data obtained so far would not support such a contention. Ongoing testing by other methods such as immunohistochemistry and mRNA analysis will help to verify the data obtained from the Western blots. Future research will be discussed in detail in Chapter 5.

Both the blood pressure recordings and the Western blots, indicate that there is no correlation between blood pressure and Cx43 protein expression levels. In addition, two mice (one in the double transgenic truncated-promoter group and one in the single transgenic full-promoter group) that consistently had high blood pressure measurements did not have increased Cx43 expression in either the aorta or tail artery. Although it would seem likely that increased Cx43 expression does not pre-dispose the mouse to hypertension at this age, it may be that these mice may develop hypertension or even hypotension later in life as has been noted for other hypertensive models (McGuire and Twietmeyer, 1985; O'Sullivan and Harrap, 1995; Hill *et al.* unpublished results).

Differences due to strain are not applicable in the current study as all mice used were BALB/c - only the chimaeras had a mixed BALB/c x C57BL/6 background.

The data obtained from the preliminary analyses in the current study showed that there was a difference both between and within the transgenic truncated and full-promoter mouse lines. However, more work is required to fully elucidate these differences and correspondingly, the phenotypes. In terms of the Cx43 expression data and the blood pressure measurements, it would seem that increased Cx43 expression does not cause hypertension or hypotension in the mouse. However, no definite conclusions can be drawn at this stage without further study, and perhaps even repeating the microinjection protocol so that comparisons with other full-promoter transgenic mice can be made. The significance of much of the available data with respect to vascular function remains to be elucidated.

Chapter 5 – General Discussion

Gene technology developed over the last ten to fifteen years, has allowed the introduction of foreign gene/s into the germ-line of mice, permitting new insights into a wide variety of biological mechanisms. This has resulted in biomedical research making use of transgenic mice which are specific to a particular molecular genetic question (Jaenisch, 1988; Hanahan, 1989; Babinet, 2000; Janssen and Smits, 2002). This methodology has a wide range of applications (Connelly *et al*. 1989; Babinet, 2000), from the regulation of gene expression *in vivo* and analysis of gene manipulation, to the establishment of disease models for the study of pathogenesis.

The primary aim of this thesis was to determine the role of Cx43 in hypertensive states by producing a transgenic mouse model that would selectively overexpress Cx43 in the arterial system. Two genetically modified mice were in fact produced: one containing a truncated form of the restricted SM22α promoter coupled to the Cx43 gene, and the other containing the entire restricted SM22α promoter coupled to the Cx43 gene. Preliminary studies were undertaken on the mice to investigate their phenotypes and the level of Cx43 expression in the vasculature.

Briefly, the tail artery tissues of all transgenic mice were more fragile than the control mouse, and the blood pressures of all mice were within the normal range. The Cx43 protein levels in the aortae and tail arteries of the single transgenic-promoter mice were not significantly increased, but in the double transgenic truncated-promoter mice, the Cx43 protein levels were significantly increased in the aorta, with no change in the tail artery. This indicated that the truncated-promoter was minimally functional. In the single transgenic full-promoter mice, aortic Cx43 protein levels were significantly increased with a trend towards increased Cx43 in the tail arteries, which demonstrated that the SM22α / Cx43 construct may be functional *in vivo*.

A number of germane areas were identified during the preliminary studies: the transient transfection system, the low expression level of the SM22α construct and the subsequent analysis of Cx43 expression by Western Blotting. These will now be discussed.

Data presented from the transfections of the construct in Chapter 3, showed that the SM22α / Cx43 construct was tissue specific. The low expression rates for the construct in the smooth muscle cells are of concern when viewed in conjunction with the expression rates for the control CMV-EGFP plasmid, and results from previous papers utilizing SM22α promoter constructs (Kemp *et al.* 1995; Solway *et al.* 1995; Li *et al.* 1996; Moessler *et al.* 1996). Solway *et al.* (1995) found that in both primary rat aortic smooth muscle cells and the smooth muscle cell line A7r5, the transfected murine 482 bp SM22α promoter (bp –441 to +41) was active and increased transcription of the luciferase reporter gene to a high level. Passage three cells were used, together with Lipofectin Reagent (Life Technologies). The 493 bp SM22α promoter (bp -438 to +56) used in the current study was based on this promoter.

Several SM22α promoter constructs of varying lengths have been transfected into primary cultured rabbit aortic cell lines, both with and without 10% serum, and using the Lipofectamine Reagent (Moessler *et al.* 1996). The best transfection rates (3-fold increase in expression of β-galactosidase) were with the 510 bp promoter (bp -445 to +65) which was again longer, by seven bases at the 5' (proximal) end and seven at the 3' (distal) end, than the promoter used in the current study. Expression was reduced when using promoters of a shorter length (417 bp; bp -352 to +65) and absent (low background only) when at 271 bp (bp -206 to +65). The truncated-promoter in the current study contained somewhere between 204 and 103 bp of the restricted 493 bp SM22α promoter and consequently, based on the above study, would not be capable of directing transcription *in vivo*. In comparison, Solway *et al.* (1995) showed that in transfections of their 482 bp promoter (bp -441 to +41), expression of luciferase was

increased by 250-300 fold compared to control, especially in the smooth muscle cell line, whilst no expression was detected in all non-smooth muscle cells. This represents a considerable difference in expression levels. Shorter promoter lengths of 365 bp (bp –300 to +65; 50% reduction) and 227 bp (bp –162 to +65; 90% reduction) were also transfected, with only background expression levels being observed for the latter. This again suggested that the truncated-promoter in the present study would not be functional *in vivo*. Actually, the truncated-promoter was found to have tissue specificity *in vivo* (Chapter 4), despite these previous studies suggesting that no expression would occur.

The only difference between the 482 bp promoter used by Solway *et al*. (1995) and the one used in the current study, is the absence of five bases at the 5' end of the promoter, and an extra fifteen bases on the 3' (exon 1) end. The omission of three bases (AGT) in the design of the construct was not thought to be of concern as they form part of the *Pst*I restriction enzyme site only. However, as two more bases at the forward end were lost during the cloning of the respective constructs, the possible functional significance of these missing bases needs to be considered when reviewing the results presented herein.

Similar results to that of Solway *et al*. (1995) were observed in the cloning and analysis of the promoter region of the rat SM22α gene by Kemp *et al*. (1995) which has 98% homology with the mouse SM22α protein (Li *et al*. 1996). Promoters of similar length to those already made in the mouse, were coupled to the reporter CAT (choramphenicol acetyltransferase) gene and transfected by electroporation into cultured adult rat aortic vascular smooth muscle cells and Rat-1 fibroblasts. The highest expression levels were recorded for the 368 bp promoter (bp –303 to +65; 295%) in both cell types, followed by the 258 bp promoter (bp –193 to +65; 44% in vascular smooth muscle cells) and the 182 bp promoter (bp –117 to +65; 39% in vascular smooth muscle cells). For both the 258 and 182 bp fragments, no CAT activity was detected in the fibroblasts. The residual promoter activity for the smallest promoter suggested that

factors binding to the proximal 182 bases of the SM22α promoter play an important role in restricting the expression of the SM22α gene to smooth muscle cells. Interestingly, these results differ from the data presented for the mouse promoter *in vitro* (Moessler *et al*. 1996).

Direct comparisons between the expression levels for the different promoter lengths are difficult to substantiate, as different plasmids, cell lines and types (which affect transfection efficiency and thus gene expression), detection methods and transfection reagents and methods were used. In the literature, murine aortic smooth muscle cells have not been chosen as the vehicle in which to study the murine SM22α promoter constructs. One mitigating factor could be that, as the current study determined, published data concerning the culture and transfection of these cells *in vitro* is lacking and at present, there is no recommended transfection reagent for murine aortic smooth muscle cells. Hamm *et al*. (2002) have recently reported on the successful use of the Nucleofectortrade mark technology in the transfection of human coronary smooth muscle cells, but its applicability to murine smooth muscle cells remains to be ascertained.

The differentiation state of the smooth muscle cells was of the utmost importance, and the most difficult to determine. As discussed in Chapter 3, Solway *et al*. (1995) used rat aortic cells at passage three, together with Lipofectin Reagent, whilst Moessler *et al*. (1996) tested the same promoter region in primary cultured rabbit aortic smooth muscle cells, both with and without 10% serum and using the Lipofectamine Reagent. In the latter, high-level expression was detected in the absence of serum (differentiated cells) with a 3-fold lower expression in the cells cultured with 10% serum (proliferating cells). As smooth muscle cells are known to readily de-differentiate *in vitro* (Moessler *et al*. 1996), procedural modifications were invoked to confirm the status of the cells and to promote differentiation by the use of insulin, for example. However, no improvement in expression levels for any construct was

observed. This indicates that the experimental conditions were still not optimal for expression of the SM22α construct, especially as the CMV-EGFP transfection rates remained relatively constant and at an acceptably high level throughout the experiments. Interestingly, it has recently been shown that the SM22α promoter activities in canine tracheal myocytes were decreased by 8-fold in long-term serum deprived smooth muscle cells compared with serum-fed cells, whilst the activity of a viral promoter was not affected (Camoretti-Mercado *et al*. 2000).

These points raise the question about the possible effect of the coupling of the SM22α promoter to various reporter genes. It is possible from the data in the current study to hypothesize that the coupling of the SM22α promoter to the Cx43 gene, may have affected the performance of the promoter. However, it may simply reflect the differences in detection sensitivity or alternatively, the CMV promoter may be more effective than the SM22α promoter. The data in the present study as well as from other studies (Gerolami *et al*. 2000; Ribault *et al*. 2001) would support either tenet.

In terms of coupling and expression levels, it is possible that combined, the omission of the seven bases at the 5' end of the SM22α promoter fragment (compared to other promoters where no bases, and fourteen bases, were missing), and the loss of seven bases at the 3' end (compared to the optimally expressing promoter lengths), affected the functioning of the SM22α promoter when it was coupled to the Cx43 gene. As all published work to date has included all of exon 1 in the cloning of the SM22α promoter, it would be advisable to include this entire region in future cloning exercises involving the murine SM22α promoter. The inclusion of more bases at the forward end of the restricted SM22α promoter region is recommended to ensure adequate and high expression levels of the gene of interest. Nevertheless, overexpression of Cx43 in the aortae of single transgenic full-promoter mice was observed in the current study and it is likely that with further testing, the 2-fold trend towards increased Cx43 expression in the tail arteries, will also prove to be significant.

In vivo data from the single transgenic truncated-promoter and the double transgenic full-promoter mice did not support the *in vitro* evidence presented above by Solway *et al.* (1995) and Kemp *et al.* (1995) that the truncated-promoter (between 204 and 103 bp) could not function in either of its tissue specific or gene-driving roles *in vivo*. The data indicated that truncated-promoter was minimally functional, especially in driving tissue specificity which, until the number of bases present is accurately determined, either extends or confirms the findings by Kemp *et al.* (1995) who found residual promoter activity with a 182 bp SM22α promoter fragment. If the construct had been incorporated into the genome and was under the control of another promoter, tissue-specificity would have been lost.

The increased Cx43 expression in the aorta and the trend towards increased Cx43 expression in the tail artery of the single transgenic full-promoter mice, indicate that the SM22α / Cx43 construct is functional *in vivo*, though to what extent remains to be determined by the ongoing studies. Tang *et al.* (2000) found a 76% increase in the GFA (glutamine:fructose-6-phosphate amidotransferase) single transgenic mice compared to the littermate controls. Others, such as Wang *et al.* (1997), reported a 3.5 to 4-fold to 10-fold increase over controls in transgenic mice overexpressing IGF-I. The trend towards increased Cx43 expression in the tail arteries for the single and double transgenic truncated-promoter mice and the single transgenic full-promoter mice, may simply be a reflection of the relatively small sample sizes. Perhaps as only one single transgenic full-promoter founder mouse was made, compared to the norm of four or five, it is possible that due to gene copy number and position effects in this mouse, this mouse is not capable of giving the best result in terms of Cx43 expression.

Three problems were identified in the analysis of Cx43 expression levels in the aortae and tail arteries of the transgenic and control mice using Western blots. Firstly, the tissue extraction component of the procedure needs to be considered. The basic assumption in this procedure was that each sample (artery) gave an equal amount of

membrane protein. So for four mice tails, this would equate to 12 mg wet weight / 10 µl (4 tails combined); the minimum amount of tissue required for visualization on a gel. However, after determining the wet weight of each sample, it is impossible to control the tissue extraction so that complete homogenization of each tissue sample occurs. I only used visual observation for determining when homogenization of the tissue was complete, although in the future, spectrophotometry could be used. Tissues that are easier to homogenize such as those with less connective tissue, are more likely to have higher membrane protein values. All the transgenic mice in the current study were observed to have fragile aortae and tail arteries compared to the controls and this may have influenced the Cx43 protein values to some degree. Anatomical studies are needed to ascertain the cause of the fragility.

There did not appear to be any difference in the intensity of the actin bands between groups macroscopically, but when the bands were analyzed with the AIS program slight, though non-significant, differences were observed. This highlights the fact that for actin, the value of Western blots for detecting change in protein expression is limited when the gels are viewed by 'eye' only. The same however cannot be said for detecting Cx43 expression in the aortae, where gross changes in bandwidth and intensity could be seen. For the tail artery, changes observed macroscopically became more significant when assessed with the AIS program.

The consistent variation in the Cx43 values between the groups and the constant actin values give credibility to the results presented in this work. It also points to the role of actin as an important and conserved entity in vascular smooth muscle. The value of using a control such as β-actin is evident. However, as the values were derived from relatively small (combined) sample sizes, especially for the double transgenic truncated-promoter and single transgenic full-promoter mice, it is recommended that further experiments be conducted using this standard to confirm the trends seen in the current study. In addition, protein assays cannot be viewed as a strictly valid determinator of

the membrane protein, and hence Cx43 protein present, in the tissue samples due to the presence of other proteins such as enzymes, that may not be directly present in smooth muscle.

The data from this thesis indicate that increased Cx43 expression can occur without a concomitant increase or decrease in blood pressure. Both the double transgenic truncated-promoter mice, and the single transgenic full-promoter mice, had increased Cx43 expression in the aortae with a trend towards increased Cx43 expression in the tail arteries, without any increase or decrease in blood pressure. This opens up a wide variety of opportunities for future studies on these mice, with potentially important implications for the study of hypertension, as increased blood pressure has traditionally been associated with an increase in Cx43 expression (Blackburn *et al.* 1997; Donaldson *et al.* 1997, Haefliger *et al.* 1997a,b; Haefliger and Meda, 2000). Recently, however, a decrease in Cx43 expression in the aorta of L-NAME hypertensive rats has been reported (Haefliger *et al.* 1999). Exactly what causes increased expression of Cx43 in hypertension is open to speculation, whilst the effect of increased Cx43 expression on vascular function remains to be elucidated. This represents an exciting area of further investigation.

Future Studies

It is unfortunate that time restrictions prevented the realisation of a more definitive picture of the characteristics of the mice produced - particularly the double transgenic full-promoter mice. My work has indicated several directions for future study, including immunohistochemistry and semi-quantitative mRNA using reverse transcription PCR (RT-PCR). This is work that should be included in a series of further studies.

To assess the effect of the increased Cx43 expression on the vascular responses physiological experiments such as electrophysiology and myography, should also be

undertaken. This work has demonstrated that not only must a substantial number of mice need to be subjected to blood pressure recordings, but also an increased number of recordings for each individual must be employed. This latter requirement suggests that it would be worthwhile trialling telemetry for continuous recording of blood pressure in future studies. This would also have the benefit of eliminating, or at least minimising, blood pressure altering stresses inherent in handling and restraint.

Comparison of data from ongoing studies using such techniques as immunohistochemistry, dye-tracer studies and / or calcium imaging of gap junction activity on both the control and transgenic mice should yield, for example, information on age-related and disease-related alterations in second messenger levels, metabolism and diffusion, sympathetic and sensory innervations, and neurotransmitter receptors.

A further area of interest for continuing study, and an alternative method for producing transgenic mice, is the use of the Tetracycline Expression System (Tet) to control the temporal expression of Cx43. To accomplish this, both tissue specific activity (using the restricted portion of the SM22α promoter) and temporal specific activity (using Tet to turn the Cx43 gene on in adulthood) must be present. Briefly, the transgenic mice separately produced by injection of these constructs, would be intercrossed to produce a doubly transgenic mouse line in which both constructs were present in the same cell. It would be hoped that Cx43 expression will be driven by the SM22α promoter under the temporal control of tetracycline. More detail is provided in Appendix II which also describes the work accomplished on this exciting area.

Conclusion

Finally, the results of this study should provide the groundwork for further experimentation into the physiological effects of Cx43 overexpression in the vasculature and changes in vascular reactivity.

Reference List

Aalkjaer, C. and Mulvany, M. J. (1995). Morphology of isolated small arteries from patients with essential hypertension. *Blood Pressure Supplement* **2**: 113-116.

Abel, A., Bone, L. J., Messing, A., Scherer, S. S., and Fischbeck, K. H. (1999). Studies in transgenic mice indicate a loss of connexin32 function in X-linked Charcot-Marie-Tooth disease. *Journal of Neuropathology and Experimental Neurology* **58**: 702-710.

Aburto, T. K., Lajoie, C., and Morgan, K. G. (1993). Mechanisms of signal transduction during alpha 2-adrenergic receptor-mediated contraction of vascular smooth muscle. *Circulation Research* **72**: 778-785.

Ackland-Berglund, C. E. and Leib, D. A. (1995). Efficacy of tetracycline-controlled gene expression is influenced by cell type. *BioTechniques* **18**: 196-200.

Almouzni, G. and Wolffe, A. P. (1993). Replication-coupled chromatin assembly is required for the repression of basal transcription in vivo. *Genes and Development* **7**: 2033-2047.

Altman, J. D., Trendelenburg, A. U., Macmillan, L., Bernstein, D., Limbird, L., Starke, K., Kobilka, B. K., and Hein, L. (1999). Abnormal regulation of the sympathetic nervous system in α_{2A}-adrenergic receptor knockout mice. *Molecular Pharmacology* **56**: 154-161.

Andreeva, E. R., Serebryakov, V. N., and Orekhov, A. N. (1995). Gap junctional communication in primary culture of cells derived from human aortic intima. *Tissue Cell* **27**: 591-597.

Anzini, P., Neuberg, D. H. H., Schachner, M., Nelles, E., Willecke, K., Zielasek, J., Toyka, K. V., Suter, U., and Martini, R. (1997). Structural abnormalities and deficient maintenance of peripheral nerve myelin in mice lacking the gap junction protein connexin 32. *Journal of Neuroscience* **17**: 4545-4551.

Arii, T., Ohyanagi, M., Shibuya, J., and Iwasaki, T. (1999). Increased function of the voltage-dependent calcium channels, without increase of Ca^{2+} release from the sarcoplasmic reticulum in the arterioles of spontaneous hypertensive rats. *American Journal of Hypertension* **12**: 1236-1242.

Arnal, J. F., Dinh-Xuan, A. T., Pueyo, M., Darblade, B., and Rami, J. (1999). Endothelium-derived nitric oxide and vascular physiology and pathology. *Cellular and Molecular Life Sciences* **55**: 1078-1087.

Babinet, C. (2000). Transgenic mice: an irreplaceable tool for the study of mammalian development and biology. *Journal of the American Society of Nephrology* **11**: S88-S94.

Babinet, C., Morello, D., and Renard, J. P. (1989). Transgenic mice. *Genome* **31**: 938-949.

Baldwin, C. T., Schwartz, F., Baima, J., Burzstyn, M., DeStefano, A. L., Gavras, I., Handy, D. E., Joost, O., Martel, T., Manolis, A., Nicolaou, M., Bresnahan, M., Farrer, L., and Gavras, H. (1999). Identification of a polymorphic glutamic acid stretch in the α_{2B}-adrenergic receptor and lack of linkage with essential hypertension. *American Journal of Hypertension* **12**: 853-857.

Baron, U., Gossen, M., and Bujard, H. (1997). Tetracycline-controlled transcription in eukaryotes: novel transactivators with graded transactivation potential. *Nucleic Acids Research* **25**: 2723-2729.

Barrio, L. C., Suchyna, T., Bargiello, T., Xu, L. X., Roginski, R. S., Bennett, M. V., and Nicholson, B. J. (1991). Gap junctions formed by connexins 26 and 32 alone and in combination are differently affected by applied voltage [published erratum appears in Proc Natl Acad Sci U S A 1992 May 1;89(9):4220]. *Proceedings of the National Academy of Sciences (USA)* **88**: 8410-8414.

Bastiaanse, E. M., Jongsma, H. J., van der Laarse, A., and Takens-Kwak, B. R. (1993). Heptanol-induced decrease in cardiac gap junctional conductance is mediated by a decrease in the fluidity of membranous cholesterol-rich domains. *Journal of Membrane Biology* **136**: 135-145.

Bastide, B., Neyses, L., Ganten, D., Paul, M., Willecke, K., and Traub, O. (1993). Gap junction protein connexin40 is preferentially expressed in vascular endothelium and conductive bundles of rat myocardium and is increased under hypertensive conditions. *Circulation Research* **73**: 1138-1149.

Baumbach, G. L. (1996). Effects of increased pulse pressure on cerebral arterioles. *Hypertension* **27**: 159-167.

Baumbach, G. L., Siems, J. E., and Heistad, D. D. (1991). Effects of local reduction in pressure on distensibility and composition of cerebral arterioles. *Circulation Research* **68**: 338-351.

Beardslee, M. A., Laing, J. G., and Saffitz, J. E. (1998). Rapid turnover of connexin43 in the adult rat heart. *Circulation Research* **83**: 629-635.

Beblo, D. A. and Veenstra, R. D. (1997). Monovalent cation permeation through the connexin40 gap junction channel. Cs, Rb, K, Na, Li, TEA, TMA, TBA, and effects of anions Br, Cl, F, acetate, aspartate, glutamate, and NO_3. *Journal of General Physiology* **109**: 509-522.

Beblo, D. A., Wang, H.-Z., Beyer, E. C., Westphale, E. M., and Veenstra, R. D. (1995). Unique conductance, gating, and selective permeability properties of gap junction channels formed by connexin40. *Circulation Research* **77**: 813-822.

Bennett, M. V., Barrio, L. C., Bargiello, T. A., Spray, D. C., Hertzberg, E., and Saez, J. C. (1991). Gap junctions: new tools, new answers, new questions. *Neuron* **6**: 305-320.

Bennett, M. V. L., Zheng, X., and Sogin, M. L. (1995). The Connexin Family Tree. In: *Intercellular Communication Through Gap Junctions.* Y. Kanno, K. Kataoka, and Y. Shiba (eds.) Elsevier Science, Amsterdam. p.3-8.

Benowitz, N. L. and Bourne, H. R. (1989). Antihypertensive Agents. In: *Basic and Clinical Pharmacology*. B. G. Katsung (ed.) Prentice-Hall International Inc., London. p.119-140.

Beny, J.-L. (1999). Information networks in the arterial wall. *News in Physiological Sciences* **14**: 68-73.

Beny, J.-L. and Pacicca, C. (1994). Bidirectional electrical communication between smooth muscle and endothelial cells in the pig coronary artery. *American Journal of Physiology* **266**: H1465-H1472.

Bergoffen, J., Scherer, S. S., Wang, S., Scott, M. O., Bone, L. J., Paul, D. L., Chen, K., Lensch, M. W., Chance, P. F., and Fischbeck, K. H. (1993). Connexin mutations in X-linked Charcot-Marie-Tooth disease. *Science* **262**: 2039-2042.

Berk, B. C., Vallega, G., Muslin, A. J., Gordon, H. M., Canessa, M., and Alexander, R. W. (1989). Spontaneously hypertensive rat vascular smooth muscle cells in culture exhibit increased growth and Na^+/H^+ exchange [published erratum appears in J Clin Invest 1989 Dec;84(6):2029]. *Journal of Clinical Investigation* **83**: 822-829.

Berne, R. M. and Levy, M. N. (1989). The Cardiovascular System. In: *Physiology*. The C. V. Mosby Company, St Louis. p.395-572.

Bevan, J. A. (1988). Basal tone in resistance arteries: role of wall stretch, flow and receptor specialization. In: *Vascular Neuroeffector Mechanisms*. J. A. Bevan, H. Majewski, R. A. Maxwell, and D. F. Story (eds.) ICSU Press, Oxford. p.1-14.

Bevan, J. A. and Purdy, R. E. (1973). Variations in adrenergic innervation and contractile responses of the rabbit saphenous artery. *Circulation Research* **32**: 746-751.

Bevan, J. A. and Torok, J. (1970). Movement of norepinephrine through the media of rabbit aorta. *Circulation Research* **27**: 325-331.

Bevans, C. G. and Harris, A. L. (1999). Direct high affinity modulation of connexin channel activity by cyclic nucleotides. *Journal of Biological Chemistry* **274**: 3720-3725.

Bevans, C. G., Kordel, M., Rhee, S. K., and Harris, A. L. (1998). Isoform composition of connexin channels determines selectivity among second messengers and uncharged molecules. *Journal of Biological Chemistry* **273**: 2808-2816.

Beyer, E. C., Paul, D. L., and Goodenough, D. A. (1990). Connexin family of gap junction proteins. *Journal of Membrane Biology* **116**: 187-194.

Beyer, E. C., Reed, K. E., Westphale, E. M., Kanter, H. L., and Larson, D. M. (1992). Molecular cloning and expression of rat connexin40, a gap junction protein expressed in vascular smooth muscle. *Journal of Membrane Biology* **127**: 69-76.

Beyer, E. C. and Steinberg, T. H. (1991). Evidence that the gap junction protein connexin-43 is the ATP-induced pore of mouse macrophages. *Journal of Biological Chemistry* **266**: 7971-7974.

Birukov, K. G., Shirinsky, V. P., Stepanova, O. V., Tkachuk, V. A., Hahn, A. W., Resink, T. J., and Smirnov, V. N. (1995). Stretch affects phenotype and proliferation of vascular smooth muscle cells. *Molecular and Cellular Biochemistry* **144**: 131-139.

Blackburn, J. P., Connat, J.-L., Severs, N. J., and Green, C. R. (1997). Connexin43 gap junction levels during development of the thoracic aorta are temporarily correlated with elastic laminae deposition and increased blood pressure. *Cell Biology International* **21**: 87-97.

Blackburn, J. P., Peters, N. S., Yeh, H.-I., Rothery, S., Green, C. R., and Severs, N. J. (1995). Upregulation of connexin43 gap junctions during early stages of human coronary atherosclerosis. *Arteriosclerosis, Thrombosis and Vascular Biology* **15**: 1219-1228.

Bogeroger, H. and Gruss, P. (1999). Functional determinants for the tetracycline-dependent transactivator tTA in transgenic mouse embryos. *Mechanisms of Development* **83**: 141-153.

Bohr, D. F. and Dominiczak, A. F. (1991). Experimental hypertension. *Hypertension* **17**: I39-I44.

Bohr, D. F., Dominiczak, A. F., and Webb, R. C. (1991a). Pathophysiology of the vasculature in hypertension. *Hypertension* **18**: III69-III75.

Bohr, D. F., Furspan, P. B., and Dominiczak, A. F. (1991b). Many membrane abnormalities in hypertension result from one primary defect. *Advances in Experimental Medicine and Biology* **304**: 291-302.

Bonifer, C., Huber, M. C., Jagle, U., Faust, N., and Sippel, A. E. (1996). Prerequisites for tissue specific and position independent expression of a gene locus in transgenic mice. *Journal of Molecular Medicine* **74**: 663-671.

Bonifer, C., Yannoutsos, N., Kruger, G., Grosveld, F., and Sippel, A. E. (1994). Dissection of the locus control function located on the chicken lysozyme gene domain in transgenic mice. *Nucleic Acids Research* **22**: 4202-4210.

Bortolotto, L. A., Hanon, O., Franconi, G., Boutouyrie, P., Legrain, S., and Girerd, X. (1999). The aging process modifies the distensibility of elastic but not muscular arteries. *Hypertension* **34**: 889-892.

Boulanger, C. M. (1999). Secondary endothelial dysfunction: hypertension and heart failure. *Journal of Molecular and Cellular Cardiology* **31**: 39-49.

Bradley, A., Ramirez-Solis, R., Zheng, H., Hasty, P., and Davis, A. (1992). Genetic manipulation of the mouse via gene targeting in embryonic stem cells. *Ciba Foundation Symposium* **165**: 256-269.

Bredt, D. S. and Snyder, S. H. (1992). Nitric oxide, a novel neuronal messenger. *Neuron* **8**: 3-11.

Brightman, M. W. and Reese, T. S. (1969). Junctions between intimately apposed cell membranes in the vertebrate brain. *Journal of Cell Biology* **40**: 648-677.

Brink, P. R. (1998). Gap junctions in vascular smooth muscle. *Acta Physiologica Scandinavia* **164**: 349-356.

Brink, P. R., Cronin, K., Banach, K., Peterson, E., Westphale, E. M., Seul, K. H., Ramanan, S. V., and Beyer, E. C. (1997). Evidence for heteromeric gap junction channels formed from rat connexin43 and human connexin37. *American Journal of Physiology* **273**: C1386-C1396.

Brink, P. R., Ramanan, S. V., and Christ, G. J. (1996). Human connexin 43 gap junction channel gating: evidence for mode shifts and/or heterogeneity. *American Journal of Physiology* **271**: C321-C331.

Brink, P.R., Ricotta, J., and Christ, G.J. (2000). Biophysical characteristics of gap junctions in vascular wall calls: implications for vascular biology and disease. *Brazilian Journal of Medical and Biological Research* **33**: 415-422.

Brissette, J. L., Kumar, N. M., Gilula, N. B., Hall, J. E., and Dotto, G. P. (1994). Switch in gap junction protein expression is associated with selective changes in junctional permeability during keratinocyte differentiation. *Proceedings of the National Academy of Sciences (USA)* **91**: 6453-6457.

Britz-Cunningham, S. H., Shah, M. M., Zuppan, C. W., and Fletcher, W. H. (1995). Mutations of the connexin43 gap junction gene in patients with heart

malformations and defects of laterality. *New England Journal of Medicine* **332**: 1323-1329.

Bruzzone, R., White, T. W., and Paul, D. L. (1994). Expression of chimeric connexins reveals new properties of the formation and gating behavior of gap junction channels. *Journal of Cell Science* **107**: 955-967.

Bruzzone, R., White, T. W., and Paul, D. L. (1996). Connections with connexins: the molecular basis of direct intercellular signalling. *European Journal of Biochemistry* **238**: 1-27.

Buckbinder, L., Talbott, R., Seizinger, B. R., and Kley, N. (1994). Gene regulation by temperature-sensitive p53 mutants: identification of p53 response genes. *Proceedings of the National Academy of Sciences (USA)* **91**: 10640-10644.

Bukauskas, F. F., Elfgang, C., Willecke, K., and Weingart, R. (1995). Heterotypic gap junction channels (connexin26-connexin32) violate the paradigm of unitary conductance. *Pflugers Arch: European Journal of Physiology* **429**: 870-872.

Bukauskas, F. F., Jordan, K., Bukauskiene, A., Bennett, M. V. L., Lampe, P. D., and Laird, D. W. (2000). Clustering of connexin 43-enhanced green fluorescent protein gap junction channels and functional coupling in living cells. *Proceedings of the National Academy of Sciences (USA)* **97**: 2556-2561.

Bunag, R. D. (1983). Facts and fallacies about measuring blood pressure in rats. *Clinical and Experimental Hypertension* **5**: 1659-1681.

Bunce, D. F. (1970). Morphology of human umbilical cord vessels. *Journal of the American Osteopathic Association* **69**: 1018-1019.

Burnstock, G. (1970). Structure of smooth muscle and its innervation. In: *Smooth Muscle*. E. Bulbring, A. F. Brading, A. W. Jones, and T. Tomita (eds.) Edward Arnold Ltd., London. p.1-69.

Burnstock, G. (1999). Release of vasoactive substances from endothelial cells by shear stress and purinergic mechanosensory transduction. *Journal of Anatomy* **194**: 335-342.

Burnstock, G. and Ralevic, V. (1994). New insights into the local regulation of blood flow by perivascular nerves and endothelium. *British Journal of Plastic Surgery* **47**: 527-543.

Burt, J. M. and Spray, D. C. (1988). Inotropic agents modulate gap junctional conductance between cardiac myocytes. *American Journal of Physiology* **254**: H1206-H1210.

Burt, J. M. and Spray, D. C. (1989). Volatile anesthetics block intercellular communication between neonatal rat myocardial cells. *Circulation Research* **65**: 829-837.

Butz, G.M. and Davisson, R.L. (2001). Long-term telemetric measurement of cardiovascular parameters in awake mice: a physiological genomics tool. *Physiological Genomics* **5**: 89-97.

Bylund, D. B. (1995). Pharmacological characteristics of alpha-$_2$ adrenergic receptor subtypes. *Annals of the New York Academy of Sciences* **763:** 1-7.

Calero, G., Kanemitsu, M., Taffet, S. M., Lau, A. F., and Delmar, M. (1998). A 17mer peptide interferes with acidification-induced uncoupling of connexin43. *Circulation Research* **82**: 929-935.

Callus, B. A. and Mathey-Prevot, B. (1999). Rapid selection of tetracycline-controlled inducible cell lines using a green fluorescent-transactivator fusion protein. *Biochemical and Biophysical Research Communications* **257**: 874-878.

Camoretti-Mercado, B., Liu, H-W., Halayko, A.J., Forsythe, S.M., Kyle, J.W., Li, B., Fu, Y., McConville, J., Kogut, P., Vieira, J.E., Patel, N.M., Hershenson, M.B., Fuchs, E., Sinha, S., Miano, J.M., Parmacek, M.S., Burkhardt, J.K., and Solway, J. (2000). Physiological control of smooth muscle-specific gene expression through regulated nuclear translocation of serum response factor. *Journal of Biological Chemistry* **275**: 30387-30393.

Campbell, G. R., Chamley-Campbell, J., Short, N., Robinson, R. B., and Hermsmeyer, K. (1981). Effect of cross-transplantation on normotensive and spontaneously hypertensive rat arterial muscle membrane. *Hypertension* **3**: 534-543.

Casey, J. L., Coley, A. M., Tilley, L. M., and Foley, M. (2000). Green fluorescent antibodies: novel in vitro tools. *Protein Engineering* **13**: 445-452.

Caspar, D. L., Goodenough, D. A., Makowski, L., and Phillips, W. C. (1977). Gap junction structures. I. Correlated electron microscopy and x-ray diffraction. *Journal of Cell Biology* **74**: 605-628.

Castro, C., Gomez-Hernandez, J. M., Silander, K., and Barrio, L. C. (1999). Altered formation of hemichannels and gap junction channels caused by C- terminal connexin-32 mutations. *Journal of Neuroscience* **19**: 3752-3760.

Chalfie, M., Tu, Y., Eukirchen, G., Ward, W. W., and Prasher, D. C. (1994). *Science* **263**: 802-805.

Chan, S. Y. and Evans, M. J. (1991). In situ freezing of embryonic stem cells in multiwell plates. *Trends in Genetics* **7**: 76.

Chanson, M., Scerri, I., and Suter, S. (1999). Defective regulation of gap junctional coupling in cystic fibrosis pancreatic duct cells. *Journal of Clinical Investigation* **103**: 1677-1684.

Chaytor, A. T., Evans, W. H., and Griffith, T. M. (1997). Peptides homologous to extracellular loop motifs of connexin 43 reversibly abolish rhythmic contractile activity in rabbit arteries. *Journal of Physiology* **503**: 99-110.

Chaytor, A. T., Evans, W. H., and Griffith, T. M. (1998). Central role of heterocellular gap junctional communication in endothelium-dependent relaxations of rabbit arteries. *Journal of Physiology* **508**: 561-573.

Chen, J., Kelz, M. B., Zeng, G., Sakai, N., Steffen, C., Shockett, P., Picciotto, M. R., Duman, R. S., and Nestler, E. J. (1998). Transgenic animals with inducible, targeted gene expression. *Molecular Pharmacology* **54**: 495-503.

Chen, Y.-F. and Meng, Q.-M. (1991). Sexual dimorphism of blood pressure in spontaneously hypertensive rats is androgen dependent. *Life Sciences* **48**: 85-96.

Chiocchetti, A., Tolosano, E., Hirsch, E., Silengo, L., and Altruda, F. (1997). Green fluorescent protein as a reporter of gene expression in transgenic mice. *Biochimica et Biophysica Acta* **1352**: 193-202.

Christ, G. J., Brink, P. R., Melman, A., and Spray, D. C. (1993a). The role of gap junctions and ion channels in the modulation of electrical and chemical signals in human corpus cavernosum smooth muscle. *International Journal of Impotence Research* **5**: 77-96.

Christ, G. J., Brink, P. R., Zhao, W., Moss, J., Gondre, C. M., and Roy, C. S. (1993b). Gap junctions modulate tissue contractility and alpha 1 adrenergic agonist efficacy in isolated rat aorta. *Journal of Pharmacology and Experimental Therapeutics* **266**: 1054-1065.

Christ, G. J., Spray, D. C., El-Sabban, M., Moore, L. K., and Brink, P. R. (1996). Gap junctions in vascular tissues. *Circulation Research* **79**: 631-646.

Christensen, K. L. (1991). Reducing pulse pressure in hypertension may normalize small artery structure. *Hypertension* **18**: 722-727.

Chung, O. and Unger, T. (1999). Angiotensin II receptor blockade and end-organ protection. *American Journal of Hypertension* **12**: 150S-156S.

Cliff, W. J. (1967). The aortic tunica media in growing rats studied with the electron microscope. *Laboratory Investigation* **17**: 599-615.

Clontech Catalogue (1997, 2000)

Clontech Laboratories. (2000). *Tet Systems User Manual.*

Connelly, C. S., Fahl, W. E., and Iannaccone, P. M. (1989). The role of transgenic animals in the analysis of various biological aspects of normal and pathologic states. *Experimental Cell Research* **183**: 257-276.

Cooper, A. and Heagerty, A. M. (1997). Blood pressure parameters as determinants of small artery structure in human essential hypertension. *Clinical Science* **92**: 551-557.

Coppen, S. R., Kodama, I., Boyett, M. R., Dobrzynski, H., Takagishi, Y., Honjo, H., Yeh, H. I., and Severs, N. J. (1999). Connexin45, a major connexin of the rabbit sinoatrial node, is co-expressed with connexin43 in a restricted zone at the nodal-crista terminalis border. *Journal of Histochemistry and Cytochemistry* **47**: 907-918.

Cormack, B. P., Valdivia, R. H., and Falkow, S. (1996). FACS-optimized mutants of the green fluorescent protein (GFP). *Gene* **173**: 33-38.

Cowan, D. B., Lye, S. J., and Langille, B. L. (1998). Regulation of vascular connexin43 gene expression by mechanical loads. *Circulation Research* **82**: 786-793.

Crow, D. S., Beyer, E. C., Paul, D. L., Kobe, S. S., and Lau, F. F. (1990). Phosphorylation of connexin43 gap junction protein in uninfected Rous sarcoma virus transformed mammalian fibroblasts. *Molecular and Cellular Biology* **10**: 1754-1763.

Cvetkovic, B. and Sigmund, C. D. (2000). Understanding hypertension through genetic manipulation in mice. *Kidney International* **57**: 863-874.

D'Angelo, G. and Meininger, G. A. (1994). Transduction mechanisms involved in the regulation of myogenic activity. *Hypertension* **23**: 1096-1105.

Darrow, B. J., Fast, V. G., Kleber, A. G., Beyer, E. C., and Saffitz, J. E. (1996). Functional and structural assessment of intercellular communication. *Circulation Research* **79**: 174-183.

Darrow, B. J., Laing, J. G., Lampe, P. D., Saffitz, J. E., and Beyer, E. C. (1995). Expression of multiple connexins in cultured neonatal rat ventricular myocytes. *Circulation Research* **76**: 381-387.

Davidson, J. S., Baumgarten, I. M., and Harley, E. H. (1986). Reversible inhibition of intercellular junctional communication by glycyrrhetinic acid. *Biochemical and Biophysical Research Communications* **134**: 29-36.

Davies, P. F. (1995). Flow-mediated endothelial mechanotransduction. *Physiological Reviews* **75**: 519-560.

Davies, P. F., Remuzzi, A., Gordon, E. J., Dewey, C. F. Jr., and Gimbrone, M. A. Jr. (1986). Turbulent fluid shear stress induces vascular endothelial cell turnover in vitro. *Proceedings of the National Academy of Sciences (USA)* **83**: 2114-2117.

de Wit, C., Roos, F., Bolz, S.-S., Kirchhoff, S., Kruger, O., Willecke, K., and Pohl, U. (2000). Impaired conduction of vasodilation along the arterioles in connexin 40-deficient mice. *Circulation Research* **86**: 649-655.

De Sousa, S. P., Juneja, S. C., Caveney, S., Houghton, F. D., Davies, T. C., Reaume, A. G., Rossant, J., and Kidder, G. M. (1997). Normal development of preimplantation mouse embryos deficient in gap junctional coupling. *Journal of Cell Science* **110**: 1751-1758.

Delashaw, J. B. and Duling, B. R. (1991). Heterogeneity in conducted arteriolar vasomotor response is agonist dependent. *American Journal of Physiology* **260**: H1276-H1282.

Delorme, B., Dahl, E., Jarry-Guichard, T., Briand, J.-P., Willecke, K., Gros, D., and Theveniau-Ruissy, M. (1997). Expression pattern of connexin gene products at the early developmental stages of the mouse cardiovascular system. *Circulation Research* **81**: 423-437.

De Paola, N., Davies, P. F., Pritchard, W. F., Florez, L., Harbeck, N., and Polacek, D. C. (1999). Spatial and temporal regulation of gap junction connexin43 in vascular endothelial cells exposed to controlled disturbed flows in vitro. *Proceedings of the National Academy of Sciences (USA)* **96**: 3154-3159.

De Paola, N., Gimbrone, M. A. J., Davies, P. F., and Dewey, C. F. J. (1992). Vascular endothelium responds to fluid shear stress gradients [published erratum appears in Arterioscler Thromb 1993 Mar;13(3):465]. *Arteriosclerosis, Thrombosis and Vascular Biology* **12**: 1254-1257.

Detweiler, D. K. (1989). Blood circulation and the cardiovascular system. In: *Dukes' Physiology of Domestic Animals.* M. J. Swenson (ed.). Cornell University Press, New York. p.15-207.

Deutsch, D. E., Williams, J. A., and Yule, D. I. (1995). Halothane and octanol block Ca^{2+} oscillations in pancreatic acini by multiple mechanisms. *American Journal of Physiology* **269**: G779-G788.

Doevendans, P. A., Daemen, M. J., de Muinck, E. D., and Smits, J. F. (1998). Cardiovascular phenotyping in mice. *Cardiovascular Research* **39**: 34-49.

Dominiczak, A. F., Lazar, D. F., Das, A. K., and Bohr, D. F. (1991). Lipid bilayer in genetic hypertension. *Hypertension* **18**: 748-757.

Donaldson, P., Eckert, R., Green, C., and Kistler, J. (1997). Gap junction channels: new roles in disease. *Histology and Histopathology* **12**: 219-231.

Dopico, A. M., Kirber, M. T., Singer, J. J., and Walsh, J. V. J. (1994). Membrane stretch directly activates large conductance Ca(2+)-activated K+ channels in mesenteric artery smooth muscle cells. *American Journal of Hypertension* 7: 82-89.

Dora, K. A., Martin, P. M., Chaytor, A. T., Evans, W. H., Garland, C. J., and Griffith, T. M. (1999). Role of heterocellular gap junctional communication in endothelium-dependent smooth muscle hyperpolarization: inhibition by a connexin-mimetic peptide. *Biochemical and Biophysical Research Communications* **254**: 27-31.

Duband, J. L., Gimona, M., Scatena, M., Sartore, S., and Small, J. V. (1993). Calponin and SM22 as differentiation markers of smooth muscle: spatiotemporal distribution during avian embryonic development. *Differentiation* **55**: 1-11.

Duling, B. R. and Berne, R. M. (1970). Propagated vasodilation in the microcirculation of the hamster cheek pouch. *Circulation Research* **26**: 163-170.

Duling, B. R., Matsuki, T., and Segal, S. S. (1991). Conduction in the resistance-vessel wall. In: *The Resistance Vasculature*. J. A. Bevan (ed.) Humana Press. p.193-215.

Duprex, W. P., Mcquaid, S., Roscic-Mrkic, B., Cattaneo, R., Mccallister, C., and Rima, B. K. (2000). In vitro and in vivo infection of neural cells by a recombinant measles virus expressing enhanced green fluorescent protein. *Journal of Virology* **74**: 7972-7979.

Dzau, V. J., Morishita, R., and Gibbons, G. H. (1993). Gene therapy for cardiovascular disease. *Trends in Biotechnology* **11**: 205-210.

Ebihara, L., Xu, X., Oberti, C., and Berthoud, V. M. (1999). Co-expression of lens fiber connexins modifies hemi-gap-junctional channel behaviour. *Biophysical Journal* **76**: 198-206.

Ek-Vitorin, J. F., Calero, G., Morley, G. E., Coombs, W., Taffet, S. M., and Delmar, M. (1996). pH regulation of connexin43: molecular analysis of the gating particle. *Biophysical Journal* **71**: 1273-1284.

Emerson, G. G. and Segal, S. S. (2000). Electrical coupling between endothelial cells and smooth muscle cells in hamster feed arteries - role in vasomotor control. *Circulation Research* **87**: 474-479.

Escriou, V., Ciolina, C., Lacroix, F., Byk, G., Scherman, D., and Wils, P. (1998). Cationic lipid-mediated gene transfer: effect of serum on cellular uptake and intracellular fate of lipopolyamine/DNA complexes. *Biochimica et Biophysica Acta* **1368**: 276-288.

Eugenin, E. A., Gonzalez, H., Saez, C. G., and Saez, J. C. (1998). Gap junctional communication coordinates vasopressin-induced glycogenolysis in rat hepatocytes. *American Journal of Physiology* **274**: G1109-G1116.

Ewart, J. L., Cohen, M. F., Meyer, R. A., Huang, G. Y., Wessels, A., Gourdie, R. G., Chin, A. J., Park, S. M. J., Lazatin, B. O., Villabon, S., and Lo, C. W. (1997). Heart and neural tube defects in transgenic mice overexpressing the Cx43 gap junction gene. *Development* **124**: 1281-1292.

Falk, M. M. (2000). Biosynthesis and structural composition of gap junction intercellular membrane channels. *European Journal of Cell Biology* **79**: 564-574.

Fallon, R. F. and Goodenough, D. A. (1981). Five-hour half-life of mouse liver gap-junction protein. *Journal of Cell Biology* **90**: 521-526.

Faraci, F. M. and Sigmund, C. D. (1999). Vascular biology in genetically altered mice: smaller vessels, bigger insight. *Circulation Research* **85**: 1214-1225.

Feletou, M. and Vanhoutte, P. M. (1999). The alternative: EDHF. *Journal of Molecular and Cellular Cardiology* **31**: 15-22.

Ferrari, A. U., Daffonchio, A., and Albergati, F. M. G. (1986). Limitations of the tail-cuff method for measuring blood pressure in rats. *Journal of Hypertension* **4**: S179-S181.

Fishman, G. I. (1998). Timing is everything in life - conditional transgene expression in the cardiovascular system. *Circulation Research* **82**: 837-844.

Flagg-Newton, J., Simpson, I., and Loewenstein, W. R. (1979). Permeability of the cell-to-cell membrane channels in mammalian cell juncton. *Science* **205**: 404-407.

Fleming, I. and Busse, R. (1995). Control and consequences of endothelial nitric oxide formation. *Advances in Pharmacology* **34**: 187-206.

Fleming, I. and Busse, R. (1999). NO: the primary EDRF. *Journal of Molecular and Cellular Cardiology* **31**: 5-14.

Folkow, B. (1978). The Fourth Volhard Lecture: cardiovascular structural adaptation; its role in the initiation and maintenance of primary hypertension. *Clinical Science and Molecular Medicine Supplement* **4**: 3s-22s.

Folkow, B. (1982). Physiological aspects of primary hypertension. *Physiological Reviews* **62**: 347-504.

Forster, K., Helbl, V., Lederer, T., Urlinger, S., Wittenburg, N., and Hillen, W. (1999). Tetracycline-inducible expression systems with reduced basal activity in mammalian cells. *Nucleic Acids Research* **27**: 708-710.

Francis, D., Stergiopoulos, K., Ek-Vitorin, J. F., Cao, F. L., Taffet, S. M., and Delmar, M. (1999). Connexin diversity and gap junction regulation by pHi. *Developmental Genetics* **24**: 123-136.

Freundlieb, S., Schirra-Muller, C., and Bujard, H. (1999). A tetracycline controlled activation/repression system with increased potential for gene transfer into mammalian cells. *Journal of Gene Medicine* **1**: 4-12.

Frid, M. G., Dempsey, E. C., Durmowicz, A. G., and Stenmark, K. R. (1997). Smooth muscle cell heterogeneity in pulmonary and systemic vessels. Importance in vascular disease. *Arteriosclerosis, Thrombosis and Vascular Biology* **17**: 1203-1209.

Furchgott, R. F. (1983). Role of endothelium in responses of vascular smooth muscle. *Circulation Research* **53**: 557-573.

Furchgott, R. F. and Zawadzki, J. V. (1980). The obligatory role of endothelial cells in the relaxation of arterial smooth muscle by acetylcholine. *Nature* **288**: 373-376.

Furth, P. A., St Onge, L., Boger, H., Gruss, P., Gossen, M., Kistner, A., Bujard, H., and Hennighausen, L. (1994). Temporal control of gene expression in transgenic mice by a tetracycline-responsive promoter. *Proceedings of the National Academy of Sciences (USA)* **91**: 9302-9306.

Gabella, G. (1973). Cellular structures and electrophysiological behaviour. *Philosophical Transactions of the Royal Society of London. Series B.* **265**: 7-16.

Gabella, G. (1981). Structure of Smooth Muscles. In: *Smooth muscle: an assessment of current knowledge.* E. Bulbring (ed.) Edward Arnold, London. p.1-46.

Gabella, G. (1991). Ultrastructure of the tracheal muscle in developing, adult and ageing guinea-pigs. *Anatomy and Embryology* **183**: 71-79.

Gabriels, J. E. and Paul, D. L. (1998). Connexin43 is highly localized to sites of disturbed flow in rat aortic endothelium but connexin37 and connexin40 are more uniformly distributed. *Circulation Research* **83**: 636-643.

Garbers, D. L. and Dubois, S. K. (1999). The molecular basis of hypertension. *Annual Review of Biochemistry* **68**: 127-155.

Gerolami, R., Uch, R., Jordier, F., Chapel, S., Bagnis, C., Brechot, C., and Mannoni, P. (2000). Gene transfer to hepatocellular carcinoma: transduction efficacy and transgene expression kinetics by using retroviral and lentiviral vectors. *Cancer Gene Therapy* 7: 1286-1292.

Giannattasio, C., Cattaneo, B. M., Mangoni, A. A., Carugo, S., Stella, M. L., Failla, M., Trazzi, S., Sega, R., Grassi, G., and Mancia, G. (1995). Cardiac and vascular structural changes in normotensive subjects with parental hypertension. *Journal of Hypertension* **13**: 259-264.

Giaretta, I., Madeo, D., Bonaguro, R., Cappellari, A., Rodeghiero, F., and Giorgio, P. (2000). A comparative evaluation of gene transfer into blood cells using the same retroviral backbone for independent expression of the EGFP and deltaLNGFR marker genes. *Haematologica* **85**: 680-689.

Gimlich, R. L., Kumar, N. M., and Gilula, N. B. (1990). Differential regulation of the levels of three gap junction mRNAs in Xenopus embryos. *Journal of Cell Biology* **110**: 597-605.

Giuriato, L., Chiavegato, A., Pauletto, P., and Sartore, S. (1995). Correlation between the presence of an immature smooth muscle cell population in tunica media and the development of atherosclerotic lesion. A study on different-sized rabbit arteries from cholesterol-fed and Watanabe heritable hyperlipemic rabbits. *Atherosclerosis* **116**: 77-92.

Goodenough, D. A., Goliger, J. A., and Paul, D. L. (1996). Connexins, connexons, and intercellular communication. *Annual Review of Biochemistry* **65**: 475-502.

Goodenough, D. A. and Revel, J. P. (1970). A fine structural analysis of intercellular junctions in the mouse liver. *Journal of Cell Biology* **45**: 272-290.

Gordon, J. W. and Ruddle, F. H. (1981). Integration and stable germ line transmission of genes injected into mouse pronuclei. *Science* **214**: 1244-1246.

Gordon, J. W. and Ruddle, F. H. (1983). Gene transfer into mouse embryos: production of transgenic mice by pronuclear injection. *Methods in Enzymology* **101**: 411-433.

Gordon, J. W., Scangos, G. A., Plotkin, D. J., Barbosa, J. A., and Ruddle, F. H. (1980). Genetic transformation of mouse embryos by microinjection of purified DNA. *Proceedings of the National Academy of Sciences (USA)* **77**: 7380-7384.

Gossen, M., Bonin, A. L., and Bujard, H. (1993). Control of gene activity in higher eukaryotic cells by prokaryotic regulatory elements. *Trends in Biochemical Sciences* **18**: 471-475.

Gossen, M. and Bujard, H. (1992). Tight control of gene expression in mammalian cells by tetracycline-responsive promoters. *Proceedings of the National Academy of Sciences (USA)* **89**: 5547-5551.

Gossen, M. and Bujard, H. (1993). Anhydrotetracycline, a novel effector for tetracycline controlled gene expression systems in eukaryotic cells. *Nucleic Acids Research* **21**: 4411-4412.

Gossen, M. and Bujard, H. (1995). Efficacy of tetracycline-controlled gene expression is influenced by cell type: commentary. *BioTechniques* **19**: 213-217.

Gossen, M., Freundlieb, S., Bender, G., Muller, G., Hillen, W., and Bujard, H. (1995). Transcriptional activation by tetracyclines in mammalian cells. *Science* **268**: 1766-1769.

Gossler, A., Doetschman, T. C., Korn, R., Serfling, E., and Kemler, R. (1986). Transgenesis by means of blastocyst-derived embryonic stem cell lines. *Proceedings of the National Academy of Sciences (USA)* **83**: 9065-9069.

Griffith, T. M., Edwards, D. H., Davies, R. L., Harrison, T. J., and Evans, K. T. (1988). Endothelium-derived relaxing factor (EDRF) and resistance vessels in an intact vascular bed: a microangiographic study of the rabbit isolated ear. *British Journal of Pharmacology* **93**: 654-662.

Griffith, T. M. and Henderson, A. H. (1989). EDRF and the regulation of vascular tone. *International Journal of Microcirculation: Clinical and Experimental* **8**: 383-396.

Griffith, T. M. and Taylor, H. J. (1999). Cyclic AMP mediates EDHF-type relaxations of rabbit jugular vein. *Biochemical and Biophysical Research Communications* **263**: 52-57.

Grosveld, F., van Assendelft, G. B., Greaves, D. R., and Kollias, G. (1987). Position-independent, high-level expression of the human beta-globin gene in transgenic mice. *Cell* **51**: 975-985.

Grundemann, D. and Schomig, E. (1996). Protection of DNA during preparative agarose gel electrophoresis against damage induced by ultraviolet light. *BioTechniques* **21**: 898-903.

Grunwald, J., Robenek, H., Mey, J., and Hauss, W. H. (1982). In vivo and in vitro cellular changes in experimental hypertension: electronmicroscopic and morphometric studies of aortic smooth muscle cells. *Experimental and Molecular Pathology* **36**: 164-176.

Gu, H., Ek-Vitorin, J. F., Taffet, S. M., and Delmar, M. (2000). Coexpression of connexins 40 and 43 enhances the pH sensitivity of gap junctions. *Circulation Research* **86**: e98-e103.

Gustafsson, F. and Holstein-Rathlou, N.-H. (1999). Conducted vasomotor responses in arterioles: characteristics, mechanisms and physiological significance. *Acta Physiologica Scandinavia* **167**: 11-21.

Gutterman, D. D. (1999). Adventitia-dependent influences on vascular function. *American Journal of Physiology* **277**: H1265-H1272.

Guyton, A. C., Montani, J. P., Hall, J. E., and Manning, R. D. J. (1988). Computer models for designing hypertension experiments and studying concepts. *American Journal of Medical Science* **295**: 320-326.

Haefliger, J. A., Bruzzone, R., Jenkins, N. A., Gilbert, D. J., Copeland, N. G., and Paul, D. L. (1992). Four novel members of the connexin family of gap junction proteins. Molecular cloning, expression, and chromosome mapping. *Journal of Biological Chemistry* **267**: 2057-2064.

Haefliger, J. A., Castillo, E., Waeber, G., Aubert, J.-F., Nicod, P., Waeber, B., and Meda, P. (1997a). Hypertension differentially affects the expression of the gap junction protein connexin43 in cardiac myocytes and aortic smooth muscle cells.

In: *Hypertension and the Heart.* A. Zanchetti (ed.) Plenum Press, New York. p.71-82.

Haefliger, J. A., Castillo, E., Waeber, G., Bergonzelli, G. E., Aubert, J.-F., Sutter, E., Nicod, P., Waeber, B., and Meda, P. (1997b). Hypertension increases connexin43 in a tissue-specific manner. *Circulation* **95**: 1007-1014.

Haefliger, J. A. and Meda, P. (2000). Chronic hypertension alters the expression of Cx43 in cardiovascular muscle cells. *Brazilian Journal of Medical and Biological Research* **33**: 431-438.

Haefliger, J. A., Meda, P., Formenton, A., Wiesel, P., Zanchi, A., Brunner, H. R., Nicod, P., and Hayoz, D. (1999). Aortic connexin43 is decreased during hypertension induced by inhibition of nitric oxide synthase. *Arteriosclerosis, Thrombosis and Vascular Biology* **19**: 1615-1622.

Halayko, A.J. and Solway, J. (2001). Molecular mechanisms of phenotypic plasticity in smooth muscle cells. *Journal of Applied Physiology* **90**: 358-368.

Hamm, A., Krott, N., Breibach, I., Blindt, R., and Bosserhoff, A.K. (2002). Efficient transfection method for primary cells. *Tissue Engineering* **8**: 235-245.

Hanahan, D. (1989). Transgenic mice as probes into complex systems. *Science* **246**: 1265-1275.

Hartman, P. S. (1991). Transillumination can profoundly reduce transformation frequencies. *BioTechniques* **11**: 747-748.

Hayoz, D. and Brunner, H. R. (1997). Remodelling of conduit arteries in hypertension: special emphasis on the mechanical and metabolic consequences of vascular hypertrophy. *Blood Pressure* **2**: 39-42.

He, D. S. and Burt, J. M. (2000). Mechanism and selectivity of the effects of halothane on gap junction channel function. *Circulation Research* **86**: e104-e109.

He, D. S., Jiang, J. X., Taffet, S. M., and Burt, J. M. (1999). Formation of heteromeric gap junction channels by connexins 40 and 43 in vascular smooth muscle cells. *Proceedings of the National Academy of Sciences (USA)* **96**: 6495-6500.

Heagerty, A. M., Aalkjaer, C., Bund, S. J., Korsgaard, N., and Mulvany, M. J. (1993). Small artery structure in hypertension. Dual processes of remodeling and growth. *Hypertension* **21**: 391-397.

Hein, L., Barsh, G. S., Pratt, R. E., Dzau, V. J., and Kobilka, B. K. (1995). Behavioural and cardiovascular effects of disrupting the angiotensin II type-2 receptor in mice. *Nature* **377**: 744-747.

Hennighausen, L., Wall, R. J., Tillmann, U., Li, M., and Furth, P. A. (1995). Conditional gene expression in secretory tissues and skin of transgenic mice using the MMTV-LTR and the tetracycline responsive system. *Journal of Cellular Biochemistry* **59**: 463-472.

Henry, S. C., Schmader, K., Brown, T. T., Miller, S. E., Howell, D. N., Daley, G. G., and Hamilton, J. D. (2000). Enhanced green fluorescent protein as a marker for localizing murine cytomegalovirus in acute and latent infection. *Journal of Virological Methods* **89**: 61-73.

Hertig, C. M., Butz, S., Koch, S., Eppenberger-Eberhardt, M., Kemler, R., and Eppenberger, H. M. (1996). N-cadherin in adult rat cardiomyocytes in culture. II. Spatio-temporal appearance of proteins involved in cell-cell contact and communication. Formation of two distinct N-cadherin/catenin complexes. *Journal of Cell Science* **109**: 11-20.

Hertlein, B., Butterweck, A., Haubrich, S., Willecke, K., and Traub, O. (1998). Phosphorylated carboxy terminal serine residues stabilize the mouse gap junction protein connexin45 against degradation. *Journal of Membrane Biology* **162**: 247-257.

Hill, C., Rummery, N., Hickey, H., and Sandow, S. (2002). Heterogeneity in the distribution of vascular gap junctions and connexins: implications for function. *Clinical and Experimental Pharmacology and Physiology* **29**: 620-625.

Hill, C. E., Phillips, J. K., and Sandow, S. L. (1999). Development of peripheral autonomic synapses: neurotransmitter receptors, neuroeffector associations and neural influences. *Clinical and Experimental Physiology* **26**: 581-590.

Hill, C. E., Phillips, J. K., and Sandow, S. L. (2001). Heterogeneous control of blood flow amongst different vascular beds. *Medical Research Reviews* **21**: 1-60.

Hirschi, K. K., Xu, C. E., Tsukamoto, T., and Sager, R. (1996). Gap junction genes Cx26 and Cx43 individually suppress the cancer phenotype of human mammary carcinoma cells and restore differentiation potential. *Cell Growth and Differentiation* **7**: 861-870.

Hirst, G. D. and Edwards, F. R. (1989). Sympathetic neuroeffector transmission in arteries and arterioles. *Physiological Reviews* **69**: 546-604.

Hitt, A. L. and Luna, E. J. (1994). Membrane interactions with the actin cytoskeleton. *Current Opinion in Cell Biology* **6**: 120-130.

Hogan, B., Beddington, R., Costantini, F., and Lacy, E. (1994). *Manipulating the mouse embryo - a laboratory manual*. Cold Spring Harbor Laboratory Press, New York.

Hoit, B. D. (2001). New approaches to phenotypic analysis in adult mice. *Journal of Molecular and Cellular Cardiology* **33**: 27-35.

Houghton, F. D., Thonnissen, E., Kidder, G. M., Naus, C. C. G., Willecke, K., and Winterhager, E. (1999). Doubly mutant mice, deficient in connexin32 and 43, show normal prenatal development of organs where the two gap junction proteins are expressed in the same cells. *Developmental Genetics* **24**: 5-12.

Howe, J. R., Skryabin, B. V., Belcher, S. M., Zerillo, C. A., and Schmauss, C. (1995). The responsiveness of a tetracycline-sensitive expression system differs in different cell lines. *Journal of Cell Biology* **270**: 14168-14174.

Huang, G. Y., Wessels, A., Smith, B. R., Linask, K. K., Ewart, J. L., and Lo, C. W. (1998). Alteration in connexin 43 gap junction gene dosage impairs conotruncal heart development. *Developmental Biology* **198**: 32-44.

Hutcheson, I. R., Chaytor, A. T., Evans, W. H., and Griffith, T. M. (1999). Nitric oxide-independent relaxations to acetylcholine and A23187 involve different routes of heterocellular communication. Role of gap junctions and phospholipase A_2. *Circulation Research* **84**: 53-63.

Huttner, I., Mo Costabella, P., De Chastonay, C., and Gabbiani, G. (1982). Volume, surface, and junctions of rat aortic endothelium during experimental hypertension. *Laboratory Investigation* **46**: 489-504.

Huttner, K. M., Barbosa, J. A., Scangos, G. A., Pratcheva, D. D., and Ruddle, F. H. (1981). DNA-mediated gene transfer without carrier DNA. *Journal of Cell Biology* **91**: 153-156.

Ignarro, L. J., Buga, G. M., Wood, K. S., Byrns, R. E., and Chaudhuri, G. (1987). Endothelium-derived relaxing factor produced and released from artery and vein is nitric oxide. *Proceedings of the National Academy of Sciences (USA)* **84**: 9265-9269.

Ikeda, K., Nara, Y., and Yamori, Y. (1991). Indirect systolic and mean blood pressure determination by a new tail cuff method in spontaneously hypertensive rats. *Laboratory Animal* **25**: 26-29.

Inoue, N., Kawashima, S., Hirata, K. I., Rikitake, Y., Takeshita, S., Yamochi, W., Akita, H., and Yokoyama, M. (1998). Stretch force on vascular smooth muscle cells enhances oxidation of LDL via superoxide production. *American Journal of Physiology* **274**: H1928-H1932.

Isoyama, S., Ito, N., Satoh, K., and Takishima, T. (1992). Collagen deposition and the reversal of coronary reserve in cardiac hypertrophy. *Hypertension* **20**: 491-500.

Jackson, C. L. and Schwartz, S. M. (1992). Pharmacology of smooth muscle cell replication. *Hypertension* **20**: 713-736.

Jacobsen, N. O., Jorgensen, F., and Thoen, A. C. (1966). An electron microscopic study of small arteries and arterioles in the normal human kidney. *Nephron* **3**: 17-39.

Jaenisch, R. (1988). Transgenic animals. *Science* **240**: 1468-1474.

Jagger, D. J. and Ashmore, J. F. (1999). Regulation of ionic currents by protein kinase A and intracellular calcium in outer hair cells isolated from the guinea-pig cochlea. *Pflugers Archiv: European Journal of Physiology* **437**: 409-416.

Janssen, B.J.A., and Smits, J.F.M. (2002). Autonomic control of blood pressure in mice: basic physiology and effects of genetic modification. *American Journal of Physiology: Regulatory Integrative and Comparative Physiology* **282**: R1545-R1564.

Jara, P. I., Boric, M. P., and Saez, J. C. (1995). Leukocytes express connexin 43 after activation with lipopolysaccharide and appear to form gap junctions with endothelial cells after ischemia-reperfusion. *Proceedings of the National Academy of Sciences (USA)* **92**: 7011-7015.

Johns, C., Gavras, I., Handy, D. E., Salomao, A., and Gavras, H. (1996). Models of experimental hypertension in mice. *Hypertension* **28**: 1064-1069.

Johnson, E. A., Sharp, D. S., and Miller, D. B. (2000). Restraint as a stressor in mice: against the dopaminergic neurotoxicity of D-MDMA, low body weight mitigates restraint-induced hypothermia and consequent neuroprotection. *Brain Research* **875**: 107-118.

Johnson, P. C. (1978). Principles of peripheral circulatory control. In: *Peripheral Circulation*. P. C. Johnson (ed.) John Wiley & Sons, New York. p.111-139.

Jones, L. R., Besch, H. R. J., and Watanabe, A. M. (1978). Regulation of the calcium pump of cardiac sarcoplasmic reticulum. Interactive roles of potassium and ATP on the phosphoprotein intermediate of the (K^+,Ca^{2+})-ATPase. *Journal of Biological Chemistry* **253**: 1643-1653.

Jordan, K., Solan, J. L., Dominguez, M., Sia, M., Hand, A., and Lampe, P. D. (1999). Trafficking, assembly, and function of a connexin43-green fluorescent protein chimaera in live mammalian cells. *Molecular Biology of the Cell* **10**: 2033-2050.

Kannan, M. S. and Daniel, E. E. (1978). Formation of gap junctions by treatment in vitro with potassium conductance blockers. *Journal of Cell Biology* **78**: 338-348.

Kanter, H. L., Laing, J. G., Beyer, E. C., Green, K. G., and Saffitz, J. E. (1993). Multiple connexins colocalize in canine ventricular myocyte gap junctions. *Circulation Research* **73**: 344-350.

Kanter, H. L., Saffitz, J. E., and Beyer, E. C. (1992). Cardiac myocytes express multiple gap junction proteins. *Circulation Research* **70**: 438-444.

Kaufman, R. J. (1997). DNA transfection to study translational control in mammalian cells. *Methods: A Companion to Methods in Enzymology* **11**: 361-370.

Kemp, P. R., Osbourn, J. K., Grainger, D. J., and Metcalfe, J. C. (1995). Cloning and analysis of the promotor region of the rat SM22α gene. *Biochemistry Journal* **310**: 1037-1043.

Kim, S. and Iwao.H. (2000). Molecular and cellular mechanisms of angiotensin II-mediated cardiovascular and renal diseases. *Pharmacological Reviews* **52**: 11-34.

Kirchhoff, S., Nelles, E., Hagendorff, A., Kruger, O., Traub, O. and Willecke, K. (1998). Reduced cardiac conduction velocity and predisposition to arrhythmias in connexin40-deficient mice. *Current Biology* **9**: 299-302.

Kirchhoff, S., Kim, J.-S., Hagendorff, A., Thonnissen, E., Kruger, O., Lamers, W. H. and Willecke, K. (2000). Abnormal cardiac conduction and morphogenesis in connexin40 and connexin43 double-deficient mice. *Circulation Research* **87**: 399-405.

Kisseberth, W. C., Brettingen, N. T., Lohse, J. K., and Sandgren, E. P. (1999). Ubiquitous expression of marker transgenes in mice and rats. *Developmental Biology* **214**: 128-138.

Kistner, A., Gossen, M., Zimmermann, F., Jerecic, J., Ullmer, C., Lubbert, H., and Bujard, H. (1996). Doxycycline-mediated quantitative and tissue-specific control of gene expression in transgenic mice. *Proceedings of the National Academy of Sciences (USA)* **93**: 10933-10938.

Ko, Y. S., Yeh, H. I., Haw, M., Dupont, E., Kaba, R., Plenz, G., Robenek, H., and Severs, N. J. (1999). Differential expression of connexin43 and desmin defines two subpopulations of medial smooth muscle cells in the human internal mammary artery. *Arteriosclerosis, Thrombosis and Vascular Biology* **19**: 1669-1680.

Koepke, J. P., Jones, S. and DiBona, G. F. (1988). Sodium responsiveness of central alpha 2-adrenergic receptors in spontaneously hypertensive rats. *Hypertension* **11**: 326-333.

Kohler, A., Jostarndt-Fogen, K., Rottner, K., Alliegro, M. C., and Draeger, A. (1999). Intima-like smooth muscle cells: developmental link between endothelium and media? *Anatomy and Embryology* **200**: 313-323.

Komori, K. and Suzuki, H. (1987). Electrical responses of smooth muscle cells during cholinergic vasodilation in the rabbit saphenous artery. *Circulation Research* **61**: 586-593.

Komuro, T., Desaki, J., and Uehara, Y. (1982). Three-dimensional organization of smooth muscle cells in blood vessels of laboratory rodents. *Cell Tissue Research* **227**: 429-437.

Korner, P. I. and Angus, J. A. (1992). Structural determinants of vascular resistance properties in hypertension. Haemodynamic and model analysis [published erratum

appears in J Vasc Res 1995 Mar-Apr;32(2):119]. *Journal of Vascular Research* **29**: 293-312.

Koval, M., Geist, S. T., Westphale, E. M., Kemendy, A. E., Civitelli, R., Beyer, E. C., and Steinberg, T. H. (1995). Transfected connexin45 alters gap junction permeability in cells expressing endogenous connexin43. *Journal of Cell Biology* **130**: 987-995.

Kramer, K., van Acker, S. A., Voss, H. P., Grimbergen, J. A., van der Vijgh, W. J., and Bast, A. (1993). Use of telemetry to record electrocardiogram and heart rate in freely moving mice. *Journal of Pharmacology and Toxicological Methods* **30**: 209-215.

Krege, J. H., Hodgin, J. B., Hagaman, J. R., and Smithies, O. (1995). A noninvasive computerized tail-cuff system for measuring blood pressure in mice. *Hypertension* **25**: 1111-1115.

Krenacs, T. and Rosendaal, M. (1995). Immunohistological detection of gap junctions in human lymphoid tissue: connexin43 in follicular dendritic and lymphoendothelial cells. *Journal of Histochemistochemistry and Cytochemistry* **43**: 1125-1137.

Kreutz, R., Higuchi, M., and Ganten, D. (1992). Molecular genetics of hypertension. *Clinical and Experimental Hypertension* **14**: 15-34.

Kringstein, A. M., Rossi, F. M. V., Hofmann, A., and Blau, H. M. (1998). Graded transcriptional response to different concentrations of a single transactivator. *Proceedings of the National Academy of Sciences (USA)* **95**: 13670-13675.

Kruger, O., Plum, A., Kim, J.-S., Winterhager, E., Maxeiner, S., Hallas, G., Kirchhoff, S., Traub, O., Lamers, W. H., and Willecke, K. (2000). Defective vascular development in connexin 45-deficient mice. *Development* **127**: 4179-4193.

Kumai, M., Nishii, K., Nakamura, K., Takeda, N., Suzuki, M., and Shibata, Y. (2000). Loss of connexin45 causes a cushion defect in early cardiogenesis. *Development* **127**: 3501-3512.

Kumar, N. M. and Gilula, N. B. (1986). Cloning and characterization of human and rat liver cDNAs coding for a gap junction protein. *Journal of Cell Biology* **103**: 767-776.

Kumar, N. M. and Gilula, N. B. (1992). Molecular biology and genetics of gap junction channels. *Seminars in Cell Biology* **3**: 3-16.

Kumar, N. M. and Gilula, N. B. (1996). The gap junction communication channel. *Cell* **84**: 381-388.

Kunsch, C. and Medford, R. M. (1999). Oxidative stress as a regulator of gene expression in the vasculature. *Circulation Research* **85**: 753-766.

Kurtz, T. W. and St Lezin, E. M. (1992). Gene mapping in experimental hypertension. *Journal of the American Society of Nephrology* **3**: 28-34.

Kwak, B. R., Hermans, M. M., De Jonge HR, Lohmann, S. M., Jongsma, H. J., and Chanson, M. (1995a). Differential regulation of distinct types of gap junction channels by similar phosphorylating conditions. *Molecular Biology of the Cell* **6**: 1707-1719.

Kwak, B. R. and Jongsma, H. (1996). Regulation of cardiac gap junction channel permeability and conductance by several phosphorylating conditions. *Molecular and Cellular Biochemistry* **157**: 93-99.

Kwak, B. R. and Jongsma, H. J. (1999). Selective inhibition of gap junction channel activity by synthetic peptides. *Journal of Physiology* **516**: 679-685.

Kwak, B.R., Mulhaupt, F., Veillard, N., Gros, D.B., and Mach, F. (2002). Altered pattern of vascular connexin expression in atherosclerotic plaques. *Arteriosclerosis, Thrombosis and Vascular Biology* **22**: 225-230.

Kwak, B. R., Saez, J. C., Wilders, R., Chanson, M., Fishman, G. I., Hertzberg, E. L., Spray, D. C., and Jongsma, H. J. (1995b). Effects of cGMP-dependent phosphorylation on rat and human connexin43 gap junction channels. *Pflugers Archiv: European Journal of Physiology* **430**: 770-778.

Laing, J. G. and Beyer, E. C. (1995). The gap junction protein connexin43 is degraded via the ubiquitin proteasome pathway. *Journal of Biological Chemistry* **270**: 26399-26403.

Laing, J. G., Tadros, P. N., Westphale, E. M., and Beyer, E. C. (1997). Degradation of connexin43 gap junctions involves both the proteasome and the lysosome. *Experimental Cell Research* **236**: 482-492.

Laird, D. W. (1996). The life cycle of a connexin: gap junction formation, removal, and degradation. *Journal of Bioenergetics and Biomembranes* **28**: 311-318.

Laird, D. W., Puranam, K. L., and Revel, J. P. (1991). Turnover and phosphorylation dynamics of connexin43 gap junction protein in cultured cardiac myocytes. *Biochemical Journal* **273**: 67-72.

Lakatta, E. G. and Mitchell, J. H. (1987). Human aging: changes in structure and function. *Journal of the American College of Cardiology* **10**: 42A-47A.

Lampe, P. D., Kistler, J., Hefti, A., Bond, J., Muller, S., Johnson, R. G., and Engel, A. (1991). In vitro assembly of gap junctions. *Journal of Structural Biology* **107**: 281-290.

Langille, B. L. (1993). Remodeling of developing and mature arteries: endothelium, smooth muscle, and matrix. *Journal of Cardiovascular Pharmacology* **21**: S11-S17.

Langton, P. D. (1993). Calcium channel currents recorded from isolated myocytes of rat basilar artery are stretch sensitive. *Journal of Physiology (London)* **471**: 1-11.

Largo, C., Tombaugh, G. C., Aitken, P. G., Herreras, O., and Somjen, G. G. (1997). Heptanol but not fluoroacetate prevents the propagation of spreading depression in rat hippocampal slices. *Journal of Neurophysiology* **77**: 9-16.

Larsen, W. J., Tung, H. N., Murray, S. A., and Swenson, C. A. (1979). Evidence for the participation of actin microfilaments and bristle coats in the internalization of gap junction membrane. *Journal of Cell Biology* **83**: 576-587.

Lassalle, J. M., Halley, H., and Roullet, P. (1994). Analysis of behavioural and hippocampal variation in congenic albino and pigmented BALB mice. *Behavior Genetics* **24**: 161-169.

Lau, A. F., Kurata, W. E., Kanemitsu, M. Y., Loo, L. W., Warn-Cramer, B. J., Eckhart, W., and Lampe, P. D. (1996). Regulation of connexin43 function by activated tyrosine protein kinases. *Journal of Bioenergetics and Biomembranes* **28**: 359-368.

Lee, R. M., Garfield, R. E., Forrest, J. B., and Daniel, E. E. (1983). Morphometric study of structural changes in the mesenteric blood vessels of spontaneously hypertensive rats. *Blood Vessels* **20**: 57-71.

Lees-Miller, J. P., Heeley, D. H., and Smillie, L. B. (1987). An abundant and novel protein of 22kDa (SM22) is widely distributed in smooth muscles. Purification from bovine aorta. *Biochemical Journal* **244**: 705-709.

Lembo, G., Morisco, C., Lanni, F., Barbato, E., Vecchione, C., Fratta, L., and Trimarco, B. (1998). Systemic hypertension and coronary artery disease: the link. *American Journal of Cardiology* **82**: 2H-7H.

Li, L., Miano, J. M., Mercer, B., and Olson, E. N. (1996). Expression of the SM22a promoter in transgenic mice provides evidence for distinct transcriptional regulatory programs in vascular and visceral smooth muscle cells. *Journal of Cell Biology* **132**: 849-859.

Li, X. and Simard, J. M. (1999). Multiple connexins form gap junction channels in rat basilar artery smooth muscle cells. *Circulation Research* **84**: 1277-1284.

Life Science Catalogue (2000).

Lindop, G. B., Boyle, J. J., McEwan, P., and Kenyon, C. J. (1995). Vascular structure, smooth muscle cell phenotype and growth in hypertension. *Journal of Human Hypertension* **9**: 475-478.

Little, T. L., Beyer, E. C., and Duling, B. R. (1995a). Connexin 43 and connexin 40 gap junctional proteins are present in arteriolar smooth muscle and endothelium in vivo. *American Journal of Physiology* **268**: H729-H739.

Little, T. L., Xia, J., and Duling, B. R. (1995b). Dye tracers define differential endothelial and smooth muscle coupling patterns within the arteriolar wall. *Circulation Research* **76**: 498-504.

Lo, C. W. (1996). The role of gap junction membrane channels in development. *Journal of Bioenergetics and Biomembranes* **28**: 379-385.

Lo, C. W. (1999). Genes, gene knockouts, and mutations in the analysis of gap junctions. *Developmental Genetics* **24**: 1-4.

Locke, D. (1998). Gap junctions in normal and neoplastic mammary gland. *Journal of Pathology* **186**: 343-349.

Loewenstein, W. R. (1979). Junctional intercellular communication and the control of growth. *Biochimica et Biophysica Acta* **560**: 1-65.

Loewenstein, W. R. (1980). Molecular and morphological aspects of cell-cell communication. Introductory remarks to the symposium. *In Vitro* **16**: 1007-1009.

Loewenstein, W. R. (1981). Junctional intercellular communication: the cell-to-cell membrane channel. *Physiological Reviews* **61**: 829-913.

Loewenstein, W. R. (1987). The cell-to-cell channel of gap junctions. *Cell* **48**: 725-726.

Loewenstein, W. R. and Rose, B. (1992). The cell-cell channel in the control of growth. *Seminars in Cell Biology* **3**: 59-79.

London, G. M. and Safar, M. E. (1996). Arterial wall remodelling and stiffness in hypertension: heterogeneous aspects. *Clinical and Experimental Pharmacology and Physiology* **23**: S1-S5.

Luff, S. E. (1991). The ultrastructure of arterioles. In: *The Resistance Vasculature*. J. A. Bevan (ed.) Humana Press. p.93-113.

Lumme, A., Vanhatalo, S., and Soinila, S. (1996). Axonal transport of nitric oxide synthase in autonomic nerves. *Journal of the Autonomic Nervous System* **56**: 207-214.

Makaritsis, K. P., Handy, D. E., Johns, C., Kobilka, B., Gavras, I., and Gavras, H. (1999a). Role of the alpha2B-adrenergic receptor in the development of salt-induced hypertension. *Hypertension* **33**: 14-17.

Makaritsis, K. P., Johns, C., Gavras, I., Altman, J. D., Handy, D. E., Bresnahan, M. R., and Gavras, H. (1999b). Sympathoinhibitory function of the alpha(2A)-adrenergic receptor subtype. *Hypertension* **34**: 403-407.

Makowski, L., Caspar, D. L., Phillips, W. C., Baker, T. S., and Goodenough, D. A. (1984). Gap junction structures.VI.Variation and conservation in connexon conformation and packing. *Biophysical Journal* **45**: 208-218.

Makowski, L., Caspar, D. L., Phillips, W. C., and Goodenough, D. A. (1977). Gap junction structures.II.Analysis of the x-ray diffraction data. *Journal of Cell Biology* **74**: 629-645.

Malek, A. M., Gibbons, G. H., Dzau, V. J., and Izumo, S. (1993). Fluid shear stress differentially modulates expression of genes encoding basic fibroblast growth factor and platelet-derived growth factor B chain in vascular endothelium. *Journal of Clinical Investigation* **92**: 2013-2021.

Mancia, G. (1997). Bjorn Folkow Award Lecture. The sympathetic nervous system in hypertension. *Journal of Hypertension* **15**: 1553-1565.

Mansuy, I. M., Winder, D. G., Moallem, T. M., Osman, M., Mayford, M., Hawkins, R. D., and Kandel, E. R. (1998). Inducible and reversible gene expression with the rtTA system for the study of memory. *Neuron* **21**: 257-265.

Manthey, D., Bukauskas, F., Lee, C. G., Kozak, C. A., and Willecke, K. (1999). Molecular cloning and functional expression of the mouse gap junction gene connexin-57 in human HeLa cells. *Journal of Biological Chemistry* **274**: 14716-14723.

Martens, J. R. and Gelband, C. H. (1998). Ion channels in vascular smooth muscle: alterations in essential hypertension. *Proceedings of the Society of Experimental and Biological Medicine* **218**: 192-203.

Martyn, K. D., Kurata, W. E., Warn-Cramer, B. J., Burt, J. M., TenBroek, E., and Lau, A. F. (1997). Immortalized connexin43 knockout cell lines display a subset of biological properties associated with the transformed phenotype. *Cell Growth and Differentiation* **8**: 1015-1027.

Maueler, W., Kyas, A., Brocker, F., and Epplen, J. T. (1994). Altered electrophoretic behavior of DNA due to short-time UV-B irradiation. *Electrophoresis* **15**: 1499-1505.

Mayo, K. E., Warren, R., and Palmiter, R. D. (1982). The mouse metallothionein-I gene is transcriptionally regulated by cadmium following transfection into human or mouse cells. *Cell* **29**: 99-108.

McDonald, L. J. and Murad, F. (1995). Nitric oxide and cGMP signaling. *Advances in Pharmacology* **34**: 263-275.

McGuire, P. G. and Twietmeyer, T. A. (1985). Aortic endothelial junctions in developing hypertension. *Hypertension* **7**: 483-490.

Meda, P., Pepper, M. S., Traub, O., Willecke, K., Gros, D., Beyer, E., Nicholson, B., Paul, D., and Orci, L. (1993). Differential expression of gap junction connexins in endocrine and exocrine glands. *Endocrinology* **133**: 2371-2378.

Mehta, P. P., Hotz-Wagenblatt, A., Rose, B., Shalloway, D., and Loewenstein, W. R. (1991). Incorporation of the gene for a cell-cell channel protein into transformed cells leads to normalization of growth. *Journal of Membrane Biology* **124**: 207-225.

Mehta, P. P., Perez-Stable, C., Nadji, M., Mian, M., and Roos, B. A. (1999). Suppression of human prostate cancer cell growth by forced expression of connexin genes. *Developmental Genetics* **24**: 91-110.

Mensink, A., Brouwer, A., Van den Burg, E. H., Geurts, S., Jongen, W. M., Lakemond, C. M., Meijerman, I., and Van der Wijk, T. (1996). Modulation of intercellular communication between smooth muscle cells by growth factors and cytokines. *European Journal of Pharmacology* **310**: 73-81.

Milano, C. A., Dolber, P. C., Rockman, H. A., Bond, R. A., Venable, M. E., Allen, L. F., and Lefkowitz, R. J. (1994). Myocardial expression of a constitutively active alpha 1B-adrenergic receptor in transgenic mice induces cardiac hypertrophy. *Proceedings of the National Academy of Sciences (USA)* **19**: 10109-10113.

Miller, B. G., Connors, B. A., Bohlen, G., and Evan, A. P. (1987). Cell and wall morphology of intestinal arterioles from 4- to 6- and 17- to 19-week-old wistar-kyoto and spontaneously hypertensive rats. *Hypertension* **9**: 59-68.

Miller, J. H., Lebkowski, J. S., Greisen, K. S., and Calos, M. P. (1984). Specificity of mutations induced in transfected DNA by mammalian cells. *EMBO Journal* **3**: 3117-2121.

Mills, P.A., Huetteman, D.A., Brockway, B.P., Zwiers, L.M., Gelsema, A.J., Schwartz, R.S., and Kramer, K. (2000). A new method for measurement of blood pressure, heart rate, and activity in the mouse by radiotelemetry. *Journal of Applied Physiology* **88**: 1537-1544.

Minkoff, R., Bales, E. S., Kerr, C. A., and Struss, W. E. (1999). Antisense oligonucleotide blockade of connexin expression during embryonic bone formation: evidence of functional compensation within a multigene family. *Developmental Genetics* **24**: 43-56.

Misteli, T. and Spector, D. L. (1997). Applications of the green fluorescent protein in cell biology and biotechnology. *Nature Biotechnology* **15**: 961-964.

Moessler, H., Mericskay, M., Li, Z., Nagl, S., Paulin, D., and Small, J. V. (1996). The SM22 promoter directs tissue-specific expression in arterial but not in venous or visceral smooth muscle cells in transgenic mice. *Development* **122**: 2415-2425.

Mombouli, J. V. and Vanhoutte, P. M. (1997). Endothelium-derived hyperpolarizing factor(s): updating the unknown. *Trends in Pharmacological Sciences* **18**: 252-256.

Mombouli, J. V. and Vanhoutte, P. M. (1999). Endothelial dysfunction: from physiology to therapy. *Journal of Molecular and Cellular Cardiology* **31**: 61-74.

Moncada, S. and Palmer, R. M. (1991). Biosynthesis and actions of nitric oxide. *Seminars in Perinatology* **15**: 16-19.

Moore, L. K. and Burt, J. M. (1994). Selective block of gap junction channel expression with connexin-specific antisense oligodeoxynucleotides. *American Journal of Physiology* **267**: C1371-C1380.

Moreno, A. P., Saez, J. C., Fishman, G. I., and Spray, D. C. (1994). Human connexin43 gap junction channels. Regulation of unitary conductances by phosphorylation. *Circulation Research* **74**: 1050-1057.

Morley, G. E., Ek-Vitorin, J. F., Taffet, S. M., and Delmar, M. (1997). Structure of connexin43 and its regulation by pH. *Journal of Cardiovascular Electrophysiology* **8**: 939-951.

Mullins, J. J. and Ganten, D. (1990). Transgenic animals: new approaches to hypertension research. *Journal of Hypertension Supplement* **8**: S35-S37.

Mulvany, M. J. (1999). Vascular remodelling of resistance vessels: can we define this? *Cardiovascular Research* **41**: 9-13.

Mulvany, M. J. (2002a). Small artery remodeling and significance in the development of hypertension. *News in Physiological Sciences* **17**: 105-109.

Mulvany, M. J. (2002b). Small artery remodeling in hypertension. *Current Hypertension Reports* **4**: 49-55.

Mulvany, M. J. and Aalkjaer, C. (1990). Structure and function of small arteries. *Physiological Reviews* **70**: 921-961.

Mulvany, M. J., Baandrup, U., and Gundersen, H. J. (1985). Evidence for hyperplasia in mesenteric resistance vessels of spontaneously hypertensive rats using a three-dimensional dissector. *Circulation Research* **57**: 794-800.

Mulvany, M. J., Baumbach, G. L., Aalkjaer, C., Heagerty, A. M., Korsgaard, N., Schiffrin, E. L., and Heistad, D. D. (1996). Vascular remodeling. *Hypertension* **28**: 505-506.

Murray, S. A., Williams, S. Y., Dillard, C. Y., Narayanan, S. K., and McCauley, J. (1997). Relationship of cytoskeletal filaments to annular gap junction expression

in human adrenal cortical tumor cells in culture. *Experimental Cell Research* **234**: 398-404.

Musil, L. S. and Goodenough, D. A. (1991). Biochemical analysis of connexin43 intracellular transport, phosphorylation, and assembly into gap junctional plaques. *Journal of Cell Biology* **115**: 1357-1374.

Nagano, M., Shinohara, T., Avarbock, M. R., and Brinster, R. L. (2000). Retrovirus-mediated gene delivery into male germ line stem cells. *FEBS Letters* **475**: 7-10.

Nakamura, A., Isoyama, S., Watanabe, T., Katoh, M., and Sawai, T. (1998). Heterogeneous smooth muscle cell population derived from small and larger arteries. *Microvascular Research* **55**: 14-28.

Nakamura, K., Inai, T., and Shibata, Y. (1999). Distribution of gap junction protein connexin 37 in smooth muscle cells of the rat trachea and pulmonary artery. *Archives of Histology and Cytology* **62**: 27-37.

Neutel, J. M., Smith, D. H. G., and Weber, M. A. (1999). Is high blood pressure a late manifestation of the hypertension syndrome? *American Journal of Hypertension* **12**: 215S-223S.

Nicholson, B., Dermietzel, R., Teplow, D., Traub, O., Willecke, K., and Revel, J. P. (1987). Two homologous protein components of hepatic gap junctions. *Nature* **329**: 732-734.

Nicholson, B. J., Weber, P. A., Cao, F., Chang, H.-C., Lampe, P., and Goldberg, G. (2000). The molecular basis of selective permeability of connexins is complex and includes both size and charge. *Brazilian Journal of Medical and Biological Research* **33**: 369-378.

Nicholson, S. M. and Bruzzone, R. (1997). Gap junctions: getting the message through. *Current Biology* **7**: R340-R344.

O'Brien, J., Bruzzone, R., White, T. W., Al-Ubaidi, M. R., and Ripps, H. (1998). Cloning and expression of two related connexins from the perch retina define a distinct subgroup of the connexin family. *Journal of Neuroscience* **18**: 7625-7637.

O'Sullivan, J. B. and Harrap, S. B. (1995). Resetting blood pressure in spontaneously hypertensive rats - the role of bradykinin. *Hypertension* **25**: 162-165.

Obaid, A. L., Socolar, S. J., and Rose, B. (1983). Cell-to-cell channels with two independently regulated gates in series - analysis of junctional conductance modulation by membrane-potential, calcium and pH. *Journal of Membrane Biology* **73**: 69-89.

Ohya, Y., Abe, I., Fujii, K., Takata, Y., and Fujishima, M. (1993). Voltage-dependent Ca^{2+} channels in resistance arteries from spontaneously hypertensive rats. *Circulation Research* **73**: 1090-1099.

Ohya, Y., Adachi, N., Nakamura, Y., Setoguchi, M., Abe, I., and Fujishima, M. (1998). Stretch-activated channels in arterial smooth muscle of genetic hypertensive rats. *Hypertension* **31**: 254-258.

Ohya, Y., Adachi, N., Setoguchi, M., Abe, I., and Fujishima, M. (1997). Effects of CP-060S on membrane channels in vascular smooth muscle cells from guinea pig. *European Journal of Pharmacology* **330**: 93-99.

Old, M. H. and Primrose, E. J. (1985). *Principles of Genetic Manipulation.* Harper & Row Publishers Inc., New York.

Omori, Y. and Yamasaki, H. (1999). Gap junction proteins connexin32 and connexin43 partially acquire growth-suppressive function in HeLa cells by deletion of their C-terminal tails. *Carcinogenesis* **20**: 1913-1918.

Ou, C. W., Orsino, A., and Lye, S. J. (1997). Expression of connexin-43 and connexin-26 in the rat myometrium during pregnancy and labor is differentially regulated by mechanical and hormonal signals. *Endocrinology* **138**: 5398-5407.

Owens, G. K., Rabinovitch, P. S., and Schwartz, S. M. (1981). Smooth muscle cell hypertrophy versus hyperplasia in hypertension. *Proceedings of the National Academy of Sciences (USA)* **78**: 7759-7763.

Palmer, R. M., Ferrige, A. G., and Moncada, S. (1987). Nitric oxide release accounts for the biological activity of endothelium-derived relaxing factor. *Nature* **327**: 524-526.

Palmer, R. M. and Moncada, S. (1989). A novel citrulline-forming enzyme implicated in the formation of nitric oxide by vascular endothelial cells. *Biochemical and Biophysical Research Communications* **158**: 348-352.

Palmiter, R. D. and Brinster, R. L. (1986). Germ-line transformation of mice. *Annual Review of Genetics* **20**: 465-499.

Paul, D. L. (1986). Molecular cloning of cDNA for rat liver gap junction protein. *Journal of Cell Biology* **103**: 123-134.

Paul, D. L. (1995). New functions for gap junctions. *Current Opinion in Cell Biology* **7**: 665-672.

Paulus, W., Baur, I., Keyvani, K., and Senner, V. (2000). Variability of transcriptional regulation after gene transfer with the retroviral tetracycline system. *Journal of Biotechnology* **81**: 159-165.

Peracchia, C. (1991). Effects of the anesthetics heptanol, halothane and isoflurane on gap junction conductance in crayfish septate axons: a calcium- and hydrogen-independent phenomenon potentiated by caffeine and theophylline, and inhibited by 4-aminopyridine. *Journal of Membrane Biology* **121**: 67-78.

Peters, N. S. (1997). Gap junctions and clinical cardiology: From molecular biology to molecular medicine. *European Heart Journal* **18**: 1697-1702.

Peters, N. S., Coromilas, J., Severs, N. J., and Wit, A. L. (1997). Disturbed connexin43 gap junction distribution correlates with the location of reentrant circuits in the epicardial border zone of healing canine infarcts that cause ventricular tachycardia. *Circulation* **95**: 988-996.

Peters, N. S., Severs, N. J., Rothery, S. M., Lincoln, C., Yacoub, M. H., and Green, C. R. (1994). Spatiotemporal relation between gap junctions and fascia adherens junctions during postnatal development of human ventricular myocardium. *Circulation* **90**: 713-725.

Pfeffer, J. M., Pfeffer, M. A., and Frohlich, E. D. (1971). Validity of an indirect tail-cuff method for determining systolic arterial pressure in unanesthetized normotensive and spontaneously hypertensive rats. *Journal of Laboratory and Clinical Medicine* **78**: 957-962.

Pickering, J. G., Takeshita, S., Feldman, L., Losordo, D. W., and Isner, J. M. (1996). Vascular applications of human gene therapy. *Seminars in Interventional Cardiology* **1**: 84-88.

Pitts, J. D., Finbow, M. E., and Kam, E. (1988). Junctional communication and cellular differentiation. *British Journal of Cancer Supplement* **9**: 52-57.

Polacek, D., Lal, R., Volin, M. V., and Davies, P. F. (1993). Gap junctional communication between vascular cells. Induction of connexin43 messenger RNA in macrophage foam cells of atherosclerotic lesions. *American Journal of Pathology* **142**: 593-606.

Potter, H., Weir, L., and Leder, P. (1984). Enhancer-dependent expression of human kappa immunoglobulin genes introduced into mouse pre-B lymphocytes by electroporation. *Proceedings of the National Academy of Sciences (USA)* **81**: 7161-7165.

Prasher, D. C., Eckenrode, V. K., Ward, W. W., Prendergast, F. G., and Cormier, M. J. (1992). Primary structure of the *Aequorea victoria* green-fluorescent protein. *Gene* **111**: 229-233.

Proulx, A., Merrifield, P. A., and Naus, C. C. (1997). Blocking gap junctional intercellular communication in myoblasts inhibits myogenin and MRF4 expression. *Developmental Genetics* **20**: 133-144.

Purnick, P. E. M., Benjamin, D. C., Verselis, V. K., Bargiello, T. A., and Dowd, T. L. (2000). Structure of the amino terminus of a gap junction protein. *Archives of Biochemistry and Biophysics* **381**: 181-190.

Rae, R. S., Mehta, P. P., Chang, C. C., Trosko, J. E., and Ruch, R. J. (1998). Neoplastic phenotype of gap-junctional intercellular communication-deficient WB

rat liver epithelial cells and its reversal by forced expression of connexin 32. *Molecular Carcinogenesis* **22**: 120-127.

Ramirez-Solis, R., Davis, A. C., and Bradley, A. (1993). Gene targeting in embryonic stem cells. *Methods in Enzymology* **225**: 855-878.

Reaume, A. G., de Sousa, P. A., Kulkarni, S., Langille, B. L., Zhu, D., Davies, T. C., Juneja, S. C., Kidder, G. M., and Rossant, J. (1995). Cardiac malformation in neonatal mice macking connexin 43. *Science* **267**: 1831-1834.

Reckelhoff, J. F., Zhang, H., and Granger, J. P. (1998). Testosterone exacerbates hypertension and reduces pressure-natriuresis in male spontaneously hypertensive rats. *Hypertension* **31**: 435-439.

Reckelhoff, J. F., Zhang, H., Srivastava, K., and Granger, J. P. (1999). Gender differences in hypertension in spontaneously hypertensive rats: role of androgens and androgen receptor. *Hypertension* **34**: 920-923.

Redon, J. (2001). Hypertension in obesity. *Nutrition, Metabolism and Cardiovascular Disease: NMCD* **11**: 344-353.

Rennick, R. E., Connat, J.-L., Burnstock, G., Rothery, S., Severs, N. J., and Green, C. R. (1993). Expression of connexin43 gap junctions between cultured vascular smooth muscle cells is dependent upon phenotype. *Tissue Research* **271**: 323-332.

Resnitzky, D., Gossen, M., Bujard, H., and Reed, S. I. (1994). Acceleration of the G1/S phase transition by expression of cyclins D1 and E with an inducible system. *Molecular and Cellular Biochemistry* **14**: 1669-1679.

Reusch, P. H., Wagdy, R., Reusch, R., Wilson, E., and Ives, H. E. (1996). Mechanical strain induces smooth muscle and decreases nonmuscle myosin expression in rat smooth muscle cells. *Circulation Research* **79**: 1046-1053.

Revilla, A., Castro, C., and Barrio, L. C. (1999). Molecular dissection of transjunctional voltage dependence in the connexin-32 and connexin-43 junctions. *Biophysical Journal* **77**: 1374-1383.

Rhodin, J. A. G. (1967). The ultrastructure of mammalian arterioles and precapillary sphincters. *Journal of Ultrastructural Research* **18**: 181-223.

Rhodin, J. A. G. (1980). Architecture of the vessel wall. In: *The Cardiovascular System.* D. F. Bohr, A. P. Somlyo, and H. V. Sparks (eds.) American Physiology Society, Bethesda. p.1-31.

Ribault, S., Neuville, P., Mechine-Neuville, A., Auge, F., Parlakian, A., Gabbiani, G., Paulin, D., and Calenda, V. (2001). Chimeric smooth muscle-specific enhancer/promoters. *Circulation Research* **88**: 468-482.

Robbins, S. L. and Kumar, V. (1987). *Basic Pathology*. W.B. Saunders Company, Philadelphia.

Robertson, E., Bradley, A., Kuehn, M., and Evans, M. (1986). Germ-line transmission of gene introduced into cultured pluripotential cells by retroviral vector. *Nature* **323**: 445-448.

Robinson, S. R., Hampson, E. C., Munro, M. N., and Vaney, D. I. (1993). Unidirectional coupling of gap junctions between neuroglia. *Science* **262**: 1072-1074.

Romero, J. C. and Reckelhoff, J. F. (1999). State-of-the-Art lecture. Role of angiotensin and oxidative stress in essential hypertension. *Hypertension* **34**: 943-949.

Rose, B., Mehta, P. P., and Loewenstein, W. R. (1993). Gap-junction protein gene suppresses tumorigenicity. *Carcinogenesis* **14**: 1073-1075.

Rosendorff, C. (1996). The renin-angiotensin system and vascular hypertrophy. *Journal of the American College of Cardiology* **28**: 803-812.

Rosendorff, C. (1997). Endothelin, vascular hypertrophy, and hypertension. *Cardiovascular Drugs and Therapy* **10**: 795-802.

Ross, M. H. and Reith, E. J. (1985). *Histology: A text and atlas.* Harper & Row Publishers Inc., New York.

Ross, R. (1996). Genetically modified mice as models of transplant atherosclerosis. *Nature Medicine* **2**: 527-528.

Rossi, F. M. and Blau, H. M. (1998). Recent advances in inducible gene expression systems. *Current Opinion in Biotechnology* **9**: 451-456.

Roth, D. B., Porter, T. N., and Wilson, J. H. (1985). Mechanisms of nonhomologous recombination in mammalian cells. *Molecular and Cellular Biology* **5**: 2599-2607.

Roth, D. B. and Wilson, J. H. (1985). Relative rates of homologous and nonhomologous recombination in transfected DNA. *Proceedings of the National Academy of Sciences (USA)* **82**: 3355-3359.

Ruch, R. J., Cesen-Cummings, K., and Malkinson, A. M. (1998). Role of gap junctions in lung neoplasia. *Experimental Lung Research* **24**: 523-539.

Rummery, N.M., McKenzie, K.U., Whitworth, J.A., and Hill, C.E. (2002). Decreased endothelial size and connexin expression in rat caudal arteries during hypertension. *Journal of Hypertension* **20**: 247-253.

Rusch, N. J. and Hermsmeyer, K. (1988). Calcium currents are altered in the vascular muscle cell membrane of spontaneously hypertensive rats. *Circulation Research* **63**: 997-1002.

Ryan, T. M., Behringer, R. R., Martin, N. C., Townes, T. M., Palmiter, R. D., and Brinster, R. L. (1989). A single erythroid-specific DNase I super-hypersensitive site activates highlevels of human beta-globin gene expression in transgenic mice. *Genes and Development* **3**: 314-323.

Sadoshima, J. and Izumo, S. (1993). Mechanical stretch rapidly activates multiple signal transduction pathways in cardiac myocytes: potential involvement of an autocrine/paracrine mechanism. *EMBO Journal* **12**: 1681-1692.

Saez, E., No, D., West, A., and Evans, RM. (1997). Inducible gene expression in mammalian cells and transgenic mice. *Current Opinion in Biotechnology* **8**: 608-616.

Saez, J. C., Berthoud, V. M., Moreno, A. P., and Spray, D. C. (1993). Gap junctions: multiplicity of controls in differentiated and undifferentiated cells and possible functional implications. *Advances in Second Messenger Phosphorylation Research* **27**: 163-198.

Saez, J. C., Nairn, A. C., Czernik, A. J., Fishman, G. I., Spray, D. C., and Hertzberg, E. L. (1997). Phosphorylation of connexin 43 and the regulation of neonatal rat cardiac myocyte gap junctions. *Journal of Molecular and Cellular Cardiology* **29**: 2131-2145.

Sambrook, J., Fritsch, E. F., and Maniatis, T. (1989). *Molecular Cloning*. Cold Spring Harbor Laboratory Press, New York.

Sandow, S. L. and Hill, C. E. (1999). Physiological and anatomical studies of the development of the sympathetic innervation to rat iris arterioles. *Journal of the Autonomic Nervous System* **77**: 152-163.

Sarao, R. and Dumont, D. J. (1998). Conditional transgene expression in endothelial cells. *Transgenic Research* **7**: 421-427.

Schiffrin, E. L. (1995). Endothelin in hypertension. *Current Opinion in Cardiology* **10**: 485-494.

Schiffrin, E. L. and Deng, L. Y. (1999). Relationship between small-artery structure and systolic, diastolic and pulse pressure in essential hypertension. *Journal of Hypertension* **17**: 381-387.

Schiller, P. C., Mehta, P. P., Roos, B. A., and Howard, G. A. (1992). Hormonal regulation of intercellular communication: parathyroid hormone increases connexin 43 gene expression and gap-junctional communication in osteoblastic cells. *Molecular Endocrinology* **6**: 1433-1440.

Schultze, N., Burki, Y., Lang, Y., Certa, U., and Bluethmann, H. (1996). Efficient control of gene expression by single step integration of the tetracycline system in transgenic mice. *Nature Biotechnology* **14**: 499-503.

Schwartz, S. M. (1999). The intima - a new soil. *Circulation Research* **85**: 877-879.

Schwartz, S. M., Majesky, M. W., and Murry, C. E. (1995). The intima: development and monoclonal responses to injury. *Atherosclerosis* **118**: S125-140.

Schwarzmann, G., Wiegandt, H., Rose, B., Zimmerman, A., Ben-Haim, D., and Loewenstein, W. R. (1981). Diameter of the cell-to-cell junctional membrane channels as probed with neutral molecules. *Science* **213**: 551-553.

Schyvens, C., Mangos, G., Zhang, Y., McKenzie, K., and Whitworth, J. (2001). Telemetric monitoring of adrenocorticotropin-induced hypertension in mice. *Clinical and Experimental Pharmacology and Physiology* **28**: 758-760.

Segal, S. S. (1994). Cell-to-cell communication coordinates blood flow control. *Hypertension* **23**: 1113-1120.

Segal, S. S., Damon, D. N., and Duling, B. R. (1989). Propagation of vasomotor responses coordinates arteriolar resistances. *American Journal of Physiology* **256**: H832-H837.

Segal, S. S. and Duling, B. R. (1986). Flow control among microvessels coordinated by intercellular conduction. *Science* **234**: 868-870.

Seidel, C. L. (1997). Cellular heterogeneity of the vascular tunica media. Implications for vessel wall repair. *Arteriosclerosis, Thrombosis and Vascular Biology* **17**: 1868-1871.

Setoguchi, M., Ohya, Y., Abe, I., and Fujishima, M. (1997). Stretch-activated whole-cell currents in smooth muscle cells from mesenteric resistance artery of guinea-pig. *Journal of Physiology (London)* **501**: 343-353.

Severs, N. J. (1999). Cardiovascular disease. In: *Gap junction-mediated intercellular signalling*. Wiley. p.188-211.

Severs, N. J., Dupont, E., Kaprielian, R. R., Yeh, H.-I., and Rothery, S. (1996). Gap junctions and connexins in the cardiovascular system. In: *Annual of Cardiac Surgery*. M. H. Yacoub, A. Carpentier, J. Pepper, and J.-N. Fabiani (eds.) Current Science, London. p.31-44.

Shanahan, C. M., Weissberg, P. L., and Metcalfe, J. C. (1993). Isolation of gene markers of differentiated and proliferating vascular smooth muscle cells. *Circulation Research* **73**: 193-204.

Sharifi, A. M., Li, J. S., Endemann, D., and Schiffrin, E. L. (1998). Effects of enalapril and amlodipine on small-artery structure and composition, and on endothelial dysfunction in spontaneously hypertensive rats. *Journal of Hypertension* **16**: 457-466.

Sherwood, L. (1993). Blood vessels and blood pressure. In: *Human Physiology*. West Publishing Company, Minneapolis. p. 299-344.

Shimkets, R. A. and Lifton, R. P. (1996). Recent advances in the molecular genetics of hypertension. *Current Opinion in Nephrology and Hypertension* **5**: 162-165.

Shimokawa, H. (1998). Endothelial dysfunction in hypertension. *Journal of Atherosclerosis and Thrombosis* **4**: 118-127.

Shimokawa, H. (1999). Primary endothelial dysfunction: atherosclerosis. *Journal of Molecular and Cellular Cardiology* **31**: 23-37.

Shiraishi, Y., Sakaki, S., and Uehara, Y. (1986). Architecture of the media of the arterial vessels in the dog brain: A scanning electron microscope study. *Cell and Tissue Research* **243**: 329-335.

Shivers, R. R. and McVicar, L. K. (1995). Gap junctions revealed by freeze-fracture electron microscopy. *Microscopy Research and Technique* **31**: 437-445.

Sia, M. A., Woodward, T. L., Turner, J. D., and Laird, D. W. (1999). Quiescent mammary epithelial cells have reduced connexin43 but maintain a high level of gap junction intercellular communication. *Developmental Genetics* **24**: 111-122.

Simon, A. M. (1999). Gap junctions: more roles and new structural data. *Trends in Cell Biology* **9**: 169-170.

Simon, A. M., Goodenough, D. A., Li, E., and Paul, D. L. (1997). Female infertility in mice lacking connexin 37. *Nature* **385**: 525-529.

Simon, A. M., Goodenough, D. A., and Paul, D. L. (1998). Mice lacking connexin40 have cardiac conduction abnormalities characteristic of atrioventricular block and bundle-branch block. *Current Biology* **8**: 295-298.

Solway, J., Seltzer, J., Samaha, F. F., Kim, S., Alger, L. E., Niu, Q., Morrisey, E. E., Ip, H. S., and Parmacek, M. S. (1995). Structure and expression of a smooth muscle cell-specific gene, SM22α. *Journal of Biological Chemistry* **270**: 13460-13469.

Somlyo, A. P. and Somlyo, A. V. (1968). Vascular smooth muscle.1. Normal structure, pathology, biochemistry and biophysics. *Pharmacological Reviews* **20**: 197-272.

Sosinsky, G. E. (1996). Molecular organization of gap junction membrane channels. *Journal of Bioenergetics and Biomembranes* **28**: 297-309.

Soulier, S., Stinnakre, M.-G., Lepourry, L., Mercier, J.-C., and Vilotte, J.-L. (1999). Use of doxycycline-controlled gene expression to reversibly alter milk-protein composition in transgenic mice. *European Journal of Biochemistry* **260**: 533-539.

Southern, E. (1975). Detection of specific sequences among DNA fragments separated by gel electrophoresis. *Journal of Molecular Biology* **98**: 503-517.

Sponer, G., Schulz, L., and Bartsch, W. (1988). Methods for the measurement of blood pressure in conscious rats. *Contributions to Nephrology* **60**: 220-229.

Spray, D. C. (1998). Gap junction proteins - where they live and how they die. *Circulation Research* **83**: 679-681.

Spray, D. C. and Bennett, M. V. (1985). Physiology and pharmacology of gap junctions. *Annual Review of Physiology* **47**: 281-303.

Spray, D. C. and Burt, J. M. (1990). Structure-activity relations of the cardiac gap junction channel. *American Journal of Physiology* **258**: C195-C205.

Srinivas, M., Rozental, R., Kojima, T., Dermietzel, R., Mehler, M., Condorelli, D. F., Kessler, J. A., and Spray, D. C. (1999). Functional properties of channels formed by the neuronal gap junction protein connexin36. *Journal of Neuroscience* **19**: 9848-9855.

Stahl, W. and Sies, H. (1998). The role of carotenoids and retinoids in gap junctional communication. *International Journal of Vitamin and Nutrition Research* **68**: 354-359.

Stauffer, K. A. (1995). The gap junction proteins $ß_1$-connexin (connexin-32) and $ß_2$-connexin (connexin-26) can form heteromeric hemichannels. *Journal of Biological Chemistry* **270**: 6768-6772.

Stearns, T. (1995). Green fluorescent protein. The green revolution. *Current Biology* **5**: 262-264.

Stratagene Catalogue (1997).

Strathdee, C. A., McLeod, M. R., and Hall, J. R. (1999). Efficient control of tetracycline-responsive gene expression from an autoregulated bi-directional expression vector. *Gene* **229**: 21-29.

Stripecke, R., Carmen Villacres, M., Skelton, D., Satake, N., Halene, S., and Kohn, D. (1999). Immune response to green fluorescent protein: implications for gene therapy. *Gene Therapy* **6**: 1305-1312.

Sturtz, F. G., Cioffi, L., Wittmer, S., Sonk, M. J., Shafer, A., Li, Y., Leeper, N. J., Smith-Gbur, J., Shulok, J., and Platika, D. (1998). Tetracycline-regulatable

expression vectors tightly regulate in vitro gene expression of secreted proteins. *Gene* **221**: 279-285.

Sullivan, R., Huang, G. Y., Meyer, R. A., Wessels, A., Linask, K. K., and Lo, C. W. (1999). Heart malformations in transgenic mice exhibiting dominant negative inhibition of gap junctional communication in neural crest cells. *Developmental Biology* **204**: 224-234.

Sunano, S., Sasaki, F., Osugi, S., and Shimamura, K. (1994). Comparison of endothelium-dependent and -independent tension oscillation in aortae of stroke-prone spontaneously hypertensive rats and Wistar Kyoto rats. *Journal of Smooth Muscle Research* **30**: 135-145.

Sutcliffe, M. C. and Davidson, J. M. (1990). Effect of static stretching on elastin production by porcine aortic smooth muscle cells. *Matrix* **10**: 148-153.

Takamura, Y., Shimokawa, H., Zhao, H., Igarashi, H., Egashira, K., and Takeshita, A. (1999). Important role of endothelium-derived hyperpolarizing factor in shear stress-induced endothelium-dependent relaxations in the rat mesenteric artery. *Journal of Cardiovascular Pharmacology* **34**: 381-387.

Takens-Kwak, B. R., Jongsma, H. J., Rook, M. B., and Van Ginneken AC. (1992). Mechanism of heptanol-induced uncoupling of cardiac gap junctions: a perforated patch-clamp study. *American Journal of Physiology* **262**: C1531-C1538.

Tang, J., Neidigh, J. L., Cooksey, R. C., and McClain, D. A. (2000). Transgenic mice with increased hexosamine flux specifically targeted to beta-cells exhibit hyperinsulinaemia and peripheral insulin resistance. *Diabetes* **49**: 1492-1499.

Tavares, A., Handy, D. E., Bogdanova, N. N., Rosene, D. L., and Gavras, H. (1996). Localization of the alpha 2A- and alpha 2B-adrenergic receptor subtypes in brain. *Hypertension* **27**: 449-455.

Temme, A., Buchmann, A., Gabriel, H. D., Nelles, E., Schwarz, M., and Willecke, K. (1997). High incidence of spontaneous and chemically induced liver tumors in mice deficient for connexin32. *Current Biology* **7**: 713-716.

Toda, N. and Okamura, T. (1998). Cerebral vasodilators. *Japanese Journal of Pharmacology* **76**: 349-367.

Todd, M. E. (1980). Development of adrenergic innervation in rat peripheral vessels: a fluorescence microscopic study. *Journal of Anatomy* **131**: 121-133.

Todd, M. E., Laye, C. G., and Osborne, D. N. (1983). The dimensional characteristics of smooth muscle in rat blood vessels. A computer-assisted analysis. *Circulation Research* **53**: 319-331.

Tortora, G. J. and Grabowski, S. R. (1993). *Principles of Anatomy and Physiology.* HarperCollins College Publishers, New York.

Tremblay, P., Meiner, Z., Galou, M., Heinrich, C., Petromilli, C., Lisse, T., Cayetano, J., Torchia, M., Mobley, W., Bujard, H., DeArmond, S. J., and Prusiner, S. B. (1998). Doxycycline control of prion protein transgene expression modulates prion disease in mice. *Proceedings of the National Academy of Sciences (USA)* **95**: 12580-12585.

Trexler, E. B., Bukauskas, F. F., Bennett, M. V., Bargiello, T. A., and Verselis, V. K. (1999). Rapid and direct effects of pH on connexins revealed by the connexin46 hemichannel preparation. *Journal of General Physiology* **113**: 721-742.

Tsien, R. W. and Weingart, R. (1976). Inotropic effect of cyclic AMP in calf ventricular muscle studied by a cut end method. *Journal of Physiology (London)* **260**: 117-141.

Tsuda, K., Tsuda, S., Minatogawa, Y., Iwahashi, H., Kido, R., and Masuyama, Y. (1988a). Decreased membrane fluidity of erythrocytes and cultured vascular smooth muscle cells in spontaneously hypertensive rats: an electron spin resonance study. *Clinical Science* **75**: 477-480.

Tsuda, K., Tsuda, S., Minatogawa, Y., Iwahashi, H., Shima, H., Yoshikawa, H., Ura, M., Takeda, J., Kimura, K., and Nishio, I. (1988b). Membrane fluidity of erythrocytes and its relevance to renin profile in essential hypertension. *Japanese Circulation Journal* **52**: 1301-1308.

Udy, G. B. and Evans, M. J. (1994). Microplate DNA preparation, PCR screening and cell freezing for gene targeting in embryonic stem cells. *BioTechniques* **17**: 887-894.

Ullmann, A., Jacob, F., and Monod, J. (1967). Characterization by in vitro complementation of a peptide corresponding to an operator-proximal segment of the beta-galactosidase structural gene of Escherichia coli. *Journal of Molecular Biology* **24**: 339-343.

Umemura, S., Hirawa, N., Hayashi, S., Toya, Y., Minamisawa, K., Iwamoto, T., Kihara, M., and Ishii, M. (1992). Effect of dietary sodium on platelet alpha 2-adrenoceptors in young normotensive men with or without a family history of hypertension. *Journal of Hypertension* **10**: 1397-1401.

Unger, V. M., Kumar, N. M., Gilula, N. B., and Yeager, M. (1999). Electron cryo-crystallography of a recombinant cardiac gap junction channel. *Novartis Foundation Symposium* **219**: 22-30.

Ure, J. M., Fiering, S., and Smith, A. G. (1992). A rapid and efficient method for freezing and recovering clones of embryonic stem cells. *Trends in Genetics* **8**: 6.

Valiunas, V., Weingart, R., and Brink, P. R. (2000). Formation of heterotypic gap junction channels by connexins 40 and 43. *Circulation Research* **86**: e42-e56.

van Breemen, C., Chen, Q., and Laher, I. (1995). Superficial buffer barrier function of smooth muscle sarcoplasmic reticulum. *Trends in Pharmacological Sciences* **16**: 98-105.

van Kempen, M. J., ten Velde, I., Wessels, A., Oosthoek, P. W., Gros, D., Jongsma, H. J., Moorman, A. F. and Lamers, W. H. (1995). Differential connexin distribution accommodates cardiac function in different species. *Microscopy Research and Technique* **31**: 420-436.

van Rijen, H., van Kempen, M. J., Analbars, L. J., Rook, M. B., van Ginneken, A. C.; Gros, D. and Jongsma, H. J. (1997). Gap junctions in human umbilical cord endothelial cells contain multiple connexins. *American Journal of Physiology* **272**: 117-130.

Vanhoutte, P. M. and Boulanger, C. M. (1995). Endothelium-dependent responses in hypertension. *Hypertension Research* **18**: 87-98.

Vanhoutte, P. M. and Feletou, M. (1998). Endothelium-dependent hyperpolaraization. *Pharmacology and Toxicology* **83**: 51-53.

Vanhoutte, P. M. and Miller, V. M. (1989). Alpha 2-adrenoceptors and endothelium-derived relaxing factor. *American Journal of Medicine* **87**: 1S-5S.

Veenstra, R. D. (1996). Size and selectivity of gap junction channels formed from different connexins. *Journal of Bioenergetics and Biomembranes* **28**: 327-337.

Veenstra, R. D., Wang, H.-Z., and Belbo, D. A. (1994). Ion permeability of connexin specific channels, variations on a common theme? *Biophysical Journal* **66**: A259.

Veenstra, R. D., Wang, H. Z., Beblo, D. A., Chilton, M. G., Harris, A. L., Beyer, E. C., and Brink, P. R. (1995). Selectivity of connexin-specific gap junctions does not correlate with channel conductance. *Circulation Research* **77**: 1156-1165.

Veenstra, R. D., Wang, H. Z., Westphale, E. M., and Beyer, E. C. (1992). Multiple connexins confer distinct regulatory and conductance properties of gap junctions in developing heart. *Circulation Research* **71**: 1277-1283.

Verselis, V. K., Ginter, C. S., and Bargiello, T. A. (1994). Opposite voltage gating polarities of two closely related connexins. *Nature* **368**: 348-351.

Wakayama, T., Rodriguez, I., Perry, A. C., Yanagimachi, R., and Mombaerts, P. (1999). Mice cloned from embryonic stem cells. *Proceedings of the National Academy of Sciences (USA)* **96**: 14984-14989.

Waldo, K. L., Lo, C. W., and Kirby, M. L. (1999). Connexin 43 expression reflects neural crest patterns during cardiovascular development. *Developmental Biology* **208**: 307-323.

Wallace, H., Ansell, R., Clark, J., and McWhir, J. (2000). Pre-selection of integration sites imparts repeatable transgene expression. *Nucleic Acids Research* **28**: 1455-1464.

Walsh, M. P., Kargacin, G. J., Kendrick-Jones, J., and Lincoln, T. M. (1995). Intracellular mechanisms involved in the regulation of vascular smooth muscle tone. *Canadian Journal of Physiology and Pharmacology* **73**: 565-573.

Waltzman, M. N. and Spray, D. C. (1995). Exogenous expression of connexins for physiological characterization of channel properties: comparison of methods and results. In: *Intercellular Communication Through Gap Junctions.* Y. Kanno, K. Kataoka, and Y. Shiba (eds.) Elsevier Science, Amsterdam. p.9-17.

Wang, H.-Z. and Veenstra, R. D. (1997). Monovalent ion selectivity sequences of the rat connexin43 gap junction channel. *Journal of General Physiology* **109**: 491-507.

Wang, J., Niu, W., Nikiforov, Y., Naito, S., Chernausek, S., Witte, D., LeRoith, D., Strauch, A., and Fagin, J. A. (1997). Targeted overexpression of IGF-I evokes distinct patterns of organ remodeling in smooth muscle cell tissue beds on transgenic mice. *Journal of Clinical Investigation* **100**: 1425-1439.

Wang, Y. and Rose, B. (1997). An inhibition of gap-junctional communication by cadherins. *Journal of Cell Science* **110**: 301-309.

Warn-Cramer, B. J., Cottrell, G. T., Burt, J. M., and Lau, A. F. (1998). Regulation of connexin 43 gap junctional intercellular communication by mitogen-activated protein kinase. *Journal of Biological Chemistry* **273**: 9188-9196.

Warner, A. (1992). Gap junctions in development - a perspective. *Seminars in Cell Biology* **3**: 81-91.

Watts, S. W., Tsai, M. L., Loch-Caruso, R., and Webb, R. C. (1994). Gap junctional communication and vascular smooth muscle reactivity: use of tetraethylammonium chloride. *Journal of Vascular Research* **31**: 307-313.

Watts, S. W. and Webb, R. C. (1996). Vascular gap junctional communication is increased in mineralocorticoid-salt hypertension. *Hypertension* **28**: 888-893.

Webb, R. C., Schreur, K. D., and Papadopoulos, S. M. (1992). Oscillatory contractions in vertebral arteries from hypertensive subjects. *Clinical Physiology* **12**: 69-77.

Weissberg, P. L., Cary, N. R., and Shanahan, C. M. (1995). Gene expression and vascular smooth muscle cell phenotype. *Blood Pressure Supplement* **2**: 68-73.

Welsh, D. G., Jackson, W. F., and Segal, S. S. (1998). Oxygen induces electromechanical coupling in arteriolar smooth muscle cells: a role for L-type Ca2+ channels. *American Journal of Physiology* **274**: H2018-H2024.

White, T. W. and Bruzzone, R. (1996). Multiple connexin proteins in single intercellular channels: connexin compatibility and functional consequences. *Journal of Bioenergetics and Biomembranes* **28**: 339-350.

White, T. W., Bruzzone, R., and Paul, D. L. (1995). The connexin family of intercellular channel forming proteins. *Kidney International* **48**: 1148-1157.

White, T. W., Bruzzone, R., Wolfram, S., and Paul, D. L. (1994). Selective interactions among the multiple connexin proteins expressed in the vertebrate lens: The second extracellular domain is a determinant of compatibility among rodent connexins. *Journal of Cell Biology* **125**: 879-892.

White, T. W. and Paul, D. L. (1999). Genetic diseases and gene knockouts reveal diverse connexin functions. *Annual Review of Physiology* **61**: 283-310.

Whitelaw, C. B., Harris, S., McClenaghan, M., Simons, J. P., and Clark, A. J. (1992). Position-independent expression of the ovine beta-lactoglobulin gene in transgenic mice. *Biochemical Journal* **286 (Pt 1)**: 31-39.

Wiinberg, N., Hoegholm, A., Christensen, H. R., Bang, L. E., Mikkelsen, K. L., Nielsen, P. E., Svendsen, T. L., Kampmann, J. P., Madsen, N. H., and Bentzon, M. W. (1995). 24-h Ambulatory blood pressure in 352 normal Danish subjects, related to age and gender. *American Journal of Hypertension* **8**: 978-986.

Wilde, D. W., Furspan, P. B., and Szocik, J. F. (1994). Calcium current in smooth muscle cells from normotensive and genetically hypertensive rats. *Hypertension* **24**: 739-746.

Willecke, K., Hennemann, H., Dahl, E., Jungbluth, S., and Heynkes, R. (1991). The diversity of connexin genes encoding gap junctional proteins. *European Journal of Cell Biology* **56**: 1-7.

Willecke, K., Kirchhoff, S., Plum, A., Temme, A., Thonnissen, E., and Ott, T. (1999). Biological functions of connexin genes revealed by human genetic defects, dominant negative approaches and targeted deletions in the mouse. *Novartis Foundation Symposium* **219**: 76-96.

Wilson, J. A. (1979). Circulatory systems - nature and functions. In: *Principles of Animal Physiology*. Collier Macmillan, New York. p.594-644.

Wood, S. A., Allen, N. D., Rossant, J., Auerbach, A., and Nagy, A. (1993a). Non-injection methods for the production of embryonic stem cell-embryo chimaeras. *Nature* **365**: 87-89.

Wood, S. A., Allen, N. D., Rossant, J., Auerbach, A., and Nagy, A. (1993b). Simple and efficient production of embryonic stem cell-embryo chimaeras by coculture. *Proceedings of the National Academy of Sciences (USA)* **90**: 4582-4585.

Xie, H., Laird, D. W., Chang, T. H., and Hu, V. W. (1997). A mitosis-specific phosphorylation of the gap junction protein connexin43 in human vascular cells: biochemical characterization and localization. *Journal of Cell Biology* **137**: 203-210.

Xu, X. and Ebihara, L. (1999). Characterization of a mouse Cx50 mutation associated with the No2 mouse cataract. *Investigative Ophthalmology and Visual Science* **40**: 1844-1850.

Ya, J., Erdtsieck-Ernste, E. B. H. W., de Boer, P. A. J., van Kempen, M. J. A., Jongsma, H., Gros, D., Moorman, A. F. M., and Lamers, W. H. (1998). Heart defects in connexin43-deficient mice. *Circulation Research* **82**: 360-366.

Yamamoto, Y., Imaeda, K., and Suzuki, H. (1999). Endothelium-dependent hyperpolarization and intercellular electrical coupling in guinea-pig mesenteric arterioles. *Journal of Physiology* **514**: 505-513.

Yancey, S. B., Nicholson, B. J., and Revel, J. P. (1981). The dynamic state of liver gap junctions. *Journal of Supramolecular Structure and Cellular Biochemistry* **16**: 221-232.

Yarranton, G. T. (1992). Inducible vectors for expression in mammalian cells. *Current Opinion in Biotechnology* **3**: 506-511.

Yeager, M. (1995). Electron microscopic image analysis of cardiac gap junction membrane crystals. *Microscopy Research and Technique* **31**: 452-466.

Yeager, M. (1998). Structure of cardiac gap junction intercellular channels. *Journal of Structural Biology* **121**: 231-245.

Yeager, M. and Gilula, N. B. (1992). Membrane topology and quaternary structure of cardiac gap junction ion channels. *Journal of Molecular Biology* **223**: 929-948.

Yeager, M. and Nicholson, B. J. (1996). Structure of gap junction intercellular channels. *Current Opinion in Structural Biology* **6**: 183-192.

Yeh, H.-I., Dupont, E., Coppen, S., Rothery, S., and Severs, N. J. (1997). Gap junction localization and connexin expression in cytochemically identified endothelial cells of arterial tissue. *Journal of Histochemistry and Cytochemistry* **45**: 539-550.

Yeh, H.-I., Rothery, S., Dupont, E., Coppen, S., and Severs, N. J. (1998). Individual gap junction plaques contain multiple connexins in arterial endothelium. *Circulation Research* **83**: 1248-1263.

Yeh, J. L., Whitney, E. G., Lamb, S., and Brophy, C. M. (1996). Nitric oxide is an autocrine feedback inhibitor of vascular smooth muscle contraction. *Surgery* **119**: 104-109.

Yin, D. X., Zuh, L., and Schimke, R. T. (1996). Tetracycline-controlled gene expression system achieves high-level and quantitative control of gene expression. *Annals of Biochemistry* **235**: 195-201.

Yoshida, K. and Toda, N. (1997). Colocalization of acetylcholinesterase and vasoactive intestinal peptide (VIP) in nicotinamide adenine dinucleotide phosphate diaphorase (NADPH-d) positive neurons in the intralingual ganglia and perivascular nerve fibers around lingual arteries in the porcine, monkey and canine tongue. *Neuroscience Letters* **222**: 147-150.

Zhang, Y. M., Miura, M., and ter Keurs HE. (1996). Triggered propagated contractions in rat cardiac trabeculae. Inhibition by octanol and heptanol. *Circulation Research* **79**: 1077-1085.

Appendix I - Methods

This Appendix supplements the information presented in Chapter 2 – Materials and Methods.

AI.1 Restriction endonuclease digests

Restriction endonuclease digests were undertaken to verify the plasmids and the DNA constructs. Each was carried out in the appropriate NEB buffer (see Table AI.1) for each enzyme selected.

NEBuffer 1	10 mM Bis Tris Propane-HCl, 10 mM $MgCl_2$ and 1 mM dithiothreitol pH 7.0 at 25°C.
NEBuffer 2	10 mM Tris-HCl, 10 mM $MgCl_2$ and 1 mM dithiothreitol pH 7.9 at 25°C.
NEBuffer 3	50 mM Tris-HCl, 10 mM $MgCl_2$, 100 mM NaCl and 1 mM dithiothreitol pH 7.9 at 25°C.
NEBuffer 4	20 mM Tris-acetate, 10 mM magnesium acetate, 50 mM potassium acetate and 1 mM dithiothreitol pH 7.9 at 25°C.

Table AI.1 NEBuffers used in the restriction digests

AI.2 Analytical and preparative separation of DNA fragments

Lambda phage DNA digested with *Acc*I or *Hind*III or pTz / *Alu*I were electrophoresed with the DNA samples as molecular size markers (see Table AI.2). The λDNA *Eco*RI / *Hind*III marker was also used.

λ *Acc*I	13.070 kb, 11.828 kb, 6.957 kb, 5.581 kb, 3.574 kb, 2.720 kb, 2.180 kb, 1.444 kb, 0.639 kb and 0.499 kb.
λ *Hind*III	23.130 kb, 9.416 kb, 6.557 kb, 4.373 kb, 2.322 kb, 2.027 kb, 0.564 kb and 0.125 kb.
λ DNA / *Eco*RI / *Hind*III	24.756 kb, 21.226 kb, 5.148 kb, 4.973 kb, 4.268 kb, 3.530 kb, 2.027 kb, 1.904 kb, 1.584 kb, 1.375 kb, 0.947 kb, 0.831 kb, 0.564 kb and 0.125 kb.
pTz / *Alu*I	0.621 kb, 0.521 kb, 0.257 kb [x2], 0.226 kb, 0.215 kb, 0.136 kb, 0.118 kb, 0.100 kb, 0.095 kb, 0.093 kb, 0.064 kb, 0.063 kb, 0.049 kb and 0.045 kb.

Table AI.2 The molecular weight DNA standards

AI.3 Smooth muscle cell specificity

Positive staining with antibodies against smooth muscle cell myosin was used to confirm the specificity of these cultures. The method is tabulated below.

1. Aspirate DMEM from the adhered cells and rinse 3 times in PBS.
2. Fix in 4 % (w/v) paraformaldehyde in 0.1 M sodium phosphate buffer pH 7.3, for 30 minutes at room temperature.
3. Rinse in PBS, then wash 3 times in PBS; 5 minutes each.
4. Add primary antibody (rabbit anti-myosin; 1:1000) diluted in PBS containing 10 mg / ml BSA, 0.4 mg / ml sodium azide and 30 µl / ml 10% Triton X-100, and incubate overnight at room temperature in a humidified chamber.
5. Rinse in PBS, then wash 3 times in PBS; 10 minutes each.
6. Incubate with fluorescein (FITC)-conjugated affinity-purified donkey anti-rabbit (1:40; Dako) or goat anti-rabbit oregon green (1:100; Molecular Probes) diluted in PBS, for one hour at room temperature in a humidified chamber.
7. Rinse in PBS, then wash 3 times in PBS; 10 minutes each.
8. Mount in buffered glycerol and store at -20°C.

Table AI.3 Immunohistochemical protocol for smooth muscle culture specificity using myosin antibody.

AI.4 Protocol for fresh tissue immunohistochemistry

1. Pre-chill chuck in a slurry of 95% ethanol and dry ice. Add embedding compound (Cryo-M-Bed; Bright Instrument Company Ltd., England) to the chuck's surface just before placing the tissue on the chuck.
2. Place dissected tissue into cold 30% sucrose in PBS for 5 to 10 minutes, and then into 1:1 mixture of 30% sucrose and embedding compund for 5 to 10 minutes until tissue sinks.
3. Remove tissues and place on a microscope slide (max. 3 per slide). Cover preparations with chilled embedding compound. Place on dry ice to freeze whilst prepare the chuck (see point 1).
4. Invert slide on chuck and freeze completely. Then remove slide by gently warming the surface
5. Keep chuck with tissue preparations on dry ice until sectioning.
6. Section tissue at a thickness of 10 μm on cryostat, and place sections on microscope slides.
7. Section tissue at a thickness of 10 μm on cryostat, and place sections on microscope slides.
8. Fix in cold acetone for 7 minutes and air dry the slides.
9. Make circle around tissue with pap pen and pre-incubate sections in 2% BSA / 0.2% Triton-X / 0.04% sodium azide for 30 minutes.
10. Add primary antibody: anti-rabbit Cx43 antibody (1:250; Zymed, California) diluted in 2% BSA / 0.2% Triton-X / 0.04% sodium azide in PBS for 1 hr at room temperature in a humidified container.
11. Rinse quickly with PBS, and then wash in PBS 3 x 10 minutes.
12. Apply secondary antibody (1:100; Cy3-conjugated anti-rabbit immunoglobulins, Jackson Immunoresearch Laboratories Inc., PA) diluted in PBS / 0.01% Triton-X for one hour at room temperature in a humidified container.
13. Rinse quickly with PBS, then wash in PBS 3 x 10 minutes.
14. Mount in buffered glycerol and examine using a fluorescence microscope fitted with the appropriate filters.

AI.5 Western blots

The solutions used in the Western blots are shown below.

Running Buffer	28.8 g glycine, 6 g Tris-base, 2 g SDS in 2 L distilled water.
Lower Tris Buffer	15.4 g Tris-base, 3.7 g Tris-HCl in 100 ml distilled water; pH 8.8.
Anode Buffer #1	100 ml Tris-base, 33.3 ml Methanol, 33.3 ml distilled water; pH 10.4.
Anode Buffer #2	10 ml Tris-base, 80 ml Methanol, 310 ml distilled water; pH 10.4.
Cathode Buffer	10 ml 500 mM Tris-base, 310 ml distilled water, 2.099 g aminohexanoic acid, 80 ml Methanol; pH 9.4.
Tris-base	500 mM – 30.25 g / 500 ml distilled water; pH 7.4.

Table AI.4 Western blot solutions

Appendix II – Generation of the Tetracycline Response Constructs

AII.1 Introduction

A major limitation in the use of genetically modified mice for various studies is the lack of tissue and temporal control of gene expression. To date, much work has been undertaken using transgenes that are controlled by either tissue-specific promoters or promoters that are expressed in a wide variety of tissues with no temporal control of expression. In the ideal situation, control of the expression of individual genes would also allow expression at defined levels, as well as mediating on / off expression.

In the tetracycline regulatory (expression) system, target genes are placed under the control of a regulatory sequence (tetO) from the tetracycline-resistance operon of Tn*10*. This short sequence is bound by the tetracycline repressor protein (tetR) in bacteria (Hillen and Wissmann, 1989). In the presence of the tetracycline antibiotic, tetR does not bind to its operators located within the promoter region of the operon, allowing transcription to occur (Gossen and Bujard, 1992). A hybrid transactivator (tTA), as in the plasmid system used in the current study, stimulates transcription from a minimal promoter sequence, which is virtually silent in the presence of low concentrations of tetracycline. This system is called TetOff. There are in fact two complimentary versions of the Tet system: TetOff and TetOn.

The TetOn system (Figure AII.1) is based on the reverse tTA (rtTA), which differs from tTA by four amino acid changes in the TetR protein (Clontech, 1997), and activates transcription in the presence of the tetracycline antibiotics, tetracycline or doxycycline (the latter being the drug of choice as it is known that the rtTA responds poorly to tetracycline; Gossen and Bujard, 1992). Two plasmids are needed: a regulator plasmid and a response plasmid. In this thesis, the regulator plasmid was pTetOn (Clontech; Figure AII.2A) which contained the rtTA coding region, a CMV promoter (to

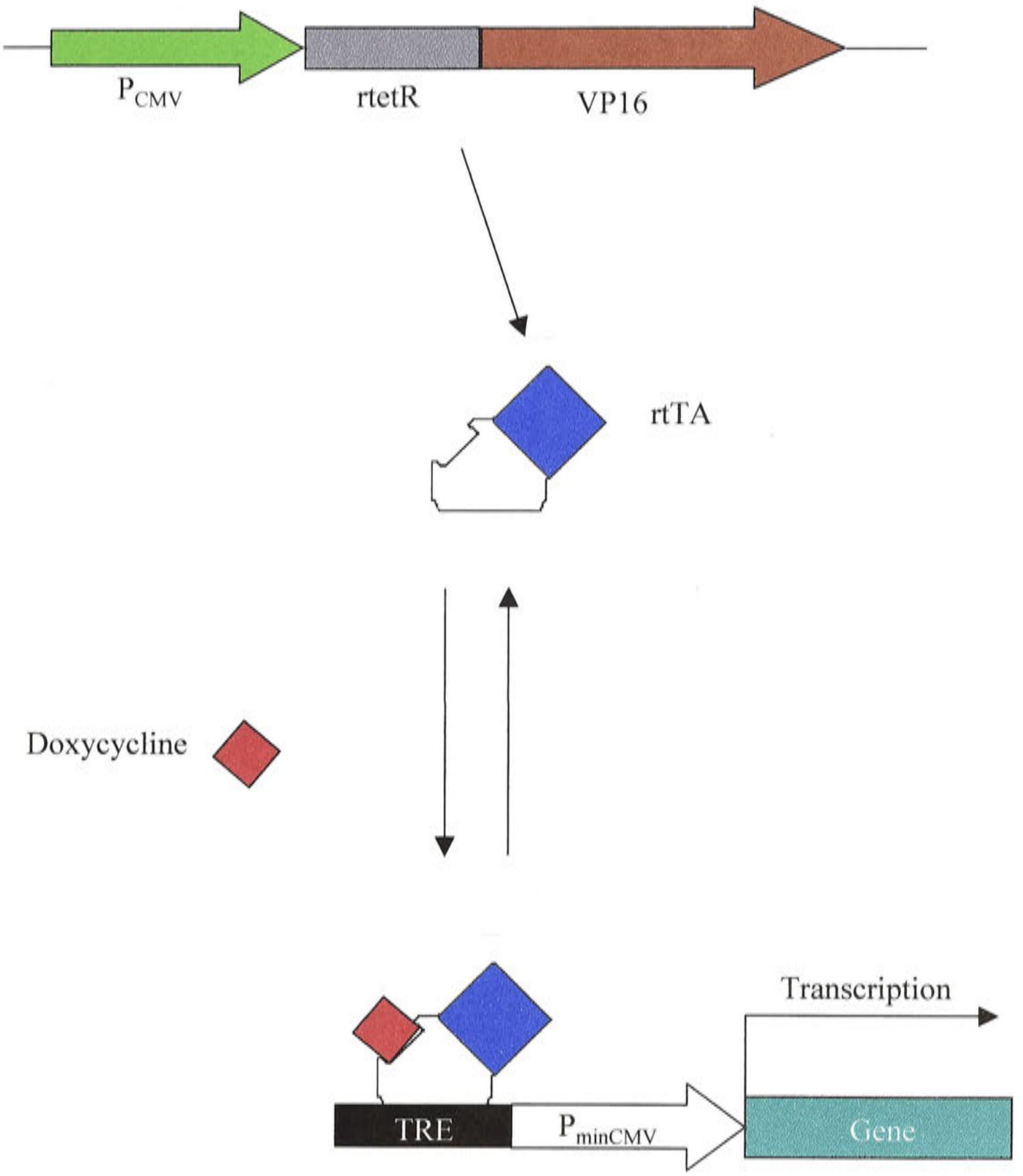

Figure AII.1 The Tetracycline Expression System

be replaced by the restricted SM22α promoter) and a SV40 polyadenylation site. The response plasmid was pBi5 (Figure AII.2B) with a silent, minimal CMV promoter, the tetracycline response element (TRE) and multiple cloning site (MCS) into which the selected Cx43 gene region was cloned (see Chapter 3).

The two DNA constructs described above would be used to generate two transgenic mouse lines. One would contain the smooth muscle specific construct in which the restricted SM22α promoter would provide tissue specificity for the expression of the tetracycline transactivator protein (rtTA; SM22α / pTetOn), and the other would contain the Cx43 temporal specific construct in which the tetracycline response element would provide temporal control of Cx43 gene expression (Cx43 / pBi5; EGFP / Cx43 / pBi5). The transgenic mice separately produced by injection of these two constructs, would be intercrossed to produce a doubly transgenic mouse line in which both constructs would be present in each cell so that Cx43 expression would be driven by the SM22α promoter under the temporal control of doxycycline (Figure AII.3).

This Appendix describes the cloning of the SM22α / pTetOn, and EGFP / Cx43 / pBi5 constructs. All constructs were evaluated *in vitro* in cultured murine embryonic fibroblasts and murine aortic smooth muscle cells.

AII.2 Additional Methods

AII.2.1 Cloning of SM22α / pTetOn

AII.2.1.1 Preparation and verification of the pTetOn plasmid

The pTetOn plasmid (7.4 kb; 500 ng / μl) was diluted in MilliQ water and a small aliquot electroporated into TOP10F' cells. Colonies were screened for the insert by cracking and one positive colony was chosen to form the stock sample. After purification, the DNA was checked by agarose gel electrophoresis and quantified by spectrophotometric analysis, before verification by restriction enzyme digests.

Figure AII.2 The TetOn plasmids

Shown are the two TetOn vectors, pTetOn (7.4 kb; **A**) and pBi5 (6.083 kb; **B**) with selected restriction enzyme sites. Neo^r and Amp^r refer to the neomycin and ampicillin resistance genes respectively.

In pTetOn, the generalized promoter (P_{CMV}) which produces the viral products rtetR and VP16 (together forming the tetracycline transactivator; rtTA), was removed and replaced with the SM22α promoter; thus giving tissue specificity to the construct. The tetracycline response element (TRE), to which the rtTA binds when doxycycline is added, is shown in the pBi5 plasmid. After binding, the TRE activates the minimal promoter (P_{bi-1} promoter) to drive transcription of the luciferase gene as well as the Cx43 gene, which was cloned into the multiple cloning site.

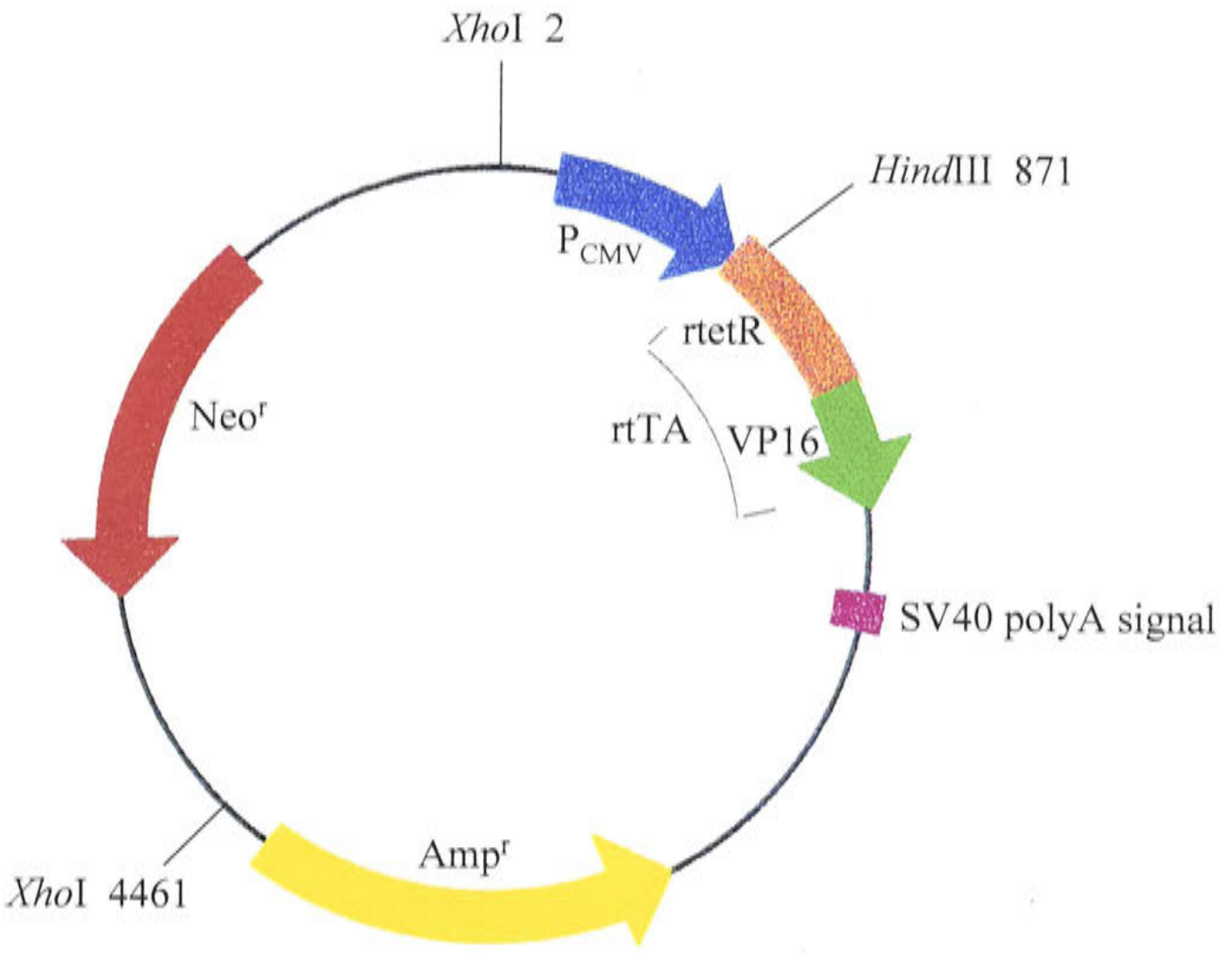

Figure AII.2A The pTetOn plasmid

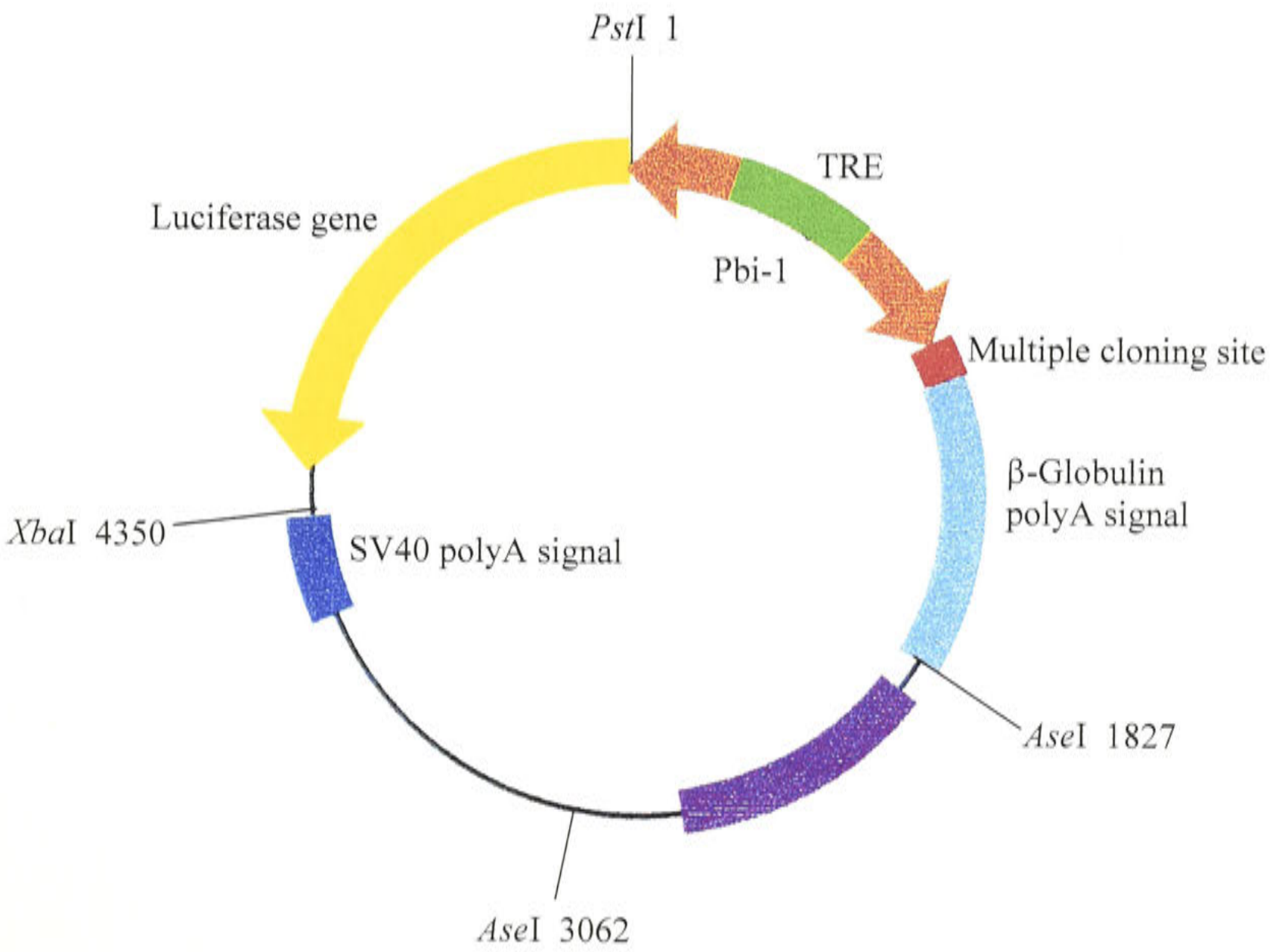

Figure AII.2B The pBi5 plasmid

Figure AII.3 Tissue and temporal specificity in the same cell

The tissue specific construct with the SM22α promoter **(A)** and the temporal specific construct with the Cx43 gene **(B)**. Mice overexpressing **A** and **B** are required.

KEY:

SM22	the restricted SM22α promoter
rtetR/VP16	rtTA (tetracycline transactivator)
Luc	luciferase gene
P_{min}	minimal promoter
TRE	tetracycline response element
Cx43	Cx43 gene

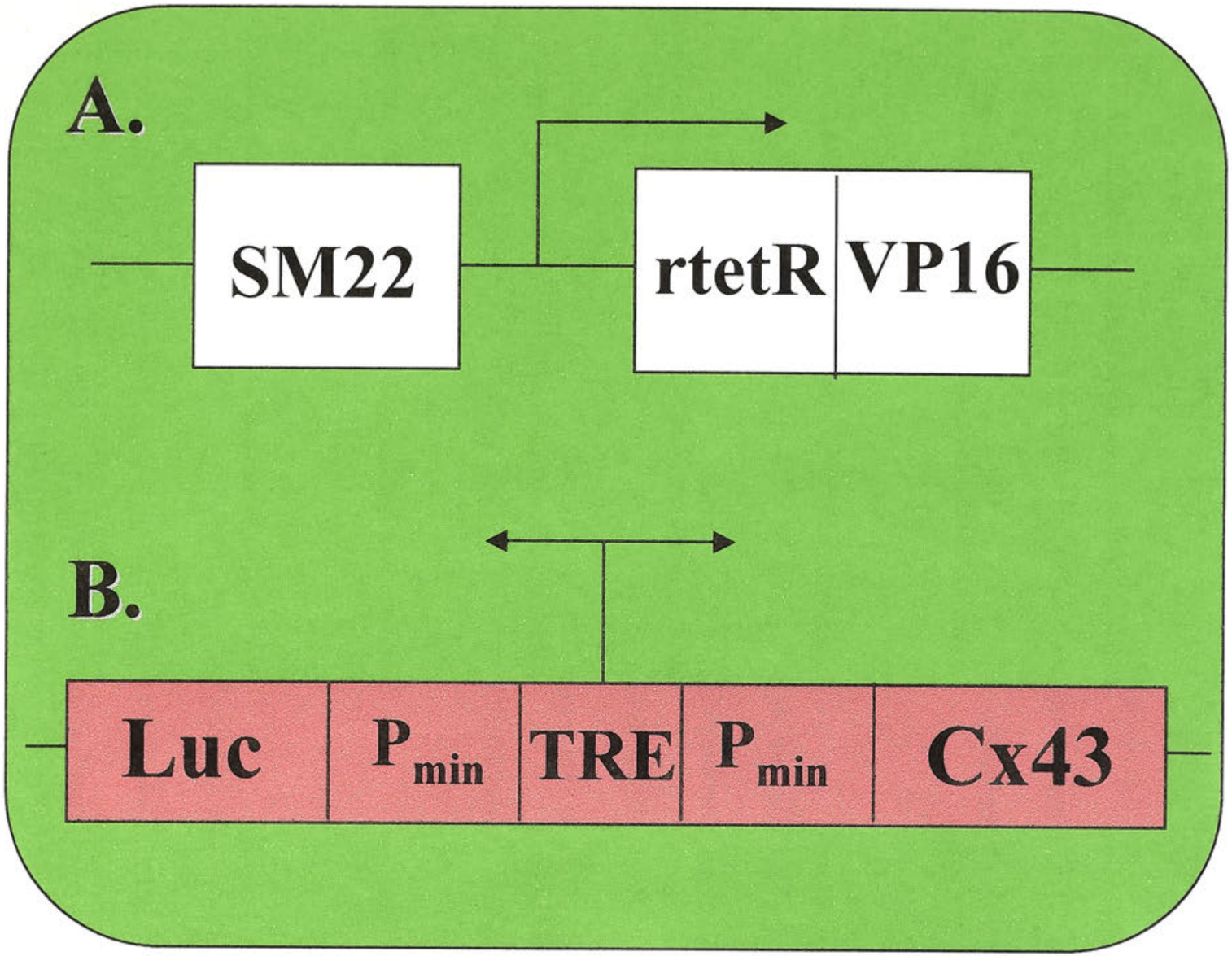
A.
SM22
rtetR
VP16
B.
Luc
P min
TRE
P min
Cx43

Briefly, the single cutters *Eco*RI and *Spe*I each gave band sizes around the predicted band size of 7.4 kb, whilst the combined *Eco*RI / *Spe*I restriction removed the CMV promoter (663 bp) leaving a fragment of around 6.7 kb. *Pvu*II, cut pTetOn five times to give the predicted fragment sizes of 3.0 kb, 2.6 kb, 0.7 kb, 0.57 kb and 0.5 kb. *Hind*III was specifically chosen to verify the plasmid as pTetOn and not pTetOff, as it has the unique feature of being a single cutter in pTetOff and a double cutter in pTetOn. Two fragments of about 1.3 kb and 6.1 kb were produced (Figure AII.4).

The CMV promoter was excised from 2 µg of the plasmid using *Eco*RI and *Spe*I, and then isolated and purified before assessment by agarose gel electrophoresis.

AII.2.1.2 Preparation of the SM22α / pBs KSII- plasmid

The SM22α promoter was excised from 400 ng of SM22α / pBs KSII- (designated Clone #121; Chapter 3) with *Eco*RI and *Spe*I. This would ensure that even with a 50% recovery rate from the gel purification, 200 ng (the calculated amount needed for subsequent cloning into pre-restricted pTetOn) would be available for cloning. After isolation and purification, the SM22α fragment was assessed by agarose gel electrophoresis.

AII.2.1.3 Cloning of SM22α / pTetOn

The *Spe*I / *Eco*RI / SM22α fragment was directionally cloned into the *Eco*RI / *Spe*I / pTetOn plasmid. The DNA was subsequently transformed, and cracking identified clones possessing an insert. Six positives were purified and assessed by agarose gel electrophoresis. Verification was by restriction enzyme digests, and bi-directional sequencing with the SM22ex1r and SM22ex1f primers (see Section AII.3). PCR screening was not undertaken, as it was deemed unnecessary due to the satisfactory results already obtained.

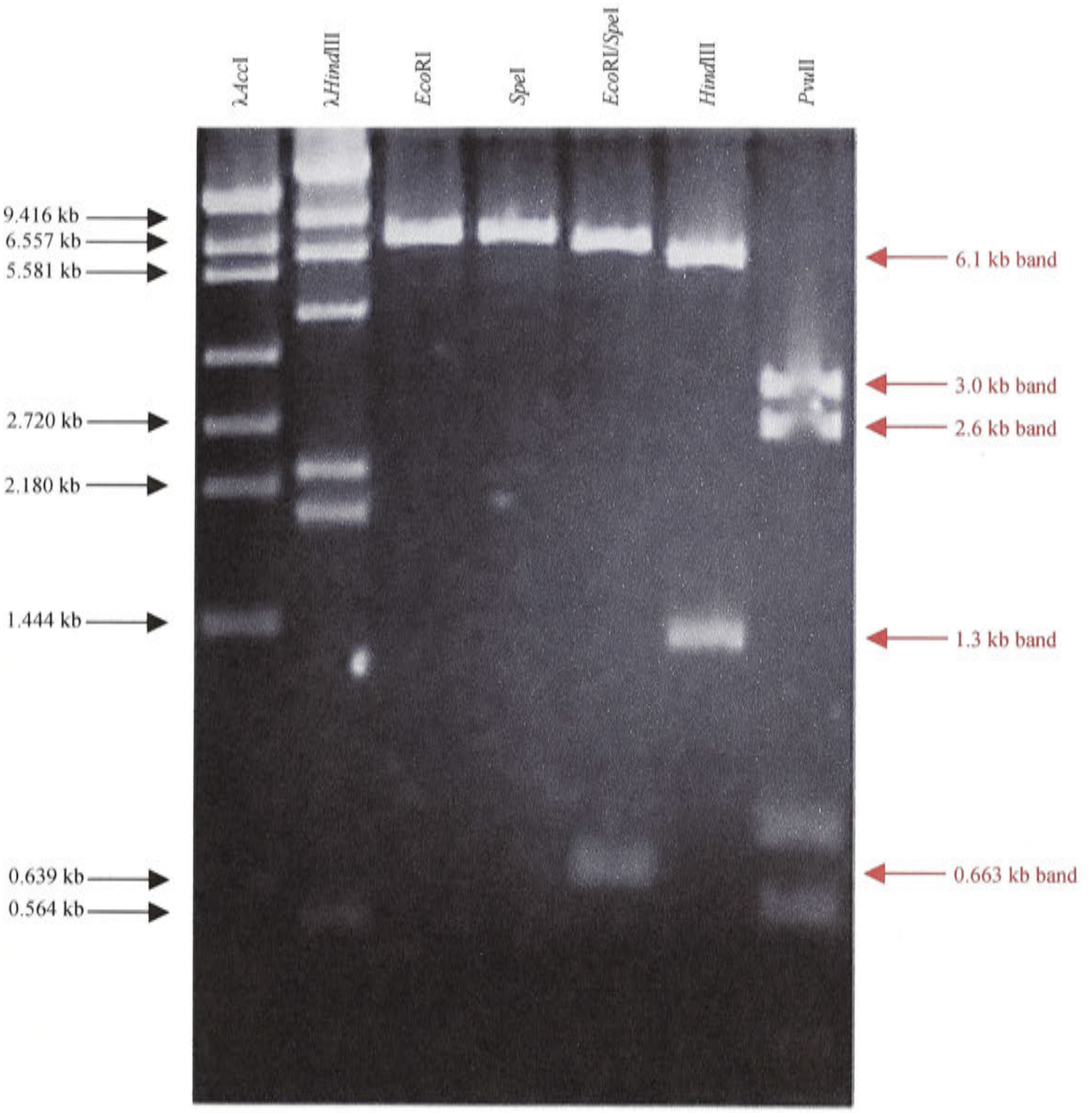

Figure AII.4 Verification of pTetOn

Both *Eco*RI and *Spe*I linearized pTetOn, giving bands of about 7.4 kb. The combined *Eco*RI / *Spe*I restriction removed the CMV promoter (663 bp). *Hind*III gave two fragments of approximately 1.3 kb and 6.1 kb, thereby verifying the plasmid as pTetOn and not pTetOff. *Pvu*II produced five bands which corresponded to the predicted fragment sizes of 3.0 kb, 2.6 kb, 0.7 kb, 0.57 kb and 0.5 kb.

AII.2.2 Cloning of Cx43 / pBi5

This construct was cloned in Chapter 3.

AII.2.3 Cloning of EGFP / Cx43 / pBi5

As the EGFP expression data from *in vitro* testing of the DNA constructs revealed that immunohistochemical detection was not as sensitive as direct detection of EGFP, the luciferase gene in the Cx43 / pBi5 construct was replaced with the EGFP gene from pEGFP-NI (4.733 kb; Figures AII.5 and AII.6). Briefly, the luciferase gene was excised from pBi5 with *Pst*I / *Spe*I and the *Pst*I / *Not*I / EGFP gene from pEGFP-NI inserted, as the polyadenylation site in the pBi5 plasmid could be used by the EGFP gene. The *Not*I and *Spe*I sites were filled in with Klenow for the blunt-end cloning.

AII.2.3.1 Preparation of the pEGFP-NI plasmid

The pEGFP-NI plasmid (4.733 kb; CMV-EGFP) was quantified by spectrophotometric analysis at OD_{260} and then verified by restriction analyses. The single cutter *Not*I (cuts pEGFP-NI at 1.402 kb) produced a linear band around the expected size of 4.7 kb. *Pst*I, also a single cutter (at 0.639 kb), gave a linear band around 4.7 kb. The *Not*I / *Pst*I double restriction removed the EGFP gene giving band sizes corresponding with the predicted sizes of 0.763 kb and 3.97 kb. *Xba*I (single cutter at 1.412 kb) did not cut the plasmid (expected a linear band of 4.7 kb). *Bam*HI cuts once at 663 bp and thus, gave a linear band approximating the predicted value of 4.7 kb.

AII.2.3.2 Preparation of the Cx43 / pBi5 plasmid

Additional restriction digests were undertaken for further verification of the Cx43 / pBi5 plasmid, and to confirm the viability of the proposed cloning strategy. *Pst*I (a single cutter in Cx43 / pBi5, specifically pBi5) gave a linear band around the

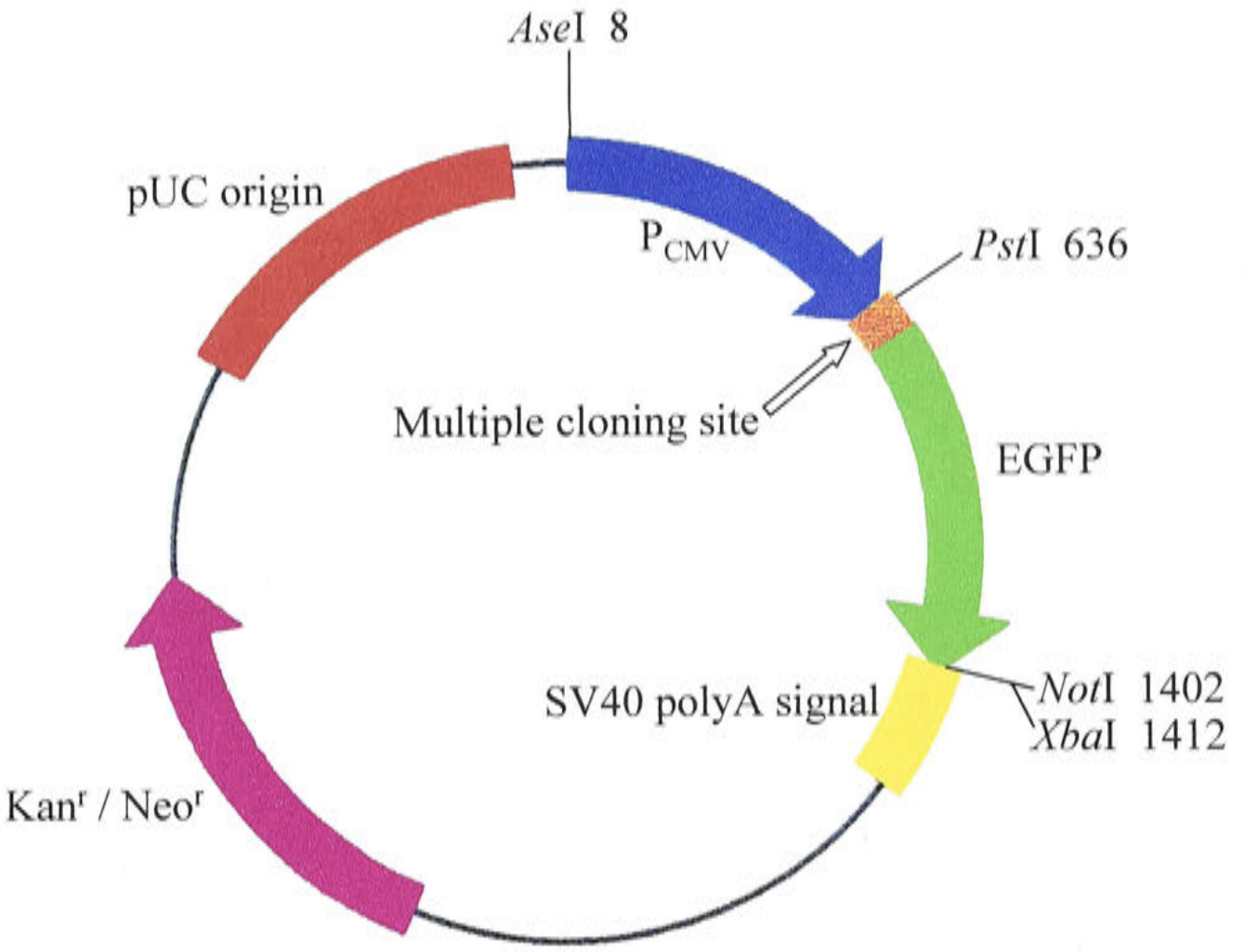

Figure AII.5 The pEGFP-NI plasmid

The pEGFP-NI plasmid (4.7 kb) is shown with selected restriction enzyme sites pertinent to this study. Kan^r / Neo^r refer to the kanamycin / neomycin resistance gene. The *Not*I site follows the EGFP stop codon. The pUC origin is the origin of replication for propagation in *E. coli*. P_{CMV} is the promoter.

Figure AII.6 Schematic diagram of the cloning of EGFP / Cx43 / pBi5

The cloning of the EGFP / Cx43 / pBi5 construct is shown in **(A)**, **(B)** and **(C)**. The luciferase gene was excised from Cx43 / pBi5 with *Pst*I and *Spe*I **(A)**, whilst the EGFP gene was excised from EGFP-NI with *Pst*I and *Not*I **(B)**. The *Pst*I / *Not*I / EGFP gene was then cloned into *Pst*I / *Spe*I / Cx43 / pBi5 **(C)**. The figures are not to scale.

(A)

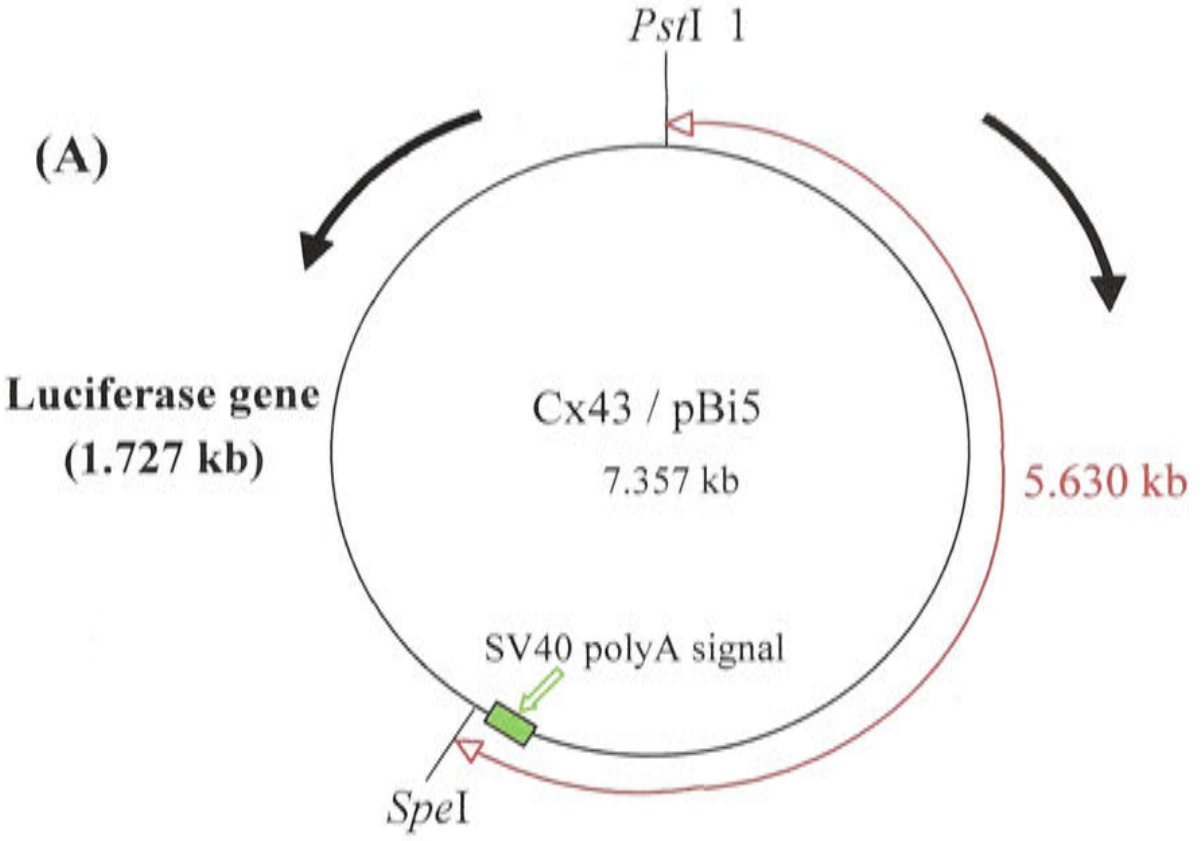
PstI 1
Luciferase gene
(1.727 kb)
Cx43 / pBi5
7.357 kb
5.630 kb
SV40 polyA signal
SpeI

(B)

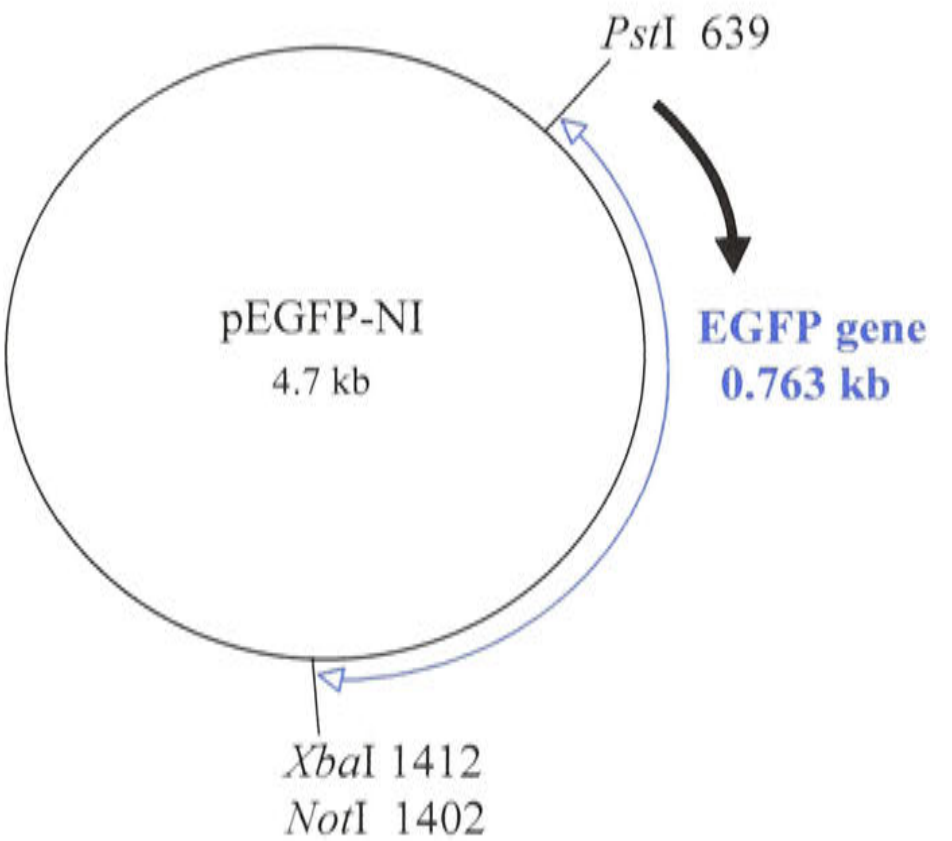
PstI 639
pEGFP-NI
4.7 kb
EGFP gene
0.763 kb
XbaI 1412
NotI 1402

(C)

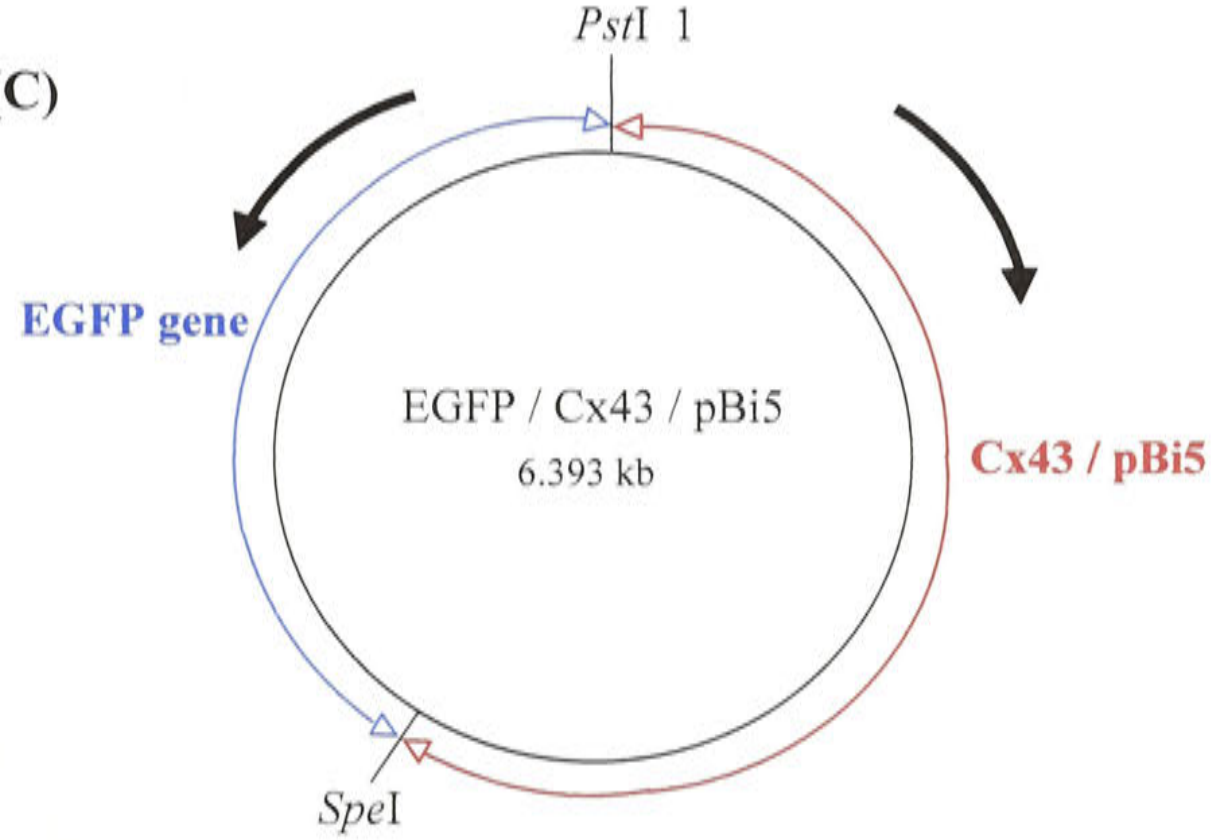
PstI 1
EGFP gene
EGFP / Cx43 / pBi5
6.393 kb
Cx43 / pBi5
SpeI

predicted band size of 7.4 kb, *Spe*I (a single cutter in Cx43 / pBi5, specifically pBi5) produced a linear band around the predicted band size of 7.4 kb, *Pst*I / *Spe*I (cuts twice in Cx43 / pBi5, specifically pBi5) removed the luciferase gene, producing bands which corresponded to the predicted bands of 5.673 kb and 1.727 kb, and a third band which was some remaining linear plasmid. *Ase*I (cuts pBi5 twice) generated two bands that were about the predicted sizes of 1.235 kb and 6.165 kb.

AII.2.3.3 Preparation of the Cx43 / pBi5 vector

The luciferase gene was excised from 2 µg of Cx43 / pBi5 in a four hour restriction digest using *Pst*I followed by *Spe*I with fresh NEBuffer, BSA and MilliQ water. The efficiency of the *Pst*I restriction was assessed by agarose gel electrophoresis prior to restriction with *Spe*I. The sample was re-checked before the fragment was isolated and purified.

AII.2.3.4 Preparation of the EGFP gene insert

*Pst*I and *Not*I excised the EGFP gene from the pEGFP-NI plasmid. After isolation, the insert was purified and assessed by agarose gel electrophoresis.

AII.2.3.5 Cloning of the insert into the vector

The *Pst*I / *Not*I / EGFP insert was ligated into the *Pst*I / *Spe*I / Cx43 / pBi5 vector with a 5:1 insert to vector ratio to maximize the cohesive (sticky-end) ligation (*Pst*I / *Pst*I). The non-ligated *Spe*I and *Not*I recessed ends were filled in with Klenow, and the mix subsequently purified. The efficacy of the sticky-end ligation was assessed by agarose gel electrophoresis before adding another 1 µl of T4 DNA Ligase to the ligation mix (for the *Spe*I / *Not*I ligation), which was then incubated as before. The sample was then transformed into TOP10F' cells with seventy-three colonies screened by cracking. The single colony containing an insert (designated C16) was purified and checked by agarose gel electrophoresis.

The EGFP / Cx43 / pBi5 clone was then verified by PCR screening using the pEGFPR and mCx435'R, and pEGFP and CxF primer combinations (Tables 2.2 and

AII.1), and by restriction enzyme digests. Two new primers were synthesized: CMVF (24 bp; T_m of 72°C; GCA GTA CAT CAA TGG GCG TGG ATA) and pEGFPR (22 bp; T_m of 70°C; GTC AGC TTG CCG TAG GTG GCA T). The new construct was evaluated in cell cultures of murine aortic smooth muscle cells and embryonic fibroblasts.

Primer Pair	Gene / Plasmid	Annealing temperature T_A (°C)	Extension Time (s) / (mins)	Predicted Fragment size (kb)	Chapter Reference
CxF pEGFPR	EGFP/Cx43/pBi5	65	2.20	1.0 kb	AII
mCx435'R pEGFPR	EGFP/Cx43/pBi5	65	2.20	none	AII

Table AII.1 PCR conditions for specific primer pairs

AII.2.4 Immunohistochemistry

Immunohistochemical studies were undertaken using antibodies against VP16 and Cx43 in order to detect the products of the individual constructs. The protocol was as described in Section 2.3.5 but with the following alterations. The primary antibodies used were either mouse anti-Cx43 (1:250; Chemicon or rabbit anti-Cx43, 1:250, Zymed) or rabbit anti-VP16 (1:50 or 1:100, Clontech) or combined). After primary incubation the cells were rinsed as before, and the pTetOn samples were incubated with fluorescein (FITC)-conjugated affinity-purified donkey anti-rabbit (1:40, Jackson Immuno-Research Laboratories Inc, PA, USA) whilst the Cx43 samples were incubated with biotinylated horse anti-mouse (1:500, Jackson Immuno-Research Laboratories Inc, PA, USA) or biotinylated donkey anti-rabbit mouse (1:500, Jackson Immuno-Research Laboratories Inc, PA, USA) at room temperature for one hour in a humidified chamber. The cells were rinsed again.

The single pTetOn transfections were mounted in buffered glycerol (glycerol: 0.5 M sodium carbonate buffer (2:1) containing 0.6% (w/v) phenylenediamine, whilst the double transfections and single Cx43 transfections were incubated in Texas Red conjugated to streptavidin (1:200, Amersham, USA) for 60 minutes at room temperature in a humidified chamber. The cells were washed and mounted in buffered glycerol.

Preparations were examined using a fluorescence microscope (BH2-RFL, Olympus) fitted with the appropriate filters for fluorescein (excitation filter IF-190 + EY455, dichroic mirror DM500, barrier filter 0-515) and Texas Red (excitation filter IF-545 + BG-36, dichroic mirror DM580, barrier filter R-610), and a confocal laser scanning microscope (Leica TCS 4D), and the number of VP16, Cx43 and EGFP labelled cells counted. Total cell counts and statistical analyses were performed as described in Section 2.3.5.

AII.3 Results

AII.3.1 Cloning of SM22α / pTetOn.

The SM22α / pTetOn clones (expected plasmid size was 7.255 kb) were verified by restriction analyses using *Spe*I / *Eco*RI, *Pvu*II, *Sac*I and *Xba*I (Figure AII.7). The *Spe*I / *Eco*RI double restriction digest (both enzymes cut in the multiple cloning site of pTetOn) removed the SM22α promoter, giving the predicted band sizes of 6.737 and 0.518 kb. *Pvu*II, a non-cutter in the restricted SM22α promoter, cuts pTetOn five times so five fragments were expected, although one was too small to visualize on a gel. *Sac*I, a single cutter in pTetOn and a non-cutter in the restricted SM22α promoter, gave a linear band of about 7.3 kb, whilst *Xba*I (cuts once in pTetOn and once in the restricted SM22α promoter fragment) generated two fragments of approximately 6.9 kb and 0.4 kb. Unfortunately, the print resolution in Figure AII.7 precluded clear visualization of all 0.4 kb bands.

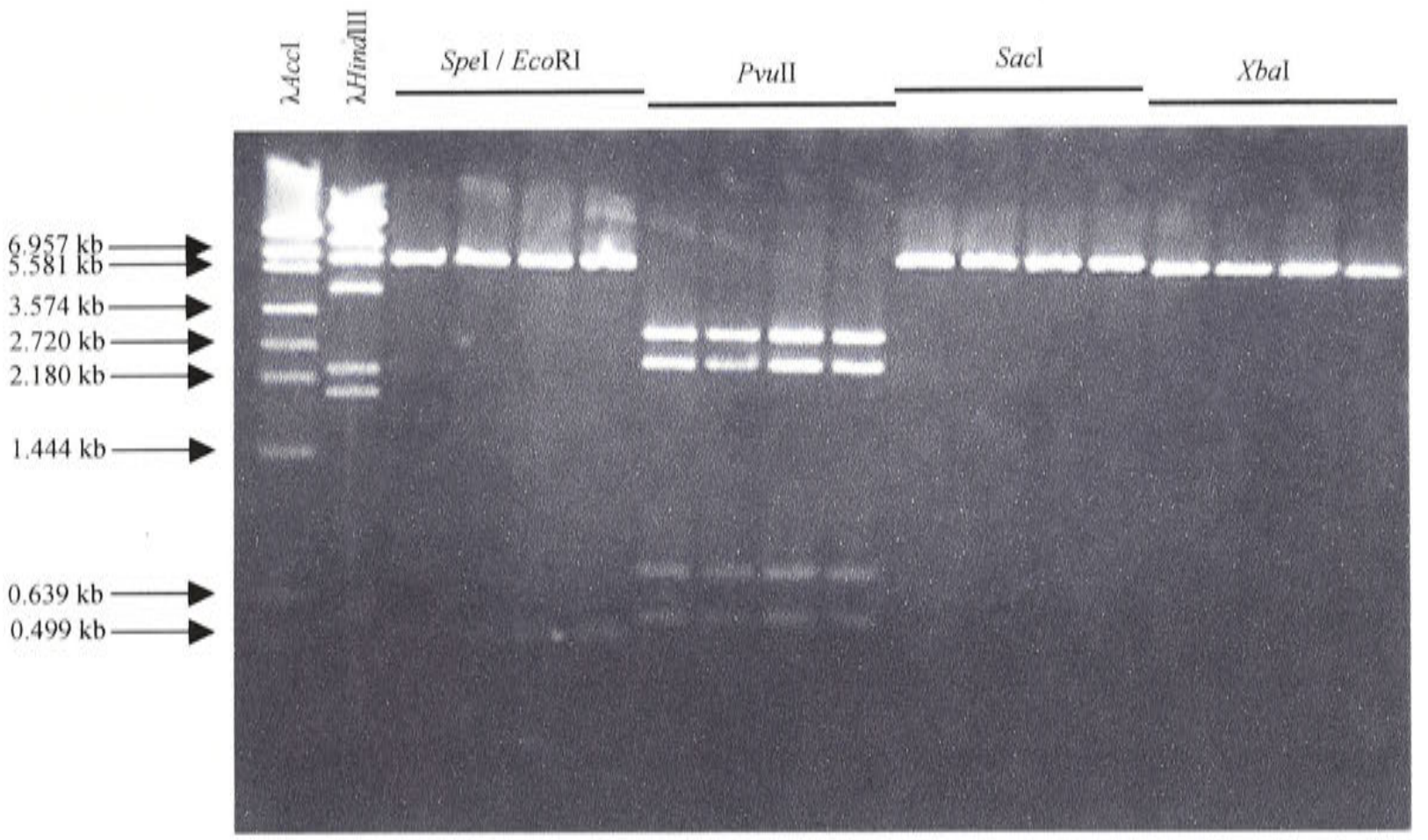

Figure AII.7 Verification of the SM22α / pTetOn colonies

The SM22α / pTetOn clones were verified using the *Spe*I / *Eco*RI, *Pvu*II, *Sac*I and *Xba*I restriction enzymes. The expected plasmid size was 7.255 kb. The *Spe*I / *Eco*RI double restriction digest removed the SM22α promoter, giving bands corresponding to the predicted band sizes of 6.737 and 0.518 kb (the latter just being visible on the gel). They also confirmed the forward orientation of the SM22α promoter in the pTetOn plasmid. *Pvu*II cut pTetOn five times so five fragments were expected, although one was too small to visualize on a gel. *Sac*I, gave a linear band of about 7.2 kb whilst *Xba*I generated two fragments of predicted lengths 6.9 kb and 0.4 kb. Unfortunately, the print resolution precluded visualization of the later band.

The clone giving the strongest bands on the gel (designated # 47) was chosen for bi-directional sequencing. Apart from the three base changes in the SM22α promoter already noted in Chapter 3, the sequence did not vary from the published sequence.

AII.3.2 Testing of the constructs in cell culture

AII.3.2.1 Electroporation experiments

Preliminary electroporative experiments were undertaken with the fibroblasts and the control plasmid pJWLacZ, followed by X-gal staining (Allen *et al.* 1988) to determine the number of transformed fibroblasts, and hence luciferase activity. As this method produced low numbers of positive healthy cells (data not shown), which meant that the luciferase activity could not be measured, it was decided to change to transfection using one of the commercial available reagents in order to introduce the DNA into the cultured fibroblasts and smooth muscle cells.

AII.3.2.2 Single and double transfections of the fibroblasts

(a) Single transfections

In the single transfections of the fibroblasts, without DNA, there were no positive CMV-pTetOn cells present and no intense staining of Cx43. Both CMV-pTetOn and Cx43 / pBi5 were expressed singly in the fibroblasts forty-eight (48) hours after transfection (Figures AII.8 and AII.9). Expression of Cx43 / pBi5 was attributed to either random integration of the plasmid or to residual basal activity of the TRE (leakiness).

The slight increase in CMV-pTetOn expression from 0.64 ± 0.05% to 0.85 ± 0.07% ($n = 5$) with the addition of doxycycline to the medium, was not statistically significant ($P > 0.05$). There was little change in Cx43 / pBi5 expression with doxycycline (0.338 ± 0.028%; $n = 5$) or without (0.339 ± 0.034%; $n = 5$). CMV-EGFP expression (4.24 ± 0.41%; $n = 5$) was significantly different to CMV-pTetOn expression

Figure AII.8 Single transfections of the fibroblasts.

Confocal images of two murine embryonic fibroblasts after transfection with CMV-pTetOn **(A)** and Cx43 / pBi5 **(B)**. Expression of both constructs was detected using immunohistochemistry. CMV-pTetOn expression was detected using a commercial antibody against VP16 (FITC; fluoresces green) **(A)** whilst Cx43 / pBi5 (Cx43) expression was detected using a commercial antibody against Cx43 (Texas Red; fluoresces red) **(B)**. Scale bar represents 500 μm.

(A)

(B)

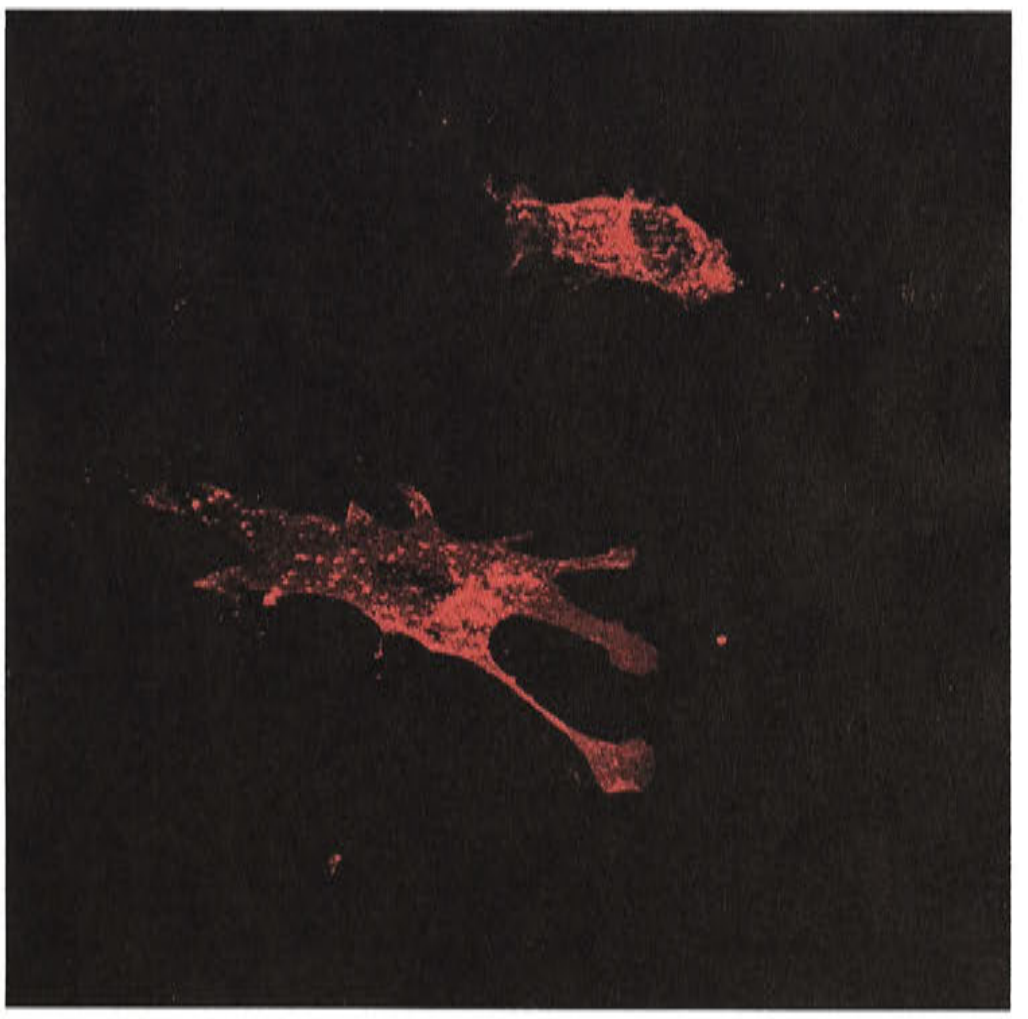

Figure AII.9 Graph of single transfections of fibroblasts.

Results from single transfections of the fibroblasts using the CMV-pTetOn and Cx43 / pBi5 plasmids, both with (+ dox) and without (-dox) the addition of doxycycline to the medium are shown. The pEGFP-NI (CMV-EGFP) plasmid was used as the control. Expression of the CMV-pTetOn and Cx43 / pBi5 constructs was detected by immunohistochemistry using commercial antibodies, whilst CMV-EGFP expression was detected by direct fluorescence microscopy. The number of labelled cells counted was expressed as a percentage of the total cell count for each slide (n = 5 experiments with duplicate wells per experiment). Each point represents the mean and standard error of the mean.

* Indicates significantly different from control

Labelled Cells (% Total)
0
1
2
3
4
5
Construct
CMV-TetOn
-dox
CMV-TetOn
+dox
Cx43/pBi5
-dox
Cx43/pBi5
+dox
CMV-EGFP
*

($P < 0.05$) and Cx43 / pBi5 expression ($P < 0.05$). As expected, there was no expression of SM22α / pTetOn in the fibroblasts.

Expression of CMV-pTetOn, Cx43 / pBi5 and CMV-EGFP following transfection was measured at 6 hourly intervals over four 48 hour periods ($n = 4$; Figure AII.10). For both CMV-pTetOn and CMV-EGFP, expression was observed in some cells at 6 hours. There was no significant change in the expression levels of CMV-pTetOn over the 48 hour period ($P > 0.05$), with expression being maximal at 12 hours. In contrast, induction of Cx43 / pBi5 was not recorded until 18 hours post-transfection. The slight variation in number of labelled cells from 18 to 24 to 48 hours was not statistically significant ($P > 0.05$), indicating that the maximum induction level of Cx43 / pBi5 had already occurred by 18 hours post-transfection. A similar time frame was obtained for double transfections using CMV-pTetOn and Cx43 / pBi5 + doxycycline ($n = 3$) where complete expression occurred 24 hours after the addition of the doxycycline to the medium.

(b) Double transfections

The results of the double transfections are presented in Figure AII.11 for cells 48 hours after transfection. In the CMV-pTetOn – doxycycline, CMV-pTetOn + doxycycline, Cx43 / pBi5 – doxycycline and Cx43 / pBi5 + doxycycline columns, the total number of cells stained with either VP16 or Cx43 were counted. As expected, doxycycline did not have an effect on CMV-pTetOn expression (1.30 ± 0.15% (without) and 1.23 ± 0.03% (with); $P > 0.05$; $n = 5$) but it did increase Cx43 expression (0.80 ± 0.07% ($n = 5$; without doxycycline) and 1.65 ± 0.10% ($n = 5$; with doxycycline)). The increase was statistically significant ($P < 0.05$).

When counts were made of cells expressing both CMV-pTetOn and Cx43 / pBi5, the numbers were reduced, suggesting that the CMV-pTetOn was inhibiting Cx43 expression, but there was still a doubling with doxycycline (0.18 ± 0.023% ($n = 5$;

Figure AII.10 Data on induction of construct expression.

Single transfections (n = 4) of the fibroblasts using CMV-pTetOn, Cx43 / pBi5 and CMV-EGFP were undertaken to determine the induction level for each. Data was collected at 6 hourly intervals over a 24 hour period and then at 48 hours. Expression of the CMV-pTetOn and Cx43 / pBi5 constructs was detected by immunohistochemistry using commercial antibodies, whilst CMV-EGFP expression was detected by direct fluorescence microscopy. The number of labelled cells counted was expressed as a percentage of the total cell count for each slide. Triplicate slides were made in each experiment for all time intervals. Each point represents the mean and standard error of the mean.

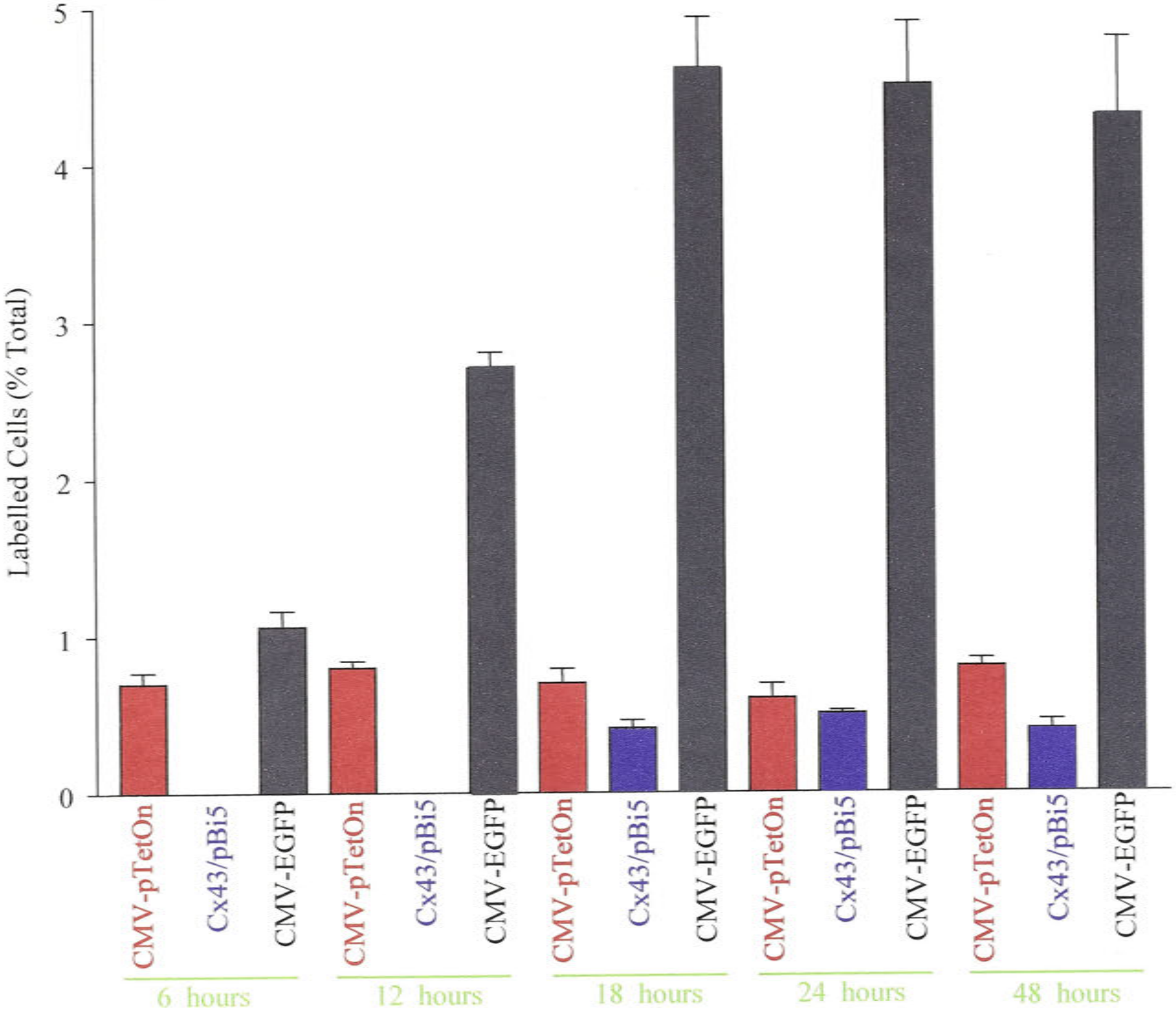
Labelled Cells (% Total)
0
1
2
3
4
5
CMV-pTetOn
Cx43/pBi5
CMV-EGFP
6 hours
12 hours
18 hours
24 hours
48 hours

Figure AII.11 Double transfections of fibroblasts.

Results from the double transfections of the fibroblasts are shown opposite. Transfections were performed using the CMV-pTetOn and Cx43 / pBi5 plasmids, both with (+ dox) and without (- dox) the addition of doxycycline to the medium. Expression of the constructs was detected by immunohistochemistry using commercial antibodies. CMV-pTetOn expression was detected using a commercial antibody against VP16 (FITC; fluoresces green), whilst Cx43 / pBi5 (Cx43) expression was detected using a commercial antibody against Cx43 (Texas Red; fluoresces red).

In the first four columns, only cells expressing either CMV-pTetOn or Cx43 / pBi5 were counted. The number of labelled cells expressing both CMV-pTetOn and Cx43 / pBi5 are shown in the last two columns. The number of labelled cells counted was expressed as a percentage of the total cell count for each slide ($n = 6$). Each point represents the mean and standard error of the mean.

* Indicates significantly different from control

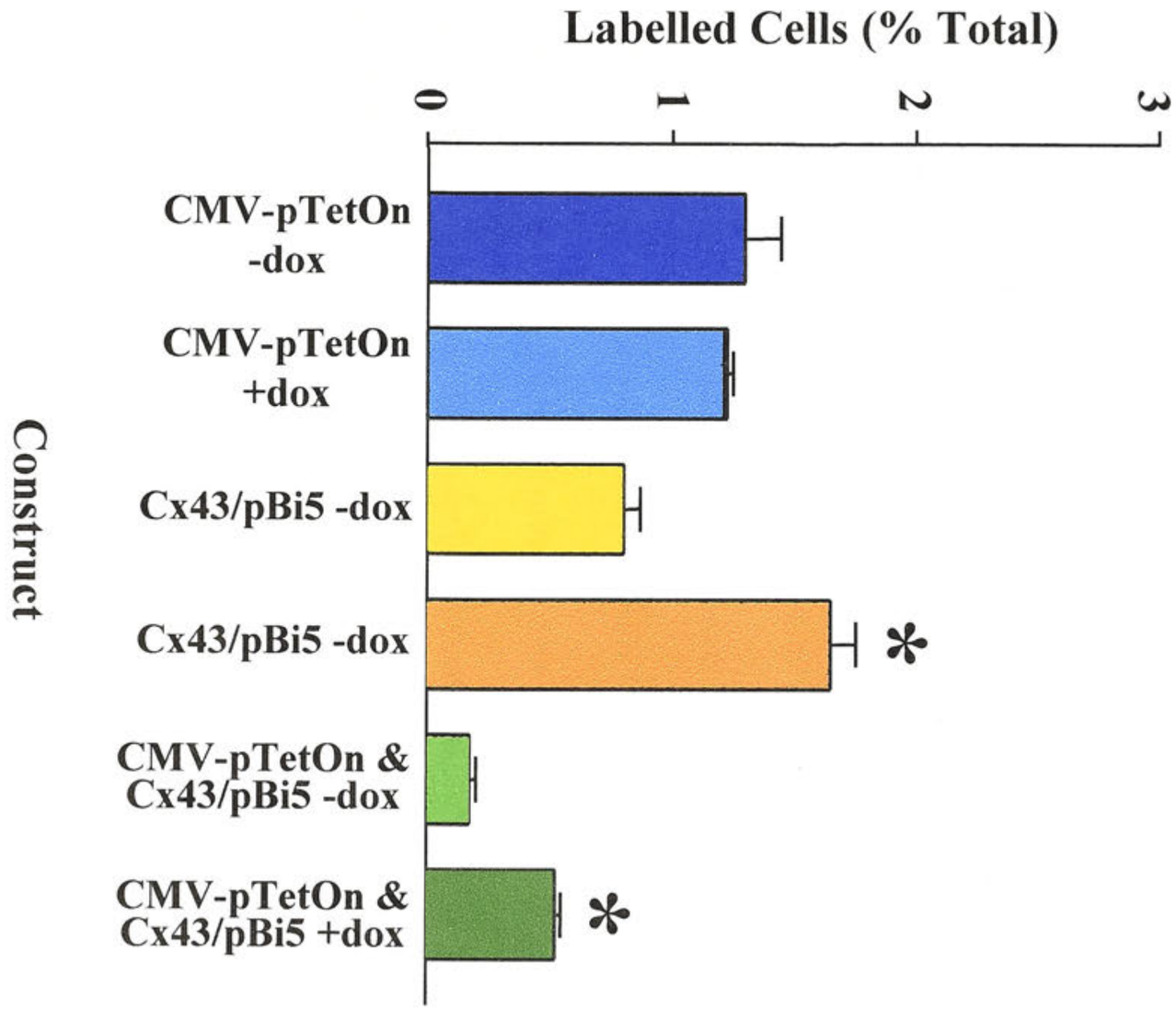
Labelled Cells (% Total)
0
1
2
3
CMV-pTetOn -dox
CMV-pTetOn +dox
Cx43/pBi5 -dox
Cx43/pBi5 -dox
CMV-pTetOn & Cx43/pBi5 -dox
CMV-pTetOn & Cx43/pBi5 +dox
*
*
Construct

without doxycycline) to 0.53 ± 0.03% (n = 5; with doxycycline)). The increase was significant ($P < 0.05$). The expression of the constructs in different parts of the same cell is shown in Figures AII.12 and AII.13.

AII.3.2.3 Single and double transfections of the smooth muscle cells

In the single transfections of the smooth muscle cells, without DNA, there were no CMV-pTetOn cells present and no intense expression of Cx43. Results from the single and double transfections are shown in Figure AII.14. All data was obtained by counting Cx43 expressing cells. In the single transfections (Cx43 / pBi5 ± doxycycline) there was no significant difference between Cx43 / pBi5 – doxycycline (1.12 ± 0.61%; n = 4) and Cx43 / pBi5 + doxycycline (1.02 ± 0.42%; n = 4) ($P > 0.05$). However, in the double transfections, doxycycline increased Cx43 expression both with CMV-pTetOn & Cx43 / pBi5 (0.93 ± 0.17% (without; n = 4) to 2.57 ± 0.81% (with; n = 4; $P > 0.05$) and SM22 / pTetOn & Cx43 / pBi5 (0.13 ± 0.02% (without; n = 4) to 0.63 ± 0.015% (with; n = 4; $P < 0.05$). EGFP expression was significantly different (4.68 ± 0.42%; n = 4; $P < 0.05$) when compared to all groups. Figure AII.15 shows the distribution of the constructs (double transfections) within the same smooth muscle cells.

AII.3.2.4 Cloning of EGFP / Cx43 / pBi5

As the EGFP expression data from the *in vitro* testing of the DNA constructs had revealed that the immunohistochemical detection was not as sensitive as the direct detection of EGFP, the luciferase gene in the Cx43 / pBi5 construct was replaced with the EGFP gene from pEGFP-NI (4.733 kb; Figures AII.6 and AII.7).

Figure AII.12 Confocal images of doubly transfected fibroblasts

Fibroblasts were transfected with both CMV-pTetOn and Cx43 / pBi5 using Lipofectamine Plus, and with the addition of doxycycline to the medium. Expression of each construct was detected by immunohistochemistry using commercial antibodies against VP16 (FITC; fluoresces green) and Cx43 (Texas Red; fluoresces red). The expression of the constructs in different parts of the same cell as seen using the confocal microscope is shown **(A)** and **(B)**. Scale bar represents 500 μm.

(A)

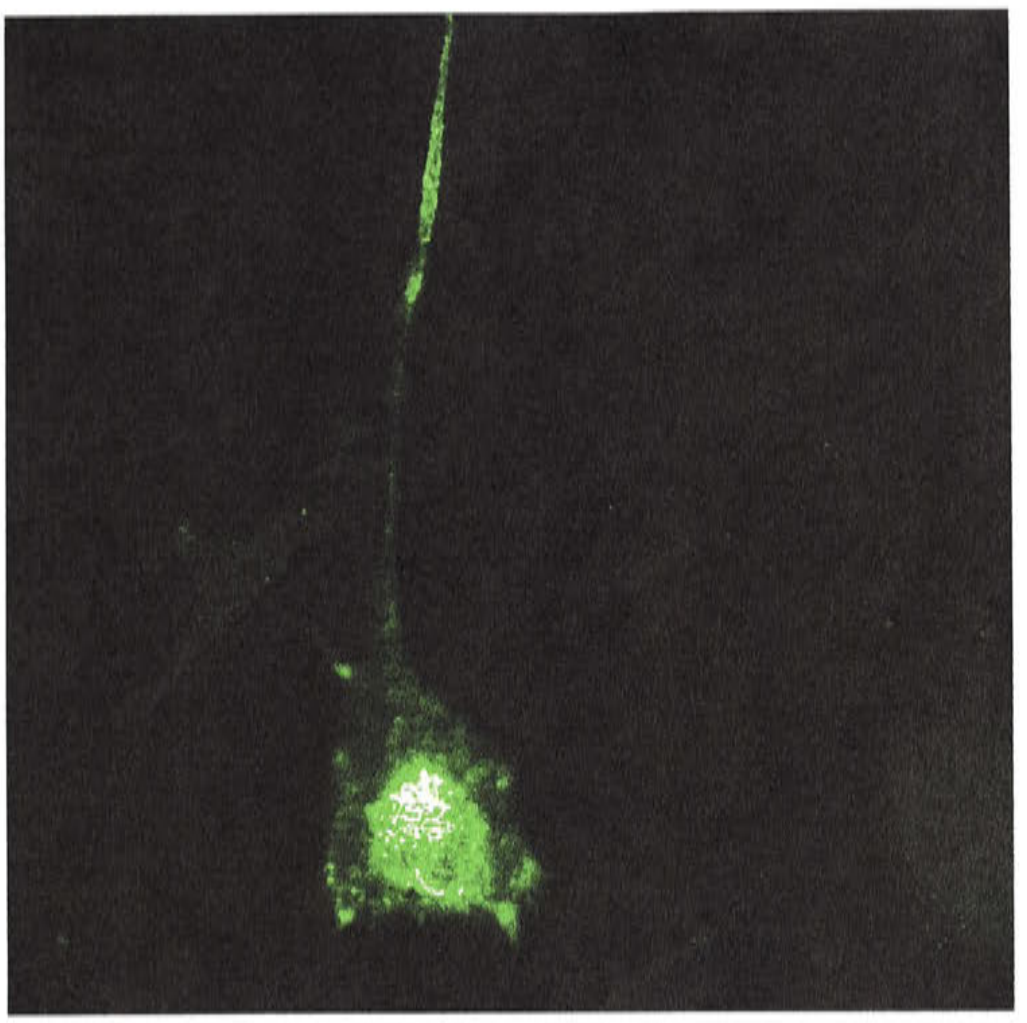

(B)

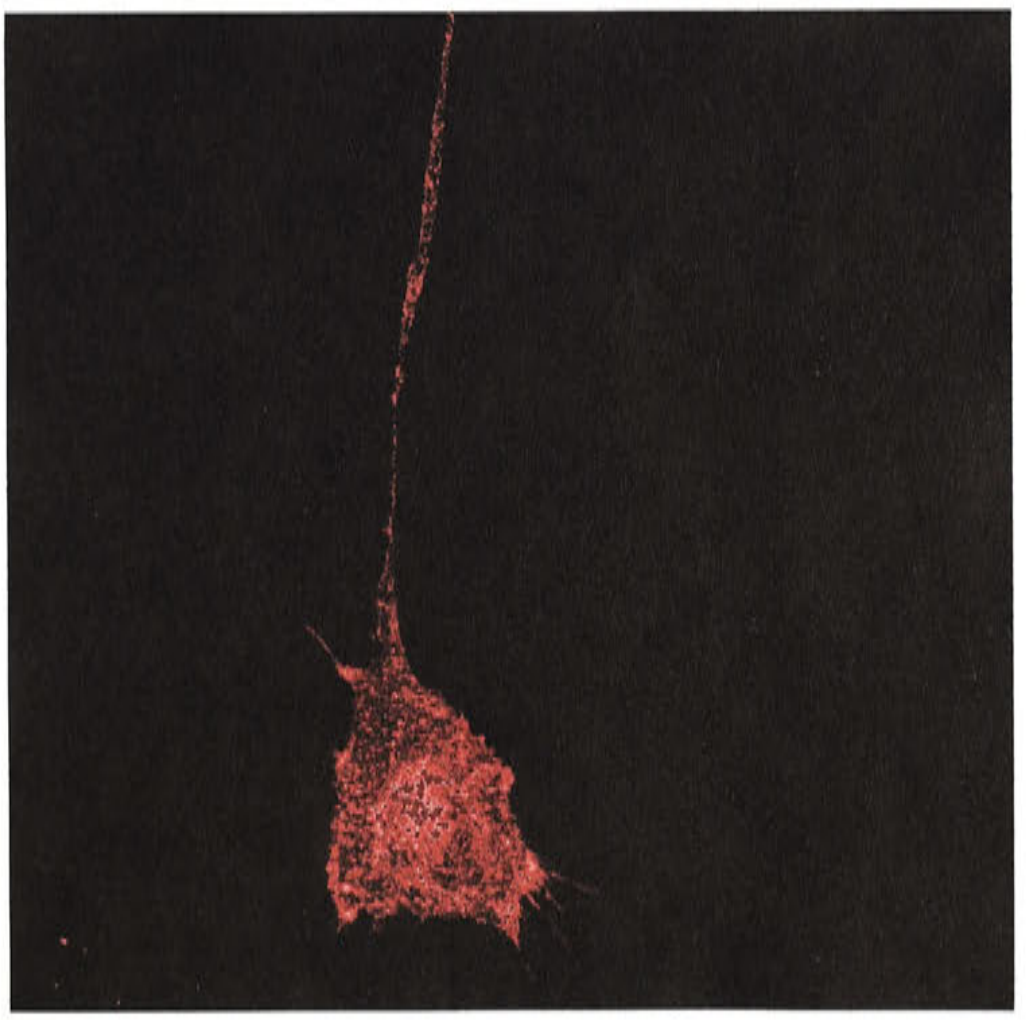

Figure AII.13 Confocal images of doubly transfected fibroblasts

Superimposed confocal images of some transfected fibroblasts are shown at high power magnification. Immunohistochemistry to detect expression of each construct was undertaken using commercial antibodies, as previously mentioned. All images saved from the confocal microscope were imported into Photoshop, where images of the same cell were superimposed on each other. Cx43 shown in red and VP16 shown in green. The expression of the constructs in different parts of the same cell is shown. Scale bar represents 500 μm.

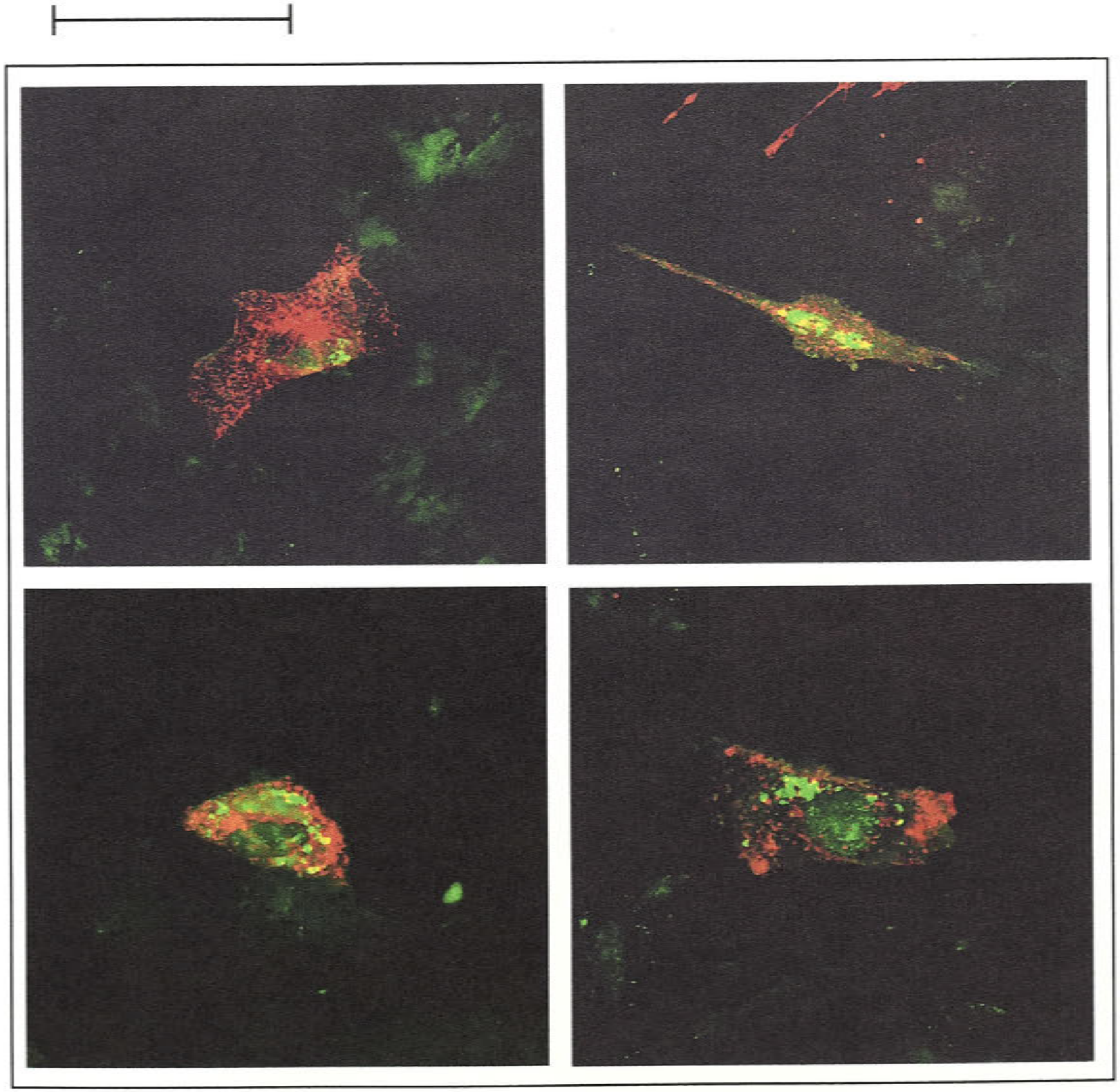

Figure AII.14 Graph of single and double transfections of murine smooth muscle cells

Single and double transfections of the murine smooth muscle cells were undertaken using the CMV-pTetOn, SM22α/ pTetOn, Cx43 / pBi5 and CMV-EGFP plasmids, both with (+ dox) and without (- dox) the addition of doxycycline to the medium. Expression was detected using commercial antibodies against VP16 (FITC) and Cx43 / pBi5 (Texas Red), with EGFP expression detected by direct fluorescence microscopy.

Single transfections are in columns one and two on the graph, and column seven. Columns three to six contain data from the double transfections. The number of labelled cells counted was expressed as a percentage of the total cell count for each slide ($n = 4$). Each point represents the mean and standard error of the mean.

* Indicates significantly different from control.

Labelled Cells (% Total)
0
1
2
3
4
5
6
Construct
single
double
Cx43/pBi5
-dox
Cx43/pBi5
+dox
CMV-pTetOn &
Cx43/pBi5-dox
CMV-pTetOn &
Cx43/pBi5+dox
SM22α/pTetOn &
Cx43/pBi5-dox
SM22α/pTetOn &
Cx43/pBi5+dox
*
CMV-EGFP
*

Figure AII.15 Confocal images of transfected smooth muscle cells

Superimposed confocal images of two transfected smooth muscle cells transfected with both CMV-pTetOn and Cx43 / pBi5, are shown at high power magnification **(A)** and **(B)**. Immunohistochemistry, using the previously mentioned commercial antibodies, detected expression of the two constructs within the same cells. VP16 shown in green and Cx43 shown in red. All images saved from the confocal microscope were imported into Photoshop, where images of the same cell were superimposed on each other. Scale bar represents 500 μm.

(A)

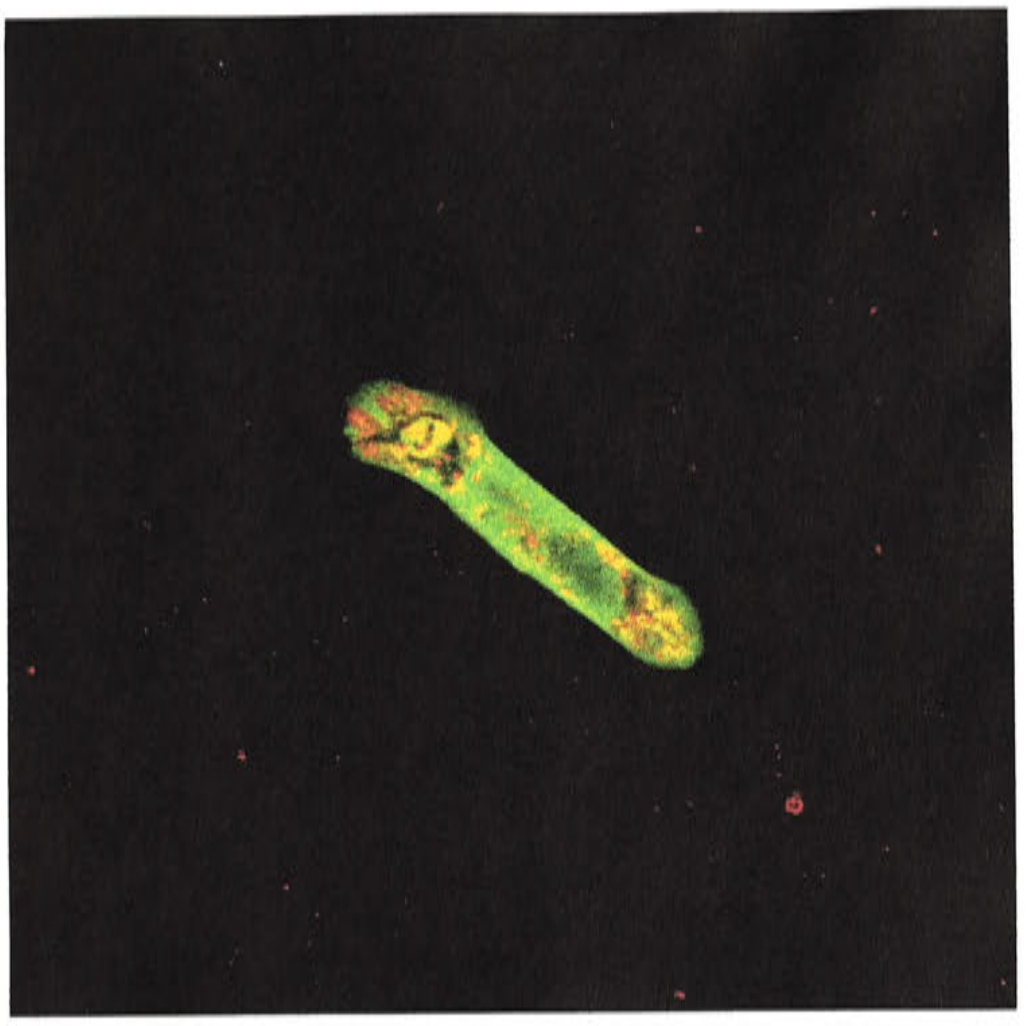

(B)

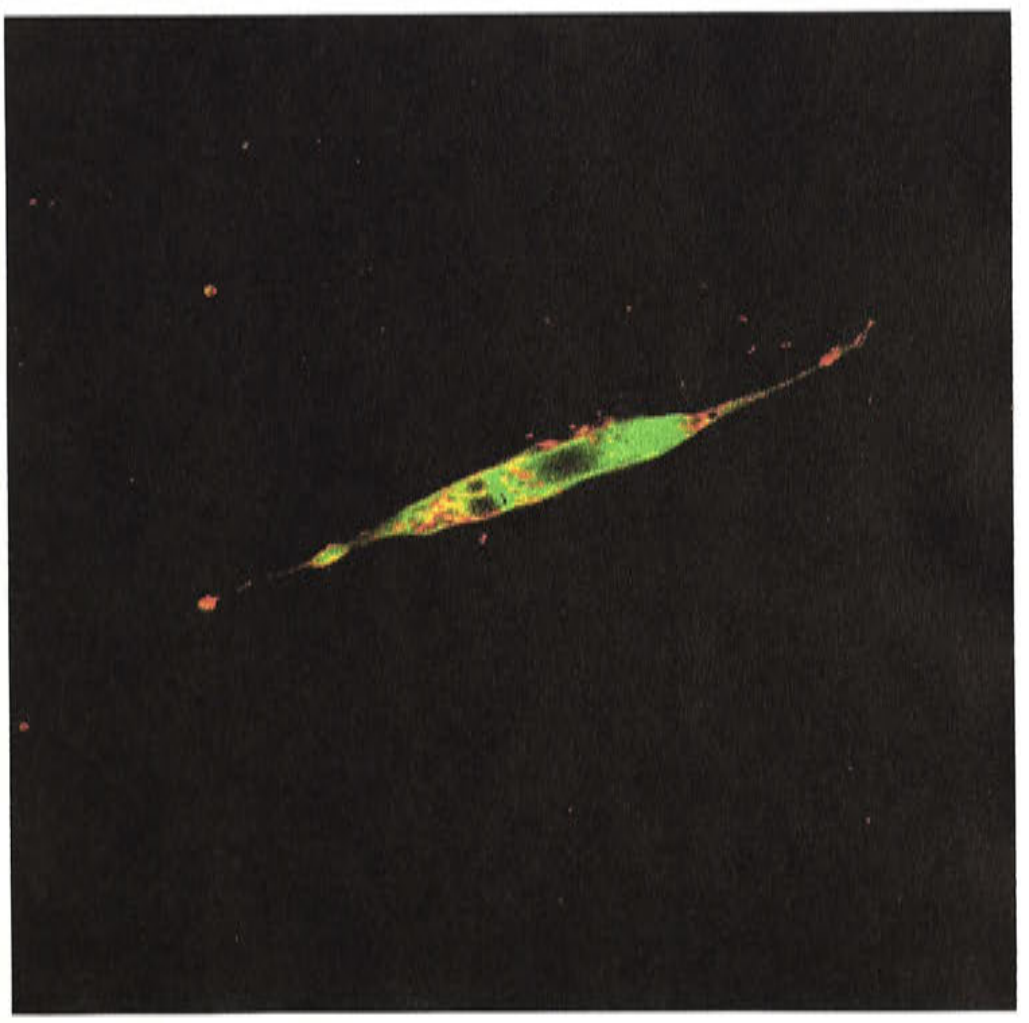

AII.3.3 Cloning of EGFP / Cx43 / pBi5

(a) Restriction analyses

The potential positive EGFP / Cx43 / pBi5 clone (C16; plasmid size 6.393 kb c.f. 7.357 kb for Cx43 / pBi5) was verified by restriction analyses using the *Xba*I, *Ase*I, *Pvu*I, *Xmn*I and *Age*I enzymes (Figure AII.16A).

*Xba*I, a double enzyme cutter in pBi5 gave one band which, due to the increased bandwidth and intensity, was assumed to be a doublet and thus did not correspond with the predicted band sizes of 3.671 kb and 2.722 kb. In view of the other results, it was judged not to have worked. *Pvu*I, a non-cutter in the EGFP and Cx43 genes, and a single cutter in pBi5, only partially cut the construct, indicating that more enzyme was needed to achieve the desired linear band. *Ase*I, a non-cutter in both the EGFP and Cx43 genes, gave two bands which corresponded to the predicted fragment sizes of 5.158 kb and 1.235 kb. *Xmn*I, which cuts once in both Cx43 and pBi5 but not in the EGFP gene, also produced two bands which were around the predicted band sizes of 3.306 kb and 3.087 kb. *Age*I, a single cutter in EGFP and a non-cutter in the Cx43 gene and pBi5 plasmid, generated a linear band which approximated the calculated size of 6.393 kb.

Correct insert orientation in the vector was confirmed by a *Bam*HI restriction (Figure AII.16B). *Bam*HI cuts EGFP once and pBi5 twice, producing three fragments that corresponded to the predicted band sizes of 5.028 kb, 0.692 kb and 0.673 kb.

(b) PCR screening

The clone was screened by PCR using the pEGFPR and mCx435'R primers (amplified a band around the predicted 1 kb), and the pEGFPR and CxF primers (no band was amplified) (Figure AII.17). Thus, in this clone, the EGFP insert had ligated into the Cx43 / pBi5 plasmid in the correct orientation.

AII.3.4 Testing of the construct in cell culture

The new construct was evaluated in combination with CMV-pTetOn, SM22α / pTetOn and EGFP-NI in murine fibroblasts and smooth muscle cells using

Figure AII.16 Restriction enzyme verification of pEGFP-NI and Cx43 / pBi5

Restriction enzyme verification of pEGFP-NI is shown in **(A)**. The single cutters *Not*I and *Pst*I each gave a linear band of around the predicted band size of 4.7 kb. The *Not*I / *Pst*I restriction removed the EGFP gene, giving bands which corresponded to the predicted band sizes of 0.763 kb and 3.937 kb (Lane 5). *Xba*I did not cut the plasmid (expected a linear band of 4.7 kb if it had) and *Bam*HI gave a linear band around 4.7 kb.

Cx43 / pBi5 was again verified using restriction enzyme digests **(B)**. The single cutters *Pst*I and *Spe*I produced linear bands which corresponded with the predicted band size of 7.4. The *Pst*I / *Spe*I restriction produced two fragments around the calculated fragment sizes of 5.673 kb and 1.727 kb (Lane 6) and also some linear plasmid. Lastly, *Ase*I gave two bands of approximately 1.235 kb and 6.122 kb.

(A)

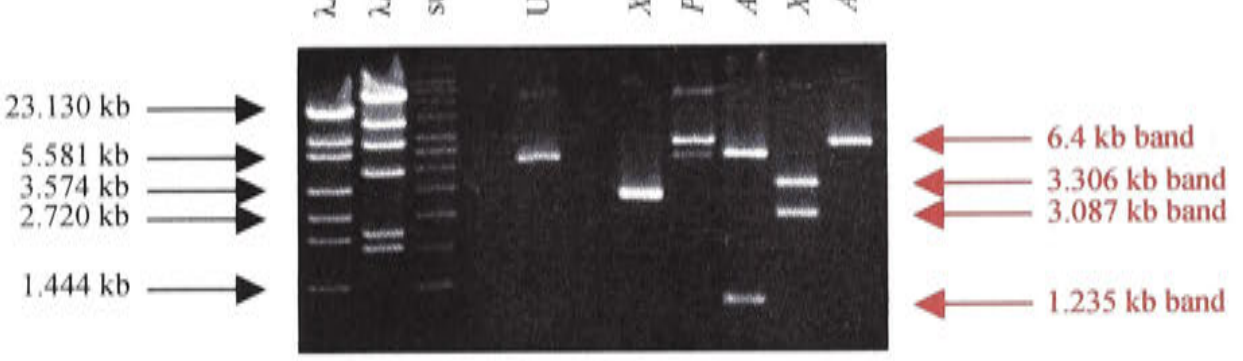
λAccI
λHindIII
supercoiled ladder
Uncut EGFP/Cx43/pBi5
XbaI
PvuI
AseI
XmnI
AgeI
23.130 kb
5.581 kb
3.574 kb
2.720 kb
1.444 kb
6.4 kb band
3.306 kb band
3.087 kb band
1.235 kb band

(B)

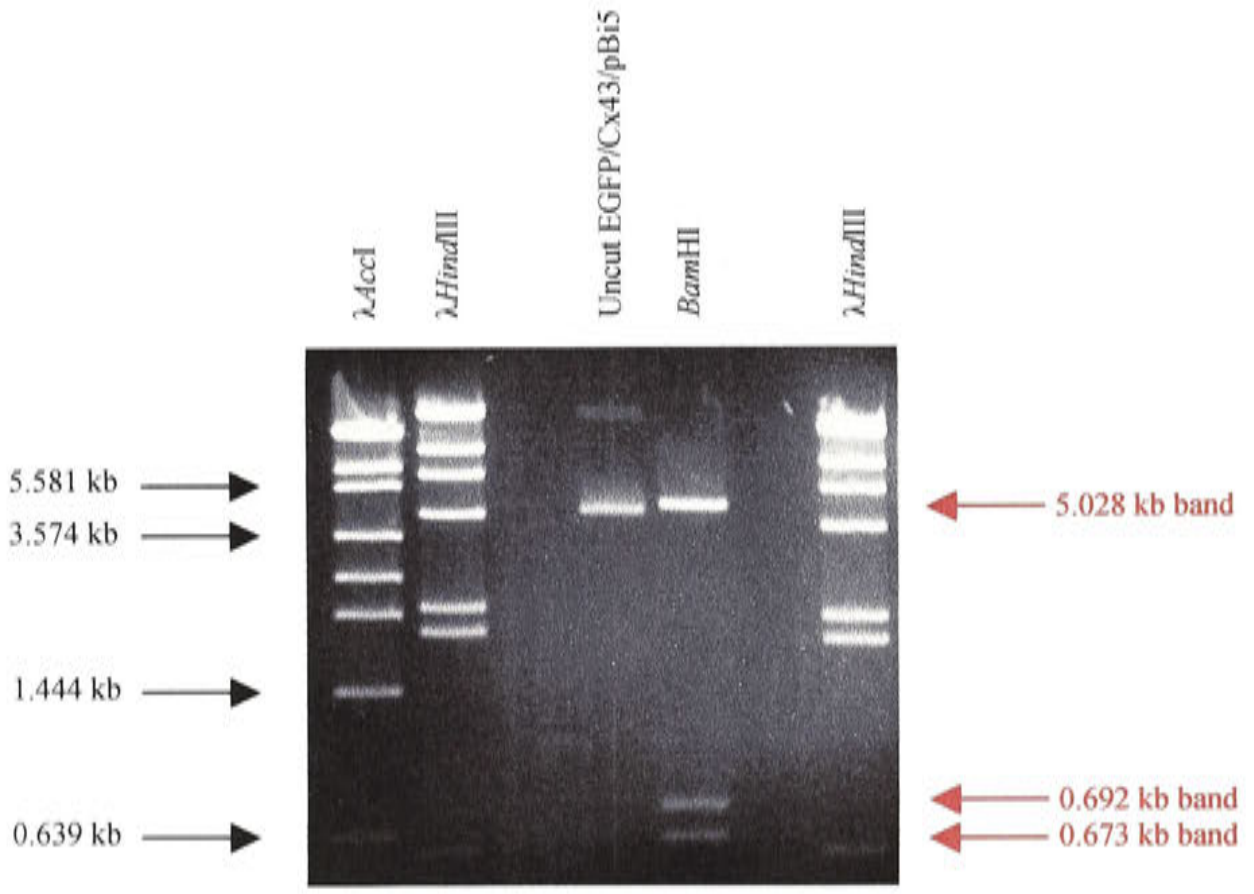
λAccI
λHindIII
Uncut EGFP/Cx43/pBi5
BamHI
λHindIII
5.581 kb
3.574 kb
1.444 kb
0.639 kb
5.028 kb band
0.692 kb band
0.673 kb band

Figure AII.17 PCR verification of EGFP / Cx43 / pBi5 clone

PCR screening of the EGFP / Cx43 / pBi5 clone using the pEGFPR and mCx435'R, and pEGFPR and CnxF primers **(A)**. The amplified band (pEGFPR and mCx435'R; Lane 1) showed that in this clone, the EGFP insert had ligated into Cx43 / pBi5 in the correct orientation (expected band size of about 1 kb). The pEGFPR and CnxF PCR did not amplify any fragment, as expected (Lane 2). The water control was in Lane 3.

A schematic diagram of the pEGFPR and mCx435'R PCR is shown in **(B)**. Here, the Cx43 gene and EGFP gene are marked, together with appropriate restriction enzyme sites for reference. The mCx435'R primer (ψ) direction is indicated by an open arrow, as is the pEGFPR primer (χ) direction. The diagram is not to scale.

(A)

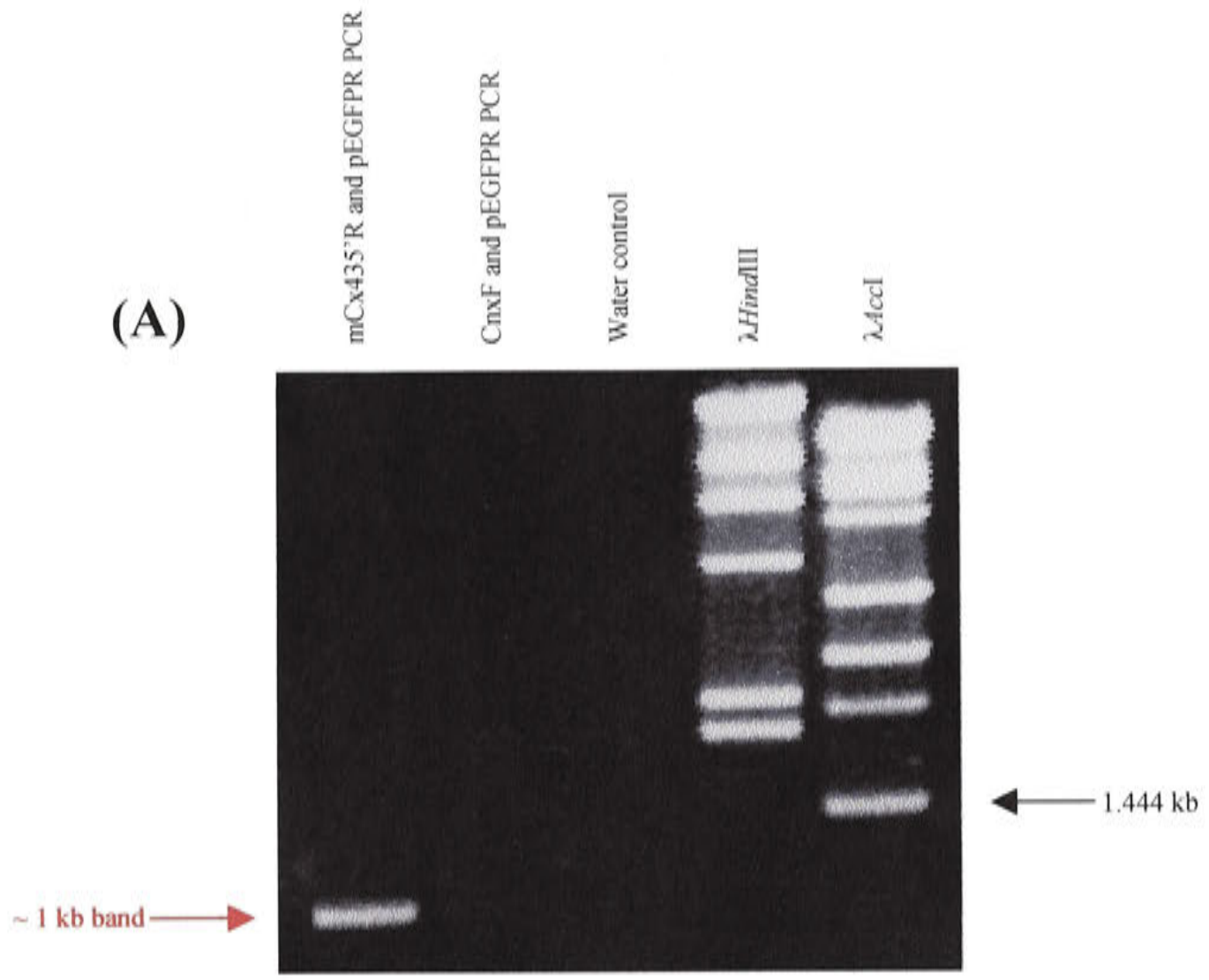
mCx43'R and pEGFPR PCR
CnxF and pEGFPR PCR
Water control
λHindIII
λAccI
~ 1 kb band
1.444 kb

(B)

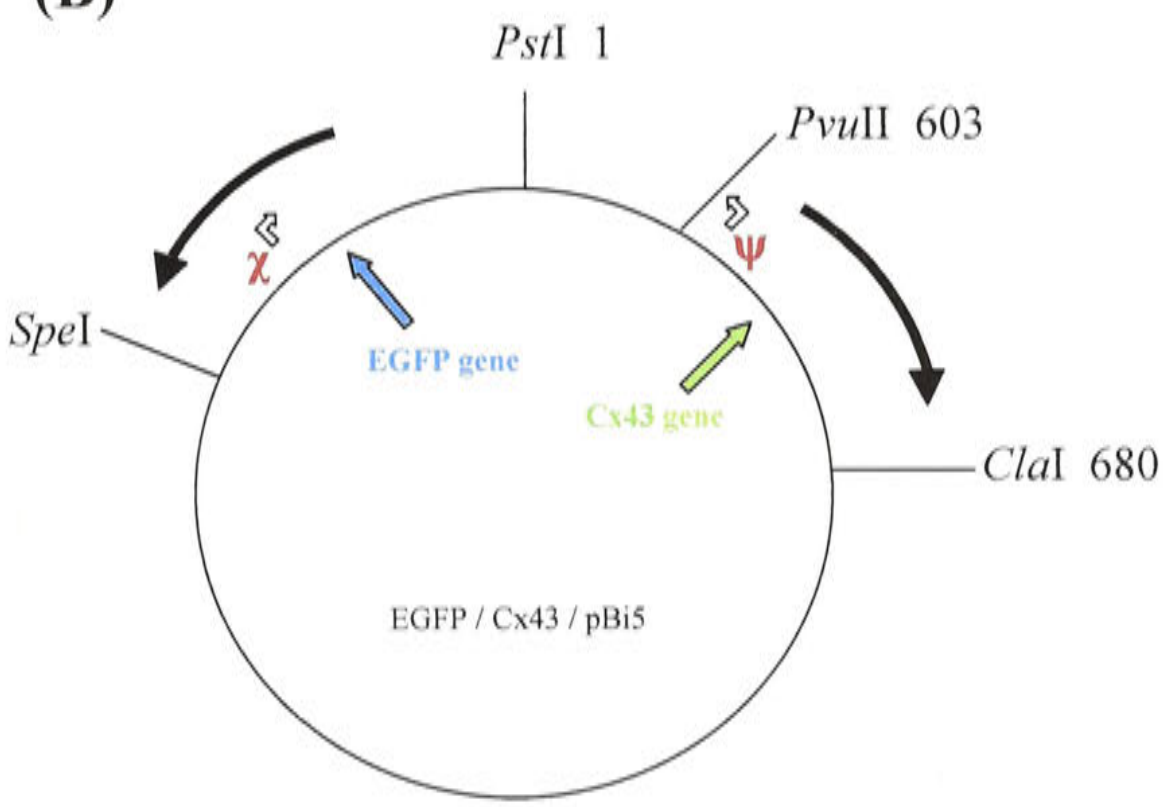
PstI 1
PvuII 603
SpeI
ClaI 680
χ
ψ
EGFP gene
Cx43 gene
EGFP / Cx43 / pBi5

Lipofectamine Plus, both with and without the addition of doxycycline to the medium. In the fibroblasts, both doxycycline free serum and foetal calf serum were used, whilst only the doxycycline free serum was used in the smooth muscle cell transfections. Expression was detected by direct fluorescence microscopy.

AII.3.4.1 Single and double transfections of the fibroblasts

(a) Single transfections

Results from the single transfections of the fibroblasts are presented in Figure AII.18. When the expression level for EGFP / Cx43 / pBi5 without doxycycline (0.22 ± 0.06%; $n = 5$) was compared to that obtained for Cx43 / pBi5 without doxycycline (0.34 ± 0.07%; $n = 5$), it was not significantly different ($P > 0.05$). Similarly with EGFP / Cx43 / pBi5 with doxycycline (0.23 ± 0.07%; $n = 5$) and Cx43 / pBi5 with doxycycline (0.34 ± 0.06%; $n = 5$) ($P > 0.05$). There was no significant difference between the expression levels for EGFP / Cx43 / pBi5 without doxycycline and EGFP / Cx43 / pBi5 with doxycycline ($n = 5$; $P > 0.05$).

The differences between the modified Cx43 / pBi5 construct with foetal calf serum (FCS) compared to doxycycline free serum (DFS), with and without the addition of doxycycline to the medium, were not significant ($P > 0.05$; $n = 5$ and $P > 0.05$; $n = 5$, respectively). In both the DFS and FCS groups, the addition of doxycycline to the medium had no effect on Cx43 expression ($P > 0.05$), as expected.

The control CMV-EGFP plasmid did not have a significantly different expression level ($P > 0.05$) compared to the earlier experiments (5.74 ± 1.26%; $n = 5$, and 4.24 ± 0.41%; $n = 5$, respectively). CMV-EGFP expression was significantly different to all EGFP / Cx43 / pBi5 transfection groups ($P < 0.05$).

Figure AII.18 Single transfections of fibroblasts using the modified construct.

Single transfections of the fibroblasts using the EGFP / Cx43 / pBi5 plasmid, both with (+ dox) and without (-dox) the addition of doxycycline to the medium containing either the doxycycline free serum (DFS) or foetal calf serum (FCS). The CMV-EGFP plasmid was used as the control. Expression of EGFP / Cx43 / pBi5 and CMV-EGFP was detected using direct fluorescence microscopy. Results are expressed as the number of labelled cells counted as a percentage of the total cell count for each slide. Each point represents the mean and standard error of the mean.

* Indicates significantly different from control

Labelled Cells (% Total)
0
1
2
3
4
5
6
7
Construct
EGFP/Cx43/pBi5
-dox +DFS
EGFP/Cx43/pBi5
+dox +DFS
EGFP/Cx43/pBi5
-dox +FCS
EGFP/Cx43/pBi5
+dox +FCS
CMV-EGFP
*

(b) Double transfections

Data from the double transfections of the fibroblasts with CMV-pTetOn and EGFP / Cx43 / pBi5 with (+ dox) and without (- dox) the addition of doxycycline to the medium containing either doxycycline free serum (DFS) or foetal calf serum (FCS) is presented in Figure AII.19. A comparison between DFS and FCS in the medium did not reveal any significant difference between the different groups ($P > 0.05$). The data also show that the addition of doxycycline to either medium induced expression of the EGFP / Cx43 / pBi5 construct; a difference that when compared to the doxycycline-free state was significant ($P < 0.05$). For DFS this was 4.60 ± 0.63% (FCS 4.74 ± 0.56%); $n = 4$, and 1.62 ± 0.09% (FCS 1.65 ± 0.16%); $n = 4$, respectively. Compared to earlier experiments, this represented a significant increase at the 5% level. The control CMV-EGFP plasmid again showed a consistent expression level when compared to previous transfections.

AII.3.4.2 Single and double transfections of the smooth muscle cells

All single and double transfections were undertaken in medium containing doxycycline free serum to abrogate the possibility of residual doxycycline in the foetal calf serum. CMV-EGFP, EGFP / Cx43 / pBi5, CMV-pTetOn and SM22α / pTetOn were transfected into the murine aortic smooth muscle cells using Lipofectamine Plus (Figure AII.20).

In the single transfections, except for CMV-EGFP, both EGFP / Cx43 / pBi5 – doxycycline and EGFP / Cx43 / pBi5 + doxycycline had low expression levels (0.26 ± 0.07%; $n = 4$, and 0.18 ± 0.04%; $n = 4$, respectively) especially when compared to the previous single transfections with Cx43 / pBi5 (av: 1.0 ± 0.05%; $n = 4$). This was not statistically significant ($P > 0.05$). The CMV-EGFP expression level was significantly different to both EGFP / Cx43 / pBi5 ± doxycycline ($P < 0.05$).

Figure AII.19 Double transfections of fibroblasts using the modified construct.

Double transfections of the fibroblasts using the EGFP / Cx43 / pBi5 and CMV-pTetOn plasmids, both with (+ dox) and without (-dox) the addition of doxycycline to the medium containing either the doxycycline free serum (DFS) or foetal calf serum are shown opposite. The CMV-EGFP plasmid was used as the control. Expression of EGFP / Cx43 / pBi5 and CMV-EGFP was detected using direct fluorescence microscopy. Results are expressed as the number of labelled cells counted as a percentage of the total cell count for each slide. Each point represents the mean and standard error of the mean.

* Indicates significantly different from control

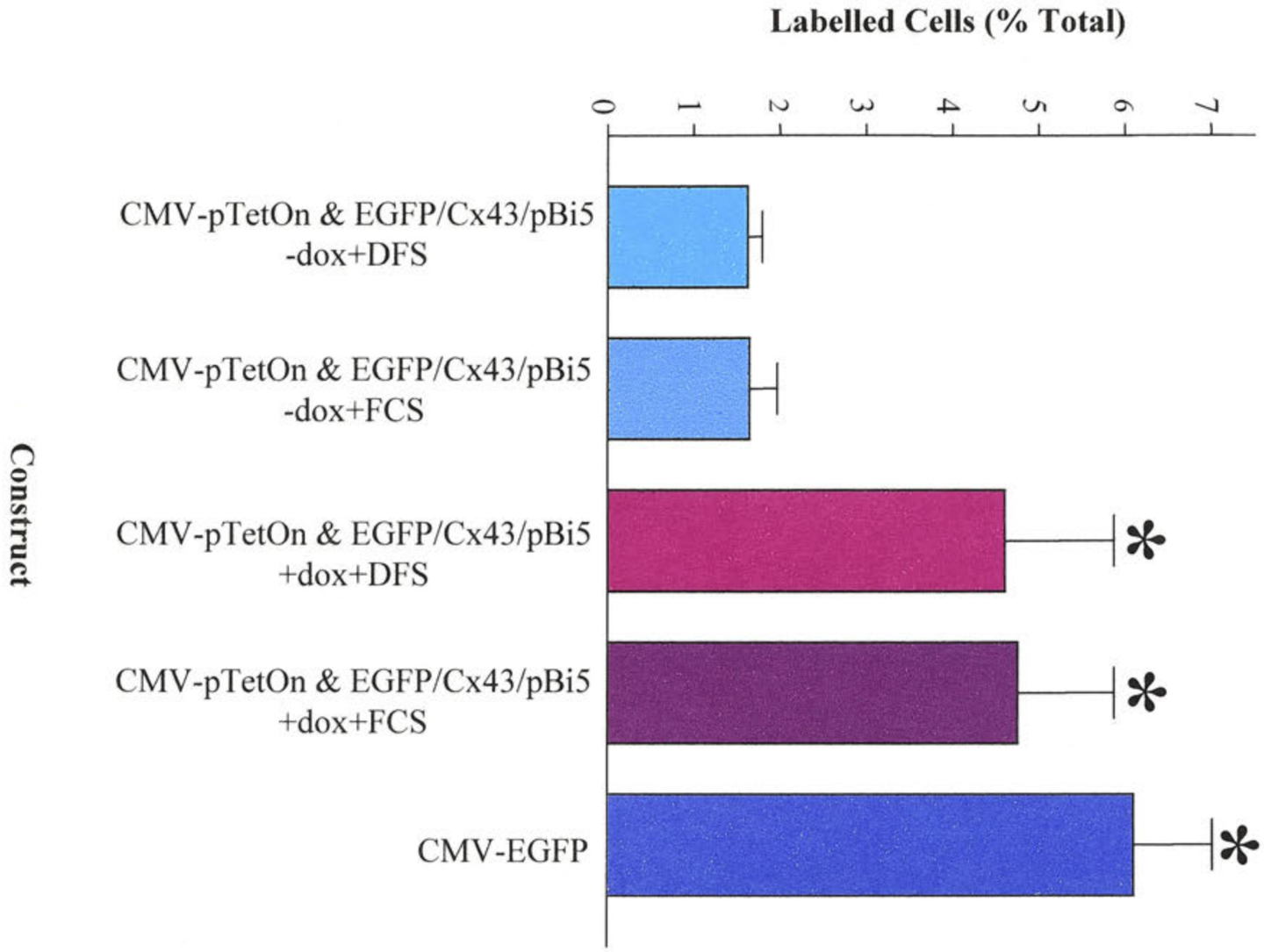
Labelled Cells (% Total)
0
1
2
3
4
5
6
7
Construct
CMV-pTetOn & EGFP/Cx43/pBi5
-dox+DFS
CMV-pTetOn & EGFP/Cx43/pBi5
-dox+FCS
CMV-pTetOn & EGFP/Cx43/pBi5
+dox+DFS
CMV-pTetOn & EGFP/Cx43/pBi5
+dox+FCS
CMV-EGFP
*
*
*

Figure AII.20 Single and double transfections of smooth muscle cells using the modified construct.

Single and double transfections of the smooth muscle cells using the EGFP / Cx43 / pBi5 plasmid with (+ dox) and without (-dox) the addition of doxycycline to the medium containing doxycycline free serum. The CMV-EGFP plasmid was used as the control. Expression of EGFP / Cx43 / pBi5 and CMV-EGFP was detected using direct fluorescence microscopy. The number of labelled cells counted is expressed as a percentage of the total cell count for each slide. Each point represents the mean and standard error of the mean.

* Indicates significantly different from control

Labelled Cells (% Total)
0.0
0.5
1.0
1.5
2.0
2.5
3.0
3.5
4.0
4.5
5.0
5.5
6.0
6.5
7.0
7.5
8.0
8.5
9.0
9.5
10.0
Construct
single
double
EGFP/Cx43/pBi5 -dox
EGFP/Cx43/pBi5 +dox
CMV-pTetOn & EGFP/Cx43/pBi5 -dox
CMV-pTetOn & EGFP/Cx43/pBi5 +dox
SM22α/pTetOn & EGFP/Cx43/pBi5 -dox
SM22α/pTetOn & EGFP/Cx43/pBi5 +dox
CMV-EGFP
*
*
*

The CMV-pTetOn and EGFP / Cx43 / pBi5 double transfections showed significantly increased expression of EGFP (and hence inferred Cx43 expression) with the addition of doxycycline to the medium (0.27 ± 0.03%; $n = 4$, and 1.37 ± 0.11%; $n = 4$, respectively; $P < 0.05$). The expression of CMV-EGFP was significantly different to CMV-pTetOn and EGFP / Cx43 / pBi5 ± doxycycline expression ($P < 0.05$).

In the double transfections with SM22α / pTetOn and EGFP / Cx43 / pBi5, doxycycline increased expression of EGFP from 0.22 ± 0.08% ($n = 4$) to 0.62 ± 0.14% ($n = 4$). The increase was statistically significant ($P < 0.05$). Although the expression levels were similar to those observed for the SM22α / pTetOn and Cx43 / pBi5 double transfections, the increase in expression with doxycycline was more marked this time, indicating that direct EGFP detection was more sensitive than immunohistochemical detection. CMV-EGFP expression was constant at 8.2 ± 1.0% ($n = 4$) and significantly different when compared to the other transfection groups ($P < 0.05$).

AII.4 Discussion

The three constructs SM22α / pTetOn, Cx43 / pBi5 and EGFP / Cx43 / pBi5 were successfully cloned, and subsequently verified using a combination of restriction analyses, PCR screening and bi-directional sequencing. The sequencing data from each construct showed that apart from the base changes already noted in the SM22α promoter, no other base changes had occurred in any construct during the cloning process and therefore, the constructs were ready for testing *in vitro* in murine embryonic fibroblasts and aortic smooth muscle cells.

The CMV-pTetOn, SM22α / pTetOn, Cx43 / pBi5, EGFP / Cx43 / pBi5 and CMV-EGFP plasmids were transfected into the fibroblasts and smooth muscle cells using the Lipofectamine Plus Reagent, albeit at varying efficiencies. CMV-pTetOn expression was detected using a commercial antibody against VP16 (FITC; fluoresces green) whilst Cx43 / pBi5 (Cx43) expression was detected using a commercial antibody

against Cx43 (Texas Red; fluoresces red). Expression of CMV-EGFP and EGFP / Cx43 / pBi5 was detected by direct fluorescence microscopy.

In the single transfections of both the fibroblasts and smooth muscle cells, without DNA, there were no CMV-pTetOn (VP16 positive) cells present and no intense staining of Cx43. CMV-pTetOn expression was observed both with and without the addition of doxycycline to the medium, albeit at low rates when compared to the control plasmid CMV-EGFP. Even lower rates of expression were observed for Cx43 / pBi5 both with and without the addition of doxycycline to the medium. In both the CMV-pTetOn and Cx43 / pBi5 single transfections, the addition of doxycycline to the medium did not increase expression levels as was expected.

The observation that there was some Cx43 expression in the single transfections of Cx43 / pBi5 suggested that there had been random integration of the plasmid. Also, as the Cx43 / pBi5 construct was not expected to show any expression, it was likely that there was some 'leakiness' of the TRE (tetracycline response element) or that there was some residual doxycycline present in the foetal calf serum. The latter possibility was ruled out by further experimentation using the doxycycline free serum, the results of which showed that there was no difference in the number of labelled cells for any transfection in the fibroblasts whether or not DFS (doxycycline free serum) or FCS (foetal calf serum) had been used. A similar result was also noted by another group working with the TetOn system *in vitro* (Ranu Mital, *pers com*). These results are further substantiated by the fact that doxycycline is rarely used in the bovine industry due to cost; tetracyclines being the drug of choice to treat bacterial infections and to increase carcase weight. Therefore, the calf and foetal calf serums used in cell culture are not likely to retain much, if any, residual doxycycline. Residual tetracycline is not likely to be of concern in the pTetOn system as the rtTA responds minimally to it (Gossen and Bujard, 1992). It has recently been stated that the pTetOn system is

responsive only to doxycycline and not to tetracycline (Gossen and Bujard, 1995; Clontech, 2000).

'Leakiness' is defined by Bujard (1996) as the intrinsic activity of the minimal promoter upon transfer into cells; the activity varying between different cell types. It is not uncommon in transient expression systems because the rtTA (or tTA) responsive transcription unit is in a non-integrated state in the cell. Whenever integration of genes responsive to either tTA or rtTA does not occur at a chromosomal site or at suitable chromosomal sites, unregulated basal transcription may be observed (Freundlieb *et al.* 1999). Some applications are known to be hampered by this residual basal activity (Furth *et al.* 1994; Howe *et al.* 1995; Kistner *et al.* 1996).

The residual activity of the minimal promoter in the current study was considered acceptable, especially as it is known that when a transcription unit controlled by a minimal promoter-tet operator sequence is integrated into the chromosome, the residual activity is drastically reduced (Bujard, 1996). If the background expression had indeed been excessive, a different minimal promoter would most likely have been selected, such as a Tk-based promoter. Recently, problems due to high background expression from tetracycline responsive promoters have been ameliorated by the use of tetracycline-sensitive transcriptional repressors / silencers (tTS) (Forster *et al.* 1999; Freundlieb *et al.* 1999; Rossi and Blau, 1998). The tTS bind promoters responsive for rtTA in the absence of the effector doxycycline, causing a ten to two hundred fold repression in transient expression systems (Freundlieb *et al.* 1999).

In the double transfections of both the fibroblasts and smooth muscle cells, the modified pBi5 plasmids responded to CMV-pTetOn (VP16) and doxycycline (Figures AII.11 and AII.14). Cx43 expression was increased in the double transfections of the smooth muscle cells using SM22α / pTetOn and Cx43 / pBi5, and with doxycycline added to the medium. Consequently, it was inferred that the SM22α / pTetOn construct had been successfully transfected into the smooth muscle cells. Also, as no expression

of this construct was detected in the fibroblasts, the tissue specificity of the construct was confirmed.

Data obtained from the time course study of the induction of expression of the CMV-pTetOn, Cx43 / pBi5 and CMV-EGFP constructs, showed a bell-shaped curve for CMV-EGFP expression, in contrast to the apparent steady-states of CMV-pTetOn and Cx43 / pBi5. This may be attributed to the more sensitive EGFP detection method compared to immunohistochemical detection; a contention which is supported by the fact that Cx43 / pBi5 expression was not detected until 18 hours post-transfection (even though the plasmid had not been expected to express at all, as previously discussed). Furthermore, low rates of expression were recorded for CMV-pTetOn compared with those for CMV-EGFP.

The results presented above suggest that immunohistochemical detection was not as sensitive as the direct EGFP detection method. The CMV-EGFP control was continually producing high levels of expression in both the fibroblasts (about 7%) and the smooth muscle cells (about 8%), compared to the other constructs. Consequently, the Cx43 / pBi5 construct was modified by replacing the luciferase gene with the EGFP gene (EGFP / Cx43 / pBi5). EGFP measurement is renowned for being easy to monitor by using standard fluorescein microscope excitation / emission filters.

Green fluorescent protein (GFP), originally isolated from the jellyfish *Aequorea victoria*, has been fused to many proteins in a range of species (eg. mice; Chiocchetti *et al*. 1997; Jordan *et al*. 1999) to produce stable chimaera which retain their normal biological activity as well as retaining the fluorescent properties of native GFP (Prasher *et al*. 1992; Chalfie *et al*. 1994; Stearns, 1995). This allows a diverse range of biological functions to be studied *in vivo*. As GFP is distributed throughout the cell, both in the nucleus and cytoplasm, it is widely used as a reporter for gene expression and as a fusion tag to monitor protein localization *in vivo* (Misteli and Spector, 1997). The autofluorescing EGFP is a red-shifted eukaryotic cytoplasmic mutant of GFP that

fluoresces thirty-five times more intensely than the wild-type GFP (Cormack *et al.* 1996), and thus has greater potential as a reporter system. As there are no mammalian homologs to EGFP, there is no specific fluorescence from endogenous GFPs in mammalian cells, although there is variable non-specific autofluorescence (Kisseberth *et al.* 1999).

Giaretta *et al.* (2000), in their comparative study of gene transfer into blood cells, concluded that EGFP marker genes are useful for rapid, safe and non-toxic detection of transduced cells; EGFP appearing particularly useful in the optimisation of gene transfer protocols *in vitro*. Similar *in vitro* conclusions have been drawn by others (Casey *et al.* 2000). Duprex *et al.* (2000) and Henry *et al.* (2000), for example, have also reported on the efficacy of using EGFP coupled to measles virus and murine cytomegalovirus respectively, both *in vivo* and *in vitro*. However, Stripecke *et al.* (1999), have shown that in mice, the immune response against EGFP and GFP is high, indicating that their widespread application *in vivo* is potentially premature.

EGFP has now been successfully fused to the TetR / VP16 DNA in order to rapidly select tetracycline-controlled inducible cell lines (Callus and Mathey-Prevot, 1999). Recently, EGFP has been coupled to the Cx43 gene to study the formation, turnover and function of this connexin in *in vitro* mammalian cells (Jordan *et al.* 1999; Bukauskas *et al.* 2000).

By using EGFP coupled to Cx43 / pBi5 in the current study, the number of labelled cells counted in the single transfections of the fibroblasts was decreased considerably compared to that of previous experiments, whilst in the double transfections, the number of labelled cells counted increased. The decrease in expression in the single and double transfections of the smooth muscle cells, may have been attributable to the use of the new serum (DFS) and not to any intrinsic property of the EGFP gene. However, it is more likely due to the elimination of false positives from the immunohistochemical detection of increased Cx43 expression, as was the case for

the single transfections of the fibroblasts. These results illustrate the effectiveness of the direct EGFP detection method compared to immunohistochemical methods for studies of this type.

The lower expression levels of Cx43 in the double transfections with SM22α / pTetOn compared with those with CMV-pTetOn may be attributable to the nature of the DNA constructs or to the CMV promoter. The cytomegalovirus promoter is known to be a promoter capable of producing high expression levels of many genes in a wide variety of cells (Almouzni and Wolfe, 1993), and especially after transfection. The same situation does not exist for the tissue specific SM22α promoter.

As discussed in Chapter 3, transient transfection of various SM22α promoter lengths has been previously reported. The expression levels obtained using the modified SM22α / pTetOn construct are clearly much lower than those for other constructs already published (c.f. Kemp *et al.* 1995; Solway *et al.* 1995; Li *et al.* 1996; Moessler *et al.* 1996). However, direct comparisons cannot be made for several reasons as discussed in Chapter 3.

Furthermore, it is possible that the coupling of the restricted SM22α promoter to the pTetOn plasmid in some way affected the performance of the promoter. Alternatively, the ubiquitous nature of the CMV promoter in pTetOn may be solely responsible. Both hypotheses could be supported by the data from the current study, where higher levels of Cx43 expression were detected when the modified pBi5 plasmids were transfected with the CMV-pTetOn plasmid compared with the SM22α / pTetOn plasmid. However, in view of the fact that several studies have shown that the CMV promoter allows a higher degree of expression of a gene compared with other promoters, such as the phosphoglycerolkinase promoter, for example (Gerolami *et al.* 2000), the latter would seem to be more plausible.

The activity (or expression) of a gene regulated by the tetracycline expression system also depends on the number of copies of the gene in the cell, which depends on the amount of DNA used for transfection (Bujard, 1996). Control experiments tested varying concentrations of CMV-EGFP and Lipofectamine Plus in the cell cultures; the optimal levels being 0.4 μg DNA and 4 μl Lipofectamine Plus in 25 μl serum free medium for each transfection (data not shown). Double transfections were performed with increased DNA concentrations (double) for each co-transfected construct, and also by maintaining each at 0.4 μg.

Transfections in the current study were undertaken with equal amounts of each vector which, in hindsight, may not have been ideal. This contention is supported by Bujard (1996), for example, who states that the ratio of the rtTA producing plasmid verses the response plasmid is critically important, with an excess of rtTA over response (up to 100-fold) being advisable to ensure high intracellular concentrations of rtTA. However, the fact that the transactivator may be toxic, thus imposing a growth disadvantage on cells expressing them at high levels, also needs to be considered (Saez *et al.* 1997; Strathdee *et al.* 1999). Hence, based on data obtained from this study, an initial titration of the regulator and response plasmids to determine the optimal ratio of the two plasmids would be recommended.

The nature of the double transfections raises another issue, that of co-transfection. Co-transfection of the regulator plasmid (CMV-pTetOn or SM22α / pTetOn) and the response plasmid (Cx43 / pBi5 or EGFP / Cx43 / pBi5) can result in high background expression of the regulated gene (Cx43), which is not affected by the presence or absence of the antibiotic (tetracycline or doxycycline; Gossen and Bujard, 1992). This is especially the case in stable co-transfections. Recently, in the Tet Systems User Manual (Clontech, 2000), it was recommended that that the regulator and response plasmids not be co-transfected for two principle reasons. Firstly, due to the induced basal expression levels as mentioned above and also, as the response plasmid

generally will not co-integrate with the regulator, giving cells with very low or no expression of the gene of interest. The background expression levels detected in the current transient experiments were relatively low but, as discussed previously, all expression levels were below that achieved by other studies using different constructs. In future experiments it would be advisable to trial separate transfections of the response and regulator plasmids, and compare the results with the data obtained in the current study. This would, of course, necessitate the use of stably transfected cells.

Consequently, it would be recommended that for future studies of this type, or if the experiments were to be repeated, stably transfected cells be used. This would eliminate the basal expression levels of pBi5 alone and the spurious results emanating from using co-transfections. In co-transfections, the response plasmid will not generally co-integrate with the regulator giving cells with very low or no expression of the gene of interest (Clontech, 2000).

The transient nature of the fibroblast and smooth muscle cell culture systems was not considered an important factor in the modulation of the various expression levels. It is recommended that the tetracycline expression system be tested first in a transient experiment with double transfections of the rtTA expression vector, an unregulated internal standard to examine the transfection efficiency and the response vector, in the absence or presence of 1 mg / ml doxycycline (Bujard, 1996). The latter factor leads to another area, which in hindsight, could have been exploited to optimize expression levels.

The antibiotics tetracycline and doxycycline are known to enter vertebrate cells by passive diffusion and thus, the concentration inside the cells correlates with the amount added to the culture medium. Although the recommended concentration of doxycycline is 1 mg / ml (Gossen and Bujard, 1992; Kringstein *et al.* 1998), it has been found that optimal concentrations for cells other than HeLa cells may vary. Furthermore, as the affinity of rtTA for doxycycline is lower than that for tTA, there is a

concentration of doxycycline at which rtTA will not bind DNA efficiently (Gossen *et al.* 1995). The same is also applicable for tTA (Rossi and Blau, 1998). Consequently, varying concentrations of doxycycline should be trialled in cell culture to optimize the functioning of the tetracycline expression system. Also, although uptake of doxycycline is very fast, it would be interesting to pre-incubate cells with doxycycline prior to transfection, as it is known that some cell lines may behave differently in such circumstances (Gossen *et al.* 1995). To date, these antibiotics have been used for many years in both animals and humans, with deleterious effects only being detected at high dosages.

A final consideration is that for all transfections, either single or double, the expression levels in the fibroblasts varied from those observed in the smooth muscle cells. This was not unduly surprising as the efficacy, sensitivity and toxicity of a transfection reagent was known to depend on a variety of parameters, some of which, have already been discussed. These include, for example, growth rates of cells (Pickering *et al.* 1996), cell type (eg. smooth muscle cell versus endothelial cell) and cell species (eg. rat versus human), absence of serum (Escriou *et al.* 1998), and DNA purity (Clontech, 2000) – which was the same for all constructs in the current study.

The majority of transfection studies so far have been performed on animal cells but unfortunately, and not surprisingly, not all cell types have been studied. To date, there is a paucity of published data examining the efficient transfection of primary murine smooth muscle cells. The success and effectiveness of the new liposomal and non-liposomal transfection reagents remains to be elucidated.

A further factor to be considered in the interpretation of the increased double transfection expression levels in the fibroblasts compared with the smooth muscle cells, is the fact that the various plasmids may respond (ie: express) differently in the two cell lines. Howe *et al.* (1995), for example, found that tetracycline-sensitive inducible expression differed between two mammalian cell lines: GH3 cells derived from the rat

pituitary and HEK293 cells derived from the human embryonic kidney. They concluded that the inducible expression system does not function optimally in HEK 293 cells. Others have also shown that efficacy of tetracycline-controlled gene expression is influenced by cell type (Ackland-Berglund and Leib, 1995; Gossen and Bujard, 1995). Therefore, this aspect must also be considered when analyzing the results from the transfections and when comparing data from other studies.

One of the advantages of the tetracycline expression systems is the high inducibility and response times. In contrast to other systems for mammalian expression, which may take up to several days, Clontech (2000) state that induction can be detected within 30 minutes in stably transfected cell lines (with doxycycline). In the current study, induction of CMV-pTetOn and CMV-EGFP expression had occurred by 6 hours post-transfection, with the maximum induction level peaking at 18 hours post-transfection for CMV-EGFP. However, the Cx43 / pBi5 construct did not show any expression until 18 hours post-transfection. A similar time frame was obtained for the double transfections using CMV-pTetOn and Cx43 / pBi5 with doxycycline where complete expression occurred 24 hours after the addition of the doxycycline to the medium. For all constructs, the expression levels did not vary significantly from the time that expression was recorded. This is in accordance with other studies. These results indicate that the expression of the three plasmids occurs within 24 hours after transfection, making them relatively highly inducible.

Kistner *et al.* (1996) showed that in transgenic mice, the administration of oral doxycycline rapidly induced synthesis of the indicator enzyme luciferase within the first four hours in some organs, with complete induction occurring after 24 hours in most organs studied. Longer induction times have, however, been recorded. Mansuy *et al.* (1998), for example, combined the rtTA with the CaMKIIalpha promoter and found that doxycycline induces maximal gene expression in neurons of the forebrain within six days. Hence, there exists a range of maximal induction times, depending on the organs

or tissues being targeted. Reversibility of the system is usually evident within 48 hours (Sturtz *et al.* 1998; Clontech, 2000).

Generally, the basic premise with rtTA is that transient experiments are more complicated than with tTA. Recently, Paulus *et al.* (2000) reported higher regulation with the conventional tet system than with the reverse tet system (rtTA) in C6 glioma and rat-1 fibroblast clones. They also noted a very high variability in absolute expression levels in rat cells *in vitro*. A further limitation of the rtTA system, which was briefly alluded to, is the fact that the full potential of the rtTA regulation system can only be exploited in stably transfected cells since it relies on two sequential stable transfections for optimal inducibility (Gossen and Bujard, 1992; Bujard, 1996). Consequently, it is not ideal for use with primary cultures.

Despite the limitations and problems inherent in the tetracycline expression system, especially with the rtTA, the data obtained in this study indicate the applicability of the system to studies involving gene manipulation. By careful adaptation of the expression vector to the host cell line, the full range of regulatory properties of tetracycline-controlled gene expression can be exploited (Hoffmann *et al.* 1997).

At present, several inducible systems have been established in transgenic mice, but all have limitations. The various eukaryotic promoters used in the 1980s to control gene activity invariably suffered from leakiness of the inactive state (basal leakiness; Mayo *et al.* 1982) or from the wide variety of effects caused by the inducing agents themselves, such as toxicity, non-specific effects such as activation of endogenous genes, increased glucocorticoid activity or elevated temperature (Yarranton, 1992). Limited availability of cell specific promoters and low levels of gene expression were also problems (Yarranton, 1992).

By the late 1980s, work on regulatory systems that do not rely on endogenous control elements had begun. This lead to the adoption of well-characterized regulatory systems from *Escherichia coli* for use in mammalian cells (Gossen *et al.* 1993).

Although transgenic systems based on the *lac* operon were unsatisfactory (Yarranton, 1992), those which were based on the tetracycline-resistance operon *tet* from the *E. coli* transposon Tn*10* enabled a new approach to be made in the control of transgene expression (Gossen and Bujard, 1992, 1993). The tetracycline regulatory system gives tight and reversible control of foreign gene activity in mammalian cells, permitting the study of particular gene functions in transfected cells (Buckbinder *et al.* 1994; Resnitzky *et al.* 1994; Yin *et al.* 1996) and *in vivo* gene transfer / regulation studies (Fishman, 1998). It has also been successfully used in transgenic mice to control expression of a transgene (Furth *et al.* 1994; Hennighausen *et al.* 1995; Kistner *et al.* 1996; Schultze *et al.* 1996; Chen *et al.* 1998; Sarao and Dumont, 1998; Tremblay *et al.* 1998; Bogeroger and Gruss, 1999 and Soulier *et al.* 1999).

In conclusion, Cx43 expression was increased in the double transfections with SM22α / pTetOn (CMV-pTetOn) and Cx43 / pBi5, and with SM22α / pTetOn (CMV-pTetOn) and EGFP / Cx43 / pBi5, with doxycycline added to the medium. Although expression levels of Cx43 (inferred from EGFP expression) were lower than expected, and lower than those produced by the CMV-pTetOn and Cx43 / pBi5 (or EGFP / Cx43 / pBi5) double transfections, the tetracycline expression system was shown to induce temporal and tissue specific expression of Cx43 in both the fibroblasts and smooth muscle cells. Thus, two constructs had been made which would form the basis of the temporal and tissue specific mouse.